



MONASH University

**Novel Techniques Using
Computed Tomography to Assess the
Functional Significance of
Coronary Artery Disease**

Dr Brian Ko

BSc (Medicine), MBBS, PhD, FRACP, FCSANZ

A thesis submitted for the degree of
Doctor in Medicine (Unsupervised) at Monash University in 2014

First submitted on 31st October 2014

Monash Cardiovascular Research Centre, MonashHEART

Department of Medicine (Monash Medical Centre),

Southern Clinical School, Monash University.

Copyright notice

© Brian Ko 2014. Except as provided in the Copyright Act 1968, this thesis may not be reproduced in any form without the written permission of the author.

THESIS CONTENTS	PAGE
ABSTRACT	4
GENERAL DECLARATION	5
ACKNOWLEDGEMENTS	8
INTRODUCTION AND AIMS OF THESIS	9
CHAPTER 1 The use of computed tomography to detect coronary ischemia	22
CHAPTER 2 Comparison of diagnostic accuracy of combined assessment using adenosine stress CT perfusion (CTP) + computed tomography angiography (CTA) with transluminal attenuation gradient (TAG320) + CTA against invasive fractional flow reserve (FFR)	104
CHAPTER 3 Diagnostic Performance of Transluminal Attenuation Gradient and Non-Invasive Fractional Flow Reserve derived from 320 detector Computed Tomography Angiography to Diagnose Hemodynamically Significant Coronary Stenosis- a NXT Substudy	139
CHAPTER 4 Rest and Stress Transluminal Attenuation Gradient and Contrast Opacification Difference for Detection of Hemodynamically Significant Stenoses in Patients with Suspected Coronary Artery Disease	175
CHAPTER 5 Diagnostic Accuracy of the ASLA Score: a Computed Tomography Angiographic Index to Predict Functionally Significant Coronary Stenoses in Lesions with Intermediate Stenosis Severity	213
CONCLUSION AND FUTURE DIRECTIONS	256

ABSTRACT:

Over the past 6 years, an important focus of CT research is the development of novel techniques to concomitantly evaluate the anatomical and functional significance of coronary artery disease which may broaden the future use of CT to assess both coronary anatomy and ischemia in a single examination. These techniques include 1) the prediction of a non-invasive fractional flow reserve (FFR_{CT}) upon applying computational fluid dynamics on CTA images, 2) the assessment of the transluminal attenuation gradient (TAG) across coronary lesions and 3) the use of CT myocardial perfusion imaging (CTP) acquired during vasodilator stress.

The aim of the thesis was first to review the novel CT techniques which have been recently evaluated to assess for coronary ischemia (chapter 1), to compare the diagnostic performance of transluminal attenuation gradient, using invasive fractional flow reserve as reference standard, with CT stress myocardial perfusion imaging (chapter 2), and non invasive fractional flow reserve derived from CT (chapter 3), to evaluate the feasibility and diagnostic performance of transluminal attenuation gradient acquired during vasodilator stress (chapter 4) and to finally assess the diagnostic accuracy of a score based on measures of area stenosis, lesion length and myocardium subtended quantified from CT coronary angiography (chapter 5).

General Declaration

Monash University

Declaration for thesis based or partially based on conjointly published or unpublished work

General Declaration

In accordance with Monash University Doctorate Regulation 17.2 Doctor of Philosophy and Research Master's regulations the following declarations are made:

I hereby declare that this thesis contains no material which has been accepted for the award of any other degree or diploma at any university or equivalent institution and that, to the best of my knowledge and belief, this thesis contains no material previously published or written by another person, except where due reference is made in the text of the thesis.

This thesis includes 3 original papers published in peer reviewed journals and 2 unpublished publications (as of 2014). The core theme of the thesis is novel CT techniques to assess the hemodynamic significance of coronary artery disease. The ideas, development and writing up of all the papers in the thesis were the principal responsibility of myself, the candidate.

In the case of chapters 1-5 my contribution to the work involved the following:

Thesis chapter	Publication title	Publication status*	Nature and extent of candidate's contribution
1	The use of computed tomography to detect coronary ischemia	Accepted for book chapter 22 titled "Myocardial Perfusion Imaging with CT" in the book titled "Non invasive perfusion imaging in clinical practice" – Publisher LWW, Editor Farhood Saremi MD	Literature review and wrote manuscript

2	Comparison of diagnostic accuracy of combined assessment using adenosine stress CT perfusion (CTP) + Computed tomography angiography (CTA) with transluminal attenuation gradient (TAG320)+CTA against invasive fractional flow reserve (FFR)	Published in Journal of the American College of Cardiology (JACC 2014, May 13; 63 (18): 1904-12)	Conception, design, analysis and interpretation of data. Drafting and revising of manuscript. Final approval of manuscript submitted.
3	Diagnostic Performance of Transluminal Attenuation Gradient and Non-Invasive Fractional Flow Reserve derived from 320 detector Computed Tomography Angiography to Diagnose Hemodynamically Significant Coronary Stenosis- a NXT substudy	Unpublished, under review in JACC cardiovascular imaging	Conceived the study, participant recruitment, acquisition of FFR, analysis and interpretation of data and wrote the manuscript.
4	Rest and Stress Transluminal Attenuation Gradient and Contrast Opacification Difference for Detection of Hemodynamically Significant Stenoses in Patients with Suspected Coronary Artery Disease	Unpublished, under review in JACC cardiovascular imaging	Conceived the study, interpretation of CT coronary angiography, statistical analysis, analysis and interpretation of data and co-wrote the manuscript.
5	Diagnostic accuracy of the ALSA score: a computed tomography angiographic index to predict functionally significant coronary stenoses in lesions with intermediate stenosis severity.	Accepted for publication in Radiology in August 2014, in press	Conceived the study, interpretation of quantitative CT coronary angiography, statistical analysis, analysis and interpretation of data and co-wrote the manuscript.

[* For example, 'published'/ 'in press'/ 'accepted'/ 'returned for revision']

I have not renumbered sections of submitted or published papers in order to generate a consistent presentation within the thesis.



Signed:

Date:16/10/2014.....

DECLARATION

This thesis contains no material which has been accepted for the award of any other degree or diploma in any university or other institution.

To the best of my knowledge the thesis contains no material previously published or written by another person, except where due reference is made in the text of the thesis.

In the manuscripts in which the work was based on joint research or publications, the relative contributions of the other contributing authors have been disclosed at the commencement of each results chapter in the 'Declaration for Thesis Chapter'.

ACKNOWLEDGEMENTS

I thank my Lord Jesus Christ for His guidance, provision and wisdom. I am deeply humbled by His grace in providing me with the opportunity to participate in this journey of scientific discovery. It has undoubtedly been His Spirit at work which has enabled me to complete this degree – the work in this PhD I pray will bring Him glory and His people health.

I thank my wife Karen for her constant love, resourcefulness and sacrifice. She has been my anchor, friend and strength. I am grateful to my children Caitlin, Elizabeth and Annaliese for their love, support and laughter. I thank my father for inspiring me to improve and complete this degree, my mother for her encouragement and prayer support and Karen's parents for sacrificing their time to come to Melbourne on many occasions to assist our family.

Lastly I thank Professor James Cameron, Associate Professor Sujith Seneviratne, Professor Ian Meredith and fellow researchers at MonashHEART to whom I will be forever in debt for inspiring me and supporting me in the rewarding field of Cardiac CT research.

But we have this treasure in jars of clay to show that this all-surpassing power is from God and not from us. 2 Corinthians 4:7

Introduction and aims of thesis

Coronary artery disease (CAD) remains a leading cause of morbidity and mortality worldwide (1) and the assessment and management of stable coronary artery disease (CAD) constitutes the daily practice of cardiologists. In symptomatic patients with suspected CAD, non invasive tests are typically performed to exclude the presence of significant coronary disease or ischemia. This may include the use of coronary computed tomography angiography (CTA) to evaluate for the presence of anatomical stenoses or functional tests to evaluate for presence of hemodynamically significant coronary stenoses resulting in myocardial ischemia. Patients identified to have either severe anatomical or functional disease are then referred for invasive angiography and consideration for revascularisation.

The advent of multi-detector CTA over the past decade has provided cardiologists with the ability to non-invasively diagnose and exclude significant anatomical coronary artery stenoses with sensitivity and negative predictive values in excess of 90% (2-4) when compared with invasive angiography. While upfront anatomical testing using coronary CT angiography is increasingly utilised as recommended in contemporary guidelines (5,6), CTA in its current form is limited in prediction of coronary ischemia. CT coronary angiography lacks specificity and positive predictive value for vessel specific ischemia which has been described to range from 48-78% and 46-77% (7-9). This is particularly important in the management of stable coronary artery disease as the functional significance of coronary stenoses determines clinical prognosis and need for revascularisation (10-12). In the presence of significant ischemia, revascularisation reduces symptoms (13) and improves overall prognosis (14-16), while in its absence, revascularisation offers little prognostic benefit and may worsen outcomes (10,17,18).

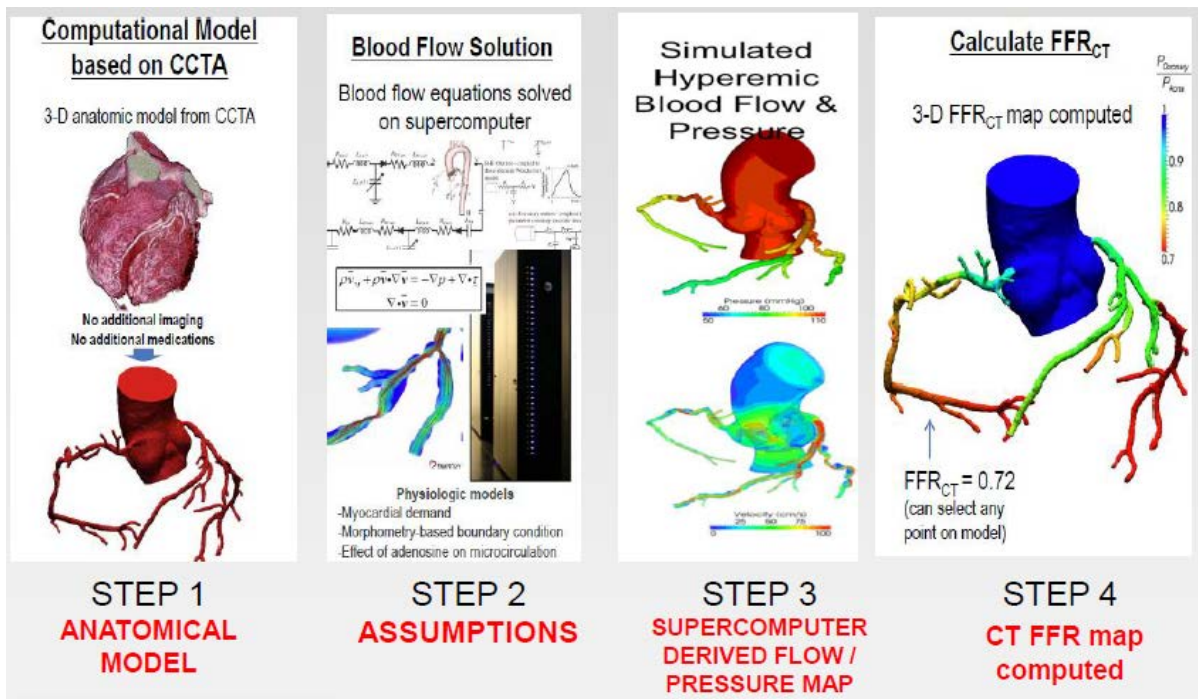
For this reason traditionally symptomatic patients with suspected coronary artery disease, have been referred for upfront non-invasive stress testing including stress electrocardiography, echocardiography, cardiac magnetic resonance (MR) imaging and single photon emission computed tomography (SPECT) myocardial perfusion imaging (MPI) to assess the burden of myocardial ischemia (19-21).

This strategy is based on literature supporting their ability to exclude severe coronary stenoses on invasive angiography (22), predict clinical prognosis (17,23-25) and cost effectiveness (26). In practice recent studies have, in contrast, demonstrated a low yield of obstructive disease on invasive angiography when functional testing is predominantly used upfront to triage patients for consideration for revascularisation. (27). Patel studied almost 400,000 patients who were referred for invasive angiography, of whom 83.9% of patients had undergone non invasive testing, which had either positive or equivocal results. In this population, 39% had no coronary disease (defined as <20% in all vessels) and patients with a positive non-invasive test result were only moderately more likely to have obstructive coronary artery disease than those who did not undergo any testing (41% vs 35%, $p<0.001$). This may pertain to the inability of current stress tests to concomitantly evaluate the patient's coronary anatomy.

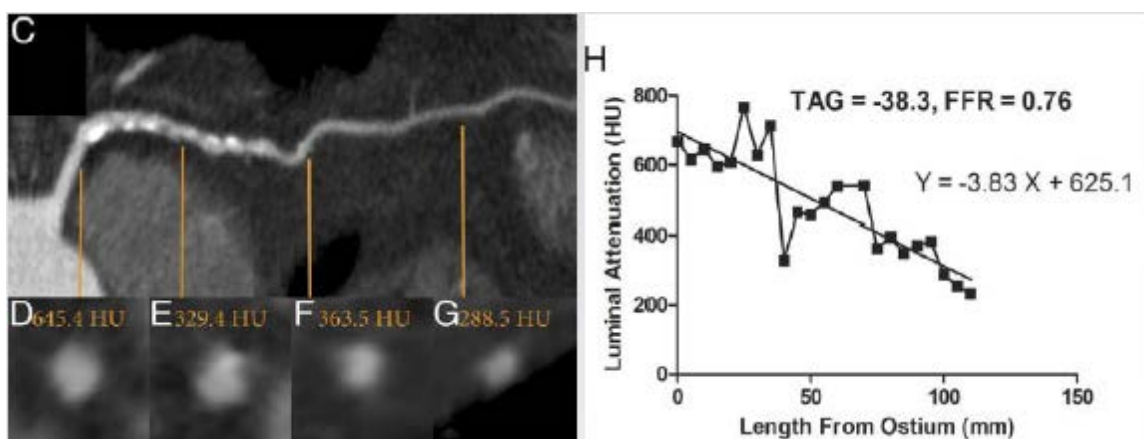
Currently there remains an unmet clinical need for a non-invasive imaging modality which may both accurately provide both coronary anatomical and functional information using a single imaging modality in one setting. Over the past 6 years, an important focus of CT research is the development of novel techniques to concomitantly evaluate the anatomical and functional significance of coronary artery disease which may broaden the future use of CT to assess both coronary anatomy and ischemia in a single examination. (28-31). These techniques include 1)

the prediction of a non-invasive fractional flow reserve (FFR_{CT}) upon applying computational fluid dynamics on CTA images, 2) the assessment of the transluminal attenuation gradient (TAG) across coronary lesions and 3) the use of CT myocardial perfusion imaging (CTP) acquired during vasodilator stress. The first two techniques can be conveniently applied on resting CTA images, while CTP requires a separate CT scan in addition to resting CTA which would require added radiation exposure and contrast usage.

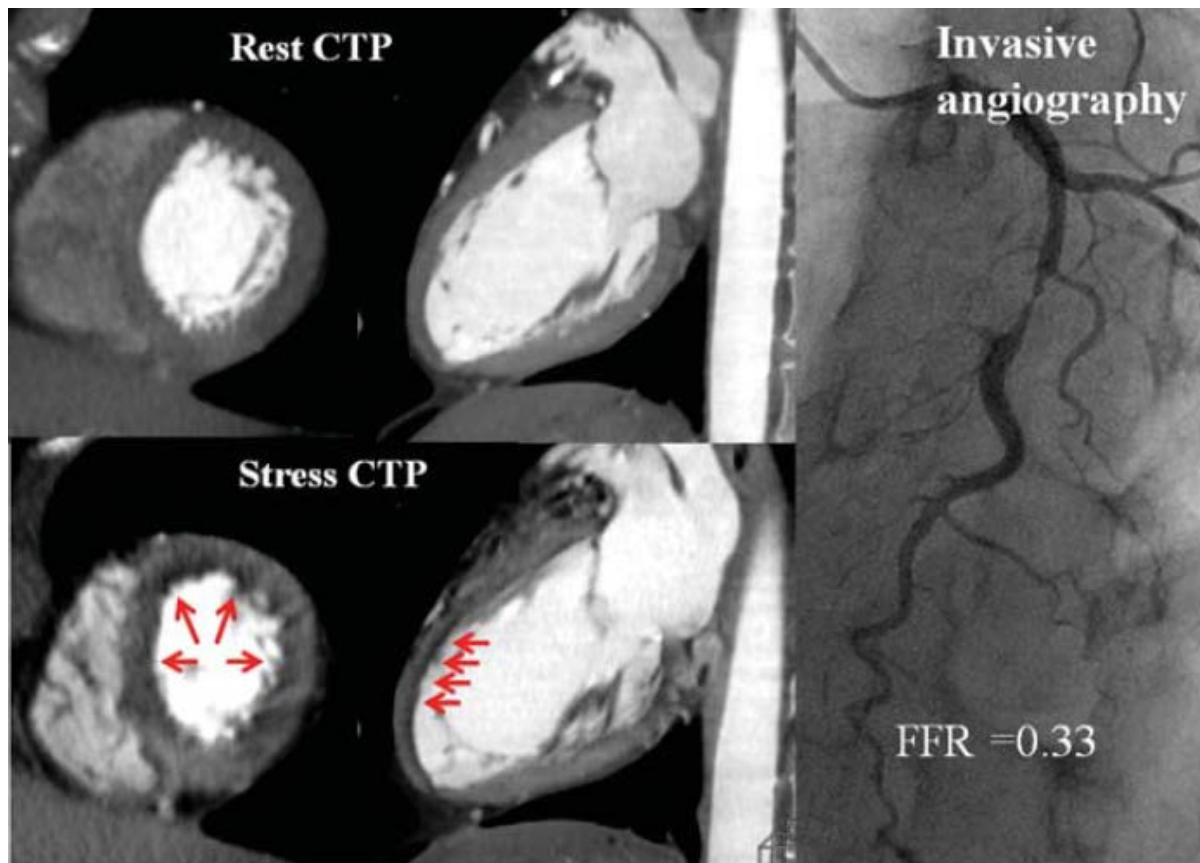
FFR_{CT} or non invasive FFR is derived by applying computational fluid dynamics to CTA vessel data. A three dimensional model of the aortic root and coronary lumen is first constructed using CTA images. Assumptions are made regarding the properties of blood assuming a constant viscosity, basal total coronary flow based on the total myocardial mass derived on CT, mean aortic pressure which matches the mean brachial pressure and total resistance coronary resistance which is inversely related to the luminal diameter (32). Using a supercomputer, three dimensional models throughout the cardiac cycle representing the pressure and flow along all points of the arteries are generated during rest and simulated maximal hyperaemic conditions. Based on the approximated pressure measurements, a non invasive FFR based on CT is derived. Its major advantage is that it can be performed without additional image reconstruction, acquisition or administration of medications. Currently the technique requires 5 hours of processing time (figure adapted from Taylor et al)(32).



Transluminal attenuation gradient (TAG) is defined as the linear regression coefficient between intraluminal attenuation (Hounsfield units) and axial distance. TAG evaluates the slope of decline in intraluminal contrast attenuation from the ostium to the distal coronary vessel (Figure, adapted from Wong et al (30)).



Myocardial perfusion imaging on CT is the acquisition of images during first pass of iodinated contrast from the arteries into the myocardium. This can be performed during rest as well as during vasodilator stress. In the absence of artifacts, hypoattenuated areas in the myocardium on CT represent areas of reduced perfusion (Figure derived from Ko et al(28)).



At the commencement of my Doctorate of Medicine (MD) in 2013, the high diagnostic performance of each of these techniques has been described when compared against the gold standard reference of invasive fractional flow reserve (28-31,33-35). Yet there has been no head to head comparison in the diagnostic performance of these novel techniques and hence it remains not known which CT test – TAG, FFRCT or CT perfusion is the best choice for functional assessment. Methodological improvements which may improve the practical implementation and diagnostic performance of these techniques also require further evaluation and validation, including the development of automated software derivation of TAG, and the

evaluation of TAG performed during vasodilator stress. Lastly the potential in the use of a score system based on multiple measurements derived from quantitative CT coronary angiography, including area stenosis, plaque burden, lesion length and volume of myocardium subtended, to better predict the functional significance of coronary stenoses remains unknown.

The aim of the thesis was first to review the novel CT techniques which have been recently evaluated to assess the hemodynamic significance of coronary stenoses (chapter 1), to compare the diagnostic performance of transluminal attenuation gradient, using invasive fractional flow reserve as reference standard, with CT stress myocardial perfusion imaging (chapter 2), and non invasive fractional flow reserve derived from CT (chapter 3), to evaluate the feasibility and diagnostic performance of transluminal attenuation gradient acquired during vasodilator stress (chapter 4) and to finally assess the diagnostic accuracy of a score based on measures of area stenosis, lesion length and myocardium subtended quantified from CT coronary angiography (chapter 5).

Reference

1. Roger VL, Go AS, Lloyd-Jones DM, et al. Heart disease and stroke statistics--2012 update: a report from the American Heart Association. *Circulation* 2012;125:e2-e220.
2. Budoff MJ, Dowe D, Jollis JG, et al. Diagnostic performance of 64-multidetector row coronary computed tomographic angiography for evaluation of coronary artery stenosis in individuals without known coronary artery disease: results from the prospective multicenter ACCURACY (Assessment by Coronary Computed Tomographic Angiography of Individuals Undergoing Invasive Coronary Angiography) trial. *J Am Coll Cardiol* 2008;52:1724-32.
3. Miller JM, Rochitte CE, Dewey M, et al. Diagnostic performance of coronary angiography by 64-row CT. *N Engl J Med* 2008;359:2324-36.
4. Meijboom WB, Meijs MF, Schuijf JD, et al. Diagnostic accuracy of 64-slice computed tomography coronary angiography: a prospective, multicenter, multivendor study. *J Am Coll Cardiol* 2008;52:2135-44.
5. Taylor AJ, Cerqueira M, Hodgson JM, et al. ACCF/SCCT/ACR/AHA/ASE/ASNC/NASCI/SCAI/SCMR 2010 Appropriate Use Criteria for Cardiac Computed Tomography. A Report of the American College of Cardiology Foundation Appropriate Use Criteria Task Force, the Society of Cardiovascular Computed Tomography, the American College of Radiology, the American Heart Association, the American Society of Echocardiography, the American Society of Nuclear Cardiology, the North American Society for Cardiovascular Imaging, the Society for Cardiovascular Angiography and Interventions, and the Society for Cardiovascular Magnetic Resonance. *Circulation* 2010;122:e525-55.
6. Shaw LJ, Marwick TH, Zoghbi WA, et al. Why all the focus on cardiac imaging? *JACC Cardiovasc Imaging* 2010;3:789-94.

7. Meijboom WB, Van Mieghem CA, van Pelt N, et al. Comprehensive assessment of coronary artery stenoses: computed tomography coronary angiography versus conventional coronary angiography and correlation with fractional flow reserve in patients with stable angina. *J Am Coll Cardiol* 2008;52:636-43.
8. Sarno G, Decraemer I, Vanhoenacker PK, et al. On the inappropriateness of noninvasive multidetector computed tomography coronary angiography to trigger coronary revascularization: a comparison with invasive angiography. *JACC Cardiovasc Interv* 2009;2:550-7.
9. Ko BS, Wong DT, Cameron JD, et al. 320-row CT coronary angiography predicts freedom from revascularisation and acts as a gatekeeper to defer invasive angiography in stable coronary artery disease: a fractional flow reserve-correlated study. *Eur Radiol* 2013;24:738-747.
10. Tonino PA, De Bruyne B, Pijls NH, et al. Fractional flow reserve versus angiography for guiding percutaneous coronary intervention. *N Engl J Med* 2009;360:213-24.
11. De Bruyne B, Pijls NH, Kalesan B, et al. Fractional flow reserve-guided PCI versus medical therapy in stable coronary disease. *N Engl J Med* 2012;367:991-1001.
12. Hachamovitch R, Berman DS, Kiat H, et al. Incremental prognostic value of adenosine stress myocardial perfusion single-photon emission computed tomography and impact on subsequent management in patients with or suspected of having myocardial ischemia. *Am J Cardiol* 1997;80:426-33.
13. Coronary angioplasty versus medical therapy for angina: the second Randomised Intervention Treatment of Angina (RITA-2) trial. RITA-2 trial participants. *Lancet* 1997;350:461-8.

14. Erne P, Schoenenberger AW, Burckhardt D, et al. Effects of percutaneous coronary interventions in silent ischemia after myocardial infarction: the SWISSI II randomized controlled trial. *JAMA* 2007;297:1985-91.
15. Shaw LJ, Berman DS, Maron DJ, et al. Optimal medical therapy with or without percutaneous coronary intervention to reduce ischemic burden: results from the Clinical Outcomes Utilizing Revascularization and Aggressive Drug Evaluation (COURAGE) trial nuclear substudy. *Circulation* 2008;117:1283-91.
16. Yusuf S, Zucker D, Peduzzi P, et al. Effect of coronary artery bypass graft surgery on survival: overview of 10-year results from randomised trials by the Coronary Artery Bypass Graft Surgery Trialists Collaboration. *Lancet* 1994;344:563-70.
17. Hachamovitch R, Rozanski A, Shaw LJ, et al. Impact of ischaemia and scar on the therapeutic benefit derived from myocardial revascularization vs. medical therapy among patients undergoing stress-rest myocardial perfusion scintigraphy. *Eur Heart J* 2011;32:1012-24.
18. Botman CJ, Schonberger J, Koolen S, et al. Does stenosis severity of native vessels influence bypass graft patency? A prospective fractional flow reserve-guided study. *Ann Thorac Surg* 2007;83:2093-7.
19. Gibbons RJ, Balady GJ, Bricker JT, et al. ACC/AHA 2002 guideline update for exercise testing: summary article: a report of the American College of Cardiology/American Heart Association Task Force on Practice Guidelines (Committee to Update the 1997 Exercise Testing Guidelines). *Circulation* 2002;106:1883-92.
20. Douglas PS, Khandheria B, Stainback RF, et al. ACCF/ASE/ACEP/AHA/ASNC/SCAI/SCCT/SCMR 2008 appropriateness criteria for stress echocardiography: a report of the American College of Cardiology Foundation Appropriateness Criteria Task Force, American Society of Echocardiography,

American College of Emergency Physicians, American Heart Association, American Society of Nuclear Cardiology, Society for Cardiovascular Angiography and Interventions, Society of Cardiovascular Computed Tomography, and Society for Cardiovascular Magnetic Resonance endorsed by the Heart Rhythm Society and the Society of Critical Care Medicine. *J Am Coll Cardiol* 2008;51:1127-47.

21. Hendel RC, Berman DS, Di Carli MF, et al. ACCF/ASNC/ACR/AHA/ASE/SCCT/SCMR/SNM 2009 Appropriate Use Criteria for Cardiac Radionuclide Imaging: A Report of the American College of Cardiology Foundation Appropriate Use Criteria Task Force, the American Society of Nuclear Cardiology, the American College of Radiology, the American Heart Association, the American Society of Echocardiography, the Society of Cardiovascular Computed Tomography, the Society for Cardiovascular Magnetic Resonance, and the Society of Nuclear Medicine. *J Am Coll Cardiol* 2009;53:2201-29.
22. Schinkel AF, Bax JJ, Geleijnse ML, et al. Noninvasive evaluation of ischaemic heart disease: myocardial perfusion imaging or stress echocardiography? *Eur Heart J* 2003;24:789-800.
23. Hachamovitch R, Hayes SW, Friedman JD, Cohen I, Berman DS. Comparison of the short-term survival benefit associated with revascularization compared with medical therapy in patients with no prior coronary artery disease undergoing stress myocardial perfusion single photon emission computed tomography. *Circulation* 2003;107:2900-7.
24. Soman P, Parsons A, Lahiri N, Lahiri A. The prognostic value of a normal Tc-99m sestamibi SPECT study in suspected coronary artery disease. *J Nucl Cardiol* 1999;6:252-6.

25. Elhendy A, Schinkel A, Bax JJ, van Domburg RT, Poldermans D. Long-term prognosis after a normal exercise stress Tc-99m sestamibi SPECT study. *J Nucl Cardiol* 2003;10:261-6.
26. Shaw LJ, Hachamovitch R, Berman DS, et al. The economic consequences of available diagnostic and prognostic strategies for the evaluation of stable angina patients: an observational assessment of the value of precatheterization ischemia. Economics of Noninvasive Diagnosis (END) Multicenter Study Group. *J Am Coll Cardiol* 1999;33:661-9.
27. Patel MR, Peterson ED, Dai D, et al. Low diagnostic yield of elective coronary angiography. *N Engl J Med* 2010;362:886-95.
28. Ko BS, Cameron JD, Meredith IT, et al. Computed tomography stress myocardial perfusion imaging in patients considered for revascularization: a comparison with fractional flow reserve. *Eur Heart J* 2012;33:67-77.
29. Bettencourt N, Chiribiri A, Schuster A, et al. Direct comparison of cardiac magnetic resonance and multidetector computed tomography stress-rest perfusion imaging for detection of coronary artery disease. *J Am Coll Cardiol* 2013;61:1099-107.
30. Wong DT, Ko BS, Cameron JD, et al. Transluminal Attenuation Gradient in Coronary Computed Tomography Angiography Is a Novel Noninvasive Approach to the Identification of Functionally Significant Coronary Artery Stenosis: A Comparison With Fractional Flow Reserve. *Journal of the American College of Cardiology* 2013;61:1271-9.
31. Koo BK, Erglis A, Doh JH, et al. Diagnosis of ischemia-causing coronary stenoses by noninvasive fractional flow reserve computed from coronary computed tomographic angiograms. Results from the prospective multicenter DISCOVER-FLOW (Diagnosis

- of Ischemia-Causing Stenoses Obtained Via Noninvasive Fractional Flow Reserve) study. *J Am Coll Cardiol* 2011;58:1989-97.
32. Taylor CA, Fonte TA, Min JK. Computational fluid dynamics applied to cardiac computed tomography for noninvasive quantification of fractional flow reserve: scientific basis. *J Am Coll Cardiol* 2013;61:2233-41.
 33. Ko BS, Cameron JD, Leung M, et al. Combined CT Coronary Angiography and Stress Myocardial Perfusion Imaging for Hemodynamically Significant Stenoses in Patients With Suspected Coronary Artery Disease: A Comparison With Fractional Flow Reserve. *JACC Cardiovasc Imaging* 2012;5:1097-111.
 34. Min JK, Leipsic J, Pencina MJ, et al. Diagnostic Accuracy of Fractional Flow Reserve From Anatomic CT Angiography. *JAMA* 2012;1-9.
 35. Bamberg F, Becker A, Schwarz F, et al. Detection of hemodynamically significant coronary artery stenosis: incremental diagnostic value of dynamic CT-based myocardial perfusion imaging. *Radiology* 2011;260:689-98.

Chapter 1

The use of computed tomography to detect coronary ischemia

PART B: Suggested Declaration for Thesis Chapter

[This declaration to be completed for each conjointly authored publication and to be placed at the start of the thesis chapter in which the publication appears.]

Monash University

Declaration for Thesis Chapter

Chapter 1: The use of computed tomography to detect coronary ischemia

Declaration by candidate

In the case of Chapter 1, the nature and extent of my contribution to the work was the following:

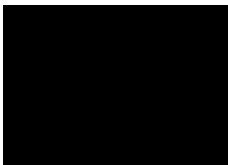
Nature of contribution	Extent of contribution (%)
Literature review and wrote manuscript	80

The following co-authors contributed to the work. If co-authors are students at Monash University, the extent of their contribution in percentage terms must be stated:

Name	Nature of contribution	Extent of contribution (%) for student co-authors only
Dennis Wong	Revision of manuscript	5
James Cameron	Revision of manuscript	
Sujith Seneviratne	Revision of manuscript	

The undersigned hereby certify that the above declaration correctly reflects the nature and extent of the candidate's and co-authors' contributions to this work*.

**Candidate's
Signature**

	Date 16/10/2014
---	---------------------------

Title

The use of computed tomography to detect coronary ischemia

Authors

Brian SH Ko BSc (Med), MBBS (Hons), PhD, FRACP , James D Cameron MBBS, MD, Dennis TL Wong BSc (Med), MBBS (Hons), PhD, FRACP, Sujith K Seneviratne MBBS, FRACP,

Affiliation of Authors

Monash Cardiovascular Research Centre, Department of Medicine (Monash Medical Centre) Monash University and Monash Heart, Southern Health, 246 Clayton Road, Clayton, 3168 VIC, Australia

Acknowledgement:

The authors wish to express their gratitude to the National Heart Foundation of Australia, and the Robertson Family Research Scholarship for assistance in funding.

Overview

(I) Introduction

(II) CT myocardial perfusion imaging

1. Fundamentals of CT perfusion imaging
2. Image acquisition
3. Image interpretation
4. Feasibility and diagnostic performance
5. Limitations

(III) Non invasive fractional flow reserve based on CT

1. Definition and derivation of FFR CT
2. Feasibility and Diagnostic Performance
3. Strengths and Limitations

(IV) Transluminal attenuation gradient

1. Definition and derivation of TAG
2. Feasibility and Diagnostic Performance
3. Strengths and Limitations

(V) Future directions

(VI) Conclusion

(I) Introduction

Coronary artery disease (CAD) remains a leading cause of morbidity and mortality worldwide

(1). The natural history of coronary artery disease (CAD) is characterised by the silent accumulation of atherosclerotic plaque in the wall of coronary arteries, progression into obstructive disease as excess plaque accumulates beyond maladaptive positive remodelling, the development of stress induced ischemia as a result of luminal encroachment and ultimate plaque rupture resulting in unstable angina, myocardial infarction and sudden cardiac death (2).

Fractional flow reserve (FFR) performed at the time of invasive coronary angiography (ICA) for combined anatomic-physiological evaluation represents the current gold standard for determining whether a coronary artery stenosis causes ischemia (3). FFR is defined as the ratio between the maximum myocardial blood flow in the presence of an epicardial stenosis and the maximum myocardial blood flow in the theoretical absence of an epicardial stenosis (4). When both epicardial and microvascular resistances are minimized by administering vasodilators and assuming microvascular resistance is similar in the presence and absence of an epicardial stenosis, coronary flow becomes proportional to coronary pressures. Because there is little pressure loss along a normal epicardial coronary artery, the proximal coronary pressure of a diseased artery is a reflection of what the distal coronary pressure would be in the absence of disease. Hence FFR can be defined as the distal coronary pressure divided by the proximal coronary pressure during maximal hyperaemia.

FFR has several unique attributes – 1) it has an unequivocal normal value of 1.0 in every patient and vessel, 2) it has a well-defined ischemic threshold determined to be 0.80 with a gray zone from 0.75 to 0.80, 3) FFR is measured during maximal hyperemia, as such it is not affected by changes in heart rate and blood pressure and is highly reproducible, 4) FFR incorporates the

contribution of collateral blood supply because distal pressure takes into account both antegrade and collateral flow, 5) FFR interrogates every epicardial vessel independent of the microvasculature, for example in the setting of an old myocardial infarct, a residual stenosis despite its angiographic appearance may have remain non-ischemic on FFR because it supplies nonviable myocardium.

FFR was first validated in 45 patients with intermediate single vessel disease by comparing the FFR value to the result from 3 different non-invasive stress tests (5). Due to the lack of a true gold standard for identifying myocardial ischemia, an abnormal result in any one of the non-invasive tests was taken to represent ischemia. Because each test has an accuracy of roughly 80%, applying sequential Bayesian analysis, the three tests in combination provided an accuracy of >95%. In this study, a threshold value of 0.75 was determined. Based on this threshold value, FFR had a 100% specificity, 88% sensitivity and an accuracy of 93%. To improve the sensitivity of FFR, the more recent clinical trial have used an FFR threshold value of 0.80 (6,7).

Deferral of percutaneous coronary intervention (PCI) for vessels with an $FFR > 0.80$ is associated with improved clinical outcomes and reduced costs compared with ICA alone-guided intervention or optimal medical therapy (6,7). Accordingly current guidelines regarding myocardial revascularisation assign a Class IA recommendation to FFR for the assessment of coronary artery stenoses with a diameter reduction ranging from 50-90% unless there is non-invasive proof ischemia(8). Due to its diagnostic accuracy, ability to provide robust vessel / lesion specific assessment of coronary stenosis and improvement in outcomes upon guiding PCI, it is currently regarded as the gold standard test for ischemia testing – a standard in which both novel and traditional non-invasive tests are increasingly benchmarked.

Over the past decade, multiple studies have demonstrated that CT coronary angiography (CTCA) is a robust non invasive method for detection of atherosclerotic plaque and obstructive coronary artery disease (defined as the presence of >50% stenosis on invasive angiography) with a high sensitivity and negative predictive value in patients with suspected coronary artery disease (9-12). Accordingly since 2010 CTCA has been recommended by the American College of Cardiology as an appropriate upfront investigation for symptomatic patients with low and intermediate risk of coronary artery disease (13,14). The use of CTCA in this population is currently a class IIa recommendation according to European Society of Cardiology and American College of Cardiology guidelines (15,16)

While CTCA accurately detects anatomical disease, in its current form it is limited in predicting lesion specific ischemia (17,18). When compared with invasive fractional flow reserve (FFR), CTCA has been found to have a high sensitivity and negative predictive value for ischemia, yet the specificity and positive predictive value is significantly limited (Table 1). This is a notable limitation as myocardial ischemia represents an important factor that determines clinical outcomes (6) and benefit from revascularisation (7,19-21). For this reason, patients with identified significant stenoses on CTCA often require further functional assessment which entails additional testing, radiation exposure, cost and inconvenience.

Current assessment for myocardial ischemia is typically performed with non-invasive stress imaging including stress echocardiography, single photon emission computed tomography (SPECT) or magnetic resonance imaging (MRI) myocardial perfusion imaging (MPI). It should be noted that with the exception of MRI MPI which is commonly available only in quaternary referral centres (22,23), stress echocardiography and SPECT MPI have been demonstrated to have poor discrimination of vessel specific ischemia(24-26). Using invasive FFR as reference standard for vessel-specific ischemia, SPECT MPI identifies ischemia territory correctly <50% of the time, with underestimation and overestimation in 36% and 22% of cases respectively

(24). Such data have evoked concerns for the ability of stress testing to effectively isolate coronary lesions that benefit from revascularisation (Table 2).

Over the past 5 to 10 years, an important focus of CT research is the development of novel techniques to evaluate each step in the pathophysiology of coronary artery disease including the assessment of the hemodynamic significance of coronary artery lesions and associated myocardial ischemia (Figure 1). These are aimed at enabling cardiac CT to act as a one-stop shop modality to assess the anatomical and physiological sequelae of coronary artery disease. The novel CT techniques which will be discussed in this book chapter include CT stress myocardial perfusion imaging (CTP) to evaluate for the presence of myocardial ischemia, the use of non invasive CT fractional flow reserve (FFR CT), and the study of transluminal attenuation gradient (TAG) across coronary lesions to assess the hemodynamic significance of coronary lesions.

(II) CT myocardial perfusion imaging

1) Fundamentals of CT myocardial perfusion imaging

Myocardial perfusion imaging on CT is facilitated by the use of iodinated contrast, which possesses the unique ability to attenuate x-rays proportional to its concentration. Imaging is acquired as contrast transits from the arteries into the myocardium and can be performed at rest, and during vasodilator stress such as adenosine (27-29), regadenoson (30,31) or dipyridamole (32). In the absence of artefacts, hypoattenuated areas in the myocardium on CT represent areas of reduced perfusion. George et al were among the first to describe the use of the technique using a canine model of LAD ischemia (33), which demonstrated the significant

difference in contrast attenuation between ischemic tissue and remote non-ischemic tissue (Figure 2).

Static and dynamic imaging

Two basic techniques can be applied for stress CTP: static imaging and dynamic imaging (Figure 3). Static stress CTP is analogous to static SPECT MPI and dynamic stress CT MPI is analogous to dynamic MRI MPI. Both static and dynamic CTP are performed during the first pass of contrast agent bolus passage through the myocardium. Differences in enhancement between normal and ischemic myocardium are maximal during the up-slope of myocardial bolus passage. During the down-slope, the differences become less and disappear (Figure 3), and the ability to distinguish enhancement differences is increased. The timing of scan acquisition is hence paramount.

In static or “snapshot” CTP imaging, only a single image stack is acquired similar to coronary CT angiography acquisition. Static imaging requires exact scan timing at a single time point during the upslope or maximum of the contrast agent bolus passage. Scan acquisition can be performed using helical or step-and-shoot techniques using narrow detector (≤ 64 detector-row CT), or prospective ECG gating using wide detector CT (256 / 320 detector- row CT). Myocardial blood flow can be assessed qualitatively and semi-quantitatively. Animal studies have shown strong nonlinear correlation between static CTP and microsphere myocardial blood flow (33). Subsequent human studies demonstrated that perfusion as assessed and quantified by transmural perfusion ratio was inversely and linearly related to percent diameter stenosis with a correlation of $R=0.63$ (29). Furthermore abnormal TPR has been found to be significantly associated with ischemia demonstrated on invasive FFR (34).

In dynamic CTP imaging, multiple stacks are acquired at multiple time points during the upslope of contrast passage through the myocardial tissue. From the series of images obtained,

a time-contrast attenuation curve (TAC) can be derived (Figure 2). The unique advantage of dynamic imaging is the ability to derive myocardial blood flow (MBF) and myocardial blood volume (MBV) from TACs using various mathematical models including a model-based deconvolution method, upslope and Patlak plot methods using available dedicated computer analysis software (28,35,36). In one of the initial reports, George et al, using 64 detector CT in a canine model of moderate to severe left anterior descending artery stenosis, demonstrated that MDCT derived MBF using model-based deconvolution analysis and 2 upslope methods strongly correlated with microsphere derived MBF ($R^2 = 0.91$, $p < 0.0001$) with a mean difference of 0.45ml/g/min (37).

Dynamic CTP when compared with static CTP requires a higher radiation exposure (36) and the use of advanced CT scanners. The technique has been thus far only been evaluated in 2nd generation dual source CT scanners using shuttle mode imaging during which the CT table rapidly alternates between two positions and as a result provides a limited coverage of the left ventricle of 73mm (35). Wide detector CT scanners may have a unique potential to overcome this by offering full coverage of the left ventricle without less than one heart beat, though feasibility studies have not been performed as yet.

Perfusion imaging has been facilitated by advances in CT technology

Technological advances over the past decade have equipped modern day cardiac CT scanners with a larger number of detector rows, faster gantry rotation speed, dual x-ray source and extended longitudinal coverage of the heart. While there is currently no one scanner which offers all of the above mentioned technology, these advances have enabled contemporary imaging to occur with superior temporal and spatial resolution and to require shorter scan and

breath hold times with reduced radiation exposure (Figure 4). These advances have been particularly advantageous for perfusion imaging (Table 3).

Wide-detector CT:

Traditional narrow detector (64 detector row) scanners typically offer 3 to 4 cm of longitudinal coverage and hence the assessment of the entire volume of the myocardium can only be completed after multiple gantry rotations over 3-4 heart beats. Myocardial contrast attenuation hence varies between the superior and inferior aspects of the heart due to the lack of temporal uniformity when image acquisition spans multiple cardiac cycles.

Wide detector scanners (256 and 320 detector row CT) offer extended longitudinal coverage of 12-16cm and hence the convenience of imaging the whole heart in one gantry rotation. This requires a shortened scan acquisition time of less than a heart beat (0.35ms) and a short patient breath-hold time of 1 to 2 seconds without the need for table movement. The shortened scan time required is an asset in myocardial perfusion imaging (CTP) as there is only a narrow time period during the early portion of first pass circulation when the iodinated contrast is predominantly intravascular and when the extravascular iodine concentration exceeds the intravascular iodine concentration (38). In addition to this, because the entire volume is imaged at the same time, there is temporal contrast distribution across the entire volume of myocardium which is ideal for myocardial perfusion assessment (39).

Dual source CT

During vasodilator stress imaging heart rates typically increases by 15-20 beats above the baseline heart rate at rest (27,40). For this reason, improvements in temporal resolution are most welcome in stress CT perfusion imaging and may assist in the minimisation of motion

artefacts encountered during image acquisition in patient with higher heart rates. Single x-ray source CT scanners offer a temporal resolution between 135 - 175ms. Accordingly images are optimised when acquired at heart rates of less than 65-70 beats per minute. Dual source CT (DSCT) scanners contain a single gantry with 2 x-ray tubes at an angle of 90 degrees and 2 corresponding x-ray detectors. This modification offers significant improvements in temporal resolution (75-83ms) which can more effectively freeze cardiac motion (41). The latest generation of DSCT also offers the ability to image in shuttle and high pitch spiral mode. During shuttle mode, images are acquired in 2 alternating table positions with the table shuttling back and forth to cover a 73mm anatomic volume (28,35). Alternatively prospective ECG-synchronised high pitch spiral mode allows acquisition of the entire myocardium within an ultrafast scan time of 0.25-0.27seconds during one end-diastolic phase due to the fast table movement, which will also ensure temporal contrast enhancement throughout the entire myocardium (42).

Dual source DSCT scanners have the added ability to operate in dual energy mode (DECT), in which one x-ray tube emits a high-energy spectra and the other a low-energy spectra during a single scan. DECT exploits the principle that tissues in the body and intravascular iodinated contrast have unique spectral characteristics when irradiated with x-rays of different energy levels. Upon processing separate image reconstructions of the high and low energy data, the iodine content within the myocardium is determined based upon the unique X-ray absorption characteristics of iodine at different kV levels(43). This provides colour-coded iodine concentration myocardial maps which offers additional information beyond the usual attenuation values and facilitates more specific tissue delineation which can be used for the detection of myocardial ischemia. DECT can be performed at a cost of increasing temporal resolution to 165ms.

2) Image Acquisition

CTCA/CTP protocol

Patient preparation

Before the scan, patients are advised to avoid caffeine which is a non-selective competitive adenosine receptor antagonist. Intravenous access is obtained in both ante-cubital veins for the administration of contrast and vasodilator stress agent (Figure 5). Given the importance of heart rate control to minimise motion artefacts, oral and or intravenous beta-blockers are administered to aim for a heart rate of <60 beats per minute prior to CT acquisition. While beta-blockers have been described to mask ischemia in exercise myocardial perfusion imaging, such an effect has not been observed on coronary flow reserve (44), vasodilator stress SPECT-MPI (45) or in CTP (27).

Image acquisition

Combined CTCA/ CTP imaging requires two separate CT scan acquisitions during rest and vasodilator stress. During the procedure, the patient is closely monitored for heart rate, blood pressure and ECG for ischemia. Both scans are performed using 50-75mLs of iodinated contrast (depending on patient size) aiming to achieve an iodine concentration of $\geq 320\text{mg I/mL}$ (40). The stress scan is performed during hyperaemia, typically attained after 3 mins of intravenous adenosine administration at 140mcg/kg/min . Real time bolus tracking is encouraged and CTP image acquisition is timed to occur in the late upslope, peak or very early downslope of the contrast bolus. In our institution this is timed to occur once the target threshold of 300HU is achieved in the descending aorta, with full volumetric imaging occurring 1-2 heart beats later (27,29). In 64-row detector scanners, there is a longer delay between bolus

tracking threshold detection and the onset of cardiac imaging, and triggering is recommended at a threshold of 100-180HU (40).

Depending on scanner type, images can be acquired using retrospective ECG gating or prospective ECG-triggering with multicycle acquisition and reconstruction. Prospective ECG gated image acquisition should ideally be timed to occur during mid to late diastole. George et al noted that the best motion free images were noted in mid to end diastole in 79% of cases, which on average occurred during 86% of the R-R interval (29,46). In our institution imaging is performed using the second generation 320-detector row CT, with a tube voltage of 100-120 kV(depending on weight), tube current adjusted to weight and a gantry rotation time of 270ms (temporal resolution =135ms). Prospective ECG gating targeting 70-90% of the R-R interval is used. Single heart beat scans are acquired if the heart rate is ≤ 65 bpm. If the heart rate is >65 bpm, a two- beat acquisition can be performed or alternatively a single beat acquisition can be performed upon widening the window to 30-80% of the R-R interval.

The protocol can be performed with a rest/ stress or a stress/rest protocol. The advantages and disadvantages of each imaging sequence is summarised in table 4. When the time interval between the 2 scans is short, the contrast used during the first acquisition may still be present in the myocardium at the time of the second acquisition, which may decrease the sensitivity for detection of infarcted and ischemic myocardium if the rest and stress scans respectively were performed as the second scan. The advantage of the stress followed by rest protocol is that the ability for the stress scan to detect ischemia is optimised. It will also allow the administration of nitrates for the subsequent rest scan, which may have otherwise been contraindicated if the rest scan was performed up front. On the contrary, initial rest-phase imaging more closely resembles clinical practice, where patients will only proceed to have CTP performed if a

coronary stenosis of at least moderate severity is identified on resting CTCA. In our institution, we most often use a rest/stress sequence (Figure 6). Contrast contamination can be avoided in our experience by leaving an interval of at least 20 minutes between the 2 scans to allow wash out of contrast from the myocardium (34,47).

3) Image Interpretation

Systematic approach for image interpretation

The use of a systematic approach for CTCA/CTP interpretation is vital in determining the diagnostic performance of the technique. A stepwise interpretation algorithm for CTCA/CTP interpretation has been described and outlined in Figure 7. The five main steps include 1) coronary CTCA interpretation, 2) CTP image reconstruction, 3) image quality assessment, 4) assessment of rest and stress CTP, and 5) correlation of coronary anatomy with perfusion defects.

Step 1: Coronary CTCA interpretation

Although blinded interpretations of coronary CTCA and myocardial CTP are often devised in research studies, the clinical use of myocardial CTP should involve a combined reading of coronary CTCA and myocardial CTP. Images of the coronary CTCA should be interpreted first. Once a potential physiologically significant stenosis is identified (in general, a stenosis $\geq 50\%$ severity), the role of myocardial CTP should be to assess the functional significance of a stenosis (Figure 8), 2) provide information about the presence of scar versus reversible perfusion abnormalities and 3) assess the burden of myocardial ischemia.

Step 2 and 3: CTP image reconstruction and image quality assessment

CTP images are reconstructed from multiple phases at 3% intervals and the cardiac phase with the least motion and artefacts is chosen for final interpretation as they can often mimic or hide perfusion abnormalities. The common causes of artefacts include motion, beam hardening, cone beam reconstruction, misalignment and poor signal to noise ratio.

Motion artefacts:

Cardiac and respiratory motion during image acquisition can result in ghosting of endocardial and epicardial edges and streaking and the presence of these features should mandate a search for alternative phases without motion (Figures 9 and 10). In our practice, the optimal phase chosen for interpretation is the one with the sharpest delineation of myocardial trabeculae.

Beam hardening artefacts:

Beam hardening occurs when x-rays pass through a radiodense or contrast filled structure with high attenuation leading to absorption of low-energy photons which results in a hypoattenuated shadowing artefact. The artefacts can occur in the context of bone (ribs, spine, sternum) or contrast enhanced LV cavity or descending aorta. The areas most likely to be affected are the basal inferior wall secondary to the contrast filled descending aorta, and the anterior wall, which may be affected by the LV cavity and overlying ribs (Figure 11). The artefacts are typically triangular, transmural and bear a hypoenhanced appearance emanating from a structure with high attenuation and for this reason do not necessarily follow the distribution of a coronary vascular bed. To minimise artefacts, CTP images are ideally reconstructed with a kernel that incorporates beam-hardening correction algorithms (FC03 in 320 detector CT (48)).

Cone beam artefacts

Cone beam artefacts typically occur in wide detector CT acquisitions and arise from the fact that the scanner isocentre and projections from the x-ray source on to the multiple detectors do

not lie in the same plane. The cone angle for a 320-detector CT is 15.2 degrees compared with 1.53 degrees for a 64-detector CT. The artefact presents as low and high attenuation bands in the image that most often affects the inferior wall and can mask or mimic hypoperfusion. The bands typically extend beyond the cardiac silhouette across the entire field of view (Figure 12). Reconstruction algorithms that involve organ-specific reconstruction, such as combination-weighted reconstruction algorithm can be effective at eliminating these artefacts (49).

Misalignment artefacts

Misalignment artefacts occur in images acquired using narrow detector CT scanners, when the entire volume of the heart is acquired over several heart beats, using helical or step and shoot protocol. Accordingly this may result in differences in contrast attenuation in the arterial bed and myocardium between the caudal and cranial portion of the z-axis, which may increase the difficulty in identifying perfusion defects.

Poor signal to noise ratio

High noise and poor signal levels may degrade the entire image. To avoid high image noise, tube and current voltages are typically chosen based on weight or body mass index.

Maintenance of adequate signal to noise ratio depends on the timely triggering of the scan to avoid premature or delayed triggering. Images are best timed to occur in the late upslope, peak or very early downslope of the contrast bolus. Premature triggering can lead to high amounts of contrast remaining in the right ventricle and inadequate contrast in the left heart and coronary circulation, which can lead to inadequate LV myocardial enhancement and significant beam hardening artefacts in the septal walls because of right ventricular contrast. Delayed triggering

can lead to inadequate contrast in the cardiac chambers and coronary circulation, leading to poor myocardial enhancement and loss of the presence of perfusion deficits secondary to diffusion (37).

Step 4: Assessment of resting and stress myocardial perfusion

Assessment of rest myocardial perfusion on CT

Areas of prior infarction and scar can be first identified on the rest images. Studies have demonstrated CT has a high sensitivity for identification of scar (50-52). Rest images should be examined for stigmata of prior myocardial infarction which may include the presence of subendocardial and transmural hypoattenuation, myocardial thinning, myocardial fat(53,54) and myocardial calcification, aneurysmal dilation and mural thrombus(40).

Methods to assess stress myocardial perfusion on CT

Recent guidelines for systematic myocardial perfusion assessment have detailed two main methods to assess myocardial perfusion including qualitative and quantitative assessment (40) (Figure 13).

Qualitative assessment of CT myocardial perfusion based on visual inspection remains the most commonly used approach in clinical studies (55) (Figure 13). Images are typically interpreted using axial, oblique and orthogonal views using dedicated computer interpretation software (Figure 14). This involves simultaneous visualization of rest and stress images for regions with hypo-enhanced myocardium compared with normally enhanced remote myocardium. Images are typically interpreted using a narrow window width and level setting

(W300/L150) and an averaged slice thickness of 3 to 5mm, which optimises the subtle differences in myocardial contrast attenuation (40). Using the standard American Heart Association 17-segment model with apex excluded (29,56) or 13 segment model (55), each myocardial segment is scored for the presence or absence of a perfusion defect and graded as transmural if it involved $\geq 50\%$ of myocardium or non-transmural. Defect reversibility is also graded (0=none, 1 = minimal, 2 = partial, 3 =complete) after comparing with the corresponding rest images. All defects should also be confirmed in at least 2 views, and should be examined in multiple phases to determine if it is a true perfusion defect or an artefact, with true perfusion defects typically present in all phases (Figure 15). Certain regions of myocardium can often be associated with lower enhancement and could mimic a perfusion defect. For example, the basal anteroseptum (membranous septum) is more fibrous in consistency which may result in the absence of photo counts on radionuclide perfusion imaging. The most distal part of the apex is also naturally thin and fibrous and should not be mistaken for prior infarction.

George et al described the use of a semi-automated quantitative interpretation (29,57). Using dedicated perfusion analysis computer software, the myocardium is equally divided into three myocardial layers – the subendocardium, mid-myocardium and subepicardium. The transmural perfusion ratio (TPR) is defined as the ratio of the averaged subendocardial attenuation of a specific segment of myocardium and the entire subepicardial attenuation (Figure 13). The TPR values for each segment can be displayed in a polar plot which allows colour coded visualisation of the variation of TPRs in each myocardial segment. In ischemic myocardium, contrast attenuation in the subendocardial layer has been demonstrated to be lower than in the subepicardial layer. Based on correlated studies using QCA (29) and invasive fractional flow reserve (FFR) (34) as reference standard, a threshold of <0.99 has been retrospectively derived to indicate abnormal perfusion. TPR is however not reliable in the presence of prior infarction

or significant artefacts which may confound the calculation of the TPR. In these settings visual based interpretation should be used to identify perfusion abnormalities.

Step 5: Correlating coronary anatomy with perfusion defects

As a final step to the analysis, the major epicardial vessels should be aligned with myocardial territories. Because of variation in coronary anatomy, the traditional assignment of vessels to myocardial segments can be enhanced by directly tracking vessels and their underlying territories on CT. It is recommended that the territory distal to an epicardial stenosis is tracked to assess for a perfusion defect occurring as a result of the stenosis. This will clarify for example when a perfusion defect in the apex is secondary to the a stenosis in a large wrap around left anterior descending artery or a lesion in a large posterior descending branch of the right coronary artery.

4) Feasibility and diagnostic performance

CT perfusion imaging has been evaluated in numerous preclinical, single-centre human studies and two multicentre studies to date (Table 5-6). The overall clinical per vessel sensitivity ranges between 71% to 97% and specificity 72% to 98% in native lesions as demonstrated using various scanner types compared with different reference standards. SPECT MPI has been chosen as the reference standard in a large number of studies (29,55,56) as it provides incremental prognostic value when used in conjunction with coronary angiography (20,58). Notably in multi-vessel disease its accuracy is limited as the technique relies on identifying relative differences in perfusion between adjacent myocardial territories (24), and separate analyses have been performed to avoid penalizing CTP for detecting multi-vessel disease (29). Accordingly recent studies have chosen modalities which are less influenced by the presence of ischemia in adjacent territories such as MRI-MPI (23,35,59,60) and fractional flow reserve (FFR) (23,27,28,34) as an appropriate reference standard for lesion specific ischemia.

Animal studies

The first animal studies illustrating feasibility of myocardial CTP were performed by George et al (33,37) in canine models (Table 5). These studies established the semiquantitative relationship between CT attenuation and blood flow based on microsphere myocardial blood flow. Mahnken et al subsequently illustrated the ability of dynamic quantitative whole heart perfusion imaging to detect the hemodynamic effect of high grade coronary artery stenosis in a canine model (61). Further work in a porcine model has confirmed that coronary flow reserve measurement by microsphere myocardial blood flow and myocardial CTP correlate well with each other (62).

Clinical studies:

Early fundamental studies:

In 2005, Kurata et al were the first to demonstrate a high agreement (83%) between rest and stress adenosine CTP and stress thallium SPECT- MPI in 12 patients with suspected CAD using 16-detector helical MDCT and retrospective ECG gating (63). Despite the favourable correlation, only 48% of coronary segments were evaluable under stress compared with 89% at rest, illustrating that myocardial CTP was not feasible at that time due to the limitations in the temporal resolution. In 2009, George et al reported the feasibility and accuracy of CTP on 40 patients with a history of abnormal SPECT-MPI who underwent adenosine stress CTP, using a 64 (n=24) and 256 (n=16) detector CT (29). When considering an abnormal TPR to be < 0.99 , combined use of CTCA / CTP was found to be 81% sensitive and 85% specific for identifying vessel territories with a $\geq 50\%$ stenosis on quantitative coronary angiography (QCA) which were associated with a perfusion defect on SPECT MPI. Similar results were reported by Blankstein et al using dual source CTP in 34 patients with a history of SPECT MPI and invasive angiography (56). The CTP protocol used included a rest, delayed phase acquisition

and stress MPI. Mean effective MDCT radiation exposure was 12.7mSv which was comparable to SPECT MPI alone. Combined CTCA and visual CTP assessment was demonstrated to have a per vessel sensitivity of 93% and specificity of 74% when compared against QCA and SPECT-MPI. Based on this cohort, Okada et al further evaluated the ability to grade the severity of perfusion defects on CT using a score (64). When applied to vessel territories at rest and stress, the score was found to compare favourably against qualitatively derived summed rest ($r=0.66$, $p<0.0001$) and stress scores ($r=0.56$ $p<0.0001$) derived from SPECT-MPI(65). Rocha-Filho demonstrated the incremental value of CTP in improving the accuracy of CTCA to detect a $\geq 50\%$ stenosis on QCA (66) resulting in an increase in sensitivity from 83% to 91%, specificity from 71% to 91%, and the area under the receiver operating curve from 0.77 to 0.90 ($p<0.005$). The addition of perfusion analysis also improved the reader confidence in stenosis classification and decreased interobserver variability (k value improved from 0.82 to 0.91).

64-detector row CTP:

The feasibility and performance of CTP using standard 64-row detector CT has been evaluated in a number of single centre studies. Cury et al demonstrated in the 36 patients, with history of abnormal SPECT-MPI, there was an moderate agreement between CTP and SPECT-MPI on a per patient analysis ($k = 0.53$), and CT-perfusion defects as qualitatively identified upon visual assessment had a sensitivity and specificity of 88% and 79% of identifying territories supplied by arteries with $\geq 50\%$ stenosis on QCA albeit requiring a high radiation dose of 14.7 – 16.8mSv (32). Bettencourt et al demonstrated in 101 patients with suspected CAD that combined CTCA/CTP detected $FFR \leq 0.8$ with 85% per vessel accuracy which was comparable with MRI-MPI (88%). The rest CTCA and stress CTP were performed using prospective ECG gating and retrospective ECG gating with tube modulation respectively with a resultant decreased radiation exposure in the combined protocol of 5.0 ± 0.96 mSv (23).

Dual Source CTP

The three techniques described to assess myocardial perfusion using DSCT include high pitch spiral mode CTP, dual energy CTP and dynamic CTP using shuttle mode.

Feuchtner et al described the feasibility in the use of high pitch prospectively ECG-synchronised spiral mode CTP using DSCT in 30 patients using MRI-MPI as reference standard(42) (Figure 16). The sensitivity and specificity was 96% and 95% respectively. The main advantage of this technique is the low associated radiation dose of <1mSv for the stress phase acquisition and 2.5mSv for the combined CTCA and CTP.

Initial investigations by Ruzsics et al demonstrated that dual energy computed tomography had a sensitivity and specificity of 96% and 95% in detecting fixed perfusion defect on SPECT(67). Furthermore DECT had a sensitivity of and specificity of 88% and 89% respectively for the detection of reversible perfusion defect, although the physiological mechanism behind such a concordance remains controversial as DECT was not performed under stress. S.Ko et al was among the first to describe the use of dual energy CTP in 41 patients with known CAD scheduled to undergo coronary angiography using MRI-MPI as reference standard (60). Stress DECT had a 91% and 72% per vessel sensitivity and specificity respectively. Using retrospective ECG-gating with tube modulation DECTP was achieved in 8.6mSv.

Bastarrika first described qualitative and quantitative assessment of MBF using dynamic CTP in ten patients using MRI-MPI as reference standard (35). The presence of perfusion defects upon visual assessment on dynamic CTP had a sensitivity and specificity of 86% and 98% respectively. Semiquantitative analysis demonstrated significant differences between ischemic and non ischemic myocardium using a CT-derived signal intensity upslope which was comparable with MRI-derived values ($p<0.05$). Overall a moderate correlation was observed between semi-quantitative CT measurements and absolute CT quantification of MBF for

hypoperfused and normal myocardial segments. Similar work was performed by Ho et al who performed dynamic CTP using shuttle mode on 128 DSCT, over a course of 30 seconds and demonstrated that the values for absolute myocardial blood flow was similar to that seen in SPECT MPI (36). The required radiation is 9mSv for the stress perfusion scan alone.

Bamberg et al extended upon this work by demonstrated that combined CTCA and dynamic CTP increased the accuracy of CTCA to predict hemodynamically significant coronary stenoses as assessed by FFR in a 36 patients with known and suspected CAD(28). The combination of a MBF below the threshold of 75ml/100mL/min together with a CTCA stenoses >50% were 93% sensitive and 87% specific for detecting stenoses with a FFR ≤ 0.75 . A notable limitation of this technique is the short z-axis of 73mm afforded by shuttle mode acquisition which results in incomplete coverage of the entire myocardium in one third of patients.

CTP using wide-detector coverage CT

B.Ko et al. reported the initial experience of CTP using 320-detector CT in 42 patients with known CAD considered for non-urgent coronary revascularisation using invasive FFR as reference standard (27). The median FFR value in territories with a perfusion defect on CTP was significantly lower than in territories with normal perfusion (FFR perfusion defect 0.72; normal myocardial 0.88, $p < 0.0001$) (Figure 17). CTP had a per-vessel territory sensitivity of 76%, specificity of 84%. Furthermore the combination of a $\geq 50\%$ stenosis on CTCA and perfusion defect on CTP was 98% specific for functionally significant stenoses as defined as FFR ≤ 0.8 , while the presence of <50% stenosis on CTCA and normal perfusion on CTP was 100% specific for exclusion of ischemia. This demonstrated the complimentary role of CTP with CTCA when the two modalities are concordant. Importantly, the mean radiation for CTP and combined CT was 5.3mSv and 11.3mSv respectively, which is much reduced from

previous retrospective ECG-gated studies. B.Ko et al subsequently applied the same study design in 40 patients with suspected coronary artery disease (34). The addition of visual CTP assessment was found to significantly improved the diagnostic accuracy of CTCA (receiver operating characteristic (ROC) area under the curve (AUC) 0.93 vs. 0.85, $p=0.0003$) and was superior to CTCA+TPR (0.93 vs. 0.79, $P=0.0003$). This improvement is largely explained by a significant improvement in specificity and positive predictive values to detect FFR significant ischemia, which is in agreement with the results reported by Bettencourt et al. using 64-detector row study (23) (Figure 18).

The use of CT perfusion has been also been studied in evaluation for stents. CTCA of coronary stents has been limited by non diagnostic studies caused by metallic stent material and coronary motion. Rief et al demonstrated in a cohort of 91 patients with stents that the addition of 320-CTP significantly improved diagnostic accuracy (ROC AUC 0.82 vs. 0.69, $P<0.001$) and non diagnostic rate when compared with CTCA alone using quantitative invasive coronary angiography as reference standard (68).

Multicentre studies

The recently published CORE 320 study is the first prospective multicentre study which included 381 patients with suspected or known CAD from 16 centres across the globe. The aim was to evaluate the diagnostic accuracy of CTCA/CTP in detecting myocardial ischemia defined as the presence of a 50% stenosis on ICA causing a perfusion defect on SPECT MPI. The patient based diagnostic accuracy defined by the area under the receiver operating characteristic curve (AUC) of CTCA/CTP for detecting or excluding myocardial ischemia was 0.87, which was statistically higher than when CTCA alone without CTP (0.82, $p\leq 0.001$) was used to predict ICA-SPECT MPI (Figure 19). The improved diagnostic accuracy was consistently reported in all 3 major epicardial vessels (ROC AUC LAD 0.89 vs. 0.84, $P\leq 0.001$,

LCx 0.86 vs. 0.81, $P=0.002$, RCA 0.86 vs. 0.81, $P=0.002$). The presence of stents, prior myocardial infarction likely influenced the diagnostic accuracy of the combined technique, and upon exclusion of patients with prior myocardial infarction and patients with known CAD, the diagnostic accuracy improved to 0.90 and 0.93 respectively (55) (Figure 19). Notably the Core 320 protocol acquired rest CTCA images before CTP. Due to the high sensitivity and negative predictive of CTCA for myocardial ischemia, the study findings support the use of stress CTP only in patients identified with intermediate degree of coronary stenosis within 1 hour of the initial CTCA diagnosis.

A multicentre multivendor study comparing regadenoson stress CTP and SPECT for visualisation of myocardial ischemia is underway (31). Patients with known or suspected CAD undergo both SPECT MPI and stress CTP which is performed using multivendor CT scanners including 64-CT, 128, 256 and 320 detector row CT. Ischemia is defined as the presence of reversible defects in ≥ 2 myocardial segments. Preliminary results based on 110 patients from 11 US sites using 6 different CT scanners demonstrate an overall agreement rate of 87% between CTP and SPECT MPI, with a sensitivity of 90% and specificity of 84% (69) using SPECT MPI as reference standard. Compared to CTCA alone, the diagnostic accuracy of combined CTCA/CTP was superior to CTCA alone (ROC AUC 0.85 vs. 0.69, $p<0.001$), which was driven primarily by improved specificity.

5. Limitations

The three main limitations related to CTP are artefacts, radiation exposure and contrast load. Artefacts can alter myocardial attenuation and interfere with myocardial perfusion analysis

which may result in the overestimation or underestimation of myocardial blood flow and perfusion defects. Artefacts include those associated with motion and beam hardening (Figures 10, 11, 15). Motion artefact can be minimised by the use of scanners with improved temporal resolution or wide-detector scanners with the capacity to perform multi-segmented acquisition and reconstruction. Routine beta-blocker administration is also important to blunt vasodilator-induced tachycardia. The development and use of various myocardial-specific beam hardening correction algorithms will help minimise these artefacts (70,71).

As stress CTP is performed as a separate additional scan to rest imaging, this increases the radiation exposure, contrast load and time required. On average the entire CT protocol can be performed in 43 mins and requires 120mls of contrast(34). For this reason it needs to be used with caution in patients with abnormal renal function.

Lastly the current evidence for CT perfusion is predominantly based on single centre studies with only one published multicentre study. The path of translation into clinical medicine will ultimately depend upon results of future multicentre studies, which will undoubtedly shape future guideline recommendations in the assessment of stable coronary artery disease. This will also determine the costs that future governments will spend to reimburse the technique.

(III) Non Invasive or Computed Tomography Fractional Flow Reserve

1) Derivation of FFR CT

In the last 5 years, advances in computational fluid dynamics have enabled calculation of coronary flow and pressure fields from anatomic image data(72). The focus of research has accordingly shifted to the application of this technique to CTCA images, which enables the

calculation of a non-invasive fractional flow reserve without additional imaging or medications. (Figure 20)(73,74).

A three dimensional model of the aortic root and coronary lumen is first constructed using CTCA images. Three key principles are then assumed and used to form boundary conditions: 1) Coronary supply meets myocardial demand at rest 2) The resistance of the microcirculation at rest is inversely but not linearly proportional to the size of the feeding vessel. 3) The microcirculation reacts predictably to maximal hyperaemic conditions in patients with normal coronary flow. (73). Blood is modelled as a Newtonian fluid with incompressible Navier-Stokes equations and upon application of the physical laws of fluid dynamics on a parallel supercomputer, three dimensional models representing the pressure and flow along all points of the arteries are generated during rest and simulated maximal hyperaemic conditions. Based on the approximated pressure measurements during hyperaemia, a non invasive FFR based on CT can be derived at any point in the coronary vascular tree (Figure 21).

2) Feasibility and Diagnostic Performance

FFR CT (HeartFlow Redwood City, CA, USA) is the first non invasive test to be validated from its inception by an outcome based gold standard- invasive FFR rather than one ultimately based on coronary stenosis measurement or non invasive functional testing. A brief summary of the FFR CT trials is summarized in Table 7. In the DISCOVER FLOW multicentre, prospective study, Koo et al demonstrated in a cohort of 103 patients (159 vessels) with suspected or known CAD that FFR CT, using a threshold of ≤ 0.8 , detected FFR-significant (≤ 0.8) stenoses with an accuracy, sensitivity and specificity 84%, 88% and 82% respectively (75). The corresponding values for CTCA alone were 59%, 91% and 40% respectively. Overall there was a good correlation between CT FFR and invasive FFR ($r=0.72$, $P<0.001$) and the

area under the ROC curve (AUC) was 0.90, which was significantly higher than CTCA alone (0.70, $p < 0.0001$).

In the subsequent prospective DeFACTO (Determination of Fractional Flow Reserve by Anatomic Computed Tomographic Angiography) multicentre international trial, Min et al reported the accuracy of FFR CT on a larger patient cohort (252 patients, 408 vessels) with suspected coronary artery disease. On a per-patient basis, FFR CT was superior to CTCA stenosis for diagnosis of ischemic lesions defined as invasive FFR ≤ 0.8 for accuracy (73% vs. 64%), sensitivity (90% vs. 84%), specificity (54% vs. 42%), PPV (67% vs. 61%) and NPV (84% vs. 72%) (76). It however did not meet the prespecified endpoint of a lower 95% confidence interval border for diagnostic accuracy of $>70\%$ (76). In patients with intermediate stenoses (30% to 70%), there was a more than 2-fold increase in sensitivity from 34% to 74% with the AUC increasing from 0.50 to 0.81 ($P = 0.0001$) (77).

The third multicentre study, An Analysis of Coronary Blood Flow Using CT Angiography: NeXt sSteps (NXT) Study was performed to characterise the diagnostic accuracy of FFR CT in patients (254 patients, 484 vessels) with suspected CAD after substantial improvements in FFR CT technology including updated proprietary software with quantitative image-quality analysis, improved image segmentation, refined physiologic models and increased automation(78). There was also strict adherence to pre-CTCA administration of beta blockers (99.6% of patients) and nitroglycerin (78% of patients) as per SCCT guidelines(79) which was aimed to optimise image quality and interpretability. Per patient sensitivity and specificity for FFR ≤ 0.8 was 86% and 79% respectively. The area under the ROC for FFR CT was 0.90, versus 0.81 for coronary CTCA ($P = 0.0008$).

Kim et al assessed the accuracy of treatment planning using computational model to simulate a virtual stent and to determine with computation of anticipated post stent FFR CT could predict

the success of stenting prior to the invasive procedure (80) (Figure 22). In a prospective cohort of 44 patients (48 lesions), the mean difference between FFR CT and FFR was 0.006 (95% limit of agreement -0.27 to 0.28) prior to intervention and 0.024 (-0.08 to 0.13) post intervention. Diagnostic accuracy to predict ischemia prior to stenting was 77% (sensitivity 85%, specificity 57%) and after stenting was 96% (sensitivity 100%, specificity 96%).

3) Strength and Limitations

The major advantage of FFR CT is that it can be performed without additional image reconstruction, acquisition or administration of medications. Hence it requires no additional contrast administration and radiation exposure.

It is also important to note that the correlation of FFRCT with FFR is good and promising yet not perfect. In the 3 multicentre trials, the Pearson correlation range between 0.63 to 0.82. Similarly the mean difference of invasive FFR and FFR CT range between 0.02 to 0.06 (± 0.07 to 0.12). This difference is particularly exaggerated in the extremes of FFRCT ischemia. This indicates over time, further technical refinements in CT-data processing, assumptions in FFRCT computation, imaging acquisition and scanner technology targeting at improvements in spatial and temporal resolution may play a role in optimisation of the technique.

The presence of artefacts on CTCA images including calcification, motion and misregistration may limit the accuracy of FFR CT. Thus adherence to protocols that ensure good quality data and facilitate accurate lumen boundary descriptions is essential(79). Furthermore the assumptions relating myocardial mass to total coronary flow, relative coronary microvascular resistance based on vessel size or reductions in resistance in response to adenosine induced hyperaemia may vary among patients, such as in populations with microvascular disease and

previous infarction. Finally no published data exist for FFR CT in the evaluation of in-stent restenosis or for coronary artery bypass grafts.

In its current form, FFR CT analyses requires 5 hours per examination (76) using a parallel computer, though iterative improvements in automation are expected to reduce processing time. Therefore it is a technology which requires offsite data analysis and attendant turnaround time.

Lastly it remains unknown whether an FFR CT value of ≤ 0.8 is sufficient to proceed with intervention or whether this may require further confirmation using invasive FFR. Further refinements in the FFR CT technology or new algorithms from other vendors may improve upon the current reported positive predictive value of 54-82%, which may render confirmation with invasive FFR unnecessary (75,76,78).

(IV) Transluminal attenuation gradient

1) Definition and derivation of TAG

Transluminal attenuation gradient (TAG) defined as the gradient of intraluminal radiological attenuation is a novel process that can evaluate the severity of coronary stenosis on CT (81). It has been found to correlate linearly with the degree of coronary artery diameter stenosis in ex vivo studies and discern normal and obstructive coronary arteries in in vivo animal and human studies (82,83) (Figure 23).

Using rest CTCA images, a centreline is determined for each major coronary artery and manually corrected if necessary. Cross sectional images perpendicular to the vessel centreline are then reconstructed. The contrast attenuation as determined by the mean Hounsfield units (HU) in a region of interest (ROI) positioned in the centre of the cross-sectional images is

recorded. The mean HU is measured at 5-10 mm intervals (81,84,85) from the ostium to a distal level where the cross-sectional area decreased to $<2.0\text{mm}^2$. TAG is defined as the change in HU per 10-mm length of coronary artery and is calculated as the linear regression coefficient between intraluminal attenuation (Hounsfield units) and axial distance typically taken from the ostium to the distal coronary vessel. (Figure 24)

2) Feasibility and Diagnostic Performance

Choi et al demonstrated, in a cohort of 127 patients (370 vessels) using 64-detector CT, that TAG64 was significantly lower in occluded vessels compared to those with lesions of 0-49% stenosis on QCA (-13.46 ± 9.59 HU/10mm vs. -2.37 ± 4.67 HU/10mm, $P < 0.001$) (81) (Figure 23). Importantly the addition of TAG64 to the interpretation of CTCA improved diagnostic accuracy for anatomical stenosis severity ($P = 0.001$), especially in vessels with calcified lesions and provided a net reclassification improvement of 0.095 (81).

CTCA with 64-detector row CT requires multiple gantry rotations which are combined for image interpretations, which will result in temporal misalignment between subvolumes for determination of coronary contrast opacification (Figure 25). TAG has hence been studied with 320-detector row CT (TAG320), which permits quantification of the spatial variation of Hounsfield Units over the coronary artery at a single point in time. Similar to the results of Choi et al, Steigner et al demonstrated in a 36 patients cohort that TAG320 measured in vessels with obstructive lesions were significantly different than in vessels considered normal by CTCA ($P < 0.021$) (82). There was no significant difference in gradients obtained in varied cardiac phases, heart rates and body mass index.

The diagnostic performance of TAG320 to predict the hemodynamic significance of coronary artery disease as assessed by invasive FFR has since been evaluated. Wong et al in a retrospective cohort of 53 stable CAD patients demonstrated that TAG assessed in FFR-

significant vessels was significantly lower than that found in FFR non-significant vessels (-21 vs. -11 HU/10mm, $p<0.001$) (84). Using a retrospectively determined TAG320 cut-off of -15.1 HU/10mm, TAG320 was reported to predict $FFR \leq 0.8$ with 77% sensitivity and 74% specificity. Importantly the AUC for the combined use of TAG320 and CCTCA was 0.88.

Over time studies which aim to compare the diagnostic accuracy of novel CT techniques in assessment of hemodynamically significant coronary stenoses across various patient populations will be important to characterise the strength and weaknesses of each technique. There are currently two studies which have compared the use of TAG with FFR CT and CT stress perfusion imaging (85,86).

Yoon et al compared the diagnostic performance of FFR CT and TAG for the diagnosis of lesion-specific ischemia in 53 consecutive patients who underwent 64-detector CTCA and FFR. The retrospectively determined optimal TAG64 cut-off to predict significant FFR of -6.4HU/10mm was much higher than that reported for 320CT(84). TAG64 was found to predict $FFR \leq 0.8$ with 37.5% sensitivity, 88% specificity. The diagnostic performance of FFR CT was found to be superior to TAG64 and CTCA stenosis (0.93 vs. 0.63, $P<0.001$ and 0.93 vs. 0.70, $P<0.001$ respectively).

Wong et al retrospectively compared the diagnostic accuracy of CTCA+ CTP with CTCA+ TAG320 in a 75 patient cohort using fractional flow reserve as reference standard (86). Due to presence of severe calcification in the TAG320 was assessable in 76% of vessels, compared with visual assessment using CTP in 97% of vessels. In the vessels where both techniques could be performed, their diagnostic accuracy was comparable for CTCA+ CTP and CTCA+ TAG320 (0.85 vs. 0.84, $P=0.98$). The diagnostic accuracy of combined CTCA, TAG320 and CTP, which defined positive vessels as the presence of $\geq 50\%$ stenosis on CTCA associated

with either a perfusion defect on CTP or significant TAG320, was superior to CTCA +TAG 320 or CTCA + CTP (AUC 0.91; P=0.01).

3) Strengths and limitations

TAG is a technique which has significant promise for the future. The advantage of the technique similar to FFR CT is that the information can be directly extracted from the resting CTCA images, without need for additional imaging, medications, radiation dose and contrast administration. Furthermore TAG evaluation does not require the need for a parallel supercomputer, but is rather performed using dedicated software at the point of care. In our experience, gradients can be derived within 10 minutes during CTCA interpretation. Future automated programs allowing instantaneous TAG320 analysis will be required for the methodology to be adopted in routine clinical practice.

Similar to FFR CT, the technique of TAG is highly dependent upon CTCA image quality and the presence of extensive luminal calcification can limit its application (86). TAG assessment has also been described to be not possible in short vessels and in the presence of significant intramyocardial bridging. This may limit the number of generated attenuation points which is required for TAG to be processed using the current available manual derivation method. Furthermore, the value of TAG remains unknown in vessels with smaller luminal sizes, major epicardial vessels with severe distal vessel or branch disease, intracoronary stents or coronary artery bypass graft surgery. While the feasibility and diagnostic accuracy of TAG320 to predict lesion specific ischemia in native coronary disease appears to be promising in single centre studies, this will require further validation in future large multicentre trials.

V Future directions

The ultimate one stop CT coronary anatomical and functional assessment technique will be one which not only improves the diagnostic performance of CTCA, but one which can be performed conveniently with minimal added radiation exposure, contrast and time. There are two important steps required in the future development of these techniques.

1) Large multicentre international registries and prospective studies aimed to evaluate the prognostic significance, cost effectiveness and downstream resource utilisation of the three novel CT techniques will be crucial in determining their adoption into guideline and reimbursement recommendations, as had been evident historically in the case of established imaging techniques including CT coronary angiography (87-89) and non-invasive stress imaging such as SPECT MPI and stress echocardiography (19,20,90,91). The ongoing multicentre “Prospective Longitudinal Trial of FFR CT: Outcome and Impact (PLATFORM) Clinical Trials.gov Identifier NCT01943903 will seek to compare the effect of FFR CT guided versus standard diagnostic evaluation on clinical outcomes, resource utilization, costs and quality of life in patients with suspected CAD. In CT perfusion, the final results of the Regadenoson Crossover (A Study of Regadenoson in Subjects Undergoing Stress Myocardial Perfusion Imaging (MPI) Using Multidetector Computed Tomography Compared to Single Photon Emission Computed Tomography (SPECT) trial will be important to assess the diagnostic performance of the technique when applied in a multivendor trial(31). Outcome studies are also underway including the PRECEPT registry, PeRfusion Evaluation by Computed tomography Procedures and Techniques is a multicentre international study which is similar in concept as the CONFIRM registry performed for CT coronary angiography(92). It currently has 14 centres participating worldwide and includes both retrospective and prospective registries of patients evaluated by CTP.

2) Technical refinements in CT scanner technology and image interpretation software remain much needed to improve the diagnostic performance and clinical application of these

techniques. In CT stress myocardial perfusion imaging, the focus of future research will aim to improve CT scanner temporal resolution to facilitate image acquisition at high heart rates during vasodilator induced hyperaemia and to evaluate dose reduction strategies to lower radiation exposure. Furthermore evaluation of dynamic wide detector CTP, refinements in dual energy CTP and improvements in artefact correction algorithms will be important areas of research to improve diagnostic performance and reader confidence to identify perfusion defects. In the case of FFR CT, there remains a need to refine automated image processing methods (75,76) and to shorten the currently required processing time of five hours (76). The current logistics requiring offsite data analysis and the attendant turnaround time (93) may limit the application of the technique especially in more symptomatic patients. Lastly in the case of TAG, the development and validation of a semi-automated program to provide instantaneous TAG analysis is much anticipated(84) and may shorten TAG processing time.

VI Conclusion

Cardiac CT has been rapidly broadened to study the functional significance of coronary artery disease, which may enable CT to act as a one stop shop to assess both coronary anatomy and associated lesion specific ischemia. The techniques of CT stress myocardial perfusion imaging and CT FFR are rapidly validated by multicentre studies and have been demonstrated to detect lesion specific ischemia with high accuracy, while TAG remains a promising technique based on single centre feasibility studies which can be conveniently derived at point of care. Future large multicentre international registries and prospective studies which aim to provide prognostic outcomes, downstream utilisation, and cost effectiveness of the three novel CT techniques will ultimately determine their transition into clinical practice.

Table 1:

Per vessel diagnostic performance of multidetector CT in prediction of hemodynamically significant stenoses compared with invasive fractional flow reserve

Author	Year	Pt no	Prevalence (per vessel %)	Sensitivity %	Specificity %	PPV %	NPV %
Meijboom et al. (18)	2008	79	18	94	48	49	93
Sarno et al. (94)	2009	81	31	79	64	46	88
Koo et al. (75)	2011	103	37	91	40	47	89
Bamberg et al. (28)	2011	33	30	100	51	47	100
B. Ko et al. (27)	2012	42	51	93	60	68	90
B. Ko et al. (34)	2012	40	33	95	68	77	93
Wong et al. (84)	2013	53	38	94	66	64	94
Bettencourt et al. (23)	2013	101	24	95	67	48	97
Norgaard et al. (78)	2014	254	21	83	60	33	92

Table 2

Per vessel diagnostic accuracy of non invasive stress imaging compared with invasive fractional flow reserve

Author	Year	Population	Patient Number	Sens / Spec (%)	PPV/ NPV (%)
SPECT MPI					
Hacker et al (26)	2005	Intermediate stenoses	50	80/76	92/53
Ragosta et al(95)	2007	Multivessel disease	36	59/85	86/57
Forster et al(96)	2009	Multivessel disease†	72	62/90	62/90
Melikian et al(24)	2010	Angiographic Multivessel disease	67	61/69	47/ 80
STRESS ECHOCARDIOGRAPHY					
Rieber et al(97)	2004	Intermediate lesions	48	67/77	Not reported
Jung et al(25)	2008	Intermediate lesions	70	56/67	48/74
MRI MPI					
Watkins et al. (22)	2009	Chest pain evaluation	103	91/94	91/94
Bettencourt et al. (23)	2013	Suspected coronary disease	101	79/93	79/93

Table 3

CT scanners used in myocardial perfusion imaging - strengths and limitations(Table adapted and revised from Ko BS, Cameron JD, De France T et al. CT stress myocardial perfusion imaging using multidetector CT- A review. Journal of Cardiovascular Computed Tomography 2011; 5:345-356 with permission from Elsevier)

	Scanner / Mode of acquisition	Strengths	Limitations
Narrow Detector CT	64 detector Helical CT	Readily available	Prolonged scan time / breath hold requirement Non-uniform temporal contrast enhancement in myocardium Slab misregistration artefacts High radiation dose
Wide detector CT	320 detector CT using prospective ECG gating	Short scan time Temporal contrast distribution in entire myocardium No slab misregistration artefacts Low radiation dose	Low Temporal resolution
Dual Source CT	1 st generation DSCT using retrospective ECG gating	High temporal resolution	Prolonged scan time Non –uniform temporal contrast enhancement in myocardium
	2 nd generation DSCT using prospective dynamic shuttle mode	High temporal resolution Real time imaging similar to MR perfusion	Limited z axis coverage (73cm) precluding assessment of some myocardial segments High radiation dose hence may not allow for complementary CTCA evaluation
	2 nd generation DSCT using prospective high pitch spiral mode	High temporal resolution Short scan time Temporal contrast distribution in entire heart volume No slab misregistration artefacts Low radiation dose	

	Dual Energy CT using 1 st or 2 nd generation DSCT	Offers additional information above contrast attenuation	Low temporal resolution
--	---	--	-------------------------

Table 4

CTCA/CTP imaging sequence. (Adapted from Techasith T. and Cury R. Stress Myocardial CT Perfusion. JACC: Cardiovascular Imaging 2011; 4:905-16 with permission from Elsevier) (47)

	Advantages	Disadvantages
Stress → Rest	<p>Better sensitivity during stress perfusion</p> <p>GTN can be given for CTA</p>	Contrast contamination of rest CTA (detect infarct)
Rest → Stress	<p>Able to stop protocol after CTA of min dsc</p> <p>Better sensitivity of rest scan (detect infarct)</p>	Late contrast enhancement during stress acquisition

Table 5.

Animal studies in CTP (Adapted from Techasith T. and Cury R. Stress Myocardial CT Perfusion. JACC: Cardiovascular Imaging 2011; 4:905-16 with permission from Elsevier)(47)

Table 3. Summary of Animal Studies Evaluating Myocardial Stress CTP					
First Author, Year (Ref. #)	Animal Model	CTP Protocol	Reference Standard	Results	Conclusion
George et al, 2006 (37)	Canine (n = 8) LAD stenosis	Adenosine stress 64-detector MDCT	Microsphere MBF	Linear relationship between myocardial signal density ratio (myocardial attenuation/left ventricular attenuation)	Adenosine stress MDCT provides semi-quantitative measurements of myocardial perfusion in canine model of LAD stenosis
George et al, 2007 (38)	Canine (n = 6) LAD stenosis	Adenosine stress 64-detector MDCT	Microsphere MBF	MDCT-derived MBF strongly correlated with microspheres ($R = 0.91$, $p < 0.0001$)	MDCT MBF measurements using upslope and model-based deconvolution methods correlate well with microsphere MBF
Christian et al, 2010 (39)	Porcine (n = 8)	Adenosine stress 64-detector MDCT	Microsphere MBF	Significant correlation between coronary flow reserve measurements between microsphere MBF and CT ($r = 0.94$, $p < 0.0001$)	CT first-pass myocardial perfusion imaging is feasible using a simple semi-quantitative analysis which provides reasonable estimates of MBF.
Mahnken et al, 2010 (43)	Porcine (n = 10) LAD stenosis Normal control	Adenosine stress 128-detector DSCT Dynamic scan mode	—	No significant differences in CT-based MBF between the stenotic and control group at rest; however, significant difference under adenosine stress ($p = 0.0024$).	DSCT permits quantitative whole heart perfusion imaging, with ability to show hemodynamic effect of high grade coronary artery stenosis.
DSCT = dual source computed tomography; LAD = left anterior descending coronary artery; MBF = myocardial blood flow; other abbreviations as in Tables 1 and 2.					

Table 6

Clinical studies in CTP (Table adapted and revised from Ko BS, Cameron JD, De France T et al. CT stress myocardial perfusion imaging using multidetector CT- A review. Journal of Cardiovascular Computed Tomography 2011; 5:345-356 with permission from Elsevier) (98)

	Scanner type	Imaging protocol	Reference standard	N°	Population	Radiation Dose (mSv) ¶	Per vessel territory Sensitivity (%)	Per vessel territory specificity (%)
Single centre studies								
Kurata et al (59)	16 detector	Retrospective	SPECT-MPI	12	Suspected CAD	Not reported	90	79
George et al (25)	64 & 256 detector	Retrospective	QCA/SPECT-MPI	27	Positive SPECT	16.8 (64 CT) 21.6 (256 CT) †	81	85
Blankstein et al (52)	64 DSCT	Retrospective	QCA/ SPECT-MPI	33	Recent SPECT and ICA	9.1	93	74
Rocha-Filho et al (62)	64 DSCT	Retrospective	QCA	34	Recent SPECT and ICA	9.8	91	91
Okada et al (61)	64 DSCT	Retrospective	SPECT-MPI	47	Recent SPECT and ICA or Positive SPECT	10.0	Pearson r = 0.56 (rest) and 0.66 (stress)	
Cury et al (28)	64 detector	Retrospective low resolution	QCA	26	Positive SPECT	3.4	88	79
Bastarrika et al (31)	128 DSCT	Dynamic shuttle mode	MRI-MPI	10	Known or suspected CAD	21.9	86 ‡	98 ‡
Ho et al (32)	128 DSCT	Dynamic shuttle mode	SPECT-MPI	35	Positive SPECT	9.2	83	78
Ko S. et al (56)	64 DSCT	Retrospective	MRI-MPI	41	Known CAD on CTCA scheduled for ICA	8.6	91	72
Tamarapoo et al (95)	64 DSCT	Retrospective	SPECT-MPI	30	Positive SPECT	15.7	92 ‡	86 ‡
Weininger et al (55)	128 DSCT	Dynamic shuttle mode (DSCT), Retrospective (DECT)	MRI-MPI	20	Acute CP w known / high likelihood CAD	12.8 (DSCT) 15.2 (DECT)	DSCT 86 ‡, DECT 93 ‡	DSCT 98 ‡, DECT 99 ‡
Feuchner et al (38)	128 DSCT	Prospective High pitch Spiral mode	MRI-MPI	30	Known and suspected CAD	0.9	96	95
Bainberg et al (24)	128 DSCT	Dynamic shuttle mode	FFR	36	Known and suspected CAD	10.0	93	87
Ko B. et al (23)	320 detector	Prospective	FFR	42	Known CAD awaiting revascularisation	5.3	76	84
George et al (53)	320 detector	Prospective	CCTCA / SPECT-MPI	50	Recent SPECT, known and suspected CAD	7.0	100	85
Nasis et al (96)	320 detector	Prospective	SPECT MPI	20	Suspected CAD	9.2	94	98
Bettencourt et al (19)	64 detector	Retrospective	FFR	101	Suspected CAD	5.0 (including rest CCTCA)	71	90
Rief et al (64)	320 detector	Prospective	QCA	91	Patients with previous coronary stenting	7.9	56	78

*Number of patients in the study who underwent both CTP and reference standard imaging modality

¶Radiation dose only for the stress perfusion acquisition, †Only the radiation dose for both stress and rest perfusion was reported, ‡ Per segment has been reported

£Assuming a summed stress score of 4 ^uper patient results available only

Table 7**Summary of FFR CT trials for per patient and per vessel detection of invasive FFR \leq 0.8**

	Koo et al Discover Flow (75)	Min et al. DeFACTO (76)	Norgaard et al NXT (78)
Year	2011	2012	2014
No of patients	103	252	251
Design	Multicentre (4 centres)	Multicentre (17 centres)	Multicentre (10 centres)
<i>Per patient</i>			
Sensitivity (%)	93	90	86
Specificity (%)	82	54	79
PPV (%)	85	67	65
NPV (%)	91	84	93
Accuracy (%)	81	73	81
<i>Per vessel</i>			
Sensitivity (%)	88	80	84
Specificity (%)	82	63	86
PPV (%)	74	56	61
NPV (%)	92	84	95
Accuracy (%)	84	69	86

Figure 1

The “one stop” anatomical and functional coronary assessment using cardiac CT.

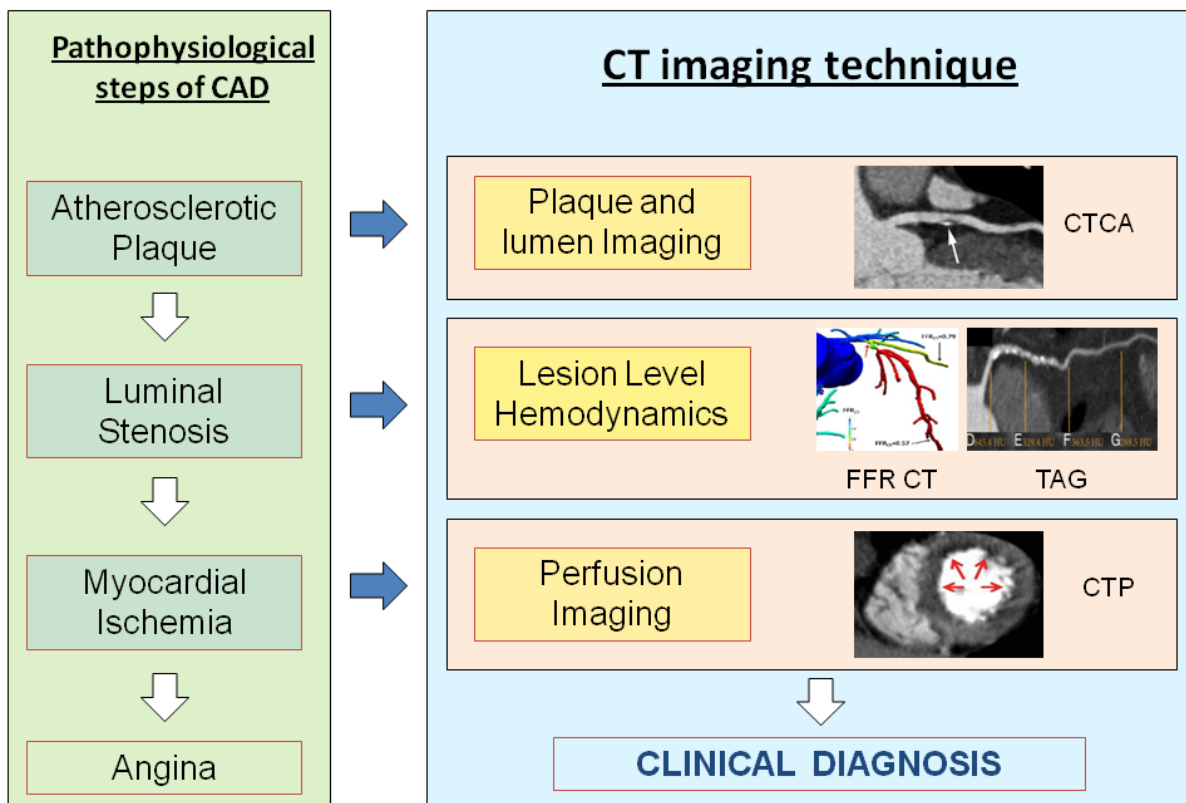


Figure 2

Perfusion defects demonstrated using a canine model of LAD ischemia.

Figure adapted from George RT, Silva C, Cordeiro MA, et al. Multidetector computed tomography myocardial perfusion imaging during adenosine stress. J Am Coll Cardiol 2006;48:153-60 with permission from Elsevier (33)

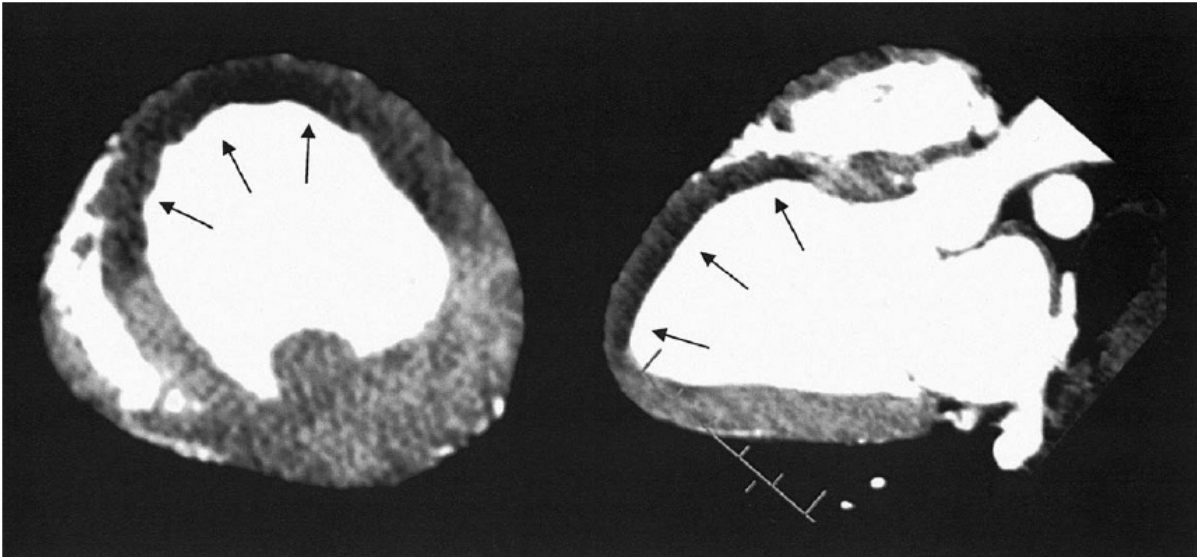


Figure 3 Dynamic and static CTP

This graph shows typical time-attenuation curve (TAC) acquired by dynamic CT myocardial perfusion imaging and 2 static images of the same mid ventricular slice, corresponding to different time points of CT MPI scan. The yellow curve (I) in the graph represents the TAC in normal tissue, the gray curve (II) that of ischemic myocardium. The red curve (III) is the TAC of the ascending aorta. Differences in enhancement between normal and ischemic myocardium are maximal during upslope of myocardial bolus passage. Image A was taken at the time point indicated by line (a) in the graph during contrast upslope. Image B was taken 6 seconds later as indicated by line (b) during early contrast downslope. The variation between the images emphasises that timing of CT image acquisition is paramount for MPI assessment. (Figure adapted from Ho KT, Chua KC, Klotz E, Panknin C. Stress and rest dynamic myocardial perfusion imaging by evaluation of complete time-attenuation curves with dual-source CT. JACC Cardiovasc Imaging 2010;3:811-20 with permission from Elsevier).

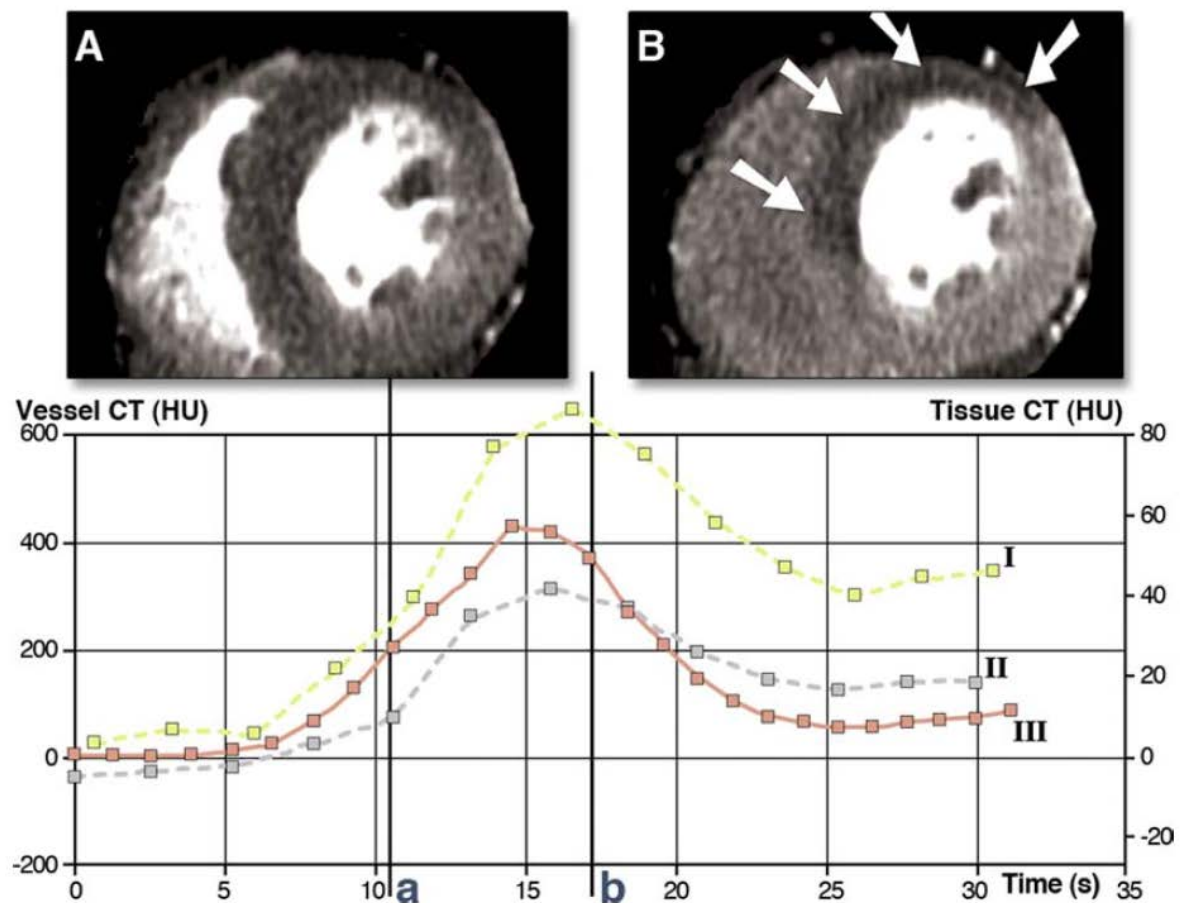


Figure 4

Advances in CT scanner technology

The advances which have been most advantageous for perfusion imaging include improvements in temporal resolution, increased longitudinal coverage and decreased scan time.

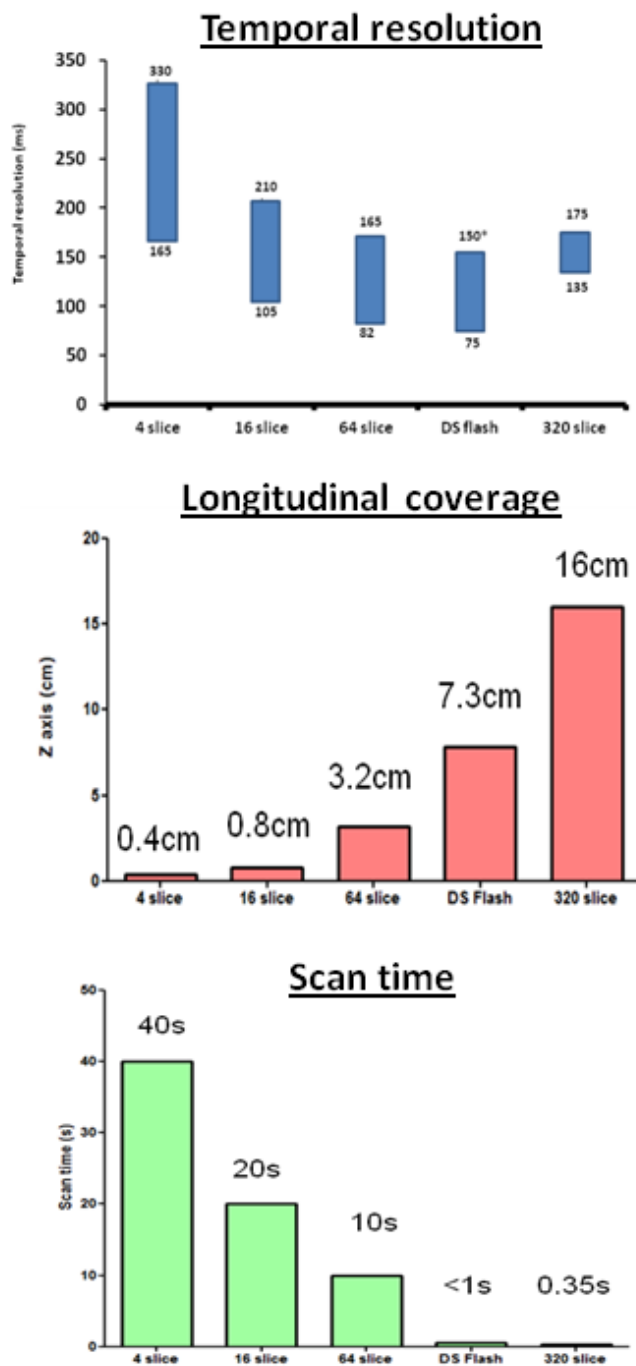


Figure 5

Image acquisition during CTCA/CTP.

Intravenous access is obtained in both antecubital veins for administration of adenosine and iodinated contrast. The average time taken for the combined rest CTCA + stress CTP protocol on the CT table is 43 minutes. (34)

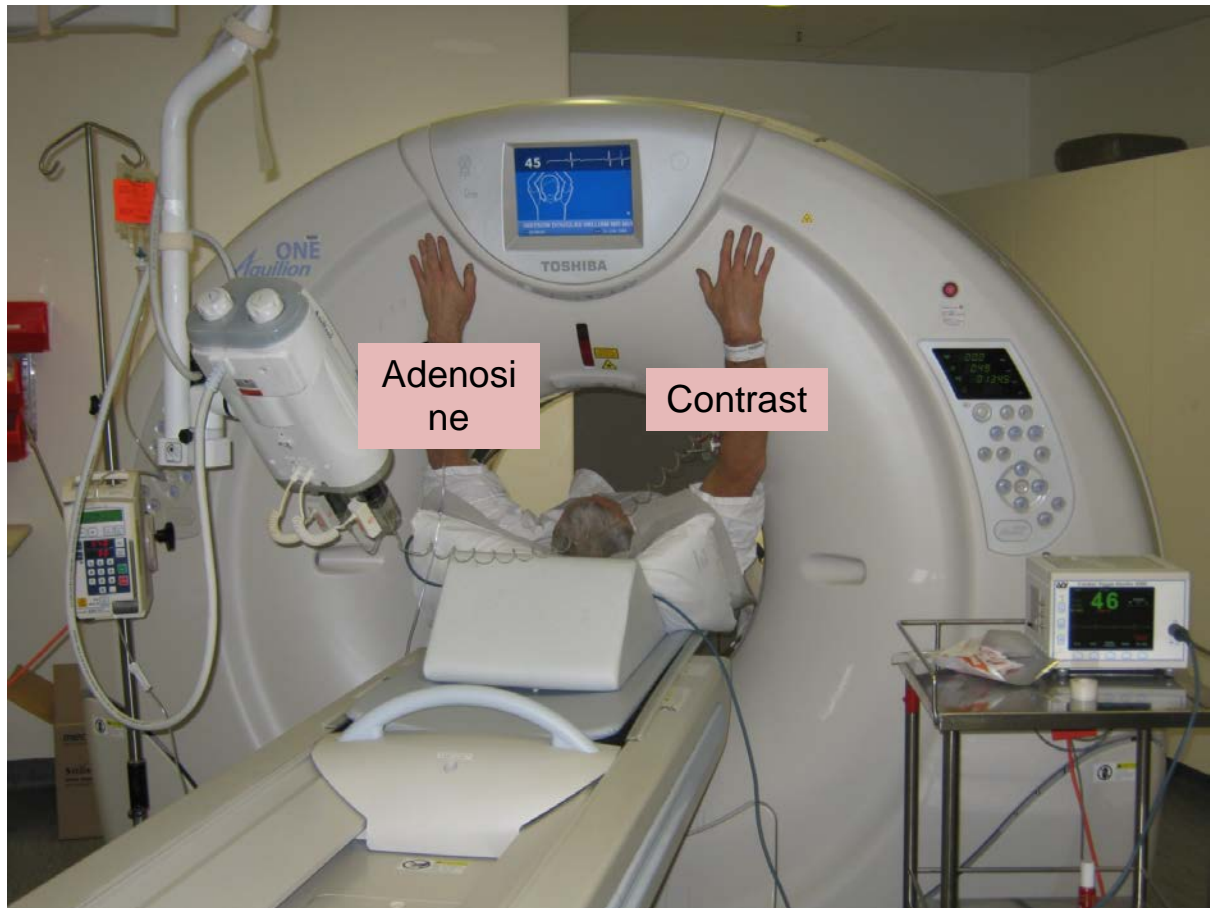


Figure 6:

CTCA/CTP imaging protocol using 320 detector CT

(Figure adapted from Ko BS, Cameron JD, De France T et al. CT stress myocardial perfusion imaging using multidetector CT- A review. Journal of Cardiovascular Computed Tomography 2011; 5:345-356 with permission from Elsevier (98))



Figure 7

Stepwise interpretation algorithm for CT-based anatomic/functional assessment This starts with evaluation of the coronary CTCA (step 1) followed by myocardial CTP image reconstruction (Step 2) , and evaluation of CTP image quality (Step 3). Serial rest and stress images are then analysed and compared for perfusion defects and other abnormalities associated with ischemia and infarction (Step 4). Finally theses analyses are correlated with anatomic localisation of coronary stenoses on CTCA (Step 5). Adapted from Mehra VC, Valdiviezo C, Arbab-Zadeh A, et al. A stepwise approach to the visual interpretation of CT-based myocardial perfusion. J Cardiovasc Comput Tomogr 2011;5:357-69 with permission from Elsevier

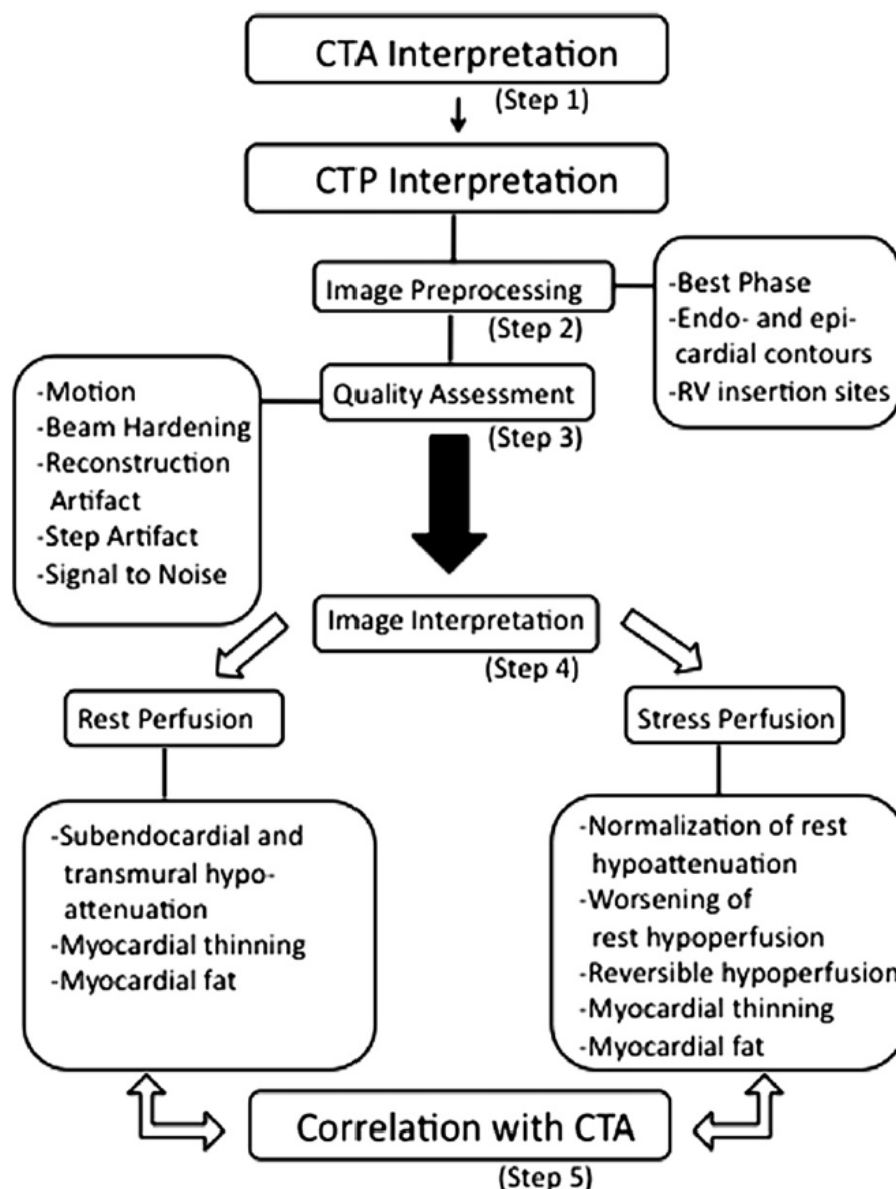


Figure 8

CTCA interpretation followed by CT perfusion assessment

The paradigm of CT-based cardiac risk assessment involves the use of CT angiography followed by CT perfusion if significant atherosclerosis is seen. As shown here, a moderate proximal left anterior descending stenosis is associated with an anterior and apical wall perfusion abnormality (arrows) just distal tot the stenosis seen on stress myocardial CTP. These perfusion defects are reversible because they are absent on rest myocardial CTP (B). Figure adapted from Mehra VC, Valdiviezo C, Arbab-Zadeh A, et al. A stepwise approach to the visual interpretation of CT-based myocardial perfusion. J Cardiovasc Comput Tomogr 2011;5:357-69.(40)

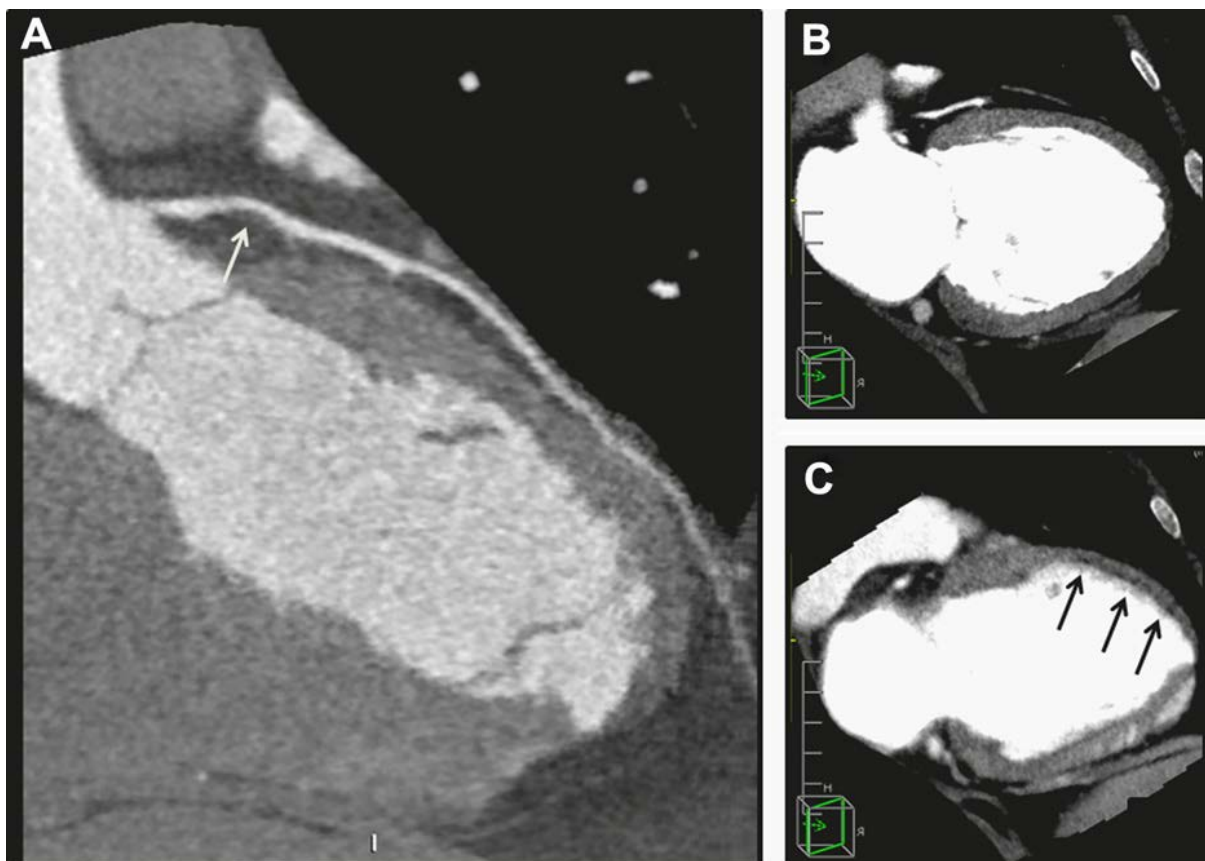


Figure 9

Example of images acquired during excessive cardiac motion.

Cardiac motion during image acquisition can lead to ghosting of endocardial and epicardial edges and streaking (arrows). Presence of these features can make detection of perfusion abnormalities difficult and should mandate a search for alternative phases without motion. Figure adapted from Mehra VC, Valdiviezo C, Arbab-Zadeh A, et al. A stepwise approach to the visual interpretation of CT-based myocardial perfusion. J Cardiovasc Comput Tomogr 2011;5:357-69.(40)

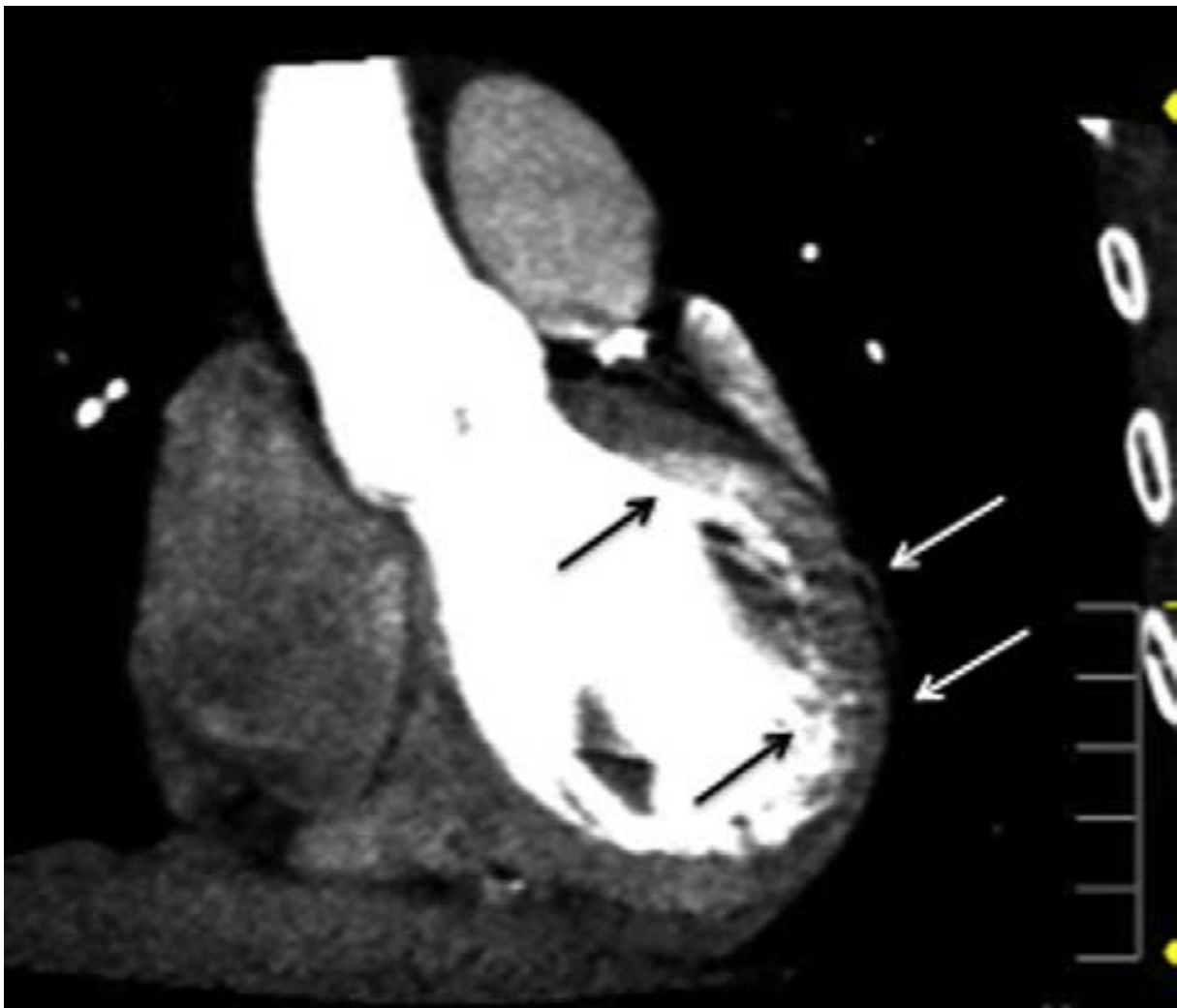


Figure 10

False positive perfusion defect due to motion artefact in a patient who underwent adenosine perfusion scanning with a heart rate of 90bpm.

CT perfusion imaging showed apparent perfusion defects in the anterolateral and inferior walls (black arrows). B) Invasive coronary angiography image of the left anterior descending artery and large diagonal branch (which supplied the anterolateral wall) demonstrated no hemodynamically significant stenoses (FFR 0.92 in diagonal branch). C Invasive coronary angiography image of the right coronary artery also revealed no significant stenosis to account for apparent inferior ischemia. Adapted from Nasis A, Seneviratne S, DeFrance T. Advances in Contrast-Enhanced Cardiovascular CT for the Evaluation of Myocardial Perfusion. Curr Cardiovasc Imaging Rep 2010;3:372-381 (99)

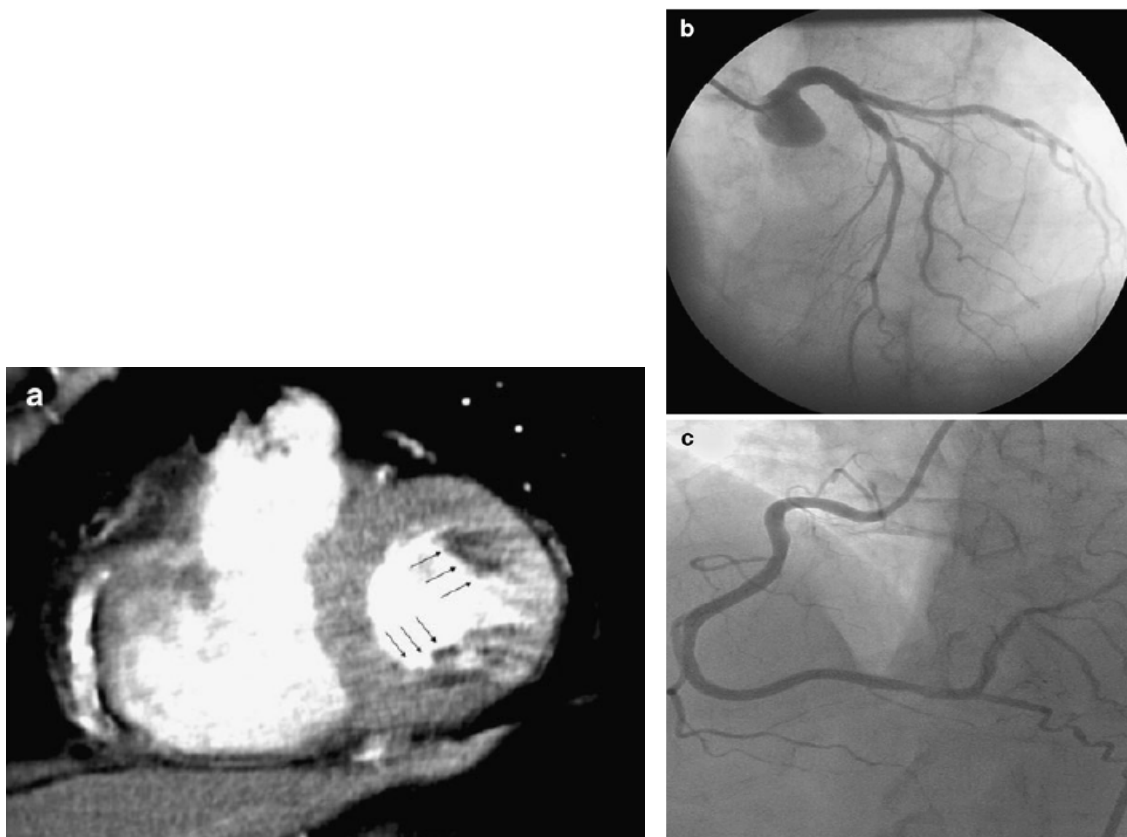


Figure 11

Beam hardening artefact correction algorithm. Beam hardening artefacts appear as areas of hypoattenuation most commonly in the basal inferior wall. A) This wall is particularly vulnerable to this artefact because of its location being between the contrast-rich left ventricular cavity and descending aorta. B) Reconstruction kernels that implement beam-hardening correction algorithm are effective in overcoming this artefact. Figure adapted from Mehra VC, Valdiviezo C, Arbab-Zadeh A, et al. A stepwise approach to the visual interpretation of CT-based myocardial perfusion. J Cardiovasc Comput Tomogr 2011;5:357-69 (40)

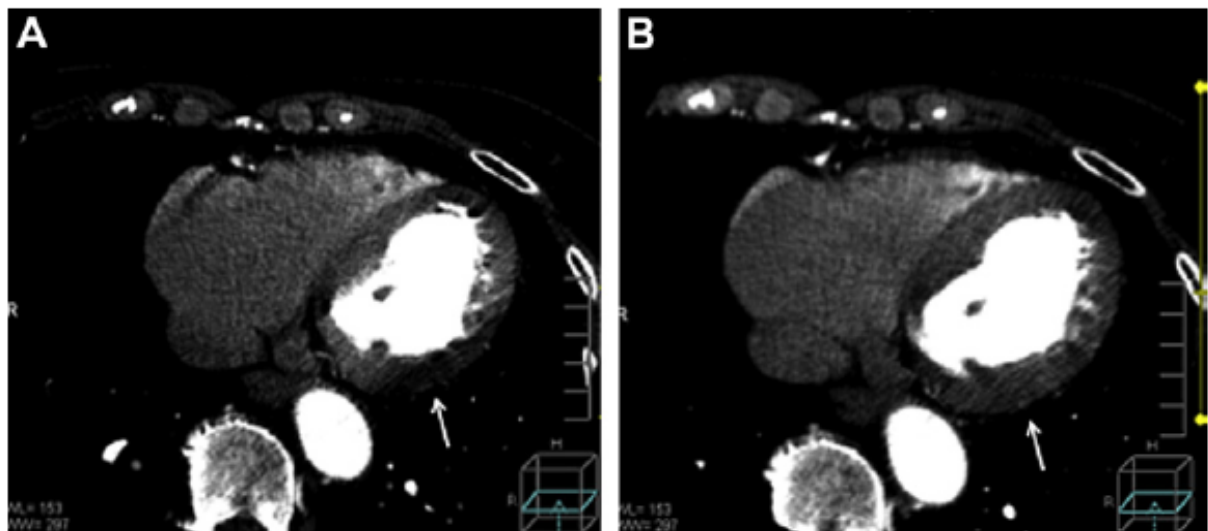


Figure 12

Cone beam artefacts

They are seen here as a continuous linear hyperenhanced artefact in the more caudal margins of the image. Figure adapted from Mehra VC, Valdiviezo C, Arbab-Zadeh A, et al. A stepwise approach to the visual interpretation of CT-based myocardial perfusion. *J Cardiovasc Comput Tomogr* 2011;5:357-69(40)

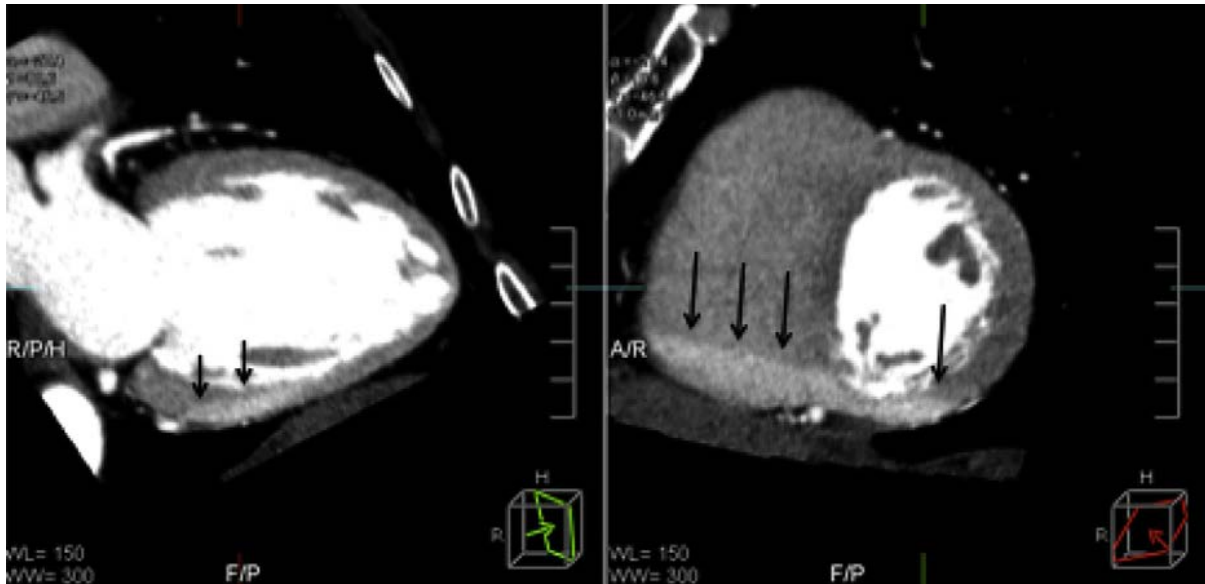
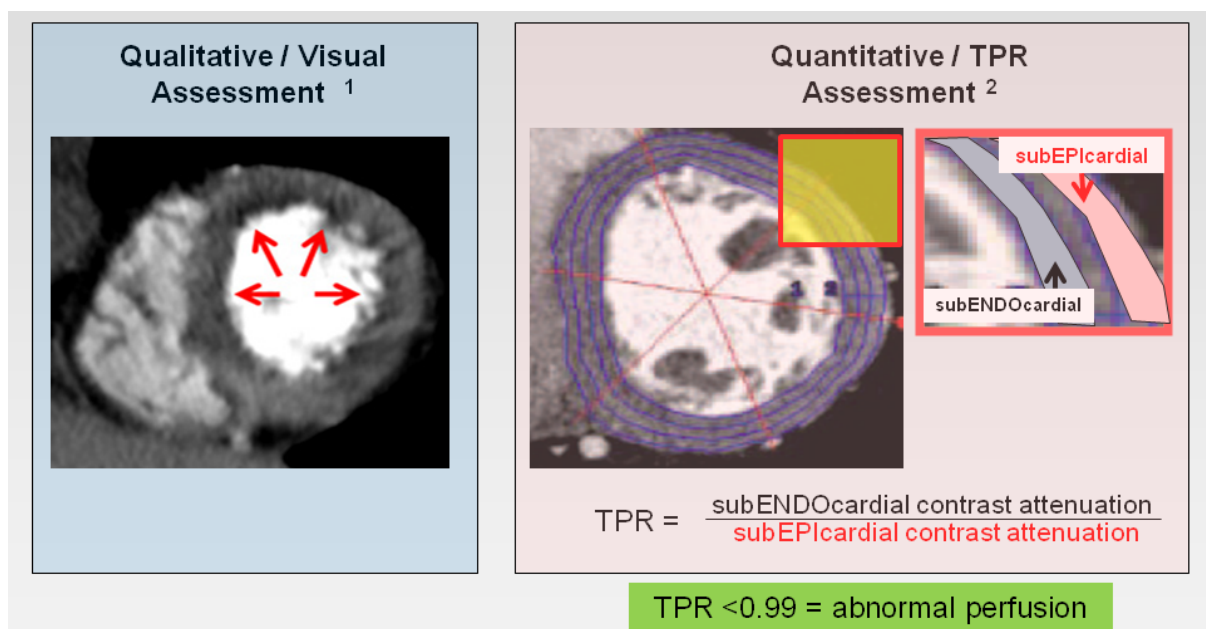


Figure 13

Qualitative and quantitative CTP interpretation on static CTP

Qualitative assessment is performed with Visual inspection 1 Figure adapted from Ko BS, Cameron JD, De France T et al. CT stress myocardial perfusion imaging using multidetector CT- A review. Journal of Cardiovascular Computed Tomography 2011; 5:345-356 with permission from Elsevier. Quantitative assessment is performed using transmural perfusion ratio (TPR) 2. Figure adapted from George RT, Arbab-Zadeh A, Miller JM, et al. Adenosine stress 64- and 256-row detector computed tomography angiography and perfusion imaging: a pilot study evaluating the transmural extent of perfusion abnormalities to predict atherosclerosis causing myocardial ischemia. Circ Cardiovasc Imaging 2009;2:174-82.with permission from AHA Journals.



Dedicated CTP interpretation software-

[illegible]

Figure 15

Multiple phases are examined to determine a true defect vs. artefact.

A true defect is typically present in all phases. This is a case of a seventy-eight year old lady who was investigated for chest pain on background of type 2 diabetes. Fractional flow reserve was not significant in all three major epicardial vessels. On CTP, the mid axial cuts demonstrate apparent perfusion abnormalities in the anterolateral wall in phase 74 (red arrows), not present in phase 83. Similarly apparent perfusion abnormalities are present in the inferoseptal wall in phase 95 (blue arrows) yet absent in phase 74. Shifting perfusion abnormalities which are not seen on all phases are secondary to artefacts. In this case, this may be secondary to contrast enhancement of the left ventricle or motion. The heart rate during image acquisition was 80bpm. Figure adapted from Ko BS, Cameron JD, Meredith IT, et al. Computed tomography stress myocardial perfusion imaging in patients considered for revascularization: a comparison with fractional flow reserve. Eur Heart J 2012;33:67-77 with permission from Oxford Press (27).

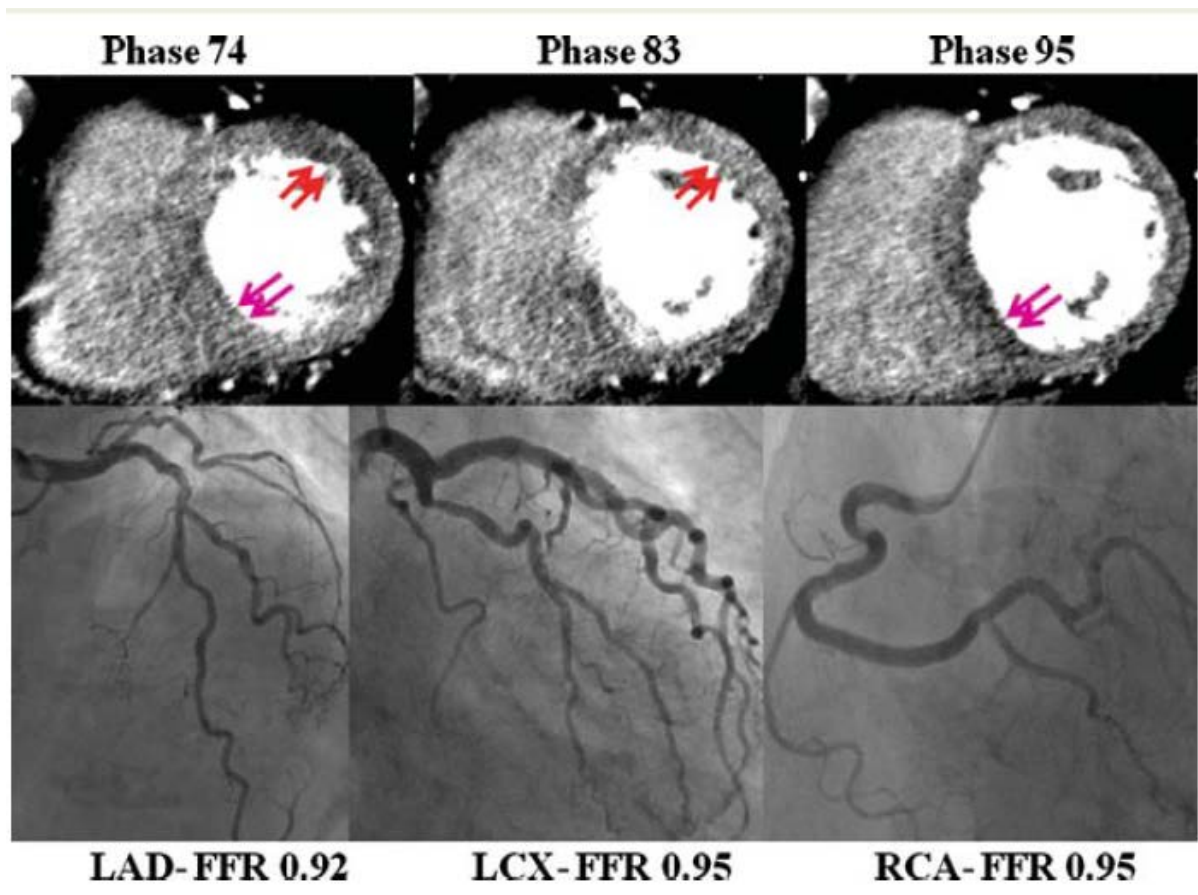


Figure 16

CT myocardial perfusion imaging using adenosine stress high pitch 128-slice dual source CT.

Reversible myocardial ischemia in the inferior and inferoseptal wall demonstrated in stress CTP (A, B) and MRI MPI (C, D). The RCA had a 60-70% stenosis proximally (E). There is also a reversible defect in the inferolateral wall on both CT and MRI, which correlates to a subtotal occlusion of the LCx (E). Adapted from Feuchtner G, Goetti R, Plass A, et al. Adenosine stress high-pitch 128-slice dual-source myocardial computed tomography perfusion for imaging of reversible myocardial ischemia: comparison with magnetic resonance imaging. *Circ Cardiovasc Imaging* 2011;4:540-9 with permission from AHA journals.

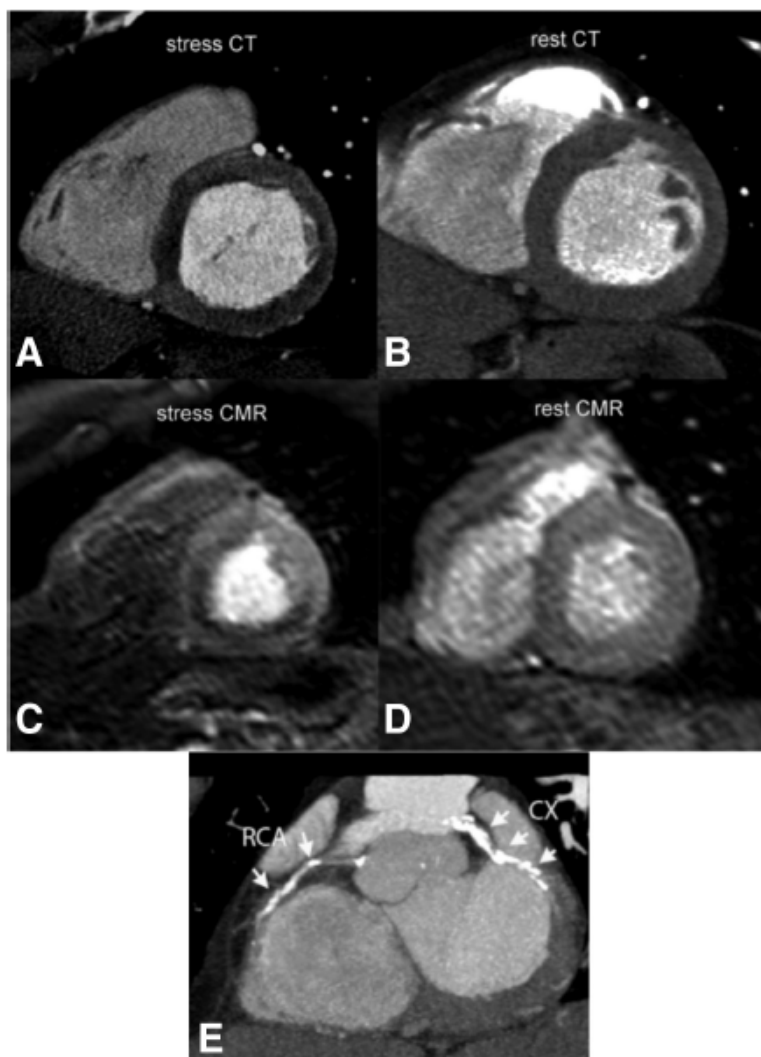


Figure 17

Relationship between CT myocardial perfusion imaging vs. fractional flow reserve.

In the studied 86 vessel territories, The median FFR is marked with a black line; 0.72 with perfusion defect vs. 0.88 with normal myocardial perfusion ($P < 0.0001$). Figure adapted from Ko BS, Cameron JD, Meredith IT, et al. Computed tomography stress myocardial perfusion imaging in patients considered for revascularization: a comparison with fractional flow reserve. Eur Heart J 2012;33:67-77 with permission from Oxford Press.(27)

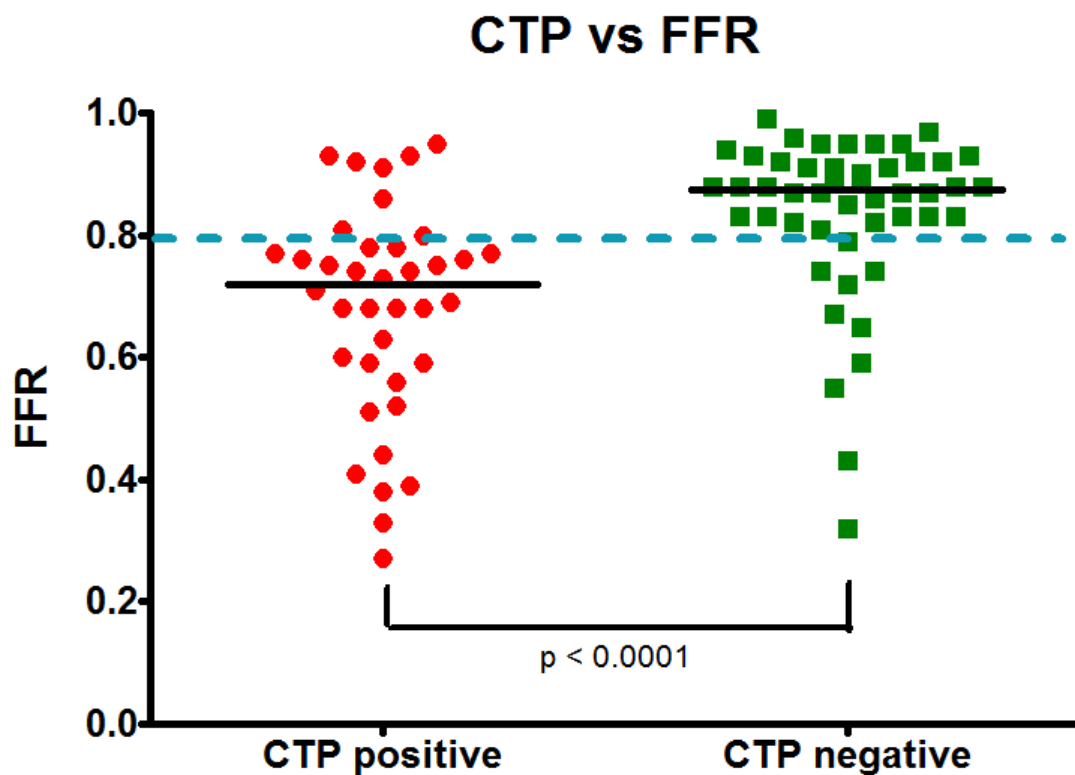


Figure 18

Incremental per vessel accuracy of 64 detector-row and 320 detector row CTCA/CTP when compared with CTCA alone to detect invasive FFR ≤ 0.8 .

Figure information obtained from Bettencourt N, Chiribiri A, Schuster A, et al. Direct comparison of cardiac magnetic resonance and multidetector computed tomography stress-rest perfusion imaging for detection of coronary artery disease. J Am Coll Cardiol 2013;61:1099-107 and Ko BS, Cameron JD, Leung M, et al. Combined CT Coronary Angiography and Stress Myocardial Perfusion Imaging for Hemodynamically Significant Stenoses in Patients With Suspected Coronary Artery Disease: A Comparison With Fractional Flow Reserve. JACC Cardiovasc Imaging 2012;5:1097-111. Both with permission from Elsevier. (23,34)

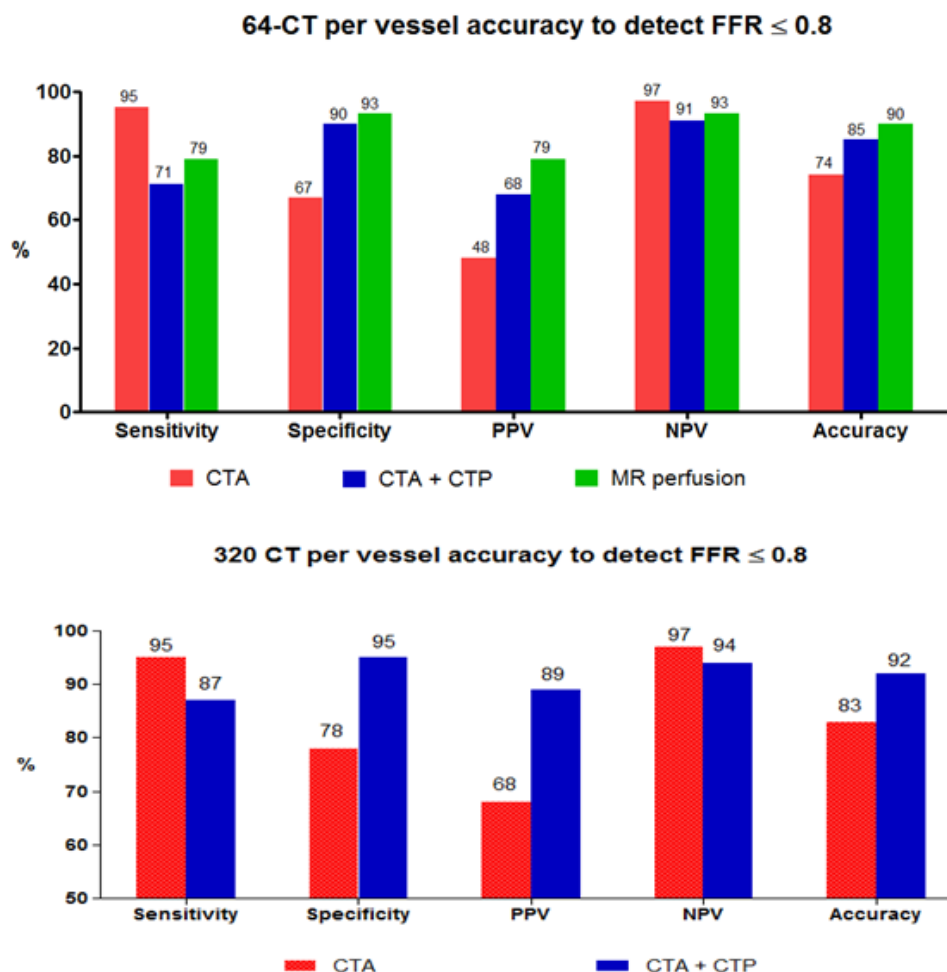


Figure 19

Receiver operating characteristic (ROC) curve and corresponding area under the curve describing the diagnostic performance of combined CTCA and CTP to identify a $\geq 50\%$ stenosis and a corresponding myocardial perfusion defect using the reference standard of invasive coronary angiography (ICA) and single photon emission computed tomography myocardial perfusion imaging (SPECT MPI) at a patient level. Figure adapted from Rochitte CE, George RT, Chen MY, et al. Computed tomography angiography and perfusion to assess coronary artery stenosis causing perfusion defects by single photon emission computed tomography: the CORE320 study. Eur Heart J 2013 with permission from Oxford Press (55)

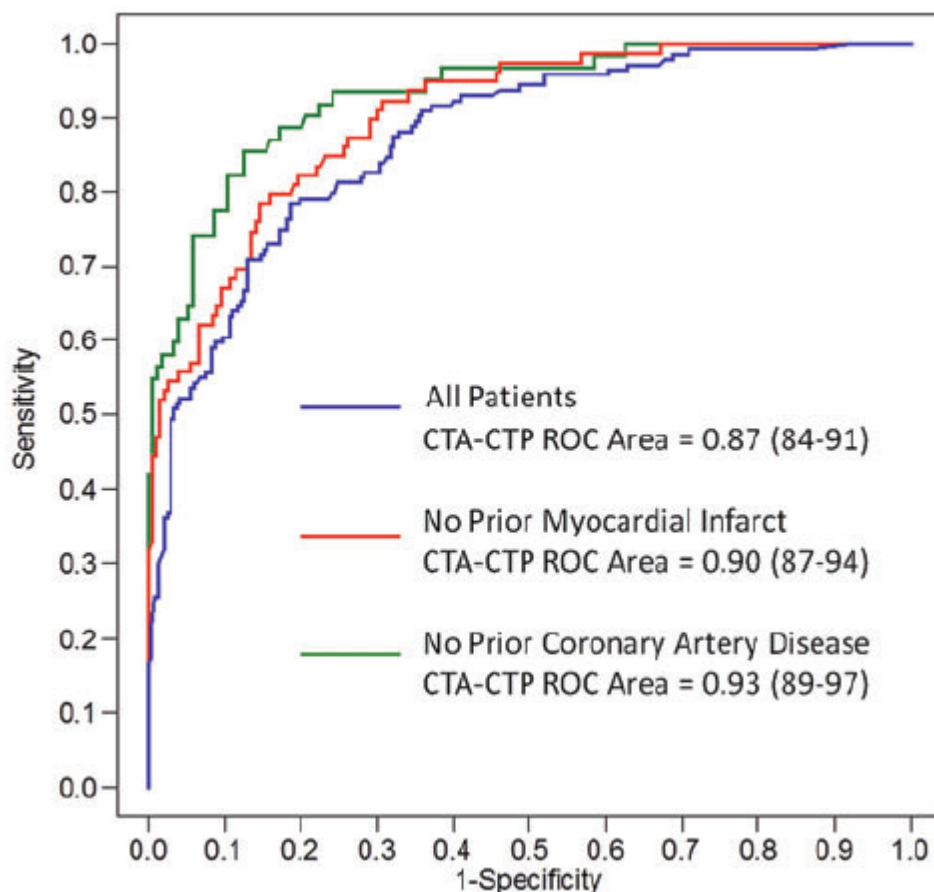


Figure 20

Technique in derivation of FFR_{CT}

Step 1: A three dimensional model of the aortic root and coronary lumen is constructed using CTCA images. Step 2: Assumptions are made regarding the properties of blood, basal total coronary flow, mean aortic pressure and total resistance coronary resistance. Step 3: Using a supercomputer, three dimensional models throughout the cardiac cycle representing the pressure and flow along all points of the arteries are generated during rest and simulated maximal hyperaemic conditions. Step 4: Based on the approximated pressure measurements, a non invasive FFR based on CT is derived. Figure Adapted from Koo BK, Erglis A, Doh JH, et al. Diagnosis of ischemia-causing coronary stenoses by non-invasive fractional flow reserve computed from coronary computed tomographic angiograms. Results from the prospective multicenter DISCOVER-FLOW (Diagnosis of Ischemia-Causing Stenoses Obtained Via Non-invasive Fractional Flow Reserve) study. J Am Coll Cardiol 2011; 58:1989-97 and Min JK, Berman DS, Budoff MJ, et al. Rationale and design of the DeFACTO (Determination of Fractional Flow Reserve by Anatomic Computed Tomographic AngiOgraphy) study. J Cardiovasc Comput Tomogr 2011;5:301-9 with permission from Elsevier.(74,75)

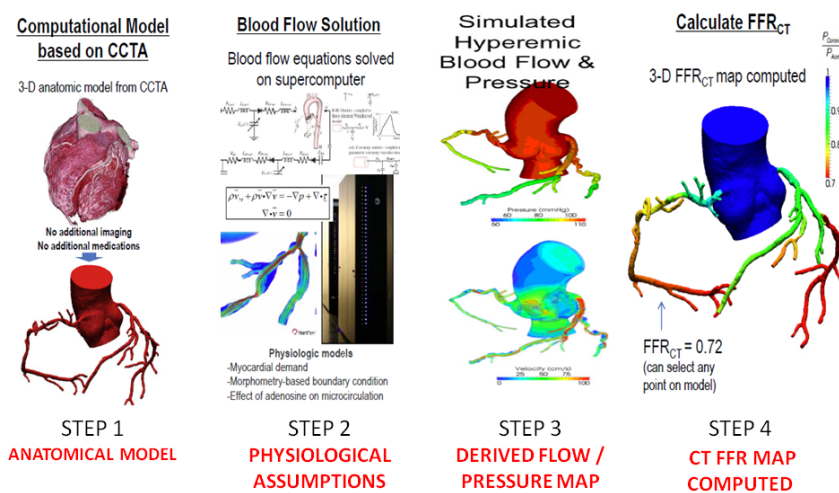


Figure 21

FFR CT results for 66 year old man with multivessel CAD and lesion specific ischemia.

A) CTCA demonstrating stenosis in the LAD. B) FFR CT demonstrates ischemia in the LAD with a computed value of 0.64. C) ICA with FFR also demonstrates ischemia in the LAD with a measured value of 0.72. D) CTCA demonstrates stenosis in the LCx. E) FFR CT demonstrates ischemia in the LCx with a computed value of 0.61. F) ICA with FFR also demonstrates ischemia in the LCx with a measured value of 0.52. Figure adapted from Taylor CA, Fonte TA, Min JK. Computational fluid dynamics applied to cardiac computed tomography for noninvasive quantification of fractional flow reserve: scientific basis. *J Am Coll Cardiol* 2013;61:2233-41 with permission from Elsevier. (73)

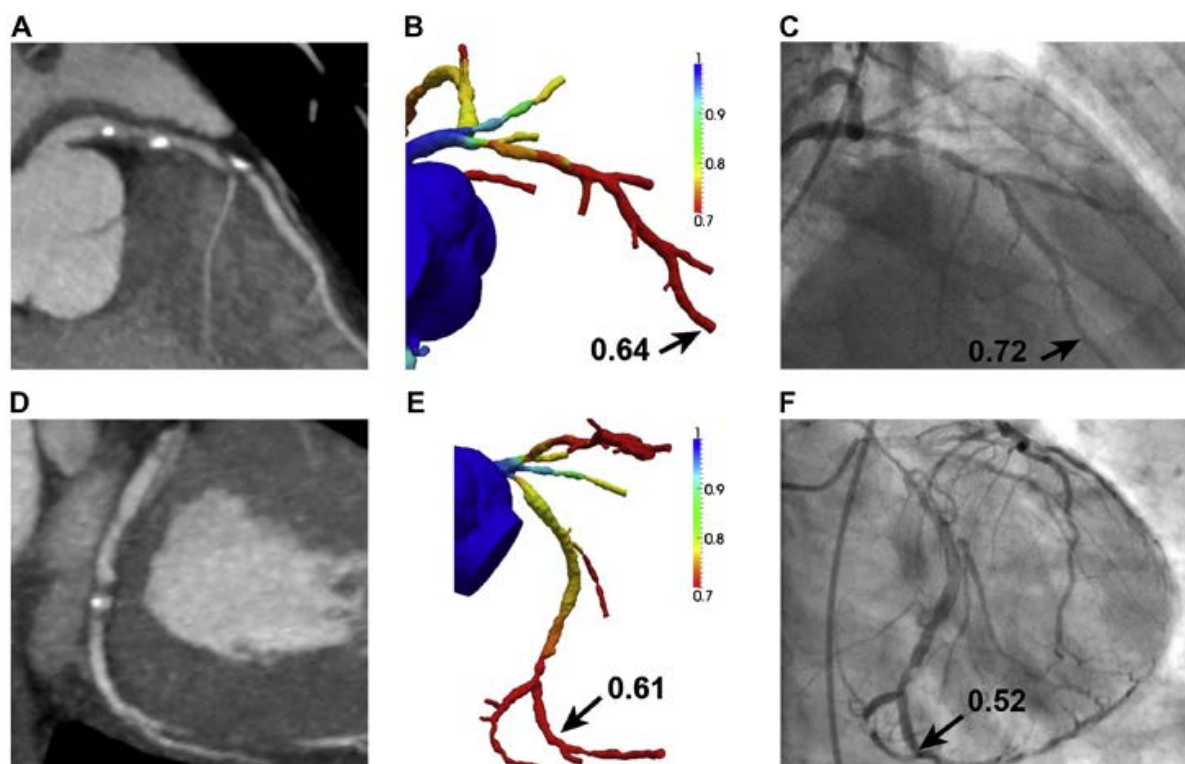


Figure 22

Comparison of FFR CT results before and after simulated PCI with stent implantation.

Figure adapted from Taylor CA, Fonte TA, Min JK. Computational fluid dynamics applied to cardiac computed tomography for noninvasive quantification of fractional flow reserve: scientific basis. J Am Coll Cardiol 2013;61:2233-41 with permission from Elsevier. (73)

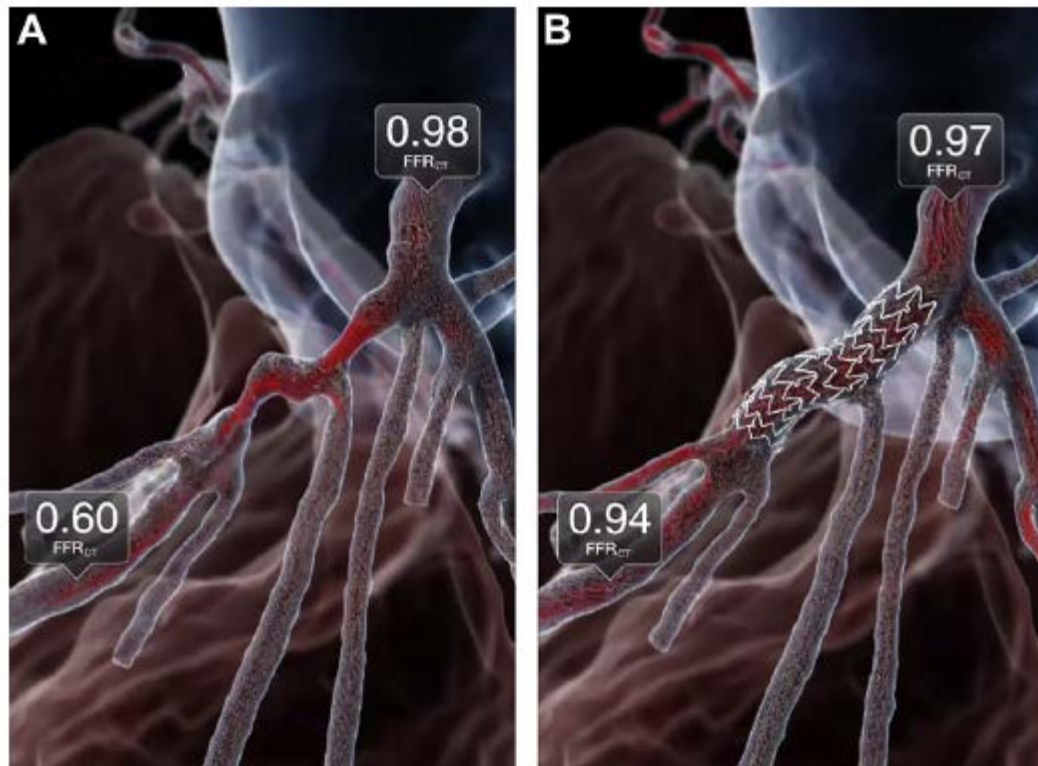


Figure 23

Transluminal attenuation gradient versus diameter stenosis (DS) by coronary CTCA.

DS 0%-49%, -1.91 ± 4.25 HU/10mm; DS 50%-69%, -3.54 ± 4.43 ; DS 70%-99% -10.55 ± 7.20 ; DS 100% -13.37 ± 9.81 ($p < 0.0001$ by ANOVA analysis, $p < 0.05$ by t test between 2 groups).

Figure adapted from Choi JH, Min JK, Labounty TM, et al. Intracoronary transluminal attenuation gradient in coronary CT angiography for determining coronary artery stenosis.

JACC Cardiovasc Imaging 2011;4:1149-57 with permission from Elsevier.(81)

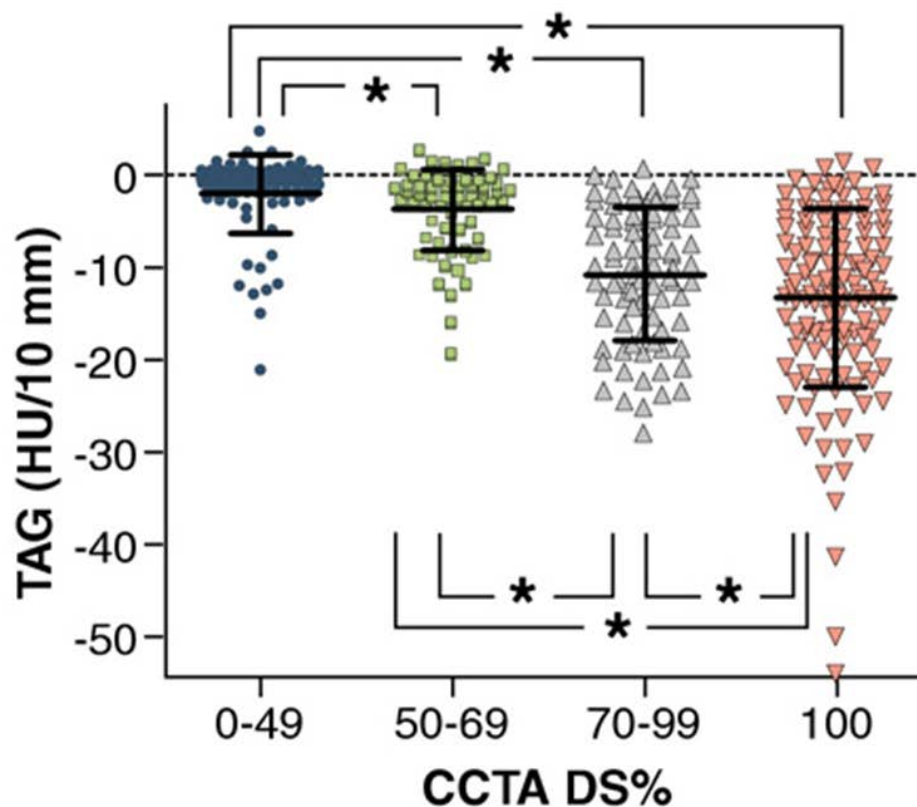


Figure 24

Transluminal Attenuation Gradient.

Left anterior descending artery with significant obstructive plaque burden imaged by CCTCA. Axial and representative cross-sectional views with corresponding luminal attenuation (HU) of CCTCA. Black square dots represent 5mm intervals at which intraluminal attenuation (HU) was measured. TAG was -38.3, and the FFR was 0.76. Figure adapted from Wong DT, Ko BS, Cameron JD, et al. Transluminal Attenuation Gradient in Coronary Computed Tomography Angiography Is a Novel Noninvasive Approach to the Identification of Functionally Significant Coronary Artery Stenosis: A Comparison With Fractional Flow Reserve. Journal of the American College of Cardiology 2013 with permission from Elsevier. (84)

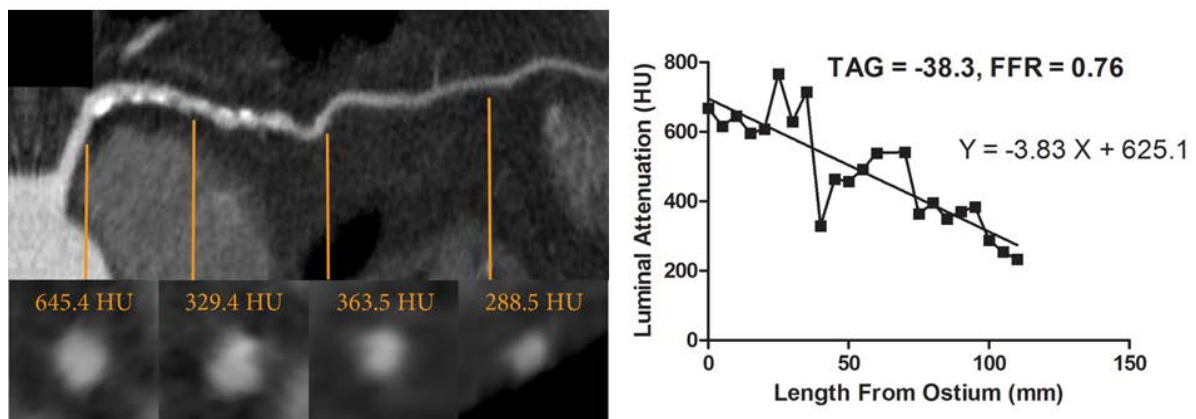


Figure 25

Contrast variability due to the lack of temporal uniformity of 64-slice CT. Contrast enhanced ECG gated cardiac computed tomography with varying contrast density (Hounsfield Units) in the aorta (red arrows) and left ventricle (yellow arrows) suggesting that the opacification of vascular structures is non uniform when image acquisition spans multiple cardiac cycles.

Figure adapted from Chow BJ, Kass M, Gagne O, et al. Can differences in corrected coronary opacification measured with computed tomography predict resting coronary artery flow? J Am Coll Cardiol 2011;57:1280-8.(100) with permission from Elsevier.



References

1. Roger VL, Go AS, Lloyd-Jones DM, et al. Heart disease and stroke statistics--2012 update: a report from the American Heart Association. *Circulation* 2012;125:e2-e220.
2. Stone GW, Maehara A, Lansky AJ, et al. A prospective natural-history study of coronary atherosclerosis. *N Engl J Med* 2011;364:226-35.
3. Pijls NH, De Bruyne B. Coronary pressure measurement and fractional flow reserve. *Heart* 1998;80:539-42.
4. Pijls NH, van Son JA, Kirkeeide RL, De Bruyne B, Gould KL. Experimental basis of determining maximum coronary, myocardial, and collateral blood flow by pressure measurements for assessing functional stenosis severity before and after percutaneous transluminal coronary angioplasty. *Circulation* 1993;87:1354-67.
5. Pijls NH, De Bruyne B, Peels K, et al. Measurement of fractional flow reserve to assess the functional severity of coronary-artery stenoses. *N Engl J Med* 1996;334:1703-8.
6. De Bruyne B, Pijls NH, Kalesan B, et al. Fractional flow reserve-guided PCI versus medical therapy in stable coronary disease. *N Engl J Med* 2012;367:991-1001.
7. Tonino PA, De Bruyne B, Pijls NH, et al. Fractional flow reserve versus angiography for guiding percutaneous coronary intervention. *N Engl J Med* 2009;360:213-24.
8. Kolh P, Windecker S. ESC/EACTS myocardial revascularization guidelines 2014. *Eur Heart J* 2014;35:3235-6.
9. Budoff MJ, Dowe D, Jollis JG, et al. Diagnostic performance of 64-multidetector row coronary computed tomographic angiography for evaluation of coronary artery stenosis in individuals without known coronary artery disease: results from the prospective multicenter ACCURACY (Assessment by Coronary Computed Tomographic Angiography of Individuals Undergoing Invasive Coronary Angiography) trial. *J Am Coll Cardiol* 2008;52:1724-32.
10. Miller JM, Rochitte CE, Dewey M, et al. Diagnostic performance of coronary angiography by 64-row CT. *N Engl J Med* 2008;359:2324-36.
11. Meijboom WB, Meijjs MF, Schuijf JD, et al. Diagnostic accuracy of 64-slice computed tomography coronary angiography: a prospective, multicenter, multivendor study. *J Am Coll Cardiol* 2008;52:2135-44.
12. Schuetz GM, Zacharopoulou NM, Schlattmann P, Dewey M. Meta-analysis: noninvasive coronary angiography using computed tomography versus magnetic resonance imaging. *Ann Intern Med* 2010;152:167-77.

13. Taylor AJ, Cerqueira M, Hodgson JM, et al. ACCF/SCCT/ACR/AHA/ASE/ASNC/NASCI/SCAI/SCMR 2010 appropriate use criteria for cardiac computed tomography. A report of the American College of Cardiology Foundation Appropriate Use Criteria Task Force, the Society of Cardiovascular Computed Tomography, the American College of Radiology, the American Heart Association, the American Society of Echocardiography, the American Society of Nuclear Cardiology, the North American Society for Cardiovascular Imaging, the Society for Cardiovascular Angiography and Interventions, and the Society for Cardiovascular Magnetic Resonance. *J Am Coll Cardiol* 2010;56:1864-94.
14. Wolk MJ, Bailey SR, Doherty JU, et al. ACCF/AHA/ASE/ASNC/HFSA/HRS/SCAI/SCCT/SCMR/STS 2013 Multimodality Appropriate Use Criteria for the Detection and Risk Assessment of Stable Ischemic Heart Disease: A Report of the American College of Cardiology Foundation Appropriate Use Criteria Task Force, American Heart Association, American Society of Echocardiography, American Society of Nuclear Cardiology, Heart Failure Society of America, Heart Rhythm Society, Society for Cardiovascular Angiography and Interventions, Society of Cardiovascular Computed Tomography, Society for Cardiovascular Magnetic Resonance, and Society of Thoracic Surgeons. *J Am Coll Cardiol* 2014;63:380-406.
15. Montalescot G, Sechtem U, Achenbach S, et al. 2013 ESC guidelines on the management of stable coronary artery disease: The Task Force on the management of stable coronary artery disease of the European Society of Cardiology. *Eur Heart J* 2013;34:2949-3003.
16. Fihn SD, Gardin JM, Abrams J, et al. 2012 ACCF/AHA/ACP/AATS/PCNA/SCAI/STS Guideline for the diagnosis and management of patients with stable ischemic heart disease: a report of the American College of Cardiology Foundation/American Heart Association Task Force on Practice Guidelines, and the American College of Physicians, American Association for Thoracic Surgery, Preventive Cardiovascular Nurses Association, Society for Cardiovascular Angiography and Interventions, and Society of Thoracic Surgeons. *J Am Coll Cardiol* 2012;60:e44-e164.
17. Ko BS, Wong DT, Cameron JD, et al. 320-row CT coronary angiography predicts freedom from revascularisation and acts as a gatekeeper to defer invasive angiography in stable coronary artery disease: a fractional flow reserve-correlated study. *Eur Radiol* 2013;24:738-747.

18. Meijboom WB, Van Mieghem CA, van Pelt N, et al. Comprehensive assessment of coronary artery stenoses: computed tomography coronary angiography versus conventional coronary angiography and correlation with fractional flow reserve in patients with stable angina. *J Am Coll Cardiol* 2008;52:636-43.
19. Hachamovitch R, Rozanski A, Shaw LJ, et al. Impact of ischaemia and scar on the therapeutic benefit derived from myocardial revascularization vs. medical therapy among patients undergoing stress-rest myocardial perfusion scintigraphy. *Eur Heart J* 2011;32:1012-24.
20. Hachamovitch R, Hayes SW, Friedman JD, Cohen I, Berman DS. Comparison of the short-term survival benefit associated with revascularization compared with medical therapy in patients with no prior coronary artery disease undergoing stress myocardial perfusion single photon emission computed tomography. *Circulation* 2003;107:2900-7.
21. Pijls NH, Fearon WF, Tonino PA, et al. Fractional Flow Reserve Versus Angiography for Guiding Percutaneous Coronary Intervention in Patients With Multivessel Coronary Artery Disease 2-Year Follow-Up of the FAME (Fractional Flow Reserve Versus Angiography for Multivessel Evaluation) Study. *J Am Coll Cardiol* 2010;56:177-184.
22. Watkins S, McGeoch R, Lyne J, et al. Validation of magnetic resonance myocardial perfusion imaging with fractional flow reserve for the detection of significant coronary heart disease. *Circulation* 2009;120:2207-13.
23. Bettencourt N, Chiribiri A, Schuster A, et al. Direct comparison of cardiac magnetic resonance and multidetector computed tomography stress-rest perfusion imaging for detection of coronary artery disease. *J Am Coll Cardiol* 2013;61:1099-107.
24. Melikian N, De Bondt P, Tonino P, et al. Fractional flow reserve and myocardial perfusion imaging in patients with angiographic multivessel coronary artery disease. *JACC Cardiovasc Interv* 2010;3:307-14.
25. Jung PH, Rieber J, Stork S, et al. Effect of contrast application on interpretability and diagnostic value of dobutamine stress echocardiography in patients with intermediate coronary lesions: comparison with myocardial fractional flow reserve. *Eur Heart J* 2008;29:2536-43.
26. Hacker M, Rieber J, Schmid R, et al. Comparison of Tc-99m sestamibi SPECT with fractional flow reserve in patients with intermediate coronary artery stenoses. *J Nucl Cardiol* 2005;12:645-54.

27. Ko BS, Cameron JD, Meredith IT, et al. Computed tomography stress myocardial perfusion imaging in patients considered for revascularization: a comparison with fractional flow reserve. *Eur Heart J* 2012;33:67-77.
28. Bamberg F, Becker A, Schwarz F, et al. Detection of hemodynamically significant coronary artery stenosis: incremental diagnostic value of dynamic CT-based myocardial perfusion imaging. *Radiology* 2011;260:689-98.
29. George RT, Arbab-Zadeh A, Miller JM, et al. Adenosine stress 64- and 256-row detector computed tomography angiography and perfusion imaging: a pilot study evaluating the transmural extent of perfusion abnormalities to predict atherosclerosis causing myocardial ischemia. *Circ Cardiovasc Imaging* 2009;2:174-82.
30. Patel AR, Lodato JA, Chandra S, et al. Detection of myocardial perfusion abnormalities using ultra-low radiation dose regadenoson stress multidetector computed tomography. *J Cardiovasc Comput Tomogr* 2011;5:247-54.
31. Cury RC, Kitt TM, Feaheny K, Akin J, George RT. Regadenoson-stress myocardial CT perfusion and single-photon emission CT: Rationale, design, and acquisition methods of a prospective, multicenter, multivendor comparison. *J Cardiovasc Comput Tomogr* 2014;8:2-12.
32. Cury RC, Magalhaes TA, Borges AC, et al. Dipyridamole stress and rest myocardial perfusion by 64-detector row computed tomography in patients with suspected coronary artery disease. *Am J Cardiol* 2010;106:310-5.
33. George RT, Silva C, Cordeiro MA, et al. Multidetector computed tomography myocardial perfusion imaging during adenosine stress. *J Am Coll Cardiol* 2006;48:153-60.
34. Ko BS, Cameron JD, Leung M, et al. Combined CT Coronary Angiography and Stress Myocardial Perfusion Imaging for Hemodynamically Significant Stenoses in Patients With Suspected Coronary Artery Disease: A Comparison With Fractional Flow Reserve. *JACC Cardiovasc Imaging* 2012;5:1097-111.
35. Bastarrika G, Ramos-Duran L, Rosenblum MA, Kang DK, Rowe GW, Schoepf UJ. Adenosine-stress dynamic myocardial CT perfusion imaging: initial clinical experience. *Invest Radiol* 2010;45:306-13.
36. Ho KT, Chua KC, Klotz E, Panknin C. Stress and rest dynamic myocardial perfusion imaging by evaluation of complete time-attenuation curves with dual-source CT. *JACC Cardiovasc Imaging* 2010;3:811-20.

37. George RT, Jerosch-Herold M, Silva C, et al. Quantification of myocardial perfusion using dynamic 64-detector computed tomography. *Invest Radiol* 2007;42:815-22.
38. Newhouse JH, Murphy RX, Jr. Tissue distribution of soluble contrast: effect of dose variation and changes with time. *AJR Am J Roentgenol* 1981;136:463-7.
39. Dewey M, Zimmermann E, Deissenrieder F, et al. Noninvasive coronary angiography by 320-row computed tomography with lower radiation exposure and maintained diagnostic accuracy: comparison of results with cardiac catheterization in a head-to-head pilot investigation. *Circulation* 2009;120:867-75.
40. Mehra VC, Valdiviezo C, Arbab-Zadeh A, et al. A stepwise approach to the visual interpretation of CT-based myocardial perfusion. *J Cardiovasc Comput Tomogr* 2011;5:357-69.
41. Achenbach S, Marwan M, Ropers D, et al. Coronary computed tomography angiography with a consistent dose below 1 mSv using prospectively electrocardiogram-triggered high-pitch spiral acquisition. *Eur Heart J* 2010;31:340-6.
42. Feuchtner G, Goetti R, Plass A, et al. Adenosine stress high-pitch 128-slice dual-source myocardial computed tomography perfusion for imaging of reversible myocardial ischemia: comparison with magnetic resonance imaging. *Circ Cardiovasc Imaging* 2011;4:540-9.
43. Douglas PS, Chen J, Gillam L, et al. Achieving Quality in Cardiovascular Imaging II: proceedings from the Second American College of Cardiology -- Duke University Medical Center Think Tank on Quality in Cardiovascular Imaging. *JACC Cardiovasc Imaging* 2009;2:231-40.
44. Bottcher M, Refsgaard J, Madsen MM, et al. Effect of antianginal medication on resting myocardial perfusion and pharmacologically induced hyperemia. *J Nucl Cardiol* 2003;10:345-52.
45. Yoon AJ, Melduni RM, Duncan SA, Ostfeld RJ, Travin MI. The effect of beta-blockers on the diagnostic accuracy of vasodilator pharmacologic SPECT myocardial perfusion imaging. *J Nucl Cardiol* 2009;16:358-67.
46. George RT, Arbab-Zadeh A, Cerci RJ, et al. Diagnostic performance of combined noninvasive coronary angiography and myocardial perfusion imaging using 320-MDCT: the CT angiography and perfusion methods of the CORE320 multicenter multinational diagnostic study. *AJR Am J Roentgenol* 2011;197:829-37.
47. Techasith T, Cury RC. Stress myocardial CT perfusion: an update and future perspective. *JACC Cardiovasc Imaging* 2011;4:905-16.

48. Kitagawa K, George RT, Arbab-Zadeh A, Lima JA, Lardo AC. Characterization and correction of beam-hardening artifacts during dynamic volume CT assessment of myocardial perfusion. *Radiology* 2010;256:111-8.
49. Mori S, Endo M, Komatsu S, Kandatsu S, Yashiro T, Baba M. A combination-weighted Feldkamp-based reconstruction algorithm for cone-beam CT. *Phys Med Biol* 2006;51:3953-65.
50. Gerber BL, Belge B, Legros GJ, et al. Characterization of acute and chronic myocardial infarcts by multidetector computed tomography: comparison with contrast-enhanced magnetic resonance. *Circulation* 2006;113:823-33.
51. Kachenoura N, Veronesi F, Lodato JA, et al. Volumetric quantification of myocardial perfusion using analysis of multi-detector computed tomography 3D datasets: comparison with nuclear perfusion imaging. *Eur Radiol* 2010;20:337-47.
52. Busch JL, Alessio AM, Caldwell JH, et al. Myocardial hypo-enhancement on resting computed tomography angiography images accurately identifies myocardial hypoperfusion. *J Cardiovasc Comput Tomogr* 2011;5:412-20.
53. Rodriguez-Granillo GA, Rosales MA, Renes P, et al. Chronic myocardial infarction detection and characterization during coronary artery calcium scoring acquisitions. *J Cardiovasc Comput Tomogr* 2010;4:99-107.
54. George RT, Lardo AC. Infarct detection or infarct characterization? Noncontrast CT and its implications for characterizing chronic myocardial scar. *J Cardiovasc Comput Tomogr*;4:108-9.
55. Rochitte CE, George RT, Chen MY, et al. Computed tomography angiography and perfusion to assess coronary artery stenosis causing perfusion defects by single photon emission computed tomography: the CORE320 study. *Eur Heart J* 2013:Epub Ahead of print 21/11/2013.
56. Blankstein R, Shturman LD, Rogers IS, et al. Adenosine-induced stress myocardial perfusion imaging using dual-source cardiac computed tomography. *J Am Coll Cardiol* 2009;54:1072-84.
57. George RT, Arbab-Zadeh A, Miller JM, et al. Computed tomography myocardial perfusion imaging with 320-row detector computed tomography accurately detects myocardial ischemia in patients with obstructive coronary artery disease. *Circ Cardiovasc Imaging* 2012;5:333-40.
58. Iskandrian AS, Chae SC, Heo J, Stanberry CD, Wasserleben V, Cave V. Independent and incremental prognostic value of exercise single-photon emission computed

- tomographic (SPECT) thallium imaging in coronary artery disease. *J Am Coll Cardiol* 1993;22:665-70.
59. Weininger M, Schoepf UJ, Ramachandra A, et al. Adenosine-stress dynamic real-time myocardial perfusion CT and adenosine-stress first-pass dual-energy myocardial perfusion CT for the assessment of acute chest pain: Initial results. *Eur J Radiol* 2012;81:3703-10.
 60. Ko SM, Choi JW, Song MG, et al. Myocardial perfusion imaging using adenosine-induced stress dual-energy computed tomography of the heart: comparison with cardiac magnetic resonance imaging and conventional coronary angiography. *Eur Radiol* 2011;21:26-35.
 61. Mahnken AH, Klotz E, Pietsch H, et al. Quantitative whole heart stress perfusion CT imaging as noninvasive assessment of hemodynamics in coronary artery stenosis: preliminary animal experience. *Invest Radiol* 2010;45:298-305.
 62. Christian TF, Frankish ML, Sisemoore JH, et al. Myocardial perfusion imaging with first-pass computed tomographic imaging: Measurement of coronary flow reserve in an animal model of regional hyperemia. *J Nucl Cardiol* 2010;17:625-30.
 63. Kurata A, Mochizuki T, Koyama Y, et al. Myocardial perfusion imaging using adenosine triphosphate stress multi-slice spiral computed tomography: alternative to stress myocardial perfusion scintigraphy. *Circ J* 2005;69:550-7.
 64. Okada DR, Ghoshhajra BB, Blankstein R, et al. Direct comparison of rest and adenosine stress myocardial perfusion CT with rest and stress SPECT. *J Nucl Cardiol* 2010;17:27-37.
 65. Okada DR, Ghoshhajra BB, Blankstein R, et al. Direct comparison of rest and adenosine stress myocardial perfusion CT with rest and stress SPECT. *J Nucl Cardiol*;17:27-37.
 66. Rocha-Filho JA, Blankstein R, Shturman LD, et al. Incremental value of adenosine-induced stress myocardial perfusion imaging with dual-source CT at cardiac CT angiography. *Radiology*;254:410-9.
 67. Ruzsics B, Schwarz F, Schoepf UJ, et al. Comparison of dual-energy computed tomography of the heart with single photon emission computed tomography for assessment of coronary artery stenosis and of the myocardial blood supply. *Am J Cardiol* 2009;104:318-26.
 68. Rief M, Zimmermann E, Stenzel F, et al. Computed tomography angiography and myocardial computed tomography perfusion in patients with coronary stents:

- prospective intraindividual comparison with conventional coronary angiography. *J Am Coll Cardiol* 2013;62:1476-85.
69. Cury R, Kitt TM, Feaheny K, Akin J, George RT. A Randomized, Multi-Center, Multi-Vnedor Study Comparing Myocardial Perfusion Imaging with Regadenoson Stress Computed Tomography Perfusion and Single Photon Emission Computed Tomography. *Journal of Cardiovascular Computed Tomography* 2013;7:S42.
 70. Perkins J, Field T, Kim J, et al. Pharmacokinetic targeting of i.v. BU with fludarabine as conditioning before hematopoietic cell transplant: the effect of first-dose area under the concentration time curve on transplant-related outcomes. *Bone Marrow Transplant* 2011;46:1418-25.
 71. So A, Hsieh J, Li JY, Lee TY. Beam hardening correction in CT myocardial perfusion measurement. *Phys Med Biol* 2009;54:3031-50.
 72. Kim HJ, Vignon-Clementel IE, Coogan JS, Figueroa CA, Jansen KE, Taylor CA. Patient-specific modeling of blood flow and pressure in human coronary arteries. *Ann Biomed Eng* 2010;38:3195-209.
 73. Taylor CA, Fonte TA, Min JK. Computational fluid dynamics applied to cardiac computed tomography for noninvasive quantification of fractional flow reserve: scientific basis. *J Am Coll Cardiol* 2013;61:2233-41.
 74. Min JK, Berman DS, Budoff MJ, et al. Rationale and design of the DeFACTO (Determination of Fractional Flow Reserve by Anatomic Computed Tomographic AngiOgraphy) study. *J Cardiovasc Comput Tomogr* 2011;5:301-9.
 75. Koo BK, Erglis A, Doh JH, et al. Diagnosis of ischemia-causing coronary stenoses by noninvasive fractional flow reserve computed from coronary computed tomographic angiograms. Results from the prospective multicenter DISCOVER-FLOW (Diagnosis of Ischemia-Causing Stenoses Obtained Via Noninvasive Fractional Flow Reserve) study. *J Am Coll Cardiol* 2011;58:1989-97.
 76. Min JK, Leipsic J, Pencina MJ, et al. Diagnostic Accuracy of Fractional Flow Reserve From Anatomic CT Angiography. *JAMA* 2012;1-9.
 77. Nakazato R, Park HB, Berman DS, et al. Noninvasive fractional flow reserve derived from computed tomography angiography for coronary lesions of intermediate stenosis severity: results from the DeFACTO study. *Circ Cardiovasc Imaging* 2013;6:881-9.
 78. Norgaard BL, Leipsic J, Gaur S, et al. Diagnostic performance of non-invasive fractional flow reserve derived from coronary CT angiography in suspected coronary artery disease: The NXT trial. *J Am Coll Cardiol* 2014;63:1145-55.

79. Abbara S, Arbab-Zadeh A, Callister TQ, et al. SCCT guidelines for performance of coronary computed tomographic angiography: a report of the Society of Cardiovascular Computed Tomography Guidelines Committee. *J Cardiovasc Comput Tomogr* 2009;3:190-204.
80. Kim KH, Doh JH, Koo BK, et al. A novel noninvasive technology for treatment planning using virtual coronary stenting and computed tomography-derived computed fractional flow reserve. *JACC Cardiovasc Interv* 2014;7:72-8.
81. Choi JH, Min JK, Labounty TM, et al. Intracoronary transluminal attenuation gradient in coronary CT angiography for determining coronary artery stenosis. *JACC Cardiovasc Imaging* 2011;4:1149-57.
82. Steigner ML, Mitsouras D, Whitmore AG, et al. Iodinated contrast opacification gradients in normal coronary arteries imaged with prospectively ECG-gated single heart beat 320-detector row computed tomography. *Circ Cardiovasc Imaging* 2010;3:179-86.
83. Lackner K, Bovenschulte H, Stutzer H, Just T, Al-Hassani H, Krug B. In vitro measurements of flow using multislice computed tomography (MSCT). *Int J Cardiovasc Imaging* 2011;27:795-804.
84. Wong DT, Ko BS, Cameron JD, et al. Transluminal Attenuation Gradient in Coronary Computed Tomography Angiography Is a Novel Noninvasive Approach to the Identification of Functionally Significant Coronary Artery Stenosis: A Comparison With Fractional Flow Reserve. *J Am Coll Cardiol* 2013;61:1271-9.
85. Yoon YE, Choi JH, Kim JH, et al. Noninvasive Diagnosis of Ischemia-Causing Coronary Stenosis Using CT Angiography: Diagnostic Value of Transluminal Attenuation Gradient and Fractional Flow Reserve Computed From Coronary CT Angiography Compared to Invasively Measured Fractional Flow Reserve. *JACC Cardiovasc Imaging* 2012;5:1088-96.
86. Wong DT, Ko BS, Cameron JD, et al. Comparison of diagnostic accuracy of combined assessment using adenosine stress CT perfusion (CTP) + computed tomography angiography (CTA) with transluminal attenuation gradient (TAG320) + CTA against invasive fractional flow reserve (FFR). *Journal of the American College of Cardiology* 2014:In press.
87. Min JK, Dunning A, Lin FY, et al. Age- and sex-related differences in all-cause mortality risk based on coronary computed tomography angiography findings results from the International Multicenter CONFIRM (Coronary CT Angiography Evaluation

- for Clinical Outcomes: An International Multicenter Registry) of 23,854 patients without known coronary artery disease. *J Am Coll Cardiol* 2011;58:849-60.
88. Hadamitzky M, Achenbach S, Al-Mallah M, et al. Optimized Prognostic Score for Coronary Computed Tomographic Angiography: Results From the CONFIRM Registry (COronary CT Angiography EvaluationN For Clinical Outcomes: An InteRnational Multicenter Registry). *J Am Coll Cardiol* 2013;62:468-76.
 89. Chow BJ, Small G, Yam Y, et al. Incremental prognostic value of cardiac computed tomography in coronary artery disease using CONFIRM: COroNary computed tomography angiography evaluation for clinical outcomes: an InteRnational Multicenter registry. *Circ Cardiovasc Imaging* 2011;4:463-72.
 90. Marwick TH, Case C, Vasey C, Allen S, Short L, Thomas JD. Prediction of mortality by exercise echocardiography: a strategy for combination with the duke treadmill score. *Circulation* 2001;103:2566-71.
 91. McCully RB, Roger VL, Mahoney DW, et al. Outcome after abnormal exercise echocardiography for patients with good exercise capacity: prognostic importance of the extent and severity of exercise-related left ventricular dysfunction. *J Am Coll Cardiol* 2002;39:1345-52.
 92. Min JK, Dunning A, Lin FY, et al. Rationale and design of the CONFIRM (COronary CT Angiography EvaluationN For Clinical Outcomes: An InteRnational Multicenter) Registry. *J Cardiovasc Comput Tomogr* 2011;5:84-92.
 93. Hecht HS. The Game Changer? *J Am Coll Cardiol* 2014.
 94. Sarno G, Decraemer I, Vanhoenacker PK, et al. On the inappropriateness of noninvasive multidetector computed tomography coronary angiography to trigger coronary revascularization: a comparison with invasive angiography. *JACC Cardiovasc Interv* 2009;2:550-7.
 95. Ragosta M, Bishop AH, Lipson LC, et al. Comparison between angiography and fractional flow reserve versus single-photon emission computed tomographic myocardial perfusion imaging for determining lesion significance in patients with multivessel coronary disease. *Am J Cardiol* 2007;99:896-902.
 96. Forster S, Rieber J, Ubleis C, et al. Tc-99m sestamibi single photon emission computed tomography for guiding percutaneous coronary intervention in patients with multivessel disease: a comparison with quantitative coronary angiography and fractional flow reserve. *Int J Cardiovasc Imaging* 2010;26:203-13.

97. Rieber J, Jung P, Erhard I, et al. Comparison of pressure measurement, dobutamine contrast stress echocardiography and SPECT for the evaluation of intermediate coronary stenoses. The COMPRESS trial. *Int J Cardiovasc Intervent* 2004;6:142-7.
98. Ko BS, Cameron JD, DeFrance T, Seneviratne SK. CT stress myocardial perfusion imaging using multidetector CT--A review. *J Cardiovasc Comput Tomogr* 2011;5:345-56.
99. Nasis A, Seneviratne S, DeFrance T. Advances in Contrast-Enhanced Cardiovascular CT for the Evaluation of Myocardial Perfusion. *Curr Cardiovasc Imaging Rep* 2010;3:372-381.
100. Chow BJ, Kass M, Gagne O, et al. Can differences in corrected coronary opacification measured with computed tomography predict resting coronary artery flow? *J Am Coll Cardiol* 2011;57:1280-8.

Chapter 2

Comparison of diagnostic accuracy of combined assessment using adenosine stress CT perfusion (CTP) + computed tomography angiography (CTA) with transluminal attenuation gradient (TAG320) + CTA against invasive fractional flow reserve (FFR)

PART B: Suggested Declaration for Thesis Chapter

[This declaration to be completed for each conjointly authored publication and to be placed at the start of the thesis chapter in which the publication appears.]

Monash University

Declaration for Thesis Chapter

Chapter 2: Comparison of diagnostic accuracy of combined assessment using adenosine stress CT perfusion (CTP) + Computed tomography angiography (CTA) with transluminal attenuation gradient (TAG320)+CTA against invasive fractional flow reserve (FFR)

Declaration by candidate

In the case of Chapter 2, the nature and extent of my contribution to the work was the following:

Nature of contribution	Extent of contribution (%)
Conception, design, analysis and interpretation of data. Drafting and revising of manuscript. Final approval of manuscript submitted.	40

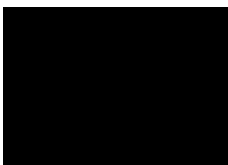
The following co-authors contributed to the work. If co-authors are students at Monash University, the extent of their contribution in percentage terms must be stated:

Name	Nature of contribution	Extent of contribution (%) for student co-authors only
Dennis Wong	Conception, design, analysis and interpretation of data. Drafting and revising of manuscript. Final approval of manuscript submitted.	40
James Cameron	Conception and design. Revising of manuscript. Final approval of manuscript submitted.	
Darryl Leong	Analysis and interpretation of data. Revising of manuscript. Final approval of manuscript submitted.	

Michael Leung	Analysis and interpretation of data. Revising of manuscript. Final approval of manuscript submitted.	
Yuvaraj Malaiapan	Analysis and interpretation of data. Revising of manuscript. Final approval of manuscript submitted.	
Nitesh Nerlekar	Analysis and interpretation of data. Revising of manuscript. Final approval of manuscript submitted.	
Marcus Crossett	Conception and design. Revising of manuscript. Final approval of manuscript submitted.	
John Troupis	Conception and design. Revising of manuscript. Final approval of manuscript submitted.	
Ian Meredith	Conception and design. Revising of manuscript. Final approval of manuscript submitted.	
Sujith Seneviratne	Conception and design. Revising of manuscript. Final approval of manuscript submitted.	

The undersigned hereby certify that the above declaration correctly reflects the nature and extent of the candidate's and co-authors' contributions to this work*.

**Candidate's
Signature**

	Date 15/10/2014
---	----------------------------------

Preface:

The strength of stress CT myocardial perfusion imaging is the existing large body of data from single and multicentre studies which demonstrate its high diagnostic accuracy when compared with various reference standards performed in patients with known and suspected coronary artery disease. However the technique is associated with additional radiation exposure, iodinated contrast usage, chest discomfort as a result of intravenous administration of vasodilator stress, increased costs and added time duration on the CT scan table.

The obvious advantage of CT transluminal attenuation gradient is that it can be conveniently applied at the point of care on typically acquired CT coronary angiography datasets, without additional radiation or contrast usage or cost.

It would be ideal hence to compare the diagnostic performance of stress CT myocardial perfusion imaging and transluminal attenuation gradient in detection of hemodynamically significant coronary stenoses, using invasive fractional flow reserve as reference standard.

Title

Comparison of diagnostic accuracy of combined assessment using adenosine stress CT perfusion (CTP) + computed tomography angiography (CTA) with transluminal attenuation gradient (TAG320) + CTA against invasive fractional flow reserve (FFR)

Authors

Dennis TL Wong MBBS (Hons), PhD^{1, 2 ‡} & Brian S Ko MBBS (Hons), PhD^{1*}, James D Cameron MBBS, MD¹, Darryl P Leong MBBS (Hons), MPH, PhD², Michael CH Leung MBBS (Hons), PhD¹, Yuvaraj Malaiapan MBBS¹, Nitesh Nerlekar MBBS¹, Marcus Crossett Ba App Sc³, John Troupis MBBS^{1,3}, Ian T Meredith MBBS (Hons), PhD¹, Sujith K Seneviratne MBBS¹*

Affiliation of Authors

¹ *Monash Cardiovascular Research Centre, Department of Medicine (Monash Medical Centre) Monash University and Monash Heart, Monash Health, 246 Clayton Road, Clayton, 3168 VIC, Australia*

² *Discipline of Medicine, University of Adelaide, Adelaide, Australia*

³ *Department of Diagnostic Imaging, MMC, Southern Health, Melbourne, Australia*

** Contributed equally to manuscript*

‡ Corresponding author

Address correspondence

Dr Dennis Thiam Leong Wong

MonashHeart, Monash Medical Centre

246 Clayton Road,

Clayton, Victoria, AUSTRALIA

[REDACTED]

[REDACTED]

[REDACTED]

Abstract

Background

Computed-tomography-coronary-angiography (CTA) has limited specificity for predicting functionally significant stenoses. Novel CT techniques including adenosine-stress-computed-tomography-myocardial-perfusion (CTP) and transluminal-attenuation-gradient (TAG320) may improve the specificity and accuracy of CTA alone to detect functionally significant coronary stenoses.

Objective

To compare the per-vessel diagnostic accuracy of combined CTP + CTA with TAG320 + CTA assessment in predicting coronary artery functional stenosis severity as determined using invasive fractional-flow-reserve (FFR). To evaluate the per-vessel diagnostic accuracy of combined assessment of CTP + TAG320 + CTA (MDCT-IP).

Method

CTA, CTP and TAG320 were assessed using 320-MDCT. We assessed per-vessel diagnostic accuracy of combined assessment of CTP + CTA, TAG320 + CTA and MDCT-IP with FFR for the evaluation of functional stenosis severity in consecutive patients who underwent CTA, CTP as well as FFR assessment on invasive-coronary-angiography. Myocardial perfusion was assessed by visual assessment. TAG320 was defined as the linear-regression-coefficient between luminal attenuation and axial distance. A TAG320 cut-off value of -15.1 HUs/10 mm as previously described was defined as significant. For combined coronary CTP and CTA and TAG320 +CTA analyses, vessels were considered significant when coronary CTA demonstrated $\geq 50\%$ stenosis and was associated with a reversible perfusion defect in the vessel's subtended territory or a significant TAG320 respectively.

MDCT-IP was classified as positive in vessels with $\geq 50\%$ CTA stenosis if a perfusion defect was detected on CTP in the corresponding territory or if the TAG320 was significant. Functionally-significant-coronary-stenosis was defined as ≤ 0.8 on FFR.

Results

In our cohort of 75 patients (age 64.1 ± 10.8 years, 52 males, 127 vessels), 44 vessels (35%) were FFR-significant. In 127 vessels, CTA predicted FFR-significant stenosis with 89% sensitivity, 65% specificity, 57% PPV and 92% NPV compared to MDCT-IP which showed 88% sensitivity, 83% specificity, 74% PPV and 93% NPV. In 97 vessels where all techniques are available, combined assessment of TAG320 + CTA (AUC = 0.844) and CTP + CTA (AUC = 0.845) had comparable diagnostic accuracy ($P = 0.98$). The diagnostic accuracy of MDCT-IP (AUC = 0.91) was superior to the combined assessment of TAG320 + CTA or CTP + CTA ($P = 0.01$).

Conclusion

Combined assessment using TAG320 + CTA and CTP + CTA provide comparable diagnostic accuracy for functional assessment of coronary artery stenosis in vessels without significant calcification or artefact in the studied cohort. Combined assessment with TAG320 + CTP + CTA (MDCT-IP) may provide the best diagnostic accuracy for functional assessment of coronary artery stenosis. Larger studies are required to determine the diagnostic and prognostic value of these assessments.

Introduction

Coronary computed tomography angiography (CTA) is an established non-invasive method for the assessment of the coronary artery anatomy. It is particularly useful for the exclusion of coronary artery disease because of its established high sensitivity and negative predictive value (1). However CTA has been shown to have limited specificity and positive predictive value for predicting functionally significant stenoses (2). Several methods such as computed tomography stress myocardial perfusion imaging (CTP), transluminal attenuation gradient (TAG) and CCTA-derived computed FFR (FFR_{CT}) have been developed to attempt to improve the diagnostic accuracy of CTA (3-5). Whilst CTP has been demonstrated to enhance detection for functionally significant stenoses, it requires additional iodinated contrast and radiation exposure (3,6,7). The diagnostic accuracy of transluminal attenuation gradient (TAG320) on a 320-detector row CT which enables near isophasic, single-beat imaging of the entire coronary tree has been recently demonstrated (4). However no studies have compared the diagnostic accuracy of CTA, CTP and TAG320. Our primary aim was to compare the diagnostic accuracy of CTA, combined assessment of CTP + CTA and combined TAG320 + CTA. Furthermore, we assessed the diagnostic accuracy of an integrated approach (MDCT-IP) which combines CTA, CTP and TAG320 assessment. Fractional flow reserve (FFR), a well-established and highly accurate invasive method to assess the functional significance of coronary stenosis, was used as the reference standard (8,9).

Methods

Patients

We examined consecutive patients who underwent CTA, CTP and FFR assessment in our institution within a 2 month interval, between July 2009 and May 2011. This included symptomatic patients with known coronary artery disease who are considered for revascularisation as well as symptomatic patients with suspected coronary artery disease awaiting invasive coronary angiography. In all cases, cardiac CT was performed for research purpose. Fractional flow reserve was performed in vessels with $\geq 30\%$ visual stenosis on diagnostic coronary angiography. Subtotally occluded and occluded vessels were excluded. Exclusion criteria included younger than 40 years of age, atrial fibrillation, high-grade atrioventricular block, renal insufficiency (estimated glomerular filtration rate < 60 ml/min/1.73m²), bronchospastic lung disease requiring long-term steroid therapy, morbid obesity (body mass index ≥ 40 kg/m²), myocardial infarction within 3 months, history of coronary artery bypass grafting or intractable heart failure and contraindications to iodinated contrast. Patients were instructed to refrain from smoking or using tea, aminophylline, calcium antagonists or nitrates for 24-hours before the tests. For TAG320 analysis, patients with more than 50% stenosis in the left main coronary artery, branch vessel disease, distal vessel disease < 2 mm in diameter or chronic total occlusions with collateral supply were not included. The study was approved by our institutional Human Research Ethics Committee.

Invasive coronary angiography and fractional flow reserve

Invasive coronary angiography was performed as per standard clinical practice via either femoral or radial approach. For FFR, the pressure wire (Certus Pressure Wire, St Jude

Medical Systems, USA) was calibrated and electronically equalised with the aortic pressure before being placed distal to the stenosis in the distal third of the coronary artery being interrogated. Intracoronary glyceryl trinitrate (100 mcg) was injected to minimise vasospasm. Intravenous adenosine was administered (140mcg/kg/min) through an intravenous line in the antecubital fossa. At steady-state hyperaemia, FFR was assessed using the RadiAnalyser Xpress (Radi Medical Systems, Sweden), calculated by dividing the mean coronary pressure measured with the pressure sensor placed distal to the stenosis by the mean aortic pressure measured through the guide catheter. Fractional flow reserve of ≤ 0.8 was taken to define ischemia in the interrogated artery and its supplied territory (8,10).

Quantitative coronary angiography

Quantitative coronary angiography (QCA) was undertaken on all coronary arteries of ≥ 1.5 mm diameter employing a 19-segment coronary model according to the SYNTAX classification (11). QCA was performed using a semi-automated edge detection system (QAngio XA 7.3, Medis, Leiden the Netherlands) by an experienced cardiologist (B.K.) who was blinded to FFR and CT findings.

Computed tomography protocol

Cardiovascular medications were ceased 48 hours prior to CTA apart from beta-blockers. On arrival, an 18-gauge intravenous line was inserted in the right antecubital vein for administration of contrast. Oral and/or intravenous metoprolol was given if the resting heart rate was >65 b.p.m. Patients were scanned on a 320-detector-row CT scanner (Aquilion ONE, Toshiba Medical Systems, Japan). The scan was acquired during injection of 55 mL of 100% Iohexal 56.6g/75 mL (Omnipaque 350) at 5 mL/s, followed by 20 mL of a 30:70 mixture of contrast and saline, followed by 30 mL of saline. Scanning was triggered in the arterial phase using automated contrast bolus tracking with the region of interest placed in the descending

aorta, and automatically triggered at 300 Hounsfield units (HU).

Scan parameters for rest coronary CTA were as follows: detector collimation 320×0.5 mm; tube current 300–500 mA [depending on body mass index (BMI)]; tube voltage 120 kV if BMI ≥ 25 (100 kV if BMI < 25); gantry rotation time 350 ms; and temporal resolution 175 ms. Prospective electrocardiogram gating was used covering 70–80% of the R–R interval. For images acquired at heart rates ≤ 65 b.p.m. scanning was completed within a single R–R interval utilizing a 180° segment. In patients with a heart rate > 65 b.p.m. data segments from two consecutive beats were used for multi-segment reconstruction with improved temporal resolution of 87 ms. Images were reconstructed using the filtered back-projection technique with FCO3 algorithm.

The stress perfusion scan was performed 20 minutes after coronary CTA with intravenous adenosine infusion ($140 \mu\text{g/kg/min}$ for 3 min), using prospective electrocardiographic gating covering phases 70% to 95% of the R–R interval, tube settings, and contrast dose as for the rest scan. The effective radiation dose was calculated by multiplying the dose-length product by a constant ($k = 0.014 \text{ mSv/mGy/cm}$) (12).

Coronary artery analysis in coronary CTA

CT angiographic images were analysed on a dedicated workstation (Vitreax FX 2.0, Vital Images, Minnetonka, MN, USA) by two experienced CT angiographers (ML and SS) blinded to QCA and FFR results. The CT angiographers read independently of each other and discrepant readings were reconciled by consensus. Image quality was determined by a three point scale: 1=poor, 2=moderate, 3=good (ML and SS). All segments ≥ 1.5 mm were analysed using the same 19-segment coronary model for QCA (11). Each coronary segment was visually

assessed for degree of luminal stenosis and a vessel considered significant if there was ≥ 1 segment which was non-evaluable or with a $\geq 50\%$ luminal stenosis.

Perfusion assessment was performed using both the stress and rest images. Datasets were reconstructed at 3% R-R intervals using a reconstruction kernel (FC03), which incorporates beam hardening correction (6,13). The phase with the least cardiac motion was selected, and images were interpreted using a narrow window width and level setting (W300/L150) and an averaged multiplanar reconstruction slice thickness of 3 to 5 mm, according to the American Heart Association 17-myocardial segment model (14) with disagreement resolved by a third reader. Segments with significant overlying artefacts were deemed uninterpretable and excluded from analysis. Each segment was scored for the presence or absence of a perfusion defect. Each myocardial segment was specifically matched to its subtending major epicardial artery, as determined by the course of the artery and its branches on coronary CTA. For the combined coronary CTA + CTP analysis, vessels were considered significant when coronary CTA demonstrated $\geq 50\%$ stenosis and was associated with a reversible perfusion defect in the vessel's subtended territory.

Transluminal attenuation gradient (TAG320)

The centreline was determined for each major coronary artery and was manually corrected if necessary. Cross-sectional images perpendicular to the vessel centreline were then reconstructed. The region of interest (ROI) contour (size - 1mm^2) was positioned in the centre of the cross-sectional images. The position of the ROI was manually adjusted. The mean luminal radiological attenuation (HU) was measured at 5-mm intervals, from the ostium to a distal level where the cross-sectional area fell below 2.0mm^2 . TAG320 was determined from the change in HU per 10-mm length of coronary artery and defined as the linear regression

coefficient between intraluminal radiological attenuation (HU) and length from the ostium (mm) (4,15). A TAG320 cut-off of -15.1 HUs/10 mm is defined as significant as previously described (4). For combined TAG320 + CTA assessment, vessels are classified as negative if CTA <50% stenosis. Vessels are classified as positive if CTA \geq 50% and TAG320 was \leq -15.1 HUs/10 mm.

The stenosis and plaque characteristics were classified in each lesion. Vessels were classified as noncalcified if the most stenotic segment was noncalcified. Vessels were classified as calcified if the most stenotic segment was calcified or partially calcified.

MDCT integrated TAG320 and CTP protocol (MDCT-IP)

The MDCT-IP was classified negative if stenosis < 50% were detected on CTA. If the CTA showed \geq 50% stenosis, the MDCT-IP was classified as positive if a perfusion defect was detected on CTP in a territory corresponding to the stenosis or if the TAG320 was \leq -15.1 HUs/10 mm (Figure 1).

Statistical analysis

Continuous variables are expressed as mean \pm SD or median (quartiles) as appropriate, whereas categorical variables are expressed as percentage. Continuous and categorical variables were compared using *t*- test, Mann-Whitney or chi-square test as appropriate. Owing to the repeated-measures nature of the study, a generalized estimating equation approach was used assuming a binomial probability distribution.

Receiver operating characteristic (ROC) analysis was performed to evaluate the

discriminatory ability of CTA, CTP + CTA, TAG320 + CTA and MDCT-IP for $\text{FFR} \leq 0.8$. The incremental value in adding TAG320 and CTP to CTA in discriminating significant FFR was assessed using the integrated discrimination improvement (IDI) index as described by Pencina et al (16):

$$\text{IDI} = (\text{IS}_{\text{new}} - \text{IS}_{\text{old}}) - (\text{IP}_{\text{new}} - \text{IP}_{\text{old}}) \text{ and}$$

Where the “new” subscript refers to a model containing a novel diagnostic tool of interest in addition to conventional risk-predictors, and “old” pertains to the model containing only the conventional risk-markers. IS and IP are the integrals of sensitivity and $(1 - \text{specificity})$ respectively. In addition, the category-free net reclassification index for identification of $\text{FFR} \leq 0.8$ using TAG320 over CTA was calculated (16).

Statistical analysis was performed with SPSS 18.0 (SPSS Inc, Chicago, IL, USA) and STATA 12.1 (StataCorp, College Station, TX, USA). A P value <0.05 was considered statistically significant.

Results

Clinical characteristics

Seventy five consecutive patients who underwent CTA, CTP and clinically indicated coronary angiography as well as fractional flow reserve, were studied. A total of 127 vessels were evaluated. TAG320 analysis could be performed in 64 patients (85%) and 97 vessels (76.4%). Non evaluable vessels were due to intramyocardial course of left anterior descending artery ($n = 3$), branch or small vessel ($n = 8$), calcified disease ($n = 15$) and significant artefact ($n = 4$). The overall patient cohort age was 64.0 ± 10.8 years with 52 (69%) males. Patient characteristics are summarised in Table 1. The mean estimated radiation effective dose for

CTA, CTP and CTA + CTP in our study was 4.6 mSv, 4.8 mSv and 9.8 mSv respectively. The computed tomography scan parameters are summarised in Table 2.

Fractional flow reserve

Fractional flow reserve was performed successfully in all 75 patients involving 127 vessels (57 left anterior descending arteries, 31 left circumflex arteries and 39 right coronary arteries). Thirty eight (51%) patients received FFR interrogation in one-vessel territory, 22 (29%) two and 15 (20%) had all three-vessel territories interrogated. Overall FFR reading ranged from 0.32 to 1.0 (mean, 0.82 ± 0.15). Forty four vessels (35%) were classified with functionally significant stenoses with $\text{FFR} \leq 0.8$ while 83 vessels had $\text{FFR} > 0.8$.

Accuracy of invasive quantitative coronary angiography compared to fractional flow reserve

On a per vessel basis, 37 (29%) vessels had $\geq 50\%$ stenosis on QCA, whereas 12 (9%) had $\geq 70\%$ stenosis. The sensitivity, specificity, PPV and NPV of QCA of $\geq 50\%$ in predicting significant FFR was 61%, 88%, 73% and 81%. Meanwhile, the sensitivity, specificity, PPV and NPV of QCA $\geq 70\%$ in predicting significant FFR were 25%, 99%, 92% and 71% (Table 3).

Accuracy of computed tomography coronary angiography compared to fractional flow reserve

There were 22 (17%) vessels which had severe calcification in which significant stenosis could not be excluded. These vessels were classified as $\geq 50\%$ stenosis and were included in the analysis. In the vessels interrogated with FFR, 68 (54%) vessels were identified to have $\geq 50\%$ stenosis on CTA. The sensitivity, specificity, PPV and NPV of CTA for the identification of FFR significant stenoses were 89%, 65%, 57% and 92% respectively (Table 3). The c-statistic of CTA for the prediction of $\text{FFR} \leq 0.8$ was 0.77 (0.68 - 0.85).

Accuracy of combined CTP and CTA assessment compared to fractional flow reserve

The combined CTP and CTA assessment could be performed in 123 (97%) vessels. CTP assessment could not be performed in 4 vessels due to artefact. On a per vessel basis, 32 (25%) vessels were identified to have $\geq 50\%$ stenosis on CTA with a corresponding perfusion defect identified on CTP. The sensitivity, specificity, PPV and NPV of combined assessment of CTP + CTA for the identification of FFR significant stenoses were 76%, 89%, 78% and 88% respectively (Table 3). The c-statistic for combined assessment of CTP + CTA for the prediction of $\text{FFR} \leq 0.8$ was 0.825 (0.74 – 0.91).

Accuracy of TAG320 and of combined TAG320 + CTA compared to fractional flow reserve

The TAG320 and combined TAG320 + CTA assessment could be performed in 97 (78%) vessels. Median TAG320 in FFR-significant vessels was significantly lower when compared with non-significant vessels [-19 (-26;-13) vs. -10 (-16;-5) HUs/10 mm, $P < 0.001$]. A TAG320 cut-off of -15.1 HUs/10 mm predicted $\text{FFR} \leq 0.8$ with a sensitivity 71%, specificity 77%, PPV 63% and NPV 83% respectively. When CTA was combined with TAG320, this yielded sensitivity 73%, specificity 97%, PPV 92% and NPV 87% (Table 3). The c-statistic for the combined assessment of TAG320 + CTA for the prediction of $\text{FFR} \leq 0.8$ was 0.848 (0.752 – 0.944).

Accuracy of MDCT-IP compared to fractional flow reserve

The MDCT-IP approach could be performed in 117 vessels. On a per vessel analysis, 35 (28%) vessels were identified to be significant. The sensitivity, specificity, PPV and NPV of CTA for the identification of FFR significant stenoses were 88%, 83%, 74% and 93% respectively (Table 3). The c-statistic for combined assessment of CTP + TAG320 + CTA (MDCT-IP) for the prediction of $\text{FFR} \leq 0.8$ was 0.854 (0.778 – 0.93).

Comparison of CTP + CTA, TAG320 + CTA and MDCT-IP in predicting FFR

In the comparison of the diagnostic accuracy of combined assessment of CTP + CTA, TAG320 + CTA and MDCT-IP, 97 vessels which could be assessed by all 3 methods were included for analysis. Using the generalised estimating equation, the predictive value of CTP + CTA ($P = 0.003$) and TAG320 + CTA ($P = 0.002$) were comparable. The c-statistic for the combined assessment of CTP + CTA (0.845) and TAG320 + CTA (0.844) were also comparable ($P = 0.98$). The c-statistic for MDCT-IP was 0.905 (Figure 4). On global comparison of ROC for all 3 methods, MDCT-IP was the best predictor of significant FFR ($P = 0.01$). The MDCT-IP approach resulted in a marked increase in sensitivity and mild decrease in specificity compared to CTA + CTP and CTA + TAG320 (Table 4). The diagnostic accuracy of the 3 methods in 97 vessels is summarised in Table 4.

Accuracy of CTP + CTA, TAG320 + CTA and MDCT-IP in predicting FFR in calcified vessels

There were 50 out of 127 vessels which were classified as calcified based on qualitative assessment. TAG320 + CTA assessment was limited to 38 vessels, CTP + CTA and MDCT-IP could be performed in 48 and 46 vessels respectively. The diagnostic accuracy of all 3 assessments is presented in Appendix 1.

Incremental value of adding CTP to CTA and TAG320 to CTA in discriminating significant FFR

There was incremental value of adding CTP to CTA assessment for detection of significant FFR by the integrated discrimination improvement (IDI) index. The IDI for the addition of CTP to CTA for detection of significant FFR was 0.18 ($P < 0.0001$) whilst the category-free net reclassification index (NRI) was 1.30 ($P < 0.0001$). There was also

incremental value of adding TAG320 to CTA assessment for detection of significant FFR by NRI (1.39, $P < 0.0001$) and IDI (0.21, $P = 0.0002$).

Incremental value of adding CTP and TAG320 to CTA in discriminating significant FFR

There was also convincing evidence of the incremental value of adding CTP and TAG320 to CTA assessment (MDCT-IP) for detection of significant FFR by NRI (1.46, $P < 0.0001$) and IDI (0.26, $P < 0.0001$). In addition, MDCT-IP also had incremental value over TAG320 + CTA assessment by NRI (0.93, $P < 0.0001$) and IDI (0.12, $P < 0.0001$). MDCT-IP also had incremental value over CTP + CTA assessment by NRI (1.45, $P < 0.0001$) and IDI (0.10, $P < 0.0001$).

Discussion

In this study we have compared for the first time the diagnostic accuracy of combined assessment of CTP + CTA and of TAG320 + CTA obtained using a 320-detector row CT with invasive functional standard – fractional flow reserve as reference. We have also demonstrated for the first time the diagnostic accuracy of an integrated approach (MDCT-IP) which combines 3 modalities (CTA, CTP and TAG320) in discriminating functionally significant coronary arterial stenoses.

TAG320, CTP and CTA assessment on 320-detector row CT with fractional flow reserve as reference standard

Based on the results from the FAME study, it is widely accepted that revascularisation based on the functional significance of coronary artery stenoses as opposed to anatomical assessment translates to lower cost and better outcome (8). Therefore FFR which is the 'gold standard' of functional assessment of coronary artery stenosis was chosen as the reference in this study. Ideally the anatomical and functional significance of disease can be determined using a single non-invasive imaging modality in a single examination. To date, the only non-invasive method which has shown promise is multi-detector computed tomography (MDCT) with previous studies having demonstrated the diagnostic accuracy and incremental predictive value of combined CTP and CTA assessment over CTA alone (6,17). However this assessment requires two separate (stress and rest) scans which require additional radiation exposure and contrast. In our study, combined CTP and CTA assessment was associated with a mean radiation dose of 9.8 mSv compared to 4.6 mSv for CTA alone. Therefore, efforts have been made to develop MDCT techniques that can assess functional significance of coronary artery stenoses without adenosine administration and additional contrast and radiation. Transluminal attenuation gradient (TAG) is a technique based on the kinetics of iodinated contrast across coronary artery stenosis which has recently shown promise for coronary artery stenosis assessment (15,18) (Figure 2). The 320-detector row CT by enabling near isophasic, single-beat imaging of the entire coronary tree is ideal for TAG assessment (4,19). We have recently demonstrated the diagnostic accuracy and incremental predictive value of combined CTA and TAG320 assessment over CTA alone on a 320-detector CT (4). Nonetheless, no studies have compared the diagnostic accuracy of combined assessment of CTP + CTA and TAG320 + CTA. In addition, the diagnostic accuracy of combined assessment of CTP + TAG320 + CTA (MDCT-IP) has not been described.

Diagnostic accuracy of CTA, combined assessment of CTP + CTA and TAG320 + CTA

The high sensitivity (89%) and negative predictive value (92%) but modest specificity (65%) and positive predictive value (57%) of CTA in our study is comparable to previous studies (2,17). Meanwhile, there have only been 3 previous studies which have compared the diagnostic accuracy of combined CTP and CTA assessment with FFR as the reference standard (3,6,17). The improved specificity (89%) but reduced sensitivity (76%) with combined CTP and CTA assessment in our study is comparable to the 3 previous studies which have described specificity that ranged from 90-95% and sensitivity of 68-87%. The diagnostic accuracy of combined TAG320 and CTA assessment has only been reported in our previous study (4). Combined TAG320 and CTA in this study showed excellent specificity (97%) with modest sensitivity (73%) whilst the c-statistic was 0.848 which is comparable to our previous study (AUC = 0.89). It is however likely to be superior to the diagnostic accuracy (AUC = 0.63) of TAG assessment on 64-detector row MDCT (20).

Comparison of diagnostic accuracy of combined CTP + CTA, combined TAG320 + CTA and combined CTP + TAG320 + CTA (MDCT-IP)

Calcified disease remains an important challenge for the interpretation of CTA. Up to 33% of patients may have unevaluable coronary segments due to the presence of extensive calcification (17,21). Our study had higher prevalence of calcified vessels (50 vessels, 39%) compared to some recent studies (24 vessels, 29%) (20) which may limit CTA and TAG320 assessment. As a result 22 vessels could not be reliably assessed by CTA whilst TAG320 assessment could not be performed in 9% of patients. As TAG320 assessment involves measurement of mean luminal radiological attenuation (HU) at 5-mm intervals from the ostium to a distal level, it is more susceptible to the influence of calcification and artefact in the entire epicardial coronary artery course (Figure 3). Its diagnostic utility is also uncertain in branch

vessel disease. These factors limited the number of vessels that could be assessed by TAG320 in this study.

In order to compare the diagnostic accuracy of CTP + CTA, TAG320 + CTA and MDCT-IP, we compared 97 vessels which were successfully assessed by all three methods. To our knowledge, this is the first study that has compared the diagnostic accuracy of these novel assessments. We found that the diagnostic accuracy of combined assessment of TAG320 + CTA (AUC = 0.844) and combined CTP + CTA (AUC = 0.845) is comparable. In addition, we demonstrated that combined assessment of CTP + TAG320 + CTA (MDCT-IP) had the best diagnostic accuracy (AUC = 0.91). The MDCT-IP approach was superior to combined assessment of TAG320 + CTA and CTP + CTA. Our study highlights a potential practical application for MDCT as a ‘one-stop-shop’ non-invasive assessment of coronary artery stenosis which might also address function. In this cohort, the addition of CTP resulted in successful evaluation of 123 (97%) vessels. The addition of CTP to CTA and TAG320 analysis significantly increased the number of vessels that could be evaluated in this study.

Limitations

Our results represent a retrospective single-centre experience involving 75 patients who underwent clinically indicated FFR and hence needs confirmation with larger prospective multicentre studies with FFR performed routinely or on a research basis. In the studied cohort, three vessel fractional flow reserve data was not available, hence limiting the general applicability of our findings. We have accordingly presented the accuracy data on a per vessel basis. Although there is incremental predictive value of TAG320 when added to CTA, its utility at this stage is limited to vessels without significant calcification, vessels with a cross-sectional area above 2.0 mm² (or diameter above 1.6mm) and vessels not affected by artefact anywhere

along its entire course. Despite the well-controlled heart rate (mean of 55 bpm) of patients in this study which has a high prevalence of patients with known coronary artery disease, TAG320 evaluation cannot be done in all vessels as heavily calcified vessels are often not evaluable by TAG320. In this study, calcium scores were not performed. We therefore could not explore whether a certain cut-off on calcium score would render TAG320 uninterpretable leading to the need for CTP as an upfront ischaemic assessment in certain patients. We also excluded chronic total and subtotal occlusion vessels, as the effect of TAG on collaterals remains unestablished. Future studies and technological advances are required to improve the utility of TAG320 in these vessels. In addition the utility of TAG320 also needs to be validated using more current acquisition and reconstruction protocols such as the model-based iterative reconstruction algorithm ("AIDR-3D"). Lastly the interpretation of CTP has been performed in the same setting as CTA which may introduce bias. Combined interpretation has been chosen as recommended by guidelines in preference to separate blinded interpretations of CTA and CTP (13).

Conclusion

Based on the results of the study, combined assessment of TAG320 + CTA and CTP + CTA provide comparable diagnostic accuracy for functional assessment of coronary artery stenosis in vessels without significant calcification or artefact. Combined assessment of TAG320 + CTP + CTA (MDCT-IP) may provide improved diagnostic accuracy for functional assessment of coronary artery stenosis. Larger studies are required to determine the diagnostic and prognostic value of these assessments.

Table 1 Patient characteristic (n =75)

Characteristic	Value
Age (years)	64.0 ± 10.8
Gender (M/F)	52/24
Diabetes, n (%)	14 (19%)
Hypertension, n (%)	62 (83%)
Hypercholesterolemia, n (%)	55 (73%)
Current smoker, n (%)	12 (16%)
Family history of IHD, n (%)	25 (33%)
Known Coronary Artery Disease	38 (51%)
Previous MI, n (%)	5 (7%)
Previous PCI, n (%)	9 (12%)
Medications	
Aspirin, n (%)	61 (81%)
Clopidogrel, n (%)	20 (27%)
Beta-blocker, n (%)	42 (56%)
ACE-inhibitor, n (%)	16 (21%)
ARB, n (%)	26 (35%)
Statin, n (%)	58 (77%)
Calcium channel blocker, n (%)	25 (33%)

Table 2 Computed tomography scan parameters (n = 75)

Parameter	CTA	CTP
Heart rate (bpm)	55.1 ± 7.5	67 ± 13
Beta blocker usage, <i>n</i> (%)		
Oral metoprolol	48 (64%)	
Intravenous metoprolol	19 (25%)	
Beta-blocker dose, mg		
Oral metoprolol	44 ± 49	
Intravenous metoprolol	3.1 ± 7.5	
Tube voltage (kV)	119 ± 4	119 ± 4
Tube current (mAs), mean ± SD	486 ± 58	421 ± 61
Dose length product (mGy-cm), mean ± SD	257 (224;295)	310 (197;446)
Estimated radiation effective dose (mSv), mean ± SD	4.6 ± 3.2	4.8 ± 3.5

Table 3 Per vessel territory diagnostic accuracy of quantitative coronary angiography (QCA), computed tomography coronary angiography (CTA), combined CTA and CTP assessment, combined CTA and transluminal attenuation gradient (TAG320) assessment and integrated CTA + CTP + TAG320 (MDCT-IP) assessment, compared with fractional flow reserve

	QCA >50% (n = 127)	QCA >70% (n = 127)	CTA (n = 127)	CTA + TAG (n = 97)	CTA + CTP (n = 123)	MDCT-IP (n = 117)
Sensitivity, %	61	25	89	73	76	88
Specificity, %	88	99	65	97	89	83
PPV, %	73	92	57	92	78	74
NPV, %	81	71	92	87	88	93

Table 4. Per vessel diagnostic accuracy of CTA + TAG320, CTA + CTP and CTA + CTP + TAG320 (MDCT-IP) methods in 97 vessels

	CTA + TAG320	CTA + CTP	CTA + CTP + TAG320 (MDCT-IP)
Sensitivity, %	73	81	97
Specificity, %	97	87	84
PPV, %	92	76	76
NPV, %	87	90	98

Figure 1. MDCT integrated TAG320 and CTP protocol (MDCT-IP)

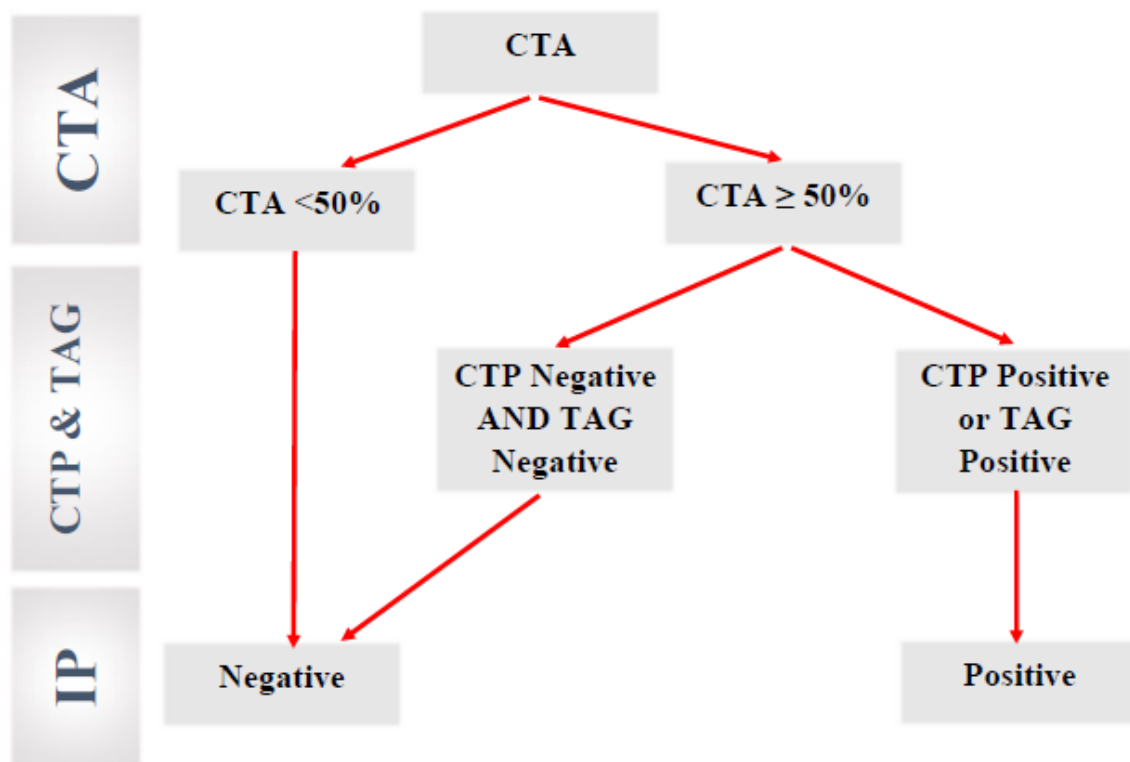


Figure 2. Representative example of left anterior descending artery with abnormal TAG320, CTP and FFR measurements. A) Left anterior descending artery with moderate obstructive plaque burden imaged by computed tomography angiography B) Transluminal attenuation gradient (TAG320) is shown. Black triangular dots represent 5-mm intervals at which intraluminal attenuation (HU) were measured. The TAG320 was -26.1 while the FFR was 0.51. C) Left anterior descending artery with severe stenosis imaged by invasive coronary angiography D) Perfusion defect noted in mid anteroseptum and anterior wall imaged by CTP

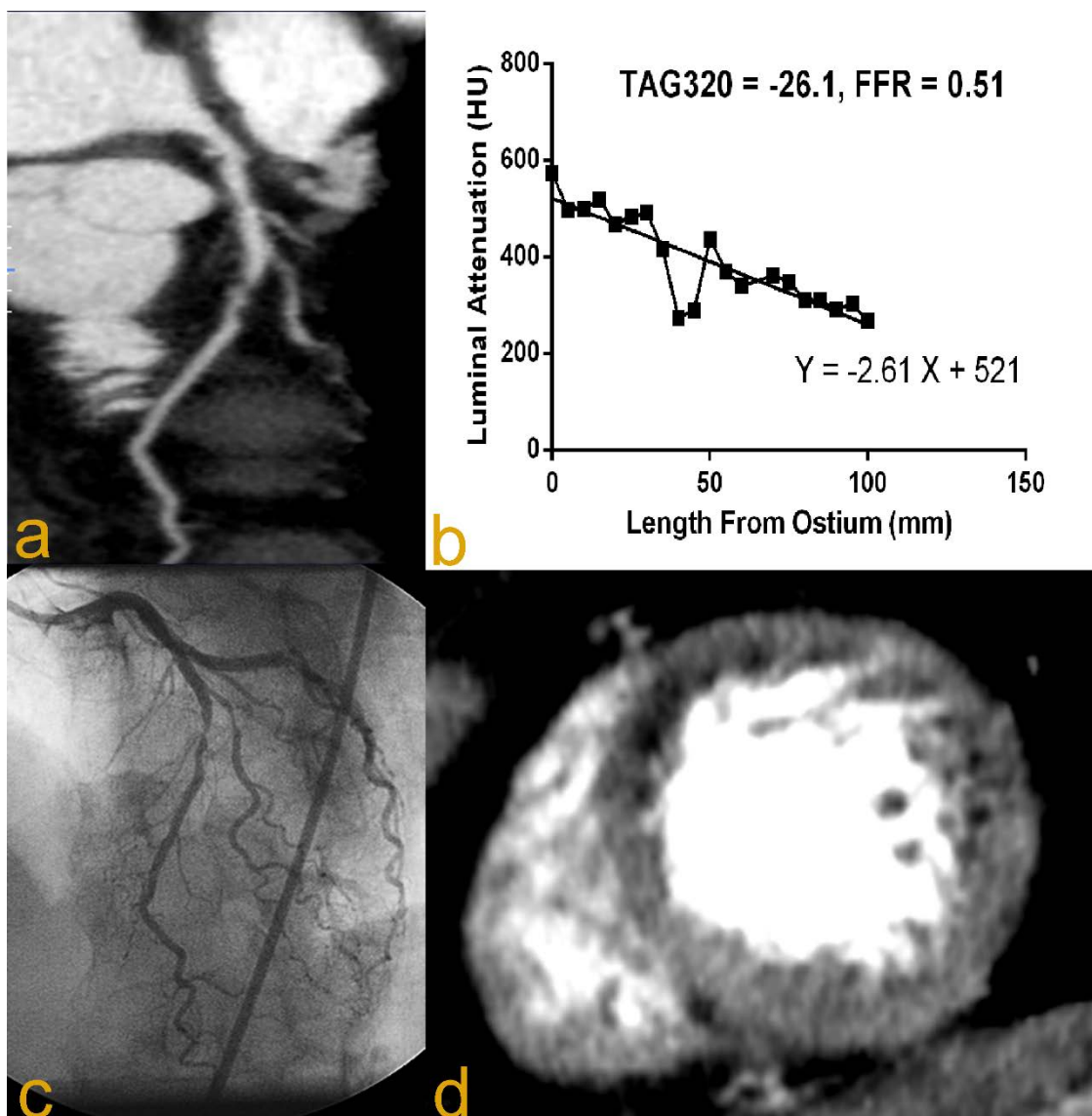


Figure 3. Representative example of left anterior descending artery with abnormal CTP and FFR measurements. Due to artefact in mid vessel, TAG320 analysis was not possible

A) Left anterior descending artery with significant artefact in mid vessel imaged by computed tomography angiography. B) Perfusion defect noted in mid anterior wall imaged by CTP C) Left anterior descending artery with severe stenosis imaged by invasive coronary angiography. The fractional flow reserve was 0.69.

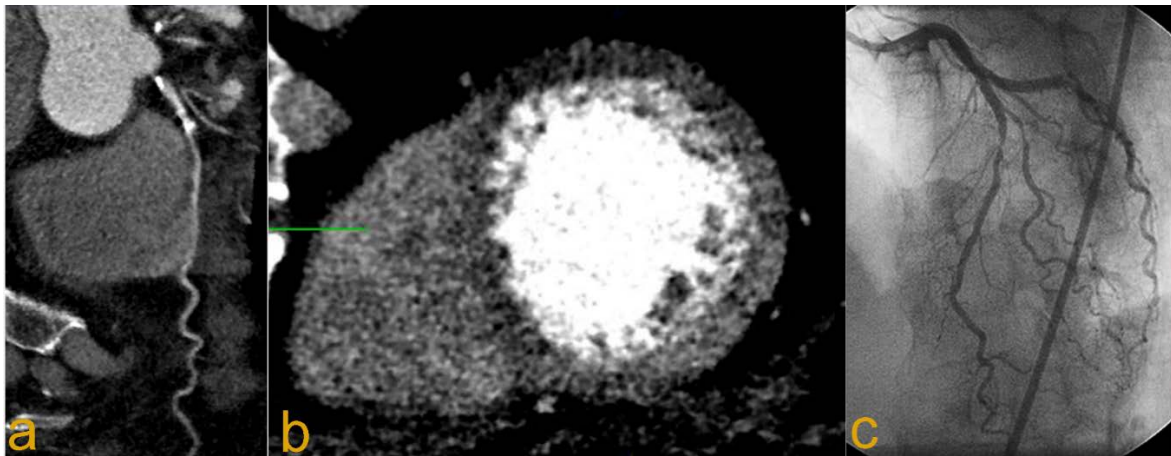
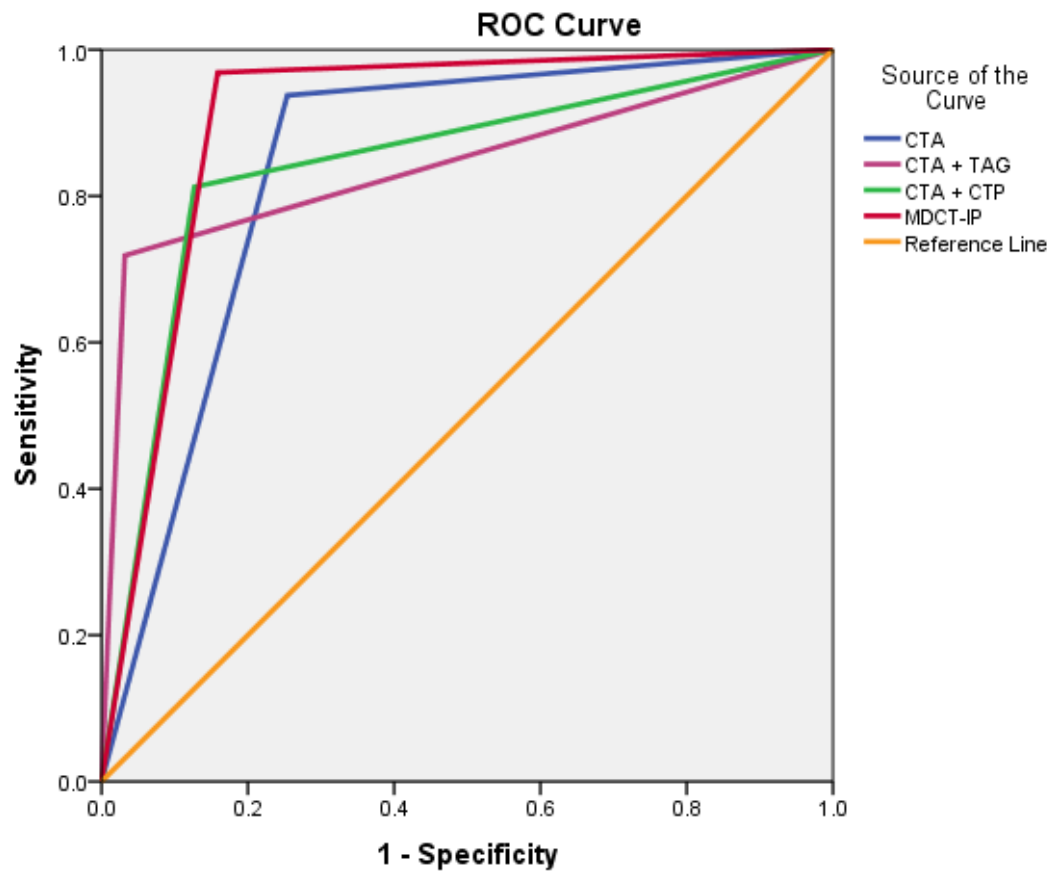


Figure 4. Receiver operating characteristics analysis showing per vessel diagnostic accuracy of CTA (0.84), CTA + TAG320 (AUC = 0.844), CTA + CTP (AUC = 0.845) and CTA + CTP + TAG320 (MDCT-IP) (AUC = 0.905) in 97 vessels.



Diagonal segments are produced by ties.

Appendix 1: Per vessel diagnostic accuracy of CTA + TAG320, CTA + CTP and CTA + CTP + TAG320 (MDCT-IP) methods in 50 calcified vessels

	CTA + TAG320 (n=38)	CTA + CTP (n=48)	MDCT-IP (n=46)
Sensitivity, %	83	87	88
Specificity, %	90	72	80
PPV, %	88	74	81
NPV, %	86	86	87
Accuracy,%	87	79	84

References

1. Budoff MJ, Dowe D, Jollis JG et al. Diagnostic performance of 64-multidetector row coronary computed tomographic angiography for evaluation of coronary artery stenosis in individuals without known coronary artery disease: results from the prospective multicenter ACCURACY (Assessment by Coronary Computed Tomographic Angiography of Individuals Undergoing Invasive Coronary Angiography) trial. *J Am Coll Cardiol* 2008;52:1724-32.
2. Meijboom WB, Van Mieghem CA, van Pelt N et al. Comprehensive assessment of coronary artery stenoses: computed tomography coronary angiography versus conventional coronary angiography and correlation with fractional flow reserve in patients with stable angina. *J Am Coll Cardiol* 2008;52:636-43.
3. Ko BS, Cameron JD, Meredith IT et al. Computed tomography stress myocardial perfusion imaging in patients considered for revascularization: a comparison with fractional flow reserve. *Eur Heart J* 2012;33:67-77.
4. Wong DT, Ko BS, Cameron JD et al. Transluminal attenuation gradient in coronary computed tomography angiography is a novel noninvasive approach to the identification of functionally significant coronary artery stenosis: a comparison with fractional flow reserve. *J Am Coll Cardiol* 2013;61:1271-9.
5. Koo BK, Erglis A, Doh JH et al. Diagnosis of ischemia-causing coronary stenoses by noninvasive fractional flow reserve computed from coronary computed tomographic angiograms. Results from the prospective multicenter DISCOVER-FLOW (Diagnosis of Ischemia-Causing Stenoses Obtained Via Noninvasive Fractional Flow Reserve) study. *J Am Coll Cardiol* 2011;58:1989-97.

6. Ko BS, Cameron JD, Leung M et al. Combined CT Coronary Angiography and Stress Myocardial Perfusion Imaging for Hemodynamically Significant Stenoses in Patients With Suspected Coronary Artery Disease: A Comparison With Fractional Flow Reserve. *JACC Cardiovasc Imaging* 2012;5:1097-111.
7. Nasis A, Ko BS, Leung MC et al. Diagnostic accuracy of combined coronary angiography and adenosine stress myocardial perfusion imaging using 320-detector computed tomography: pilot study. *Eur Radiol* 2013.
8. Tonino PA, De Bruyne B, Pijls NH et al. Fractional flow reserve versus angiography for guiding percutaneous coronary intervention. *N Engl J Med* 2009;360:213-24.
9. De Bruyne B, Pijls NH, Kalesan B et al. Fractional flow reserve-guided PCI versus medical therapy in stable coronary disease. *N Engl J Med* 2012;367:991-1001.
10. Kern MJ, Samady H. Current concepts of integrated coronary physiology in the catheterization laboratory. *J Am Coll Cardiol* 2010;55:173-85.
11. Sianos G, Morel MA, Kappetein AP et al. The SYNTAX Score: an angiographic tool grading the complexity of coronary artery disease. *EuroIntervention* 2005;1:219-27.
12. Hausleiter J, Meyer T, Hermann F et al. Estimated radiation dose associated with cardiac CT angiography. *JAMA* 2009;301:500-7.
13. Mehra VC, Valdiviezo C, Arbab-Zadeh A et al. A stepwise approach to the visual interpretation of CT-based myocardial perfusion. *J Cardiovasc Comput Tomogr* 2011;5:357-69.
14. Cerqueira MD, Weissman NJ, Dilsizian V et al. Standardized myocardial segmentation and nomenclature for tomographic imaging of the heart. A statement for healthcare professionals from the Cardiac Imaging Committee of the Council on Clinical Cardiology of the American Heart Association. *Journal of nuclear cardiology : official publication of the American Society of Nuclear Cardiology* 2002;9:240-5.

15. Choi JH, Min JK, Labounty TM et al. Intracoronary transluminal attenuation gradient in coronary CT angiography for determining coronary artery stenosis. *JACC Cardiovasc Imaging* 2011;4:1149-57.
16. Pencina MJ, D'Agostino RB, Sr., D'Agostino RB, Jr., Vasan RS. Evaluating the added predictive ability of a new marker: from area under the ROC curve to reclassification and beyond. *Statistics in medicine* 2008;27:157-72; discussion 207-12.
17. Bettencourt N, Chiribiri A, Schuster A et al. Direct comparison of cardiac magnetic resonance and multidetector computed tomography stress-rest perfusion imaging for detection of coronary artery disease. *J Am Coll Cardiol* 2013;61:1099-107.
18. Chow BJ, Kass M, Gagne O et al. Can differences in corrected coronary opacification measured with computed tomography predict resting coronary artery flow? *J Am Coll Cardiol* 2011;57:1280-8.
19. Steigner ML, Mitsouras D, Whitmore AG et al. Iodinated contrast opacification gradients in normal coronary arteries imaged with prospectively ECG-gated single heart beat 320-detector row computed tomography. *Circ Cardiovasc Imaging* 2010;3:179-86.
20. Yoon YE, Choi JH, Kim JH et al. Noninvasive diagnosis of ischemia-causing coronary stenosis using CT angiography: diagnostic value of transluminal attenuation gradient and fractional flow reserve computed from coronary CT angiography compared to invasively measured fractional flow reserve. *JACC Cardiovasc Imaging* 2012;5:1088-96.
21. Blankstein R, Shturman LD, Rogers IS et al. Adenosine-induced stress myocardial perfusion imaging using dual-source cardiac computed tomography. *J Am Coll Cardiol* 2009;54:1072-84.

Chapter 3

**Diagnostic Performance of Transluminal
Attenuation Gradient and Non-Invasive
Fractional Flow Reserve derived from 320
detector Computed Tomography Angiography
to Diagnose Hemodynamically Significant
Coronary Stenosis- a NXT substudy**

PART B: Suggested Declaration for Thesis Chapter

[This declaration to be completed for each conjointly authored publication and to be placed at the start of the thesis chapter in which the publication appears.]

Monash University

Declaration for Thesis Chapter

Chapter 3: Diagnostic Performance of Transluminal Attenuation Gradient and Non-Invasive Fractional Flow Reserve derived from 320 detector Computed Tomography Angiography to Diagnose Hemodynamically Significant Coronary Stenosis- a NXT substudy

Declaration by candidate

In the case of Chapter 3, the nature and extent of my contribution to the work was the following:

Nature of contribution	Extent of contribution (%)
Conceived the study, participant recruitment, acquisition of FFR, analysis and interpretation of data and wrote the manuscript.	70

The following co-authors contributed to the work. If co-authors are students at Monash University, the extent of their contribution in percentage terms must be stated:

Name	Nature of contribution	Extent of contribution (%) for student co-authors only
Dennis Wong	Assisted in study design and involved in analysis and interpretation of data and assisted in manuscript drafting and critical revision.	10
Bjarne Norgaard	Critical revision of manuscript.	
Darryl Leong	Statistical analysis and Revising of manuscript. Final approval of manuscript submitted.	
James Cameron	Assisted in interpretation of data and critical revision of manuscript.	

Sara Gaur	Assisted in analysis of data. Revising of manuscript. Final approval of manuscript submitted.	
Mohamed Marwan	Performed core lab analysis of CTA	
Stephan Achenbach	Performed core lab analysis of CTA	
Sachio Kuribayashi	Recruitment of participants, contributed to manuscript revision	
Takeshi Kimura	Recruitment of participants, contributed to manuscript revision	
Ian Meredith	Contributed to critical manuscript revision	
Sujith Seneviratne	Contributed to critical manuscript revision	

The undersigned hereby certify that the above declaration correctly reflects the nature and extent of the candidate's and co-authors' contributions to this work*.

**Candidate's
Signature**

	Date 15/10/2014
---	----------------------------------

Preface:

While the diagnostic performance of traditional stress modalities have been benchmarked against its ability to diagnose obstructive anatomical disease on invasive angiography, the new generation CT functional tests have been increasingly benchmarked against invasive fractional flow reserve. Non invasive fractional flow reserve (FFR_{CT}) is a modality which has been most extensively tested against invasive FFR, comprising of 3 large multicentre trials which included in excess of 700 patients. The most recent included the NXT trial, published by Norgaard in JACC in 2014, comprised of 254 patients of whom 42 were recruited from MonashHEART which was the second largest recruiting centre in the trial.

For this reason, I have been offered to be a co-author of the NXT trial manuscript, and invited to be the principal investigator of the NXT substudy to compare the diagnostic performance of TAG and FFR_{CT} in the subset patients who had undergone CT coronary angiography performed using wide detector CT.

While both CT transluminal attenuation gradient and non invasive fractional flow reserve (FFR_{CT}) can be derived from typically acquired resting CT coronary angiography datasets, the two techniques differed in how they are derived, analysed and interpreted. Being the lead investigator certainly allowed me to appreciate this.

Uniquely the transluminal attenuation gradient in this study was performed using a semi-automated method, and hence a new retrospectively determined gradient threshold was determined. The Hounsfield units were sampled at 1mm intervals down a coronary artery,

rather than at 5mm intervals. The software can also determine precisely distal point at which HU sampling may be terminated.

Title

Diagnostic Performance of Transluminal Attenuation Gradient and Non-Invasive Fractional Flow Reserve derived from 320 detector Computed Tomography Angiography to Diagnose Hemodynamically Significant Coronary Stenosis- a NXT substudy

Authors

Brian S Ko MBBS (Hons), PhD^{1}, Dennis TL Wong MBBS (Hons), PhD^{1, 2}, Bjarne L. Norgaard MD, PhD³, Darryl P Leong MBBS (Hons), MPH, PhD², James D Cameron MBBS, MD¹, Sara Gaur, MD³, Mohamed Marwan MD, PhD⁴, Stephan Achenbach MD, PhD⁴, Sachio Kuribayashi MD, PhD⁵, Takeshi Kimura MD, PhD⁶, Ian T Meredith MBBS (Hons), PhD¹ Sujith K Seneviratne MBBS¹*

Affiliation of Authors

¹ *Monash Cardiovascular Research Centre, Department of Medicine (Monash Medical Centre) Monash University and Monash Heart, Monash Health, 246 Clayton Road, Clayton, 3168 VIC, Australia*

² *Discipline of Medicine, University of Adelaide, Adelaide, Australia*

³ *Department of Cardiology, Aarhus University Hospital, Skejby, Aarhus, Denmark*

⁴ *Department of Cardiology, Erlangen University Hospital, Erlangen, Germany*

⁵ *Department of Diagnostic Radiology, Keio University, Tokyo, Japan*

⁶ *Department of Cardiovascular Medicine, Kyoto University, Kyoto, Japan*

^{*} *Corresponding author*

Financial disclosures

Dr Norgaard has received research grants from Edwards Lifesciences. Dr Achenbach has received research grants from Siemens, Guerbet and Abbott, and is a consultant for Siemens, Biotronik, and HeartFlow. Dr Seneviratne has given lectures at meetings organized by Toshiba. Dr Meredith has received honorarium from and has served as an advisor or consultant for Boston Scientific and Medtronic, and has served as a speaker or a member of the speaker's bureaus for Boston Scientific and Medtronic.

Structured abstract

Objectives: We sought to compare the diagnostic performance of 320 detector CT coronary angiography (CTA) derived computed fractional flow reserve (FFR_{CT}) and transluminal attenuation gradient (TAG320) to diagnose hemodynamically significant stenosis as determined by invasive FFR.

Background: In its current form, CCTA is limited in assessing the hemodynamic significance of coronary stenoses. Novel techniques based on CTA have been developed to improve its diagnostic performance, however there remain limited data comparing these methods.

Methods: Fifty one consecutive patients who underwent CTA and invasive coronary angiography with FFR measurement were included. Independent core laboratories determined CAD severity by CTA, TAG320, FFR_{CT} and FFR. TAG320 is defined as the linear regression coefficient between luminal attenuation and axial distance from the coronary ostium. FFR_{CT} was computed from CTA data using computational fluid dynamics technology.

Results: Among 82 vessels, 24 lesions (29%) had ischemia by FFR (FFR \leq 0.80). FFR_{CT} exhibited a stronger correlation with invasive FFR when compared with TAG320 ($R^2=0.71$ vs 0.34, $P<0.0001$). Overall per vessel accuracy, sensitivity, specificity, positive and negative predictive values for TAG320 (<15.37) was 78%, 58%, 86%, 64% and 83% respectively; and those of FFR_{CT} were 83%, 92%, 79%, 65% and 96% respectively. Receiver operating characteristic curve analysis showed a significantly larger area under the curve (AUC) for FFR_{CT} (0.93) compared to that for TAG320 (0.72, $P=0.003$) and CTA alone (0.68, $P=0.008$).

Conclusion: Non-invasive FFR computed from 320 detector CTA provides better diagnostic performance for the diagnosis of hemodynamically significant coronary stenoses compared to CTA and TAG320.

Keywords

Fractional flow reserve

CT coronary angiography

Invasive angiography

Transluminar attenuation gradient

Non invasive fractional flow reserve

Condensed abstract

This study compared the diagnostic performance of 320 detector CT coronary angiography (CTA) derived fractional flow reserve (FFR_{CT}) and transluminar attenuation gradient (TAG320) to detect hemodynamically significant stenoses as determined by invasive fractional flow reserve ($\text{FFR} \leq 0.80$). Fifty one patients, including 82 vessels, with suspected coronary artery disease were studied. Per vessel sensitivity and specificity for TAG320 (<15.37) was 78% and 58%; and FFR_{CT} (≤ 0.80) was 92% and 79% respectively. Receiver operating characteristic curve analysis showed a significantly larger area under the curve for FFR_{CT} (0.93) compared to that for TAG320 (0.72, $P=0.003$) and CTA alone (0.68, $P=0.008$). Diagnostic performance of wide detector CTA derived FFR_{CT} is comparable to invasive FFR and superior in diagnosing hemodynamically significant stenoses compared to CTA and TAG320.

Abbreviation list

CTA – CT coronary angiography

FFR_{CT} – Non invasive fractional flow reserve

TAG – Transluminal attenuation gradient

FFR- Invasive fractional flow reserve

ICA – Invasive coronary angiography

PPV- Positive predictive value

NPV – Negative predictive value

CT coronary angiography (CTA) is an established non-invasive method for anatomical assessment of coronary stenoses (1), yet has limited specificity for diagnosing their hemodynamic significance (2). Novel CT techniques have recently been developed including transluminal attenuation gradient (TAG) and non-invasive fractional flow reserve derived from CT (FFR_{CT}) in an attempt to improve the diagnostic performance of CTA.

TAG is defined as the linear regression coefficient between luminal attenuation and axial distance from the coronary ostium. The high diagnostic performance of TAG, using 320-detector CT, which enables near isophasic, single-beat imaging of the entire coronary tree, has been demonstrated (3). Computational fluid dynamics as applied to CTA images enables prediction of blood flow and pressure in coronary arteries and calculation of lesion-specific fractional flow reserve (4). FFR_{CT} has been demonstrated to have high diagnostic performance for detection and exclusion of hemodynamically significant stenoses (5-7). Both techniques can be computed from typically acquired CTA scans without need of additional image acquisition or administration of medication. However their diagnostic performance has not been compared based on images acquired using wide-detector CT.

In the present study, our primary aim was to compare in stable coronary artery disease the diagnostic performance of TAG320 and FFR_{CT} derived from 320-detector CTA to diagnose hemodynamically significant stenosis as determined by invasive FFR performed at the time of invasive angiography (ICA). The secondary aim was to evaluate the incremental value of TAG320 and FFR_{CT} to CTA alone in the diagnosis of hemodynamically significant stenosis.

Methods

From the prospective NXT study (Analysis of Coronary Blood Flow Using CT Angiography: Next Steps), consecutive patients with suspected coronary artery disease who underwent 320 detector CTA and invasive coronary angiography with FFR measurement were studied. The rationale, design and eligibility criteria of the NXT study have been previously described (8). Exclusion criteria included previous coronary intervention or coronary bypass surgery, contraindications to beta-blocking agents, nitroglycerin, or adenosine, suspected acute coronary syndrome, previous myocardial infarction <30 days before coronary CTA or between coronary CTA and ICA and body mass index $>35\text{kg/m}^2$. Patients with non-evaluable FFR, or with CTA images that were determined as non-evaluable for FFR_{CT} or TAG320 were excluded. All study patients provided written informed consent.

Protocol for CTA acquisition and analysis

CTA was performed using prospective ECG gating and 320 detector row CT (Aquilion One or Aquilion Vision, Toshiba Medical Systems, Japan). The scan was acquired during injection of 60-75ml of 100% iohexal 56.6/75mL (Omnipaque 350, GE Healthcare, United Kingdom) at 5ml/s, followed by 30ml of saline at the same rate. Scans were either manually triggered or automated triggered when the contrast attenuation reached 150HU in the descending aorta. Scan parameters were as follows: detector collimation 320 x 0.5mm; tube current 300 to 500mA (depending on BMI); tube voltage 100-135kV depending on BMI, temporal resolution 135 to 170ms. In adherence to quality standards as defined in guidelines (9), oral and/or intravenous beta-blockers were administered targeting a heart rate of <60beats/min, and sublingual nitrates were administered to ensure coronary vasodilatation. Core laboratory analysis (Erlangen, Germany) for luminal diameter stenosis in each coronary artery segment

≥ 2 mm diameter using the 18-segment coronary model was performed. Significant stenosis was defined as stenosis $\geq 50\%$ in a major epicardial coronary artery segment ≥ 2 mm in diameter.

FFR_{CT} computation

Using the most recent generation of FFR_{CT} analysis software (7), analysis was performed in a blinded fashion (Redwood City, Heartflow Inc, CA, USA). For each patient, a quantitative 3-dimensional luminal model of the aortic root and epicardial coronary arteries was generated from coronary CTA images. Coronary blood flow and pressure were computed under conditions simulating maximal hyperaemia, and FFR_{CT} was computed throughout the coronary arterial tree. For occluded arteries FFR_{CT} of 0.50 was assigned. A FFR_{CT} ≤ 0.80 was considered to be significant. For the combined FFR_{CT} + CTA assessment, vessels were classified as non-significant if there was a $< 50\%$ CTA stenosis. Vessels were classified as significant if there was a $\geq 50\%$ stenosis on CTA and FFR_{CT} was ≤ 0.80 .

TAG320 analysis

Core laboratory analysis of TAG320 was performed with a semi-automated method using dedicated computer software (Toshiba Medical Systems, Japan) in a blinded fashion (MonashHEART, Clayton, Australia). Vessel centreline and contouring was automatically determined for each major coronary artery and was manually corrected if necessary. Cross sectional images perpendicular to the vessel centreline were then reconstructed. The mean luminal radiological attenuation (in Hounsfield units) was measured at 1mm intervals, from the ostium to a distal level where the cross-sectional minimal area fell below 2mm^2 . The data points in segments with motion or blooming artefacts from luminal calcium were manually excluded from analysis. The TAG320 value was defined as the linear regression coefficient

between intraluminal radiological attenuation (in Hounsfield units) and length from the ostium (in millimetres). TAG320 was performed for both stenosed and occluded arteries(10). A retrospectively determined TAG320 cut-off was determined from the dataset and taken to indicate significant stenosis. For combined TAG320+CTA assessment, vessels were classified as non-significant if there was a <50% CTA stenosis. Vessels were classified as significant if there was a $\geq 50\%$ stenosis on CTA and TAG320 was significant.

Invasive angiography and fractional flow reserve

ICA was performed according to standard practice. Measurement of FFR (Pressure Wire, St Jude Medical, Minneapolis, USA) was performed during ICA in at least one vessel with diameter $\geq 2\text{mm}$ and stenosis $\geq 30\%$. Tracings were evaluated at an FFR core laboratory (Harrington Heart and Vascular Institute, University Hospitals, Cleveland, Ohio) to assess achievement of steady-state maximal hyperaemia, pressure drift and other artefacts that could compromise FFR interpretation. Segments showing angiographic total occlusion were assigned an FFR value of 0.50.

Statistical analysis:

Categorical variables are presented as frequencies and percentages, with continuous variables as mean \pm SD or median (interquartile range). Comparisons of continuous variables were performed using the Kruskal-Wallis test. Per vessel sensitivity, specificity, positive predictive (PPV) and negative predictive values (NPV) of CTA, TAG320, FFR_{CT}, CTA+TAG320 and CTA+FFR_{CT} are calculated and expressed with 95% confidence intervals. The discriminatory ability of both TAG320+CTA and FFR_{CT} (≤ 0.80) for the identification of hemodynamically significant stenosis was evaluated on a per vessel basis by the area-under-the-receiver operating

characteristic curve. Invasive FFR ≤ 0.80 was the reference standard. Comparisons were performed using the DeLong method (11) and Bonferroni's adjustment was made for multiple comparisons. The category-free net reclassification index was used to determine whether TAG 320 and FFR_{CT} improve vessel classification as hemodynamically significant, compared with CTA alone(12).

Statistical analysis was performed with SPSS version 18 (SPSS, Chicago, Illinois) and STATA version 13.1 (STATA Corp, College Station, Texas). A P value <0.05 was considered statistically significant.

Results

Sixty-one consecutive patients with suspected coronary artery disease underwent 320 detector CTA and invasive coronary angiography with FFR measurement in Monash Medical Centre (n=40), Kyoto Hospital (n=18) and Keio Hospital (n=3) between September 2012 and August 2013 (Figure 1). Eight patients were excluded by the FFR core lab due to FFR measurement in a <2 mm vessel (n=7); or FFR was not performed (n=1). Two patients were excluded due to inability to perform TAG (vessel deemed too small on CT to perform TAG n=1; vessel found to severe stenosis with collateral supply n=1). Finally 82 vessels were analysed from 51 patients.

Mean age was 62.2 ± 10.4 years and 74.5% were male. Of the 82 coronary arteries, 34 were left anterior descending, 23 left circumflex and 25 right coronary arteries. There were 5 occluded vessels in 5 patients in which FFR_{CT} and FFR values were assigned. Baseline patient and vessel characteristics are listed in Tables 1 and 2. CT scan parameters are listed in Table 3. The number (percentage) of vessels with FFR ≤ 0.80 was 24 (29.3%).

Relationship of TAG320 and FFR_{CT} with FFR

The median (inter-quartile range) TAG320 was significantly lower in vessels with hemodynamically significant stenoses compared to vessels without hemodynamically significant stenosis, -17.2 (-20.0 to -6.40) HU/10 mm vs -8.86 (-13.2 to -3.83) HU/10mm (P=0.002). Median (inter-quartile range) FFR_{CT} was also significantly lower in vessels with hemodynamically significant stenosis compared to vessels without ischemia, 0.68 (0.50 to 0.75) vs 0.87 (0.81 to 0.93) (P<0.001).

Figure 2 illustrates the correlation between TAG320, FFR_{CT} and invasive FFR. TAG320 demonstrated a modest correlation with invasive FFR ($R^2=0.34$, $P<0.0001$). FFR_{CT} demonstrated strong correlation with invasive FFR ($R^2=0.71$, $P<0.0001$). On Bland Altman analysis, there was good agreement with a bias of -0.04 ± 0.08 (95% CI -0.19 to 0.11).

Diagnostic performance of CTA, TAG320 and FFR_{CT}

The diagnostic performance of CTA, TAG320, FFR_{CT}, TAG320+CTA and FFR_{CT}+CTA for diagnosis of hemodynamically significant stenoses is summarised in Table 4 and Figures 2 and 3. The ROC curve analysis for CTA alone showed an AUC of 0.68 (P=0.007). The sensitivity, specificity, PPV and NPV were 79%, 59%, 44% and 87% respectively.

A cut-off value of -15.37 HU/10mm was found to be optimal, and yielded 14 true positives, 50 true negatives, 8 false positives and 10 false negatives. The sensitivity, specificity, PPV and NPV of TAG320 were 58%, 86%, 64% and 83% respectively. The ROC curve analysis for

TAG320 demonstrated an AUC of 0.72 ($P = 0.002$), which was not found to be superior to the AUC of CTA (0.72 vs 0.68; $P=0.67$). The net reclassification index for TAG320 when compared with CTA was 0.89 (standard error ± 0.24 , $P<0.0002$). When CTA findings were combined with TAG320, the ROC AUC was 0.72, and sensitivity, specificity, PPV and NPV 45.8%, 98.3%, 91.7% and 81.4% respectively. There was modest yet not significant difference in ROC AUC when comparing CTA+TAG with CTA alone (0.72 vs 0.69; $P=0.59$).

Using a threshold of ≤ 0.80 , the ROC curve analysis for FFR_{CT} demonstrated an AUC of 0.93 ($P<0.001$) which was significantly superior to both CTA ($P=0.008$) and TAG320 ($P=0.003$). This resulted in 22 true positives, 46 true negatives, 12 false positives and 2 false negatives. Sensitivity, specificity, PPV and NPV of FFR_{CT} were 92%, 79%, 65% and 96%. The net reclassification index for FFR_{CT} when compared with CTA was 1.42 (SE ± 0.24 , $P<0.0001$). The ROC AUC for $\text{FFR}_{\text{CT}}+\text{CTA}$ was 0.78, with a sensitivity, specificity, PPV and NPV of 71%, 85%, 65% and 88%.

Interobserver variability and time taken of TAG320 analysis

The medium per vessel time required for TAG320 analysis was 200 seconds (interquartile range 118 to 276). Assessment of interobserver variability of TAG320 demonstrated an intraclass coefficient 0.985 95% CI 0.961-0.994. Based on Bland Altman analysis, there was a mean variability of -0.06 ± 1.18 , and the 95% limit of agreement was 2.37 to -2.25.

Discussion

This study demonstrates that the per-vessel FFR_{CT} has better association with invasive FFR compared with TAG320 and that diagnostic performance of FFR_{CT} is superior to TAG320 for the diagnosis of hemodynamically significant stenoses determined by invasive FFR in patients suspected of stable coronary artery disease. FFR_{CT} also demonstrated a superior net reclassification index than TAG320 when both were compared to CTA alone.

Diagnostic accuracy of wide detector FFR_{CT} and TAG

Three large multicentre observations trials have thus far evaluated the performance of FFR_{CT} when compared with invasive FFR (5-7). The most recent NXT study demonstrated a per vessel sensitivity, specificity, PPV and NPV of 84%, 86%, 61% and 95% respectively, using images acquired by CT scanners with varied longitudinal coverage including 64, 128, 256 and 320 detector CT (7). The results derived from this subset of NXT patients demonstrate consistent per vessel diagnostic performance of FFR_{CT} evaluated with wide detector CT as was reported in the entire NXT cohort. The high usage of prescan nitroglycerin and beta blockers (in 99%/67% and 100%/63% of patients respectively in the NXT study and this current study), may have contributed to this high accuracy by optimising image quality. This finding also suggests that the diagnostic performance FFR_{CT} may not be affected by the longitudinal coverage of CT scanners.

In contrast the diagnostic performance of TAG has been reported to differ when applied on CT images acquired by scanners with varied longitudinal coverage (3,13,14). Previous work demonstrated that the diagnostic accuracy of TAG derived from 64 and 256 detector CTA

acquisitions was not significantly different from CTA alone (13,14), while the results based on single centre studies using 320 detector CTA have to date shown the most promise. Wong et al reported in a retrospective single centre cohort of 54 patients, including 78 vessels, that TAG320 detected $\text{FFR} \leq 0.80$ with a per vessel sensitivity of 77%, specificity 74% and ROC AUC of 0.81(3). The accuracy of the technique further improved when added to CTA alone with a ROC AUC of 0.88 (3), and the combined approach was shown to have comparable accuracy as combined rest CTA and stress CT myocardial perfusion imaging (15). The superior results derived from TAG320 may be related to the ability of the 320-detector CT scanner to image the entire heart volume in a single gantry rotation hence enabling near isophasic, single beat imaging of the entire coronary tree.

This study uniquely evaluates the diagnostic performance of TAG320 in a cohort of patients recruited from multiple international centres. It is also the first to study the accuracy of a semi-automated technique by which TAG320 can be obtained. Comparable with the findings of the previous single centre studies (3,15), TAG320 is shown to have a higher accuracy than CTA alone mainly driven by improvements in specificity and positive predictive value. However in the current study, TAG exhibited a lower sensitivity related to a large number of false negative results. The sensitivity of TAG320 in this study was 58% which is lower than its sensitivity reported in two previous studies (77% and 71% respectively) (3,15). In this present cohort there is a slightly lower per vessel prevalence of FFR significant lesions when compared with previous studies (29% in this cohort, vs. 39% and 35% in two previous studies), which should typically favour rather than diminish sensitivity.

The observed lower accuracy and sensitivity of TAG320 may relate to the technique by which TAG320 was obtained in this study. Earlier studies reported the use of a manual technique in which the HU were sampled at 5mm intervals. TAG320 was determined in this study using a new semi-automated method in which HU are sampled along a vessel's centreline at 1mm intervals and the most distal point of the vessel in which HU was sampled was guided by automated luminal contouring. This technique increased the sampled points and the number of vessels in which TAG can be performed (only 2/84 vessels were excluded vs 30/127 of vessels in a previous studies (15). However algorithmic errors in luminal contouring may result in premature cessation in HU sampling in the distal vessel which can result in an overestimation of TAG to be less negative hence potentially associated with a larger number of false negative results.

Comparison of FFR_{CT} and TAG320

Our results demonstrate that the overall accuracy of both FFR_{CT} and TAG320 is higher than CTA alone (TAG320 78%; FFR_{CT} 83% vs CTA 65%). While the overall accuracy reported of TAG320 and FFR_{CT} are similar, comparison of ROC AUC and net reclassification indices in this study indicate that the diagnostic performance of FFR_{CT} is superior to TAG320 which may relate to the superior correlation of FFR_{CT} with invasive FFR than that observed for TAG320.

The superior correlation observed for FFR_{CT} may relate to its derivation technique, which permits the computation of pressure, flow and hence FFR along the entire coronary tree. Importantly assumptions are made for conditions of maximal hyperaemia and minimal microvascular resistance which mimics invasive FFR (4). In contrast, TAG320 has been postulated to represent resting coronary blood flow. This is based on observations by Lackner

et al which demonstrated a lower peak contrast attenuation and increased time required for passage of iodinated contrast through in vitro tube cross-sections with increasing degrees of stenosis compared with normal sections (16). Subsequent studies further demonstrated that differences in contrast opacification across a lesion and TAG along a vessel varied significantly in accordance to TIMI grade flow and stenosis severity (10,17,18). Hence in the absence of maximal hyperaemia, TAG may be influenced by the resistance from both epicardial artery stenoses and microvascular circulation, and a linear relationship between flow and pressure cannot be assumed. The diagnostic performance TAG320 in vessels which have been imaged during vasodilator stress may improve yet vasodilator stress typically increases heart rate by up to 15-20 beats per minute (19), which may significantly impact upon image quality and increase prevalence of motion artefacts.

Use of FFR_{CT} and TAG320 only in lesions with >50% CT stenosis

Previous studies have suggested that the presence of >50% stenosis on CTA may act as an important gatekeeper to defer invasive angiography and revascularisation. This is based on the observation that the presence of >50% stenosis may have high sensitivity and negative predictive value for $FFR \leq 0.80$. Meijboom et al demonstrated using 64 detector CT that CTA>50% had a 94% sensitivity and 93% NPV (2). Similarly Ko et. al. demonstrated a comparably high sensitivity and NPV for $FFR \leq 0.80$ in vessels studied using 320-detector CTA(20). The specificity and PPV for $FFR \leq 0.80$ is significantly limited and accordingly in clinical practice, patients identified with disease of $\geq 50\%$ severity on CTA often require non invasive functional stress testing to confirm the presence of ischemia before referral for invasive angiography and revascularisation.

It is for this reason that analysis has been performed to evaluate the diagnostic performance of TAG320 and FFR_{CT} when they are applied in the presence of a CTA stenosis of >50%. While our results demonstrate that their overall accuracy is higher than CTA alone (TAG320+CTA 83%; FFR_{CT}+CTA 81%; CTA alone 65%), this difference is not significant based on comparison of AUC on ROC analysis. Indeed, the AUC for TAG320 +CTA was equivalent to TAG alone (0.72), and FFR_{CT}+CTA was inferior to FFR_{CT} alone (0.93 vs 0.78).

Notably in this cohort with intermediate risk of CAD, per vessel sensitivity and negative predictive of CTA was 79% and 87% respectively, which suggests that a sizeable proportion of vessels had mild diffuse yet hemodynamically significant disease. As the combined technique requires a lesion to be significant on both CTA and TAG320 or FFR_{CT} to be scored as significant, the low sensitivity of CTA observed in this cohort may limit diagnostic performance of the combined technique. Our results however emphasise the ultimate aim of the combined technique which is to improve specificity and PPV. Notably the combined use of CTA with TAG320 and FFR_{CT} is highly specific for ischemia (98% and 85% respectively). For this reason, the finding of a significant TAG320 in particular in lesions with >50% stenosis on CTA, will almost certainly justify referral for invasive angiography and revascularisation.

Limitations

This study is a multicentre retrospective analysis of a prospectively enrolled cohort. The relatively small number of study patients therefore may not provide definite evidence for the superior diagnostic performance of FFR_{CT} compared with TAG. Moreover, patients who

underwent clinically indicated invasive coronary angiography and FFR as well as CTA were enrolled in this study. Therefore the ability to assess the diagnostic performance of FFR_{CT} and TAG in all-comer consecutive patients undergoing CTA is not possible. Lastly opacification of coronary artery lumen and luminal contrast density with CTA can be influenced by contrast iodine concentration, contrast infusion rate, contrast volume, timing of image acquisition and cardiac output. Differences in contrast administration protocols may affect the overall diagnostic performance of TAG320 in this multicentre study.

Conclusion

Based on the results of the current cohort of patients acquired using wide detector CT, non-invasive FFR derived from typically acquired CTA images provides better diagnostic performance for detecting and excluding hemodynamically significant coronary artery lesions compared to gradient of transluminal radiological attenuation (TAG320) or visual stenosis grade on CTA.

Acknowledgements

Drs Ko and Wong are supported by the National Heart Foundation of Australia post doctorate fellowship, and Robertson Family Scholarship.

Reference

1. Budoff MJ, Dowe D, Jollis JG, et al. Diagnostic performance of 64-multidetector row coronary computed tomographic angiography for evaluation of coronary artery stenosis in individuals without known coronary artery disease: results from the prospective multicenter ACCURACY (Assessment by Coronary Computed Tomographic Angiography of Individuals Undergoing Invasive Coronary Angiography) trial. *J Am Coll Cardiol* 2008;52:1724-32.
2. Meijboom WB, Van Mieghem CA, van Pelt N, et al. Comprehensive assessment of coronary artery stenoses: computed tomography coronary angiography versus conventional coronary angiography and correlation with fractional flow reserve in patients with stable angina. *J Am Coll Cardiol* 2008;52:636-43.
3. Wong DT, Ko BS, Cameron JD, et al. Translumenal Attenuation Gradient in Coronary Computed Tomography Angiography Is a Novel Noninvasive Approach to the Identification of Functionally Significant Coronary Artery Stenosis: A Comparison With Fractional Flow Reserve. *Journal of the American College of Cardiology* 2013;61:1271-9.
4. Taylor CA, Fonte TA, Min JK. Computational fluid dynamics applied to cardiac computed tomography for noninvasive quantification of fractional flow reserve: scientific basis. *J Am Coll Cardiol* 2013;61:2233-41.
5. Koo BK, Erglis A, Doh JH, et al. Diagnosis of ischemia-causing coronary stenoses by noninvasive fractional flow reserve computed from coronary computed tomographic angiograms. Results from the prospective multicenter DISCOVER-FLOW (Diagnosis of Ischemia-Causing Stenoses Obtained Via Noninvasive Fractional Flow Reserve) study. *J Am Coll Cardiol* 2011;58:1989-97.
6. Min JK, Leipsic J, Pencina MJ, et al. Diagnostic Accuracy of Fractional Flow Reserve From Anatomic CT Angiography. *JAMA* 2012;1-9.

7. Norgaard BL, Leipsic J, Gaur S, et al. Diagnostic performance of non-invasive fractional flow reserve derived from coronary CT angiography in suspected coronary artery disease: The NXT trial. *J Am Coll Cardiol* 2014;63:1145-55.
8. Gaur S, Achenbach S, Leipsic J, et al. Rationale and design of the HeartFlowNXT (HeartFlow analysis of coronary blood flow using CT angiography: NeXt sTeps) study. *J Cardiovasc Comput Tomogr* 2013;7:279-88.
9. Abbara S, Arbab-Zadeh A, Callister TQ, et al. SCCT guidelines for performance of coronary computed tomographic angiography: a report of the Society of Cardiovascular Computed Tomography Guidelines Committee. *J Cardiovasc Comput Tomogr* 2009;3:190-204.
10. Choi JH, Min JK, Labounty TM, et al. Intracoronary transluminal attenuation gradient in coronary CT angiography for determining coronary artery stenosis. *JACC Cardiovasc Imaging* 2011;4:1149-57.
11. DeLong ER, DeLong DM, Clarke-Pearson DL. Comparing the areas under two or more correlated receiver operating characteristic curves: a nonparametric approach. *Biometrics* 1988;44:837-45.
12. Pencina MJ, D'Agostino RB, Sr., D'Agostino RB, Jr., Vasan RS. Evaluating the added predictive ability of a new marker: from area under the ROC curve to reclassification and beyond. *Stat Med* 2008;27:157-72; discussion 207-12.
13. Yoon YE, Choi JH, Kim JH, et al. Noninvasive Diagnosis of Ischemia-Causing Coronary Stenosis Using CT Angiography: Diagnostic Value of Transluminal Attenuation Gradient and Fractional Flow Reserve Computed From Coronary CT Angiography Compared to Invasively Measured Fractional Flow Reserve. *JACC Cardiovasc Imaging* 2012;5:1088-96.

14. Stuijzand WJ, Danad I, Raijmakers PG, et al. Additional value of transluminal attenuation gradient in CT angiography to predict hemodynamic significance of coronary artery stenosis. *JACC Cardiovasc Imaging* 2014;7:374-86.
15. Wong DT, Ko BS, Cameron JD, et al. Comparison of diagnostic accuracy of combined assessment using adenosine stress CT perfusion (CTP) + computed tomography angiography (CTA) with transluminal attenuation gradient (TAG320) + CTA against invasive fractional flow reserve (FFR). *Journal of the American College of Cardiology* 2014:In press.
16. Lackner K, Bovenschulte H, Stutzer H, Just T, Al-Hassani H, Krug B. In vitro measurements of flow using multislice computed tomography (MSCT). *Int J Cardiovasc Imaging* 2011;27:795-804.
17. Chow BJ, Kass M, Gagne O, et al. Can differences in corrected coronary opacification measured with computed tomography predict resting coronary artery flow? *J Am Coll Cardiol* 2011;57:1280-8.
18. Steigner ML, Mitsouras D, Whitmore AG, et al. Iodinated contrast opacification gradients in normal coronary arteries imaged with prospectively ECG-gated single heart beat 320-detector row computed tomography. *Circ Cardiovasc Imaging* 2010;3:179-86.
19. Ko BS, Cameron JD, Leung M, et al. Combined CT Coronary Angiography and Stress Myocardial Perfusion Imaging for Hemodynamically Significant Stenoses in Patients With Suspected Coronary Artery Disease: A Comparison With Fractional Flow Reserve. *JACC Cardiovasc Imaging* 2012;5:1097-111.
20. Ko BS, Wong DT, Cameron JD, et al. 320-row CT coronary angiography predicts freedom from revascularisation and acts as a gatekeeper to defer invasive angiography

in stable coronary artery disease: a fractional flow reserve-correlated study. Eur Radiol 2013;24:738-747.

Figures

Figure 1 Study Enrolment

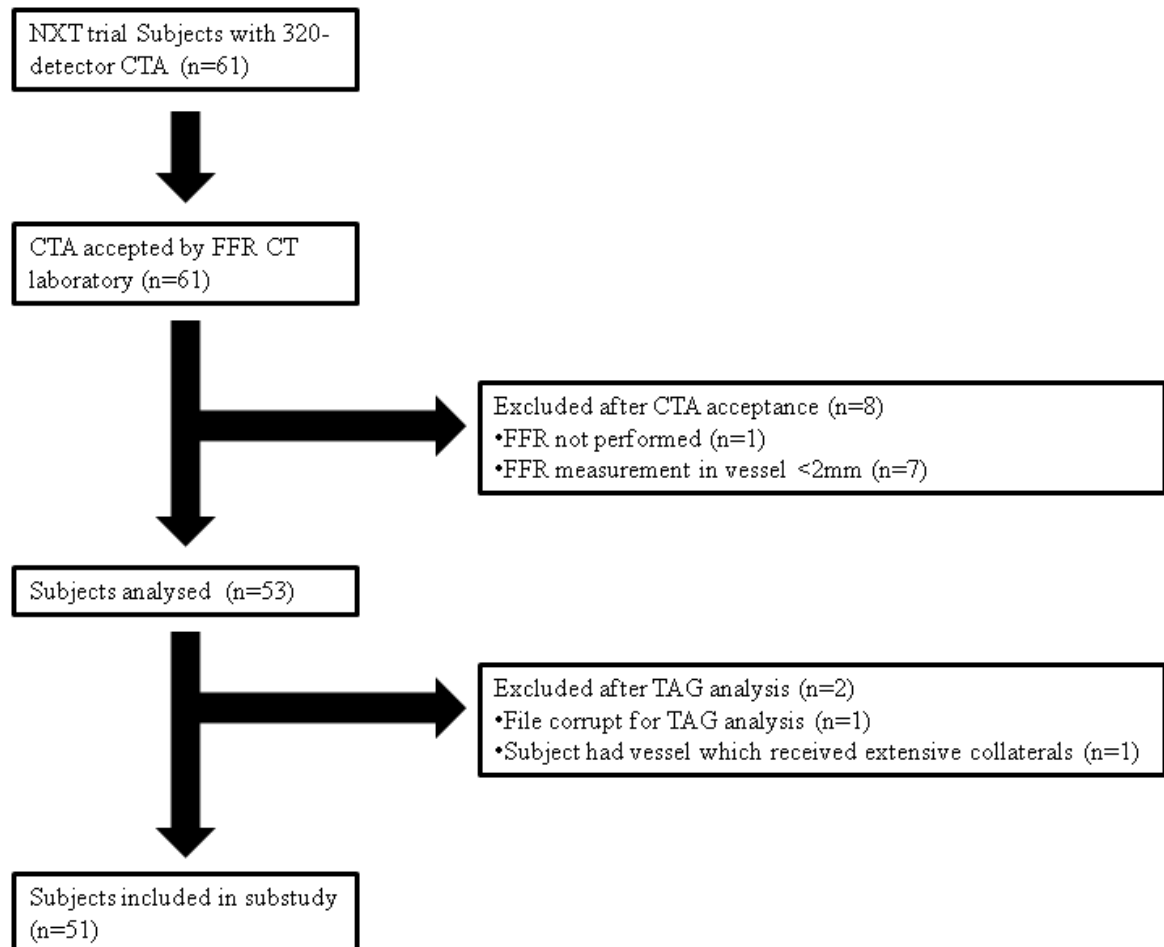
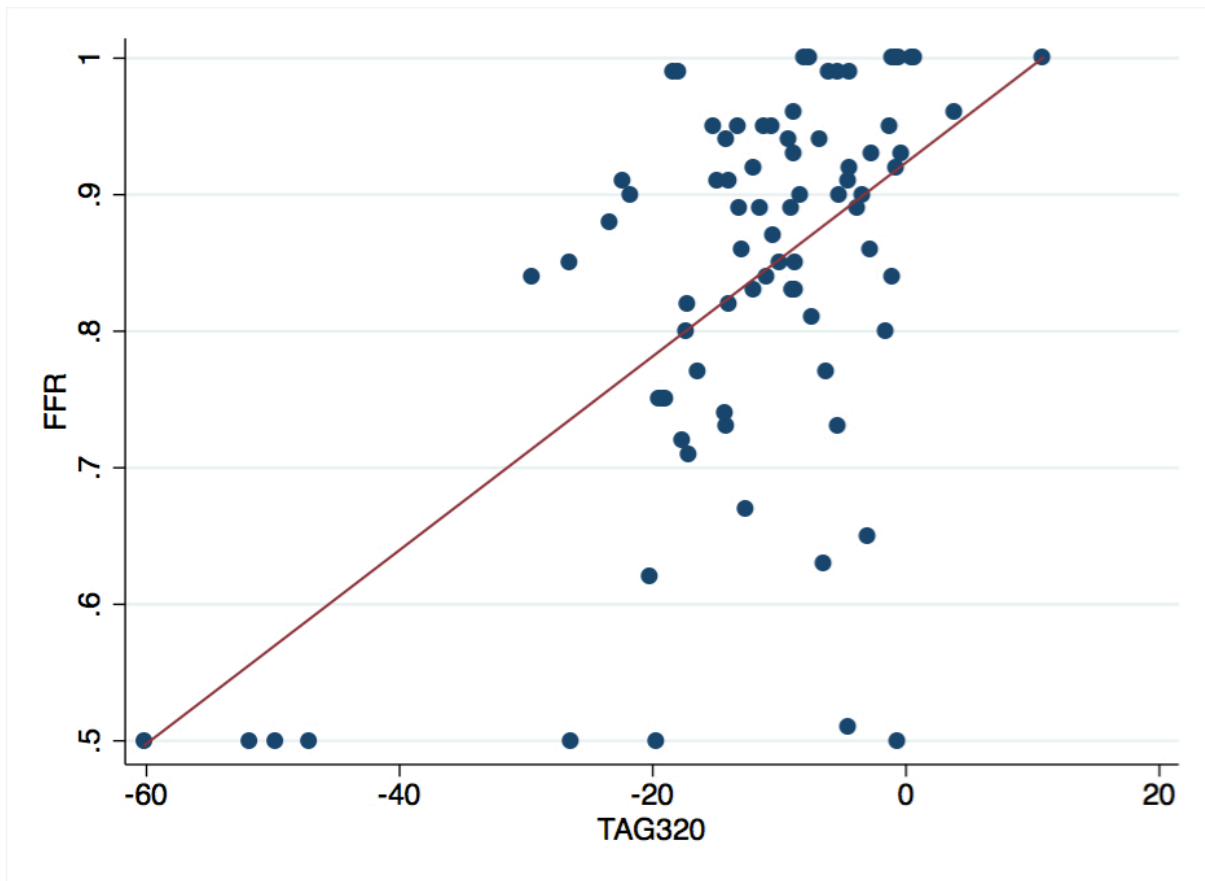


Figure 2 Correlation of TAG320 and FFR_{CT} with FFR. Bland Altman curve of FFR_{CT} vs FFR



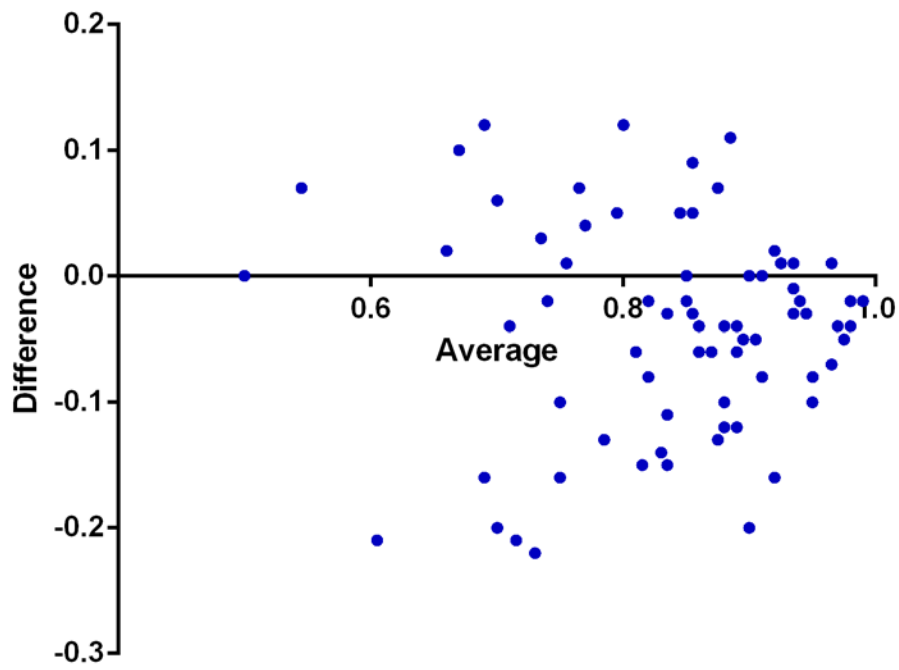
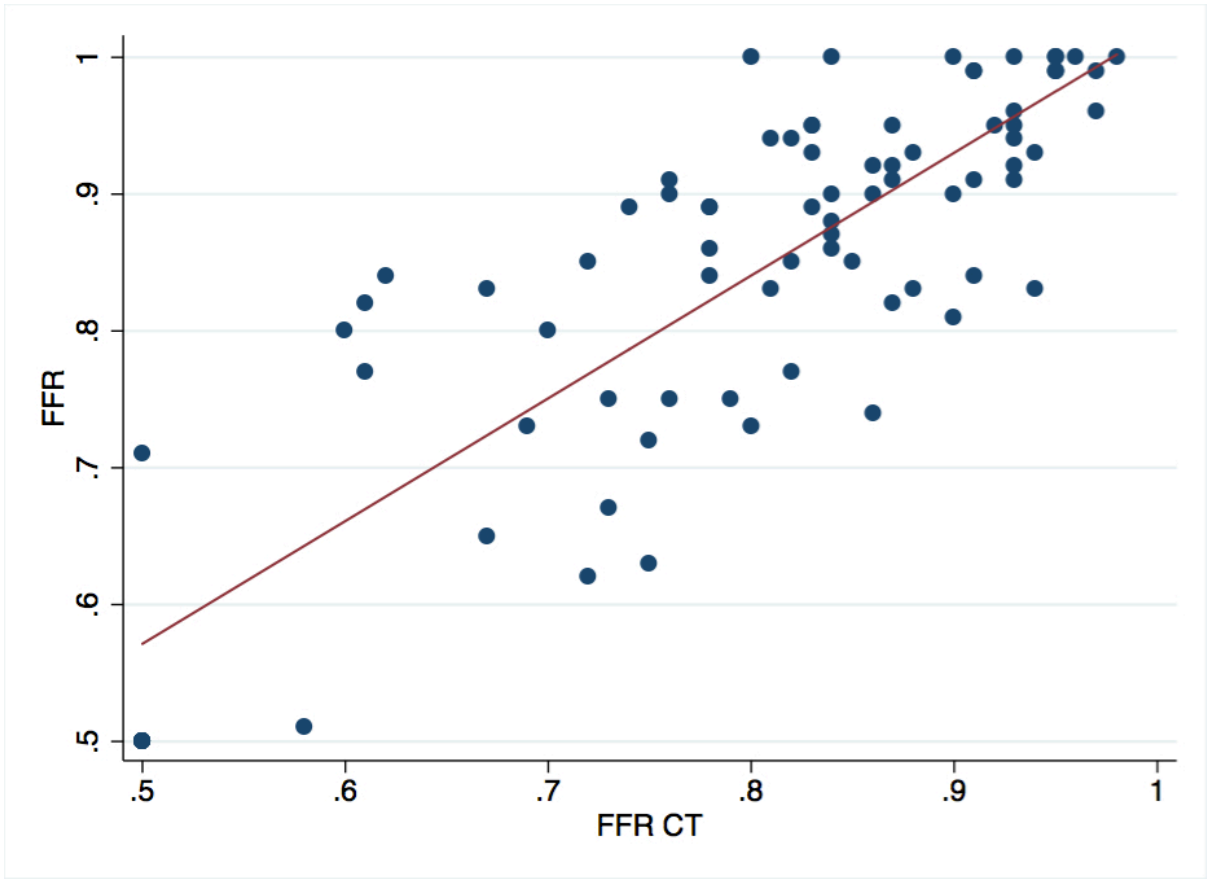
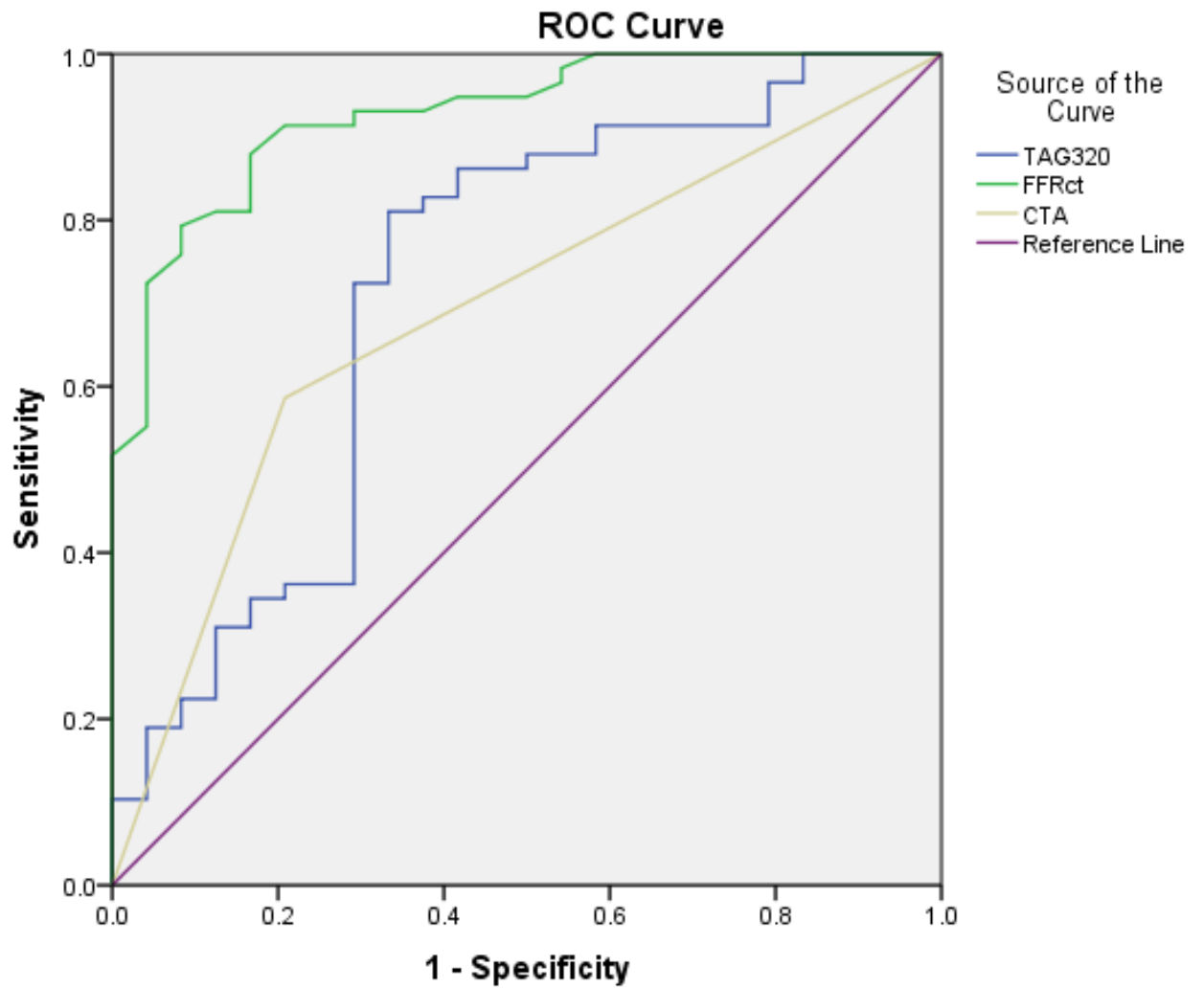


Figure 3 Receiver operating characteristic area under the curve of CTA , TAG320 and FFR_{CT}.



Tables

Table 1 Patient characteristics (n=51)

	N = 51 Patients
Age (years)	
Mean \pm SD (N)	62.2 \pm 10.4(51)
Median	64.0
Range (Min, Max)	(42.0, 81.0)
Gender	
Male	74.5% (38/51)
Female	25.5% (13/51)
Race	
Asian	52.9% (27/51)
White	43.1% (22/51)
Not Specified or Unknown	2.0% (1/51)
Other Race	2.0% (1/51)
Diabetes mellitus	33.3% (17/51)
Hypertension	70.6% (36/51)
Hyperlipidemia	84.3% (43/51)
Smoking	
Former Smoker	45.1% (23/51)
Current Smoker	17.6% (9/51)
Never Smoked	33.3% (17/51)
Unknown	3.9% (2/51)
Prior Myocardial Infarction	0.0% (0/51)
Angina Type*	
Typical	67.5% (27/40)
Atypical	30.0% (12/40)
Dyspnea	5.0% (2/40)
Angina Within the Past Month	
Yes	78.4% (40/51)
No	21.6% (11/51)
Updated Diamond-Forrester risk score, %	
Mean \pm SD (N)	59.6 \pm 19.7(51)
Intermediate (20%-80%) pre-test risk	82.4%(42/51)
Body mass index	
Mean \pm SD (N)	25.4 \pm 3.7(51)
Median	25.1

Range (Min, Max)	(19.2, 32.9)
<25	47.1% (24/51)
25-30	43.1% (22/51)
>30	9.8% (5/51)
Creatinine (mg/dL)	
Mean \pm SD (N)	0.8 \pm 0.2(51)
Median	0.8
Range (Min, Max)	(0.5, 1.2)
LVEF (%)	
Mean \pm SD (N)	66.2 \pm 8.9(18)
Median	65.0
Range (Min, Max)	(55.0, 88.0)

Table 2 Coronary CTA acquisition characteristics

CT Scan acquisition characteristics	N = 51 Patients N = 82 Vessels
Heart Rate Prior to cCTA (bpm)	
Mean \pm SD (N)	66.3 \pm 11.8(51)
Median	63.0
Range (Min, Max)	(37.0, 110.0)
Nitrates Administered	100.0% (51/51)
Beta Blockers Administered	62.7% (32/51)
Prospective Scan	64.7% (33/51)
Retrospective Scan	35.3% (18/51)
Radiation Calculated from DLP (mSv)	
Retrospective Scan	
Mean \pm SD (N)	12.7 \pm 4.8(18)
Median	12.3
Range (Min, Max)	(6.7, 27.0)
Prospective Scan	
Mean \pm SD (N)	3.3 \pm 3.8(33)
Median	2.1
Range (Min, Max)	(0.7, 16.8)
kV	
100	29.4% (15/51)
120	66.7% (34/51)
135	3.9% (2/51)
mAs	
Mean \pm SD (N)	451.27 \pm 193.14
Range (Min, Max)	(225, 900)
Single beat acquisition	100% (51/51)
Multiple beat acquisition	0% (0/51)

Table 3**Patient and vessel characteristics according to CTA, TAG320, FFR_{CT}, ICA and FFR**

Characteristics	N = 51 Patients N = 82 Vessels
cCTA Diagnostic Findings (maximum stenosis severity distribution at patient level)	
Patients with coronary CTA maximum stenosis >50%	66.7 (34/51)
Patients with coronary CTA maximum stenosis >70%	60.0 (26/51)
Patients with intermediate-range stenosis (30%-70%)	35.3 (18/51)
Patients with FFR _{CT} ≤ 0.80	54.9%(28/51)
Vessels with FFR _{CT} ≤ 0.80	41.5%(34/82)
Patients with TAG320<-15.37	39.2% (20/51)
Vessels with TAG320<-15.37	26.8% (22/82)
Calcium Score (Agaston Units)	
Mean ± SD (N)	384.2±522.3(19)
Median	195
Range (Min, Max)	(0.0, 2213.0)
Agatston score ≥ 400	31.6%(6/19)
Patients with QCA maximum stenosis >50%	41.2% (21/51)
Patients with QCA maximum stenosis >70%	13.7%(7/51)
Patients with FFR ≤ 0.80	41.2%(21/51)
Vessels with FFR ≤ 0.80	29.3%(24/82)
Patients with FFR ≤ 0.80 in >1 vessel	5.9%(3/51)

Table 4 Per vessel diagnostic performance

	CTA ($\geq 50\%$)	QCA ($\geq 50\%$)	TAG320 (< 15.37)	FFR _{CT} (≤ 0.80)	CTA+ TAG320	CTA+ FFR _{CT}
N	82	82	82	82	82	82
True positive	19	14	14	22	11	17
True negative	34	48	50	46	57	49
False positive	24	10	8	12	1	9
False negative	5	10	10	2	13	7
Accuracy	64.6	75.6	78.0	82.9	82.9	80.5
Sensitivity	79.2 (57.3-92.1)	58.3 (36.9-77.2)	58.3 (36.9-77.2)	91.7 (71.5-98.5)	45.8 (26.2-66.8)	70.8 (48.8-86.6)
Specificity	58.6 (45.0-71.1)	82.7 (70.1-91.0)	86.2 (74.1-93.4)	79.3 (66.3-88.4)	98.3 (89.5-99.9)	84.5 (72.1-92.2)
PPV	44.2 (29.4-60.0)	58.3 (36.9-77.2)	63.6 (40.8-82.0)	64.7 (46.5-79.7)	91.7 (59.8-99.6)	65.4 (44.4-82.1)
NPV	87.2 (71.8-95.2)	82.8 (70.1-91.0)	83.3 (71.0-91.3)	95.8 (84.6-99.3)	81.4 (70.0-89.4)	87.5 (75.3-94.4)
AUC	0.69	0.75	0.72	0.93	0.72	0.78

Chapter 4

Rest and Stress Transluminal Attenuation Gradient and Contrast Opacification Difference for Detection of Hemodynamically Significant Stenoses in Patients with Suspected Coronary Artery Disease

PART B: Suggested Declaration for Thesis Chapter

[This declaration to be completed for each conjointly authored publication and to be placed at the start of the thesis chapter in which the publication appears.]

Monash University

Declaration for Thesis Chapter

Chapter 4: Rest and Stress Transluminal Attenuation Gradient and Contrast Opacification Difference for Detection of Hemodynamically Significant Stenoses in Patients with Suspected Coronary Artery Disease

Declaration by candidate

In the case of Chapter 4, the nature and extent of my contribution to the work was the following:

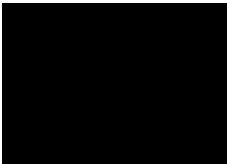
Nature of contribution	Extent of contribution (%)
Conceived the study, interpretation of CT coronary angiography, statistical analysis, analysis and interpretation of data and co-wrote the manuscript.	60

The following co-authors contributed to the work. If co-authors are students at Monash University, the extent of their contribution in percentage terms must be stated:

Name	Nature of contribution	Extent of contribution (%) for student co-authors only
Sujith Seneviratne	Assisted in manuscript revision	
James Cameron	Assisted in study design and assisted in manuscript drafting and critical revision	
Sarah Gutman	Subject recruitment and manuscript revision	
Marcus Crossett	Assisted in data collection and revision of manuscript	
Kiran Munnar	Subject recruitment and manuscript revision	2
Dennis Wong	Interpretation of CT coronary angiography, assisted in the interpretation of data and statistical analysis. Assisted in manuscript revision and presentation of the data	30

The undersigned hereby certify that the above declaration correctly reflects the nature and extent of the candidate's and co-authors' contributions to this work*.

**Candidate's
Signature**

	Date 16/10/2014
---	----------------------------------

Preface

The superior diagnostic performance demonstrated in the previous chapter in FFR_{CT} may relate to its superior correlation with invasive FFR, which in turn may be related to the technique in which FFR_{CT} is derived.

FFR_{CT} is derived with the assumption that there is maximal hyperemia and minimal microvascular resistance. In contrast, rest TAG is acquired in the absence of maximal hyperaemia. Therefore it has been hypothesised that TAG performed during maximal hyperaemia or vasodilator stress may be associated with superior diagnostic performance when compared with TAG performed at rest conditions.

This point of view has been echoed in the correspondence letters received regarding chapter 2 from Dai et al (JACC, Vol 64: 13: 1404-5).

Accordingly this has formed the basis in which the next study is performed.

Title

Rest and Stress Transluminal Attenuation Gradient and Contrast Opacification Difference for Detection of Hemodynamically Significant Stenoses in Patients with Suspected Coronary Artery Disease

Authors

Brian S Ko^{a,b}, MBBS (Hons), PhD; Sujith Seneviratne^{a,b}, MBBS; James D Cameron^{a,b}, MD; Sarah Gutman^{a,b}, MBBS; Marcus Crossett^{a,c}, BSc; Kiran Munnur^{a,b}, MBBS; Ian T Meredith^{a,b}, MBBS (Hons), PhD; Dennis Wong^{a,b}, MBBS (Hons), PhD.

Affiliations of Authors

^aMonash Cardiovascular Research Centre, School of Clinical Sciences, Monash University, Melbourne, Australia

^bMonashHEART, Monash Health, Melbourne, Australia

^cDepartment of Diagnostic Imaging , Monash Health, Melbourne, Australia

Corresponding Author

Dr Brian Ko

Monash Heart, 246 Clayton Road, Clayton, 3168 VIC, Australia

[REDACTED]

[REDACTED]

Word count

Abstract 326 words

Manuscript 4367 words including text and reference.

Abbreviations

CAD = coronary artery disease

FFR = fractional flow reserve

CTA = CT coronary angiography

TAG = transluminal attenuation gradient

CO difference = contrast opacification difference

PPV = positive predictive value

NPV = negative predictive value

ROC AUC= receiver operating characteristics area under curve

Conflicts of interest

Dr Seneviratne has been an invited speaker at a Toshiba sponsored meeting. Professor Meredith has received honoraria for serving on strategic advisory boards of Boston Scientific and Medtronic. All other authors have reported that they have no relationships relevant to the contents of this paper to disclose.

Structured abstract

Objectives: To evaluate the feasibility and diagnostic performance of transluminal attenuation gradient (TAG) and contrast opacification (CO) difference derived from computed tomography coronary angiography (CTA) performed during vasodilator stress to diagnose hemodynamically significant stenoses as determined by invasive fractional flow reserve ($\text{FFR} \leq 0.8$).

Background: CTA is limited in assessing the hemodynamic significance of coronary stenoses. CT derived TAG and CO difference are new techniques which may improve its diagnostic performance. Feasibility when derived from CT images acquired during vasodilator stress remains unknown.

Methods: Twenty seven patients prospectively underwent rest and stress 320-detector CTA and invasive coronary angiography with FFR measurement. TAG and CO difference on rest and stress CT datasets was manually determined using dedicated software. Image quality for each coronary segment was assessed using Likert score. TAG is defined as the linear regression coefficient between luminal attenuation and axial distance from the coronary ostium. CO difference is defined as the change in mean CO, proximal and distal to a coronary stenosis.

Results: 51 vessels on rest CTA and 35 vessels on stress CTA were deemed interpretable and analysed. Per vessel sensitivity and specificity for CTA alone was 77% and 56% respectively. Corresponding values for rest and stress TAG was 77%, 85% and 75%, 61% respectively; and those of rest and stress CO difference 82%, 44% and 75%, 65% respectively. Receiver operating characteristic curve analysis showed a comparable area under the curve (AUC) for rest and stress TAG (0.78 and 0.75) which was higher than CTA alone (0.68), and rest and stress CO difference (0.71 and 0.67). Compared with rest CTA, stress CTA was acquired at a higher heart rate (54bpm vs. 70bpm, $P < 0.0001$), demonstrated inferior per coronary segment

image quality (3.7 vs. 2.6 $P<0.0001$), and required a higher mean radiation exposure (3.2mSv vs. 5.1mSv, $P<0.0001$).

Conclusion: TAG and mean CO difference derived from stress CTA is less feasible and comparably accurate with that derived from rest CTA. Stress CTA required added radiation exposure and is associated with inferior image quality.

Keywords

Fractional flow reserve

CT coronary angiography

Invasive angiography

Transluminal attenuation gradient

Non invasive fractional flow reserve

Condensed abstract

This study evaluated the feasibility of stress 320 detector CT coronary angiography (CTA) derived transluminal attenuation gradient (TAG) and contrast opacification (CO) difference to detect hemodynamically significant stenoses as determined by invasive fractional flow reserve ($\text{FFR} \leq 0.80$). Twenty seven patients, including 51 vessels on rest CTA were studied. 16 (31%) vessels were not interpretable on stress CTA largely secondary to motion artefacts. Receiver operating characteristic curve analysis showed a comparable area under the curve (AUC) for rest and stress TAG (0.78 and 0.75) which was higher than CTA alone (0.68), and rest and stress CO difference (0.71 and 0.67). Compared with rest CTA, stress CTA demonstrated inferior image quality (3.7 vs. 2.6 $P < 0.0001$) and required a higher mean radiation exposure (3.2mSv vs. 5.1mSv, $P < 0.0001$). Stress TAG and CO difference is less feasible and comparably accurate as rest CTA.

Introduction

CT coronary angiography (CTA) is an established non-invasive method for anatomical assessment of coronary stenoses (1), yet has limited specificity for diagnosing their hemodynamic significance (2-4). Novel CT techniques have recently been developed including transluminal attenuation gradient (TAG) and contrast opacification (CO) difference in an attempt to improve the diagnostic performance of CTA.

TAG is defined as the linear regression coefficient between luminal attenuation and axial distance from the coronary ostium. CO difference is defined as the mean hounsfield units (HU) difference across a stenosis and has been demonstrated to predict abnormal TIMI grade flow at rest (5). Similarly previous work demonstrated that the TAG along a vessel varied significantly in accordance to TIMI grade flow and stenosis severity (5-7). Their diagnostic performance to detect hemodynamic stenoses as assessed by fractional flow reserve (FFR), when applied on rest CTA images acquired using 320-detector CT, which enables near isophasic, single-beat imaging of the entire coronary tree, has been demonstrated (8,9).

While TAG and CO difference can be typically derived from rest CTA images, performance on CTA images acquired during vasodilator stress may improve its diagnostic accuracy to predict hemodynamic stenoses as assessed by fractional flow reserve which is performed during maximal hyperaemia(10). This may however be challenging as heart rate increases on average by 15-20 bpm during vasodilator stress. Accordingly motion scan artefacts may adversely impact on the performance of stress TAG and CO difference (11).

The feasibility and diagnostic accuracy of these techniques performed during vasodilator stress to predict hemodynamically significant stenoses is not known.

Our primary aim was to determine the feasibility and diagnostic performance of stress TAG and CO difference to detect hemodynamically significant stenoses. Fractional flow reserve, a well-established and highly accurate invasive method to assess the functional significance of coronary stenoses, was used as the reference standard.

Methods

We prospectively recruited symptomatic patients with known or suspected coronary artery disease who were referred for elective invasive coronary angiography (ICA). Exclusion criteria included age <40 years, previous coronary artery bypass graft surgery, acute coronary syndrome within 7 days, atrial fibrillation, high grade atrioventricular block, renal insufficiency (eGFR <60mL/min/1.73m²), bronchospastic lung disease requiring long term steroid therapy, morbid obesity (BMI≥40), cardiomyopathy (EF<50%), severe valve dysfunction and contraindications to iodinated contrast. Patients were scheduled for rest and stress coronary CTA, within 14 days before ICA. At the time of ICA, FFR was measured in at least one major patent epicardial coronary artery at physicians discretion. FFR was not performed on lesions with >90% stenosis or angiographically smooth coronary arteries. The study was approved by the institutional human research ethics committee and all participants gave written informed consent.

Computed tomography imaging protocol

Patients underwent cardiac CT assessment using a 320-row detector CT scanner (Aquilion VISION, Toshiba Medical Systems, Japan). The CT protocol consisted of rest coronary CTA followed by stress CTA (Figure 1). Anti-anginal medications apart from beta-blockers were ceased 48 hours prior to scanning. Additional beta-blockers were administered when indicated to achieve a pre-scan heart rate of <60 beats per minute (bpm). The rest CTA was acquired after sublingual nitrate administration during injection of 60-75ml of 100% iohexal 56.6/75mL (Omnipaque 350, GE Healthcare, United Kingdom) at 5ml/s, followed by 30ml of saline at the same rate. Scans were either manually triggered or automatically triggered when the contrast attenuation reached 300HU in the descending aorta. The tube current was determined with use of automatic exposure control (^{SURE}Exposure3D, Toshiba Medical Systems) on the basis of x-ray attenuation on anterior-posterior and lateral scout images and the reconstruction kernel. Tube potential was manually set by the operator with the default set at 100 kVp, and is manually adjusted to 120 or 135 kVp when the automatic tube current selected maximum. The gantry rotation time was 275ms and temporal resolution 137.5 ms. Prospective electrocardiogram gating was used to include diastole phases covering 70-100% of the R-R interval. For images acquired at >65 bpm the acquisition window was widened to include systole and diastole (40-100%). The stress perfusion scan was performed 20 minutes after coronary CTA with intravenous adenosine infusion (140mcg/kg/min for 3 min), using prospective electrocardiogram gating, tube settings and contrast dose as for the rest scan. Effective radiation dose was calculated by multiplying the dose-length product by a constant ($k=0.014\text{mSv/mGy/cm}$) (12).

Image reconstruction and analysis

Images were reconstructed at 3% R-R intervals with a 512 x 512 matrix, 0.5 mm thick sections, and 0.25 mm increments by using kernel (FC03), which incorporates beam hardening correction (13) and iterative reconstruction with adaptive iterative dose reduction 3D

(AIDR3D, Toshiba Medical Systems) standard, and asymmetric cone beam reconstruction (14). The phase with the least cardiac motion was selected and segments with significant overlying artefacts were deemed uninterpretable and excluded from analysis. Vessels with stents were excluded from analysis.

All CT images were analysed on a dedicated workstation (Toshiba Medical Systems) by two experienced CT angiographers (BK, DW) blinded to the results of ICA and FFR as previously described in accordance to the 16 segment American Heart Association model (15). Each coronary segment was visually assessed for degree of luminal stenosis and a vessel was considered significantly stenosed if there was $\geq 50\%$ luminal stenosis. Image quality on a per-segment basis was rated by consensus agreement using a five point Likert scale (16). The Likert scale was defined as 1= poor, impaired image quality limited by excessive noise or poor vessel wall definition; 2 = adequate, reduced image quality with poor vessel wall definition or excessive image noise, limitations in low contrast resolution remain evident; 3 = good, impact of image noise, limitations of low contrast resolution and vessel margin definition are minimal; 4 = very good, good attenuation of vessel lumen and delineation of vessel walls, relative image noise is minimal, coronary wall definition and low contrast resolution well maintained and 5 = excellent, excellent attenuation of the vessel lumen and clear delineation of the vessel walls, limited perceived image noise (16). In segments scored with a score <4 , the reasons for decreased image quality were recorded including the presence of significant calcification, intramural course of the vessel, image noise, motion or beam hardening artefacts.

TAG analysis

Analysis of TAG was performed with a manual method using dedicated computer software (Toshiba Medical Systems, Japan) in a blinded fashion (BK, DW). Vessel centreline and contouring was determined for each major coronary artery and was manually corrected if

necessary. Cross sectional images perpendicular to the vessel centreline were then reconstructed. The mean luminal radiological attenuation (in Hounsfield units) was measured at 5mm intervals, from the ostium to a distal level where the cross-sectional minimal area fell below 2mm^2 . The data points in segments with motion or blooming artefacts from luminal calcium were manually excluded from analysis. The TAG value was defined as the linear regression coefficient between intraluminal radiological attenuation (in Hounsfield units) and length from the ostium (in millimetres). For rest TAG, vessels with values < -15.1 were considered to be significant. A retrospectively determined stress TAG cut-off was determined from the dataset and taken to indicate significant stenosis. For combined TAG+CTA assessment, vessels were classified as non-significant if there was a $<50\%$ CTA stenosis at rest. Vessels were classified as significant if there was a $\geq 50\%$ stenosis on CTA and TAG was significant.

CO difference

Using the same method as for TAG, the CO mean difference across stenoses were calculated as the change between mean CO proximal to the stenosis and mean CO distal to the coronary stenosis. For rest CO difference, vessels with values ≥ 55 were considered to be significant. A retrospectively determined stress CO difference cut-off was determined from the dataset and taken to indicate significant stenosis during stress.

Invasive angiography and FFR

Invasive coronary angiography was performed as per standard practice either via the femoral or radial approach. The pressure wire (Pressure wire Certus 6, St Jude Medical, USA) was calibrated and electronically equalised with the aortic pressure before being placed in the distal third of the coronary artery being interrogated. Intracoronary glyceryl trinitrate (100mcg) was injected to minimise vasospasm. Intravenous adenosine was administered (140mcg/kg/min)

through an intravenous line in the antecubital fossa. At steady-state hyperaemia, FFR was recorded on a RadiAnalyzer Xpress (St Jude Medical Systems, USA), calculated by dividing the mean coronary pressure measured with the pressure sensor placed distal to the stenosis by the mean aortic pressure measured through the guide catheter. A FFR value ≤ 0.80 was taken to define hemodynamically significant stenoses (17).

Statistical analysis

Categorical variables are presented as frequencies and percentages, with continuous variables as mean \pm SD or median (interquartile range). Comparisons of continuous variables were performed using the paired t- test. Per vessel sensitivity, specificity, positive predictive (PPV) and negative predictive values (NPV) of CTA, rest TAG, stress TAG, CTA+ rest TAG and CTA+ stress TAG are calculated and expressed with 95% confidence intervals. The discriminatory ability of both rest and stress TAG for the identification of hemodynamically significant stenosis was evaluated on a per vessel basis by the area-under-the-receiver operating characteristic curve. Invasive FFR ≤ 0.80 was the reference standard.

The incremental value in adding rest and stress TAG to CTA in discriminating significant FFR was assessed by 2 methods. The integrated discrimination improvement (IDI) index and category-free net reclassification index (NRI) were used to determine whether rest and stress TAG improve vessel classification as hemodynamically significant, compared with CTA alone(18).

Statistical analysis was performed with SPSS version 18 (SPSS, Chicago, Illinois) and STATA version 13.1 (STATA Corp, College Station, Texas). A P value <0.05 was considered statistically significant.

Results

Patient population

Twenty-seven patients (mean age 64.9 ± 9.8 years, 81.5% male) were enrolled and successfully underwent CT protocol and FFR assessment. Subject and lesion characteristics are summarised in Tables 1 and 2. Patient flow chart is illustrated in Figure 2.

All patients underwent rest and stress CTA. Oral beta-blockers were administered in 93% of patients prior to CT, and additional intravenous beta-blockers were administered in 37% of patients. The heart rate during image acquisition was significantly higher during stress than rest CTA (70bpm vs 54bpm, $P < 0.0001$) (Figure3). CT scan parameters are summarised in Table 3.

The final cohort included fifty-one major vessels which were successfully interrogated by FFR of which one third (17/51) were hemodynamically significant. The diagnostic accuracy and incremental value for rest and stress TAG in the detection of hemodynamically significant stenoses is summarised in Tables 4 and 5. An example is illustrated in Figure 4.

Rest Coronary CT angiography

Coronary CTA alone had a per vessel sensitivity for FFR-significant stenoses of 77%, a specificity of 56%, a PPV of 46%, a NPV of 83% and an accuracy of 63%. The ROC curve analysis for CTA alone showed an AUC of 0.66 (95% CI 0.53-0.80).

Rest transluminal attenuation gradient

Using a cut-off value of -15.1 HU/10mm, there were 13 true positives, 29 true negatives, 5 false positives and 4 false negatives. The sensitivity, specificity, PPV and NPV of rest TAG were 77%, 85%, 72% and 88% respectively. The ROC curve analysis for rest TAG demonstrated an AUC of 0.78 (95% CI 0.63-0.93). The incremental discrimination index for rest TAG when compared with CTA was 0.33 (standard error ± 0.07 , $P < 0.0001$). The net reclassification index for rest TAG when compared with CTA was 1.24 (standard error ± 0.30 , $P < 0.0001$). When CTA findings were combined with rest TAG, the ROC AUC was 0.76, and sensitivity, specificity, PPV and NPV 59%, 94%, 83% and 82% respectively.

Stress transluminal attenuation gradient

Stress TAG was not interpretable in 16 vessels (31.4%) respectively which were excluded from analysis for diagnostic performance. Reasons for interpretability include motion (81%, 13/16), intramyocardial course (6%, 1/16) and the vessel being too small for interpretation (13%, 2/16). In the remaining 35 vessels, 12 (34.3%) were hemodynamically significant. A cut-off value of -10 HU/10mm was found to be optimal, and yielded 9 true positives, 14 true negatives, 9 false positives and 3 false negatives. The sensitivity, specificity, PPV and NPV of stress TAG were 75%, 61%, 50% and 82% respectively. The ROC curve analysis for stress TAG demonstrated an AUC of 0.75 (95% CI 0.58-0.92). The incremental discrimination index for stress TAG

when compared with CTA was 0.07 (standard error ± 0.05 , $P=0.19$). The net reclassification index for stressTAG when compared with CTA was 0.72 (standard error ± 0.36 , $P=0.04$). When CTA findings were combined with stress TAG, the ROC AUC was 0.64, and sensitivity, specificity, PPV and NPV 50%, 78%, 55% and 75% respectively.

Mean contrast opacification difference

The rest CO mean difference threshold of 55 predicted $\text{FFR} \leq 0.80$ with a sensitivity of 82%, specificity of 44%, positive predictive value of 42% and negative predictive value of 83%. The corresponding values for stress CO mean difference, using a retrospectively determined threshold of 62 were 75%, 65%, 53% and 83%. The ROC AUC for rest and stress CO mean difference was 0.71 (95% CI 0.56-0.86) and 0.67 (95% CI 0.47-0.87) respectively.

Image quality of coronary segments assessed at rest and stress

When comparing the image quality for each coronary segment in the 51 vessels (192 segments) from the rest and stress CTA images as assessed by the Likert score, the average score for rest CTA was 3.65, which was significantly higher than the average score at stress (2.60, $P < 0.0001$). This is attributable to a higher number of coronary segments which were rated to have Likert scores of 1, 2 and 3 on rest CTA - 1 (0.5%); 10 (5%); 67 (35%) than stress CTA- 41 (21%) ; 33 (17%); 64 (33%) respectively (Figure 5).

In the 78 segments rated to have Likert scores of 1-3 on rest CTA, decreased image quality was attributable to the presence of calcification in 42% (33/78), image noise in 41% (32/78), motion

in 10% (8/78), intramyocardial course in 5% (4/78) and beam hardening 1% (1/78). In the 138 segments rated to have Likert scores of 1-3 on stress CTA, decreased image quality was attributable to the presence of motion in 62% (85/138), calcification in 20% (28/138), image noise in 17% (23/138) and intramyocardial course in 1% (2/138) (Figure 6).

Duration of CT protocol and Radiation dose

Mean radiation dose for rest coronary CTA was 3.2 ± 1.9 mSv which was significantly lower than that for the stress CTA 5.1 ± 2.3 mSv ($P < 0.0001$). Mean radiation dose for the entire CT protocol was 8.3 ± 3.7 mSv. The average duration required to perform the entire CT protocol was 39.5 ± 12.5 mins. The average duration spent in the CT department, including time before and after the scans, was 172.8 ± 44.4 mins.

Discussion

This study is the first to report the feasibility and diagnostic accuracy of stress TAG and mean CO difference to detect hemodynamically significant stenoses as assessed by fractional flow reserve. It is also the first to compare the accuracy of the techniques performed on rest and stress CTA datasets.

Previous work suggested that the measure vasodilator stress TAG or CO difference may have potential to permit the assessment of hemodynamic significance of a lesion (5). Vasodilator stress induces maximal hyperaemia in the myocardium, during which the microvascular resistance is minimised and the relationship between coronary blood flow and pressure becomes linear (19). Accordingly vasodilator stress is applied during invasive FFR and non

invasive functional stress. Maximal hyperaemia is also assumed in non invasive FFR derived from cardiac CT (FFR_{CT}) for prediction of invasive FFR (20).

Our results demonstrate that the diagnostic accuracy of stress TAG and CO difference is comparable but not superior to rest TAG and CO difference, while stress CTA required a higher radiation exposure and longer duration in the CT scanner. Notably, in both rest and stress, overall accuracy and the incremental value over and above CTA was superior when TAG is performed compared with CO difference, which is in agreement with previous work (8).

Widened window image acquisition using second generation 320 detector CT

The study has been purposefully designed to optimise the diagnostic performance of rest and stress TAG and CO difference. Firstly it has been performed using 320 detector CT, based on the results of single centre studies of TAG derived from 320 detector CT which have to date shown the most promise (8,9). Previous work demonstrated that the diagnostic accuracy of TAG derived from 64 and 256 detector CTA acquisitions was not significantly different from CTA alone (21,22). The difference may be related to the ability of the 320-detector CT scanner to image the entire heart volume in a single gantry rotation hence enabling near isophasic, single beat imaging of the entire coronary tree. Secondly all patients were scanned using the second generation 320-detector scanner which provides superior temporal resolution (135ms) when compared with the first generation scanner (175ms). This may assist in minimising the effects of artefacts especially attributable to motion. Thirdly a rigorous attempt has been made to beta block patients. Additional oral beta blockers prior to scanning were administered in 93% of subjects, and intravenous beta-blockers were used in 37% usually in between the rest

and stress CTA. Lastly the protocol used a wide image acquisition window and a large number of phases were made available for interpretation by reconstruction at 3% intervals on rest and stress CTA to enhance the ability of CT angiographers to choose a phase least affected by motion on which TAG and CO difference can be performed.

Decreased image quality related to stress CTA

Despite the measures undertaken to optimise image quality, the results highlight the difficulty in routine assessment of stress TAG or stress CO difference. The significant elevation in heart rate during CT acquisition during vasodilator stress has resulted in 31% (16/51) of vessels which had been interpretable at rest, to become uninterpretable at stress. The stress CTA also had a significantly higher incidence of uninterpretable segments and poorer overall image quality which is largely attributable to a significantly higher incidence of motion artefacts. This may have adversely influenced the overall diagnostic performance of stress TAG and CO difference. For this reason, the diagnostic performance of these techniques can be revisited upon improvements in 320-detector scanner technology including in its temporal resolution.

Limitations

Our results represent a single centre study with limited patient numbers. Secondly we did not perform calcium score imaging in this CT protocol hence we could not quantify the overall and per vessel burden of calcified disease. Thirdly patients who were referred for clinically indicated invasive coronary angiography were enrolled in this study. Therefore the ability to assess the diagnostic performance of stress and rest TAG in all-comer consecutive patients undergoing CTA is not possible. Fourthly, ideally the derivation of the optimal threshold on

the stress CO difference and TAG should be derived from a separate cohort before it is applied in the current cohort. Lastly since rest and stress CTA requires double the iodinated contrast dose compared with rest CTA alone, it needs to be used with caution in patients with abnormal renal function.

Conclusion

Based on the results of the current cohort of patients acquired using wide detector CT, transluminal attenuation gradient and mean contrast opacification difference derived from stress CTA images is less feasible and provides comparable diagnostic performance for detecting hemodynamically significant coronary artery lesions compared to rest CTA. Stress CTA is associated with added radiation exposure, inferior image quality and higher proportion of uninterpretable vessels. This work suggests that stress TAG or CO difference provides no significant incremental benefit over rest TAG or CO difference using current 320-CT scanner technology.

Reference

1. Budoff MJ, Dowe D, Jollis JG, et al. Diagnostic performance of 64-multidetector row coronary computed tomographic angiography for evaluation of coronary artery stenosis in individuals without known coronary artery disease: results from the prospective multicenter ACCURACY (Assessment by Coronary Computed Tomographic Angiography of Individuals Undergoing Invasive Coronary Angiography) trial. *J Am Coll Cardiol* 2008;52:1724-32.
2. Meijboom WB, Van Mieghem CA, van Pelt N, et al. Comprehensive assessment of coronary artery stenoses: computed tomography coronary angiography versus conventional coronary angiography and correlation with fractional flow reserve in patients with stable angina. *J Am Coll Cardiol* 2008;52:636-43.

3. Ko BS, Cameron JD, Meredith IT, et al. Computed tomography stress myocardial perfusion imaging in patients considered for revascularization: a comparison with fractional flow reserve. *Eur Heart J* 2012;33:67-77.
4. Bamberg F, Becker A, Schwarz F, et al. Detection of hemodynamically significant coronary artery stenosis: incremental diagnostic value of dynamic CT-based myocardial perfusion imaging. *Radiology* 2011;260:689-98.
5. Chow BJ, Kass M, Gagne O, et al. Can differences in corrected coronary opacification measured with computed tomography predict resting coronary artery flow? *J Am Coll Cardiol* 2011;57:1280-8.
6. Choi JH, Min JK, Labounty TM, et al. Intracoronary transluminal attenuation gradient in coronary CT angiography for determining coronary artery stenosis. *JACC Cardiovasc Imaging* 2011;4:1149-57.
7. Steigner ML, Mitsouras D, Whitmore AG, et al. Iodinated contrast opacification gradients in normal coronary arteries imaged with prospectively ECG-gated single heart beat 320-detector row computed tomography. *Circ Cardiovasc Imaging* 2010;3:179-86.
8. Wong DT, Ko BS, Cameron JD, et al. Transluminal Attenuation Gradient in Coronary Computed Tomography Angiography Is a Novel Noninvasive Approach to the Identification of Functionally Significant Coronary Artery Stenosis: A Comparison With Fractional Flow Reserve. *Journal of the American College of Cardiology* 2013;61:1271-9.
9. Wong DT, Ko BS, Cameron JD, et al. Comparison of diagnostic accuracy of combined assessment using adenosine stress CT perfusion (CTP) + computed tomography angiography (CTA) with transluminal attenuation gradient (TAG320) + CTA against invasive fractional flow reserve (FFR). *Journal of the American College of Cardiology* 2014:In press.
10. Wong DT, Ko BS, Cameron JD, Meredith IT, Seneviratne SK. Reply: Combined CT Techniques to Assess Functionally Significant Coronary Stenosis. *J Am Coll Cardiol* 2014;64:1404-5.
11. Ko BS, Cameron JD, Leung M, et al. Combined CT Coronary Angiography and Stress Myocardial Perfusion Imaging for Hemodynamically Significant Stenoses in Patients With Suspected Coronary Artery Disease: A Comparison With Fractional Flow Reserve. *JACC Cardiovasc Imaging* 2012;5:1097-111.
12. Hausleiter J, Meyer T, Hermann F, et al. Estimated radiation dose associated with cardiac CT angiography. *JAMA* 2009;301:500-7.

13. Mehra VC, Valdiviezo C, Arbab-Zadeh A, et al. A stepwise approach to the visual interpretation of CT-based myocardial perfusion. *J Cardiovasc Comput Tomogr* 2011;5:357-69.
14. Van der Molen AJ, Joemai RM, Geleijns J. Performance of longitudinal and volumetric tube current modulation in a 64-slice CT with different choices of acquisition and reconstruction parameters. *Phys Med* 2012;28:319-26.
15. Raff GL, Abidov A, Achenbach S, et al. SCCT guidelines for the interpretation and reporting of coronary computed tomographic angiography. *J Cardiovasc Comput Tomogr* 2009;3:122-36.
16. Leipsic J, Labounty TM, Heilbron B, et al. Adaptive statistical iterative reconstruction: assessment of image noise and image quality in coronary CT angiography. *AJR Am J Roentgenol* 2010;195:649-54.
17. Tonino PA, De Bruyne B, Pijls NH, et al. Fractional flow reserve versus angiography for guiding percutaneous coronary intervention. *N Engl J Med* 2009;360:213-24.
18. Pencina MJ, D'Agostino RB, Sr., D'Agostino RB, Jr., Vasan RS. Evaluating the added predictive ability of a new marker: from area under the ROC curve to reclassification and beyond. *Stat Med* 2008;27:157-72; discussion 207-12.
19. De Bruyne B, Sarma J. Fractional flow reserve: a review: invasive imaging. *Heart* 2008;94:949-59.
20. Taylor CA, Fonte TA, Min JK. Computational fluid dynamics applied to cardiac computed tomography for noninvasive quantification of fractional flow reserve: scientific basis. *J Am Coll Cardiol* 2013;61:2233-41.
21. Stuijzand WJ, Danad I, Raijmakers PG, et al. Additional value of transluminal attenuation gradient in CT angiography to predict hemodynamic significance of coronary artery stenosis. *JACC Cardiovasc Imaging* 2014;7:374-86.
22. Yoon YE, Choi JH, Kim JH, et al. Noninvasive Diagnosis of Ischemia-Causing Coronary Stenosis Using CT Angiography: Diagnostic Value of Transluminal Attenuation Gradient and Fractional Flow Reserve Computed From Coronary CT Angiography Compared to Invasively Measured Fractional Flow Reserve. *JACC Cardiovasc Imaging* 2012;5:1088-96.

Acknowledgements

Dr Ko and Dr Wong are funded by the National Heart Foundation of Australia and Robertson Family Scholarship.

Figures

Figure 1 – CT imaging protocol

Rest CTA is performed, followed by stress CTA after 20 mins.

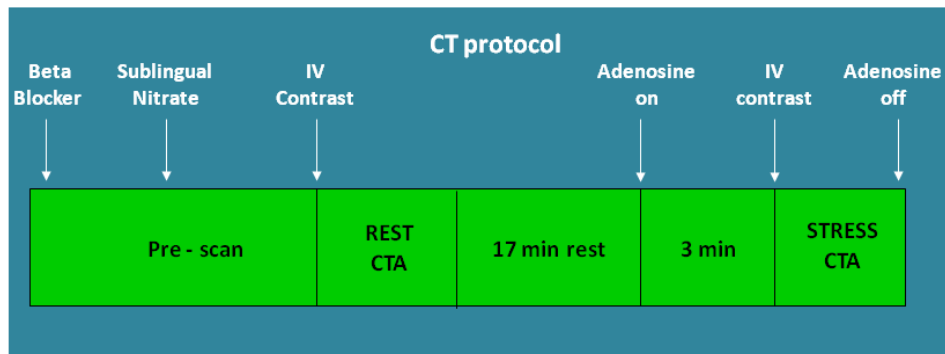


Figure 2 – Patient flow diagram

92 patients were screened and met inclusion criteria, 61 were excluded. 27 patients were enrolled and completed the entire protocol. This included 51 and 35 interpretable vessels on rest and stress CTA respectively

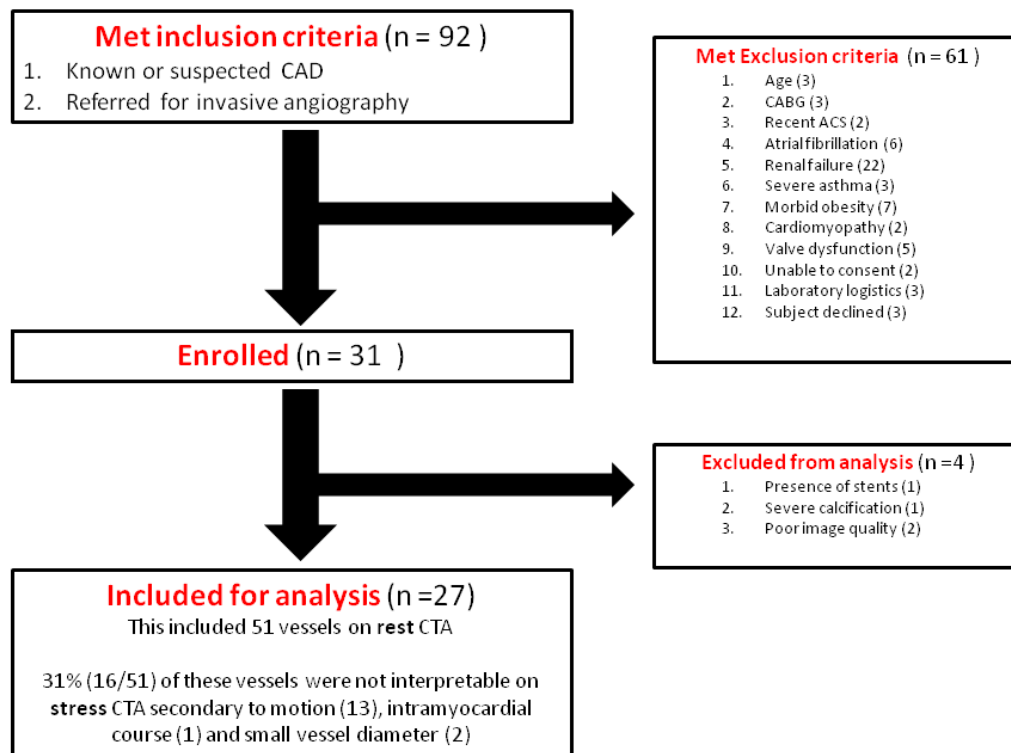


Figure 3 - Heart Rate During Scan Acquisition at Rest and Stress.

The heart rate during image acquisition significantly increased upon adenosine administration during stress CTA when compared with rest CTA (70bpm vs 54bpm, $P<0.0001$).

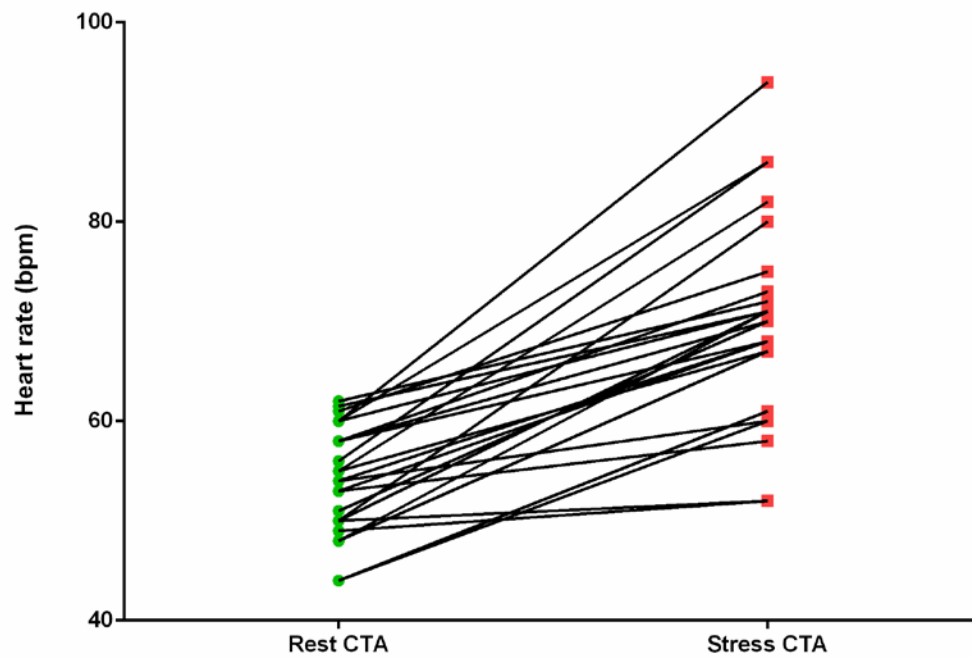
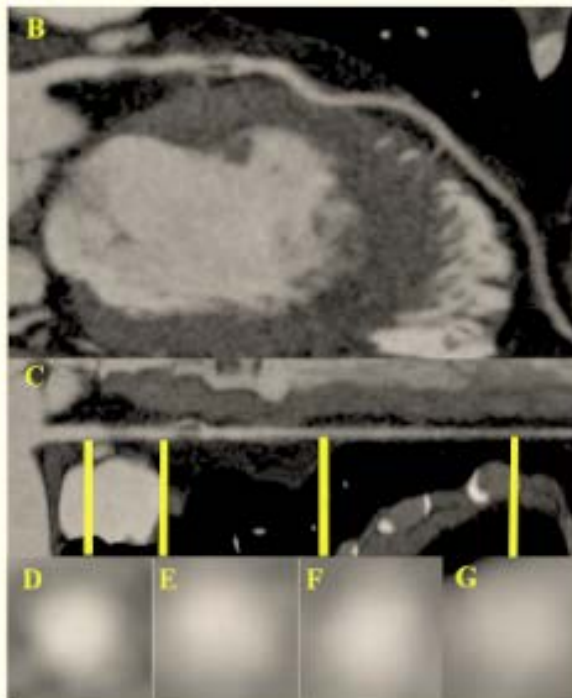
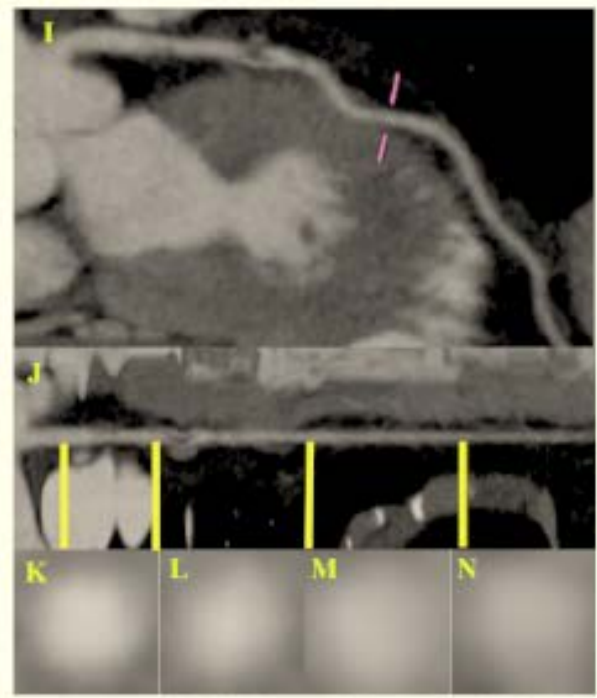


Figure 4 – Example: Rest and stress CTA.

(A) Proximal left anterior descending artery with significant stenosis as imaged by invasive coronary angiography. (B) Proximal left anterior descending artery with significant plaque burden and stenosis imaged by rest CTA. (C-G) Axial and representative cross-sectional views with corresponding luminal attenuation (HU) on rest CTA. (H) Dots represent 5mm intervals at which intraluminal attenuation (HU) was measured. Rest TAG is shown. The rest TAG was -25.9, and FFR was 0.64. (I) Proximal left anterior descending artery with significant plaque burden and stenosis imaged by stress CTA. (J-N) Axial and representative cross sectional views with corresponding luminal attenuation (HU) on stress CTA. (O) The stress TAG was -31.2.



663HU 624HU 528HU 423HU



571 HU 483 HU 398 HU 324 HU

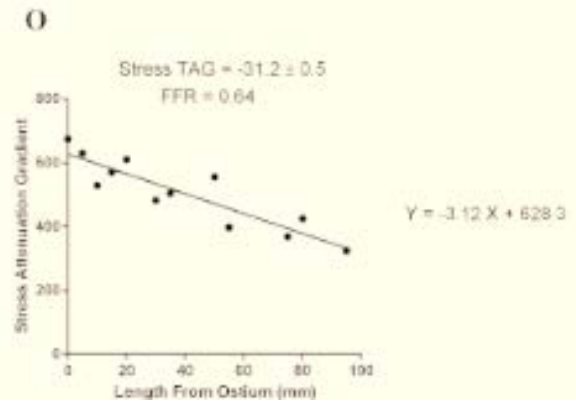
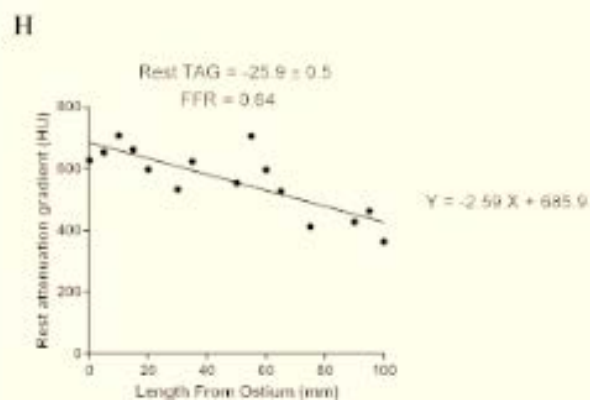


Figure 5– Image quality

51 vessels (192 coronary segments) were analysed on rest CTA. Based on likert score, image quality was graded to be 5 in 22 segments, 4 in 92 segments, 3 in 67 segments, 2 in 10 segments and 1 in 1 segment. The same corresponding 51 vessels (192 coronary segments) were analysed on stress CTA. Image quality was graded to be 5 in 5 segments, 4 in 49 segments, 3 in 67 segments, 2 in 33 segments and 1 in 41 segments. As a result 16 vessels were excluded from analysis in the stress CTA cohort.

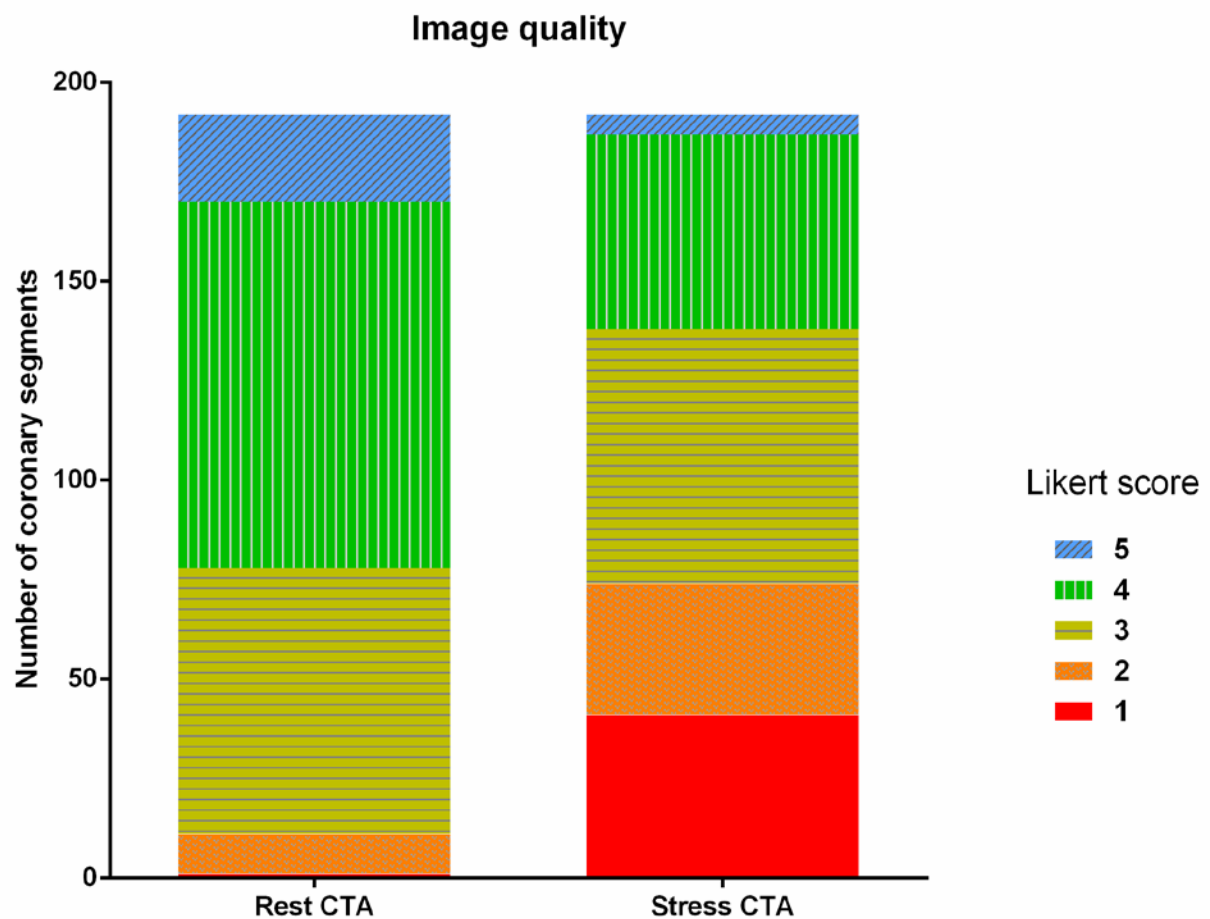
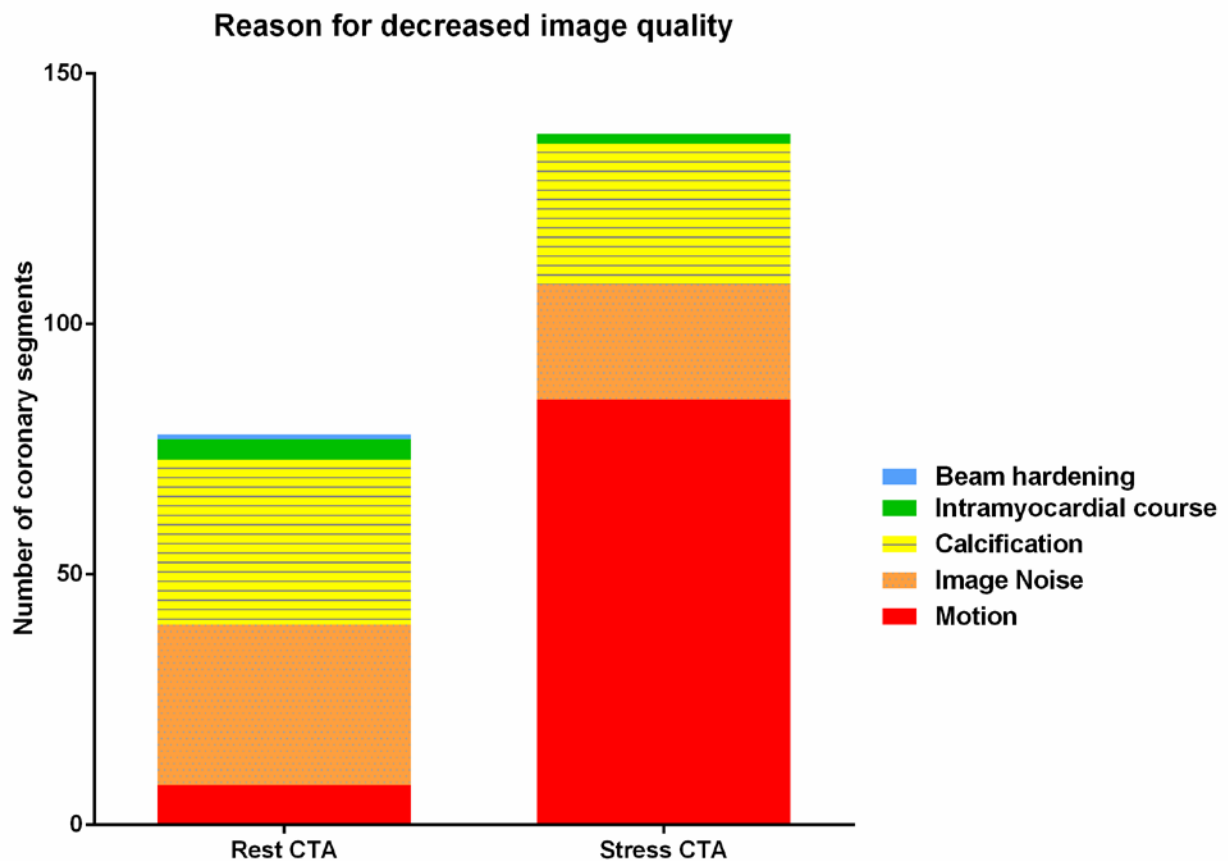


Figure 6 – Reasons for decreased image quality

In the 78 segments rated to have Likert scores of 1-3 on rest CTA, decreased image quality was attributable to the presence of calcification in 42% (33/78), image noise in 41% (32/78), motion in 10% (8/78), intramyocardial course in 5% (4/78) and beam hardening 1% (1/78). In the 138 segments rated to have Likert scores of 1-3 on stress CTA, decreased image quality was attributable to the presence of motion in 62% (85/138), calcification in 20% (28/138), image noise in 17% (23/138) and intramyocardial course in 1% (2/138).



Tables

Table 1- Patient Characteristics (n=27)

Characteristic	Value
Age (years) mean \pm SD	64.9 \pm 9.8
Male % (n)	81.5 (22)
Body mass index (kg/m ²), mean \pm SD	27.7 \pm 4.4
Creatinine (mmol/L), mean \pm SD	84.6 \pm 18.9
Cardiovascular risk factors % (n)	
Hypertension*	74.1 (20)
Hyperlipidemia†	77.8 (21)
Current Smoker	18.5 (5)
Diabetes	25.9 (7)
Family history of IHD	40.7 (11)
Obesity‡	25.9 (7)
Suspected CAD % (n)	85.2 (23)
Known CAD % (n)	14.8 (5)
Medication % (n)	
Aspirin	81.5 (22)
Clopidogrel	22.2 (6)
β Blocker	55.6 (15)
ACE inhibitor	37.0 (10)
ARB	22.2 (6)
Statin	81.5 (22)
Nitrates	7.4 (2)
Calcium Channel Blocker	30 (12)

SD indicates standard deviation; CAD, coronary artery disease; ACE, angiotensin converting enzyme; ARB, angiotensin receptor blocker. *Blood pressure >140/90 mmHg or treatment

for hypertension. †Total cholesterol >180 mg/dl or treatment for hypercholesterolemia.
‡Body mass index >30 kg/m²

Table 2 – Lesion characteristics

Lesion characteristics	Rest CTA (n=51)	Stress CTA (n=35)
CTCA findings		
$\geq 50\%$ diameter stenosis on visual assessment (n,%)	28 (54.9)	18 (51.4)
FFR findings (mean \pm SD)		
Mean FFR in all lesions	0.84 \pm 0.10	0.83 \pm 0.11
Lesions with FFR \leq 0.8 (n,%)	17 (33.3)	12 (34.3)
Lesion location (n, %)		
Proximal RCA	5 (9.8)	4 (11.4)
Mid RCA	7 (13.7)	5 (14.3)
Distal RCA	4 (7.8)	2 (5.7)
Right PDA or PLV	1 (2.0)	0 (2.0)
Proximal LAD	13 (25.5)	11 (31.4)
Mid LAD	8 (15.7)	7 (20.0)
Diagonal artery	2 (3.9)	0 (0)
Proximal LCx	7 (13.7)	4 (11.4)
Obtuse marginal artery	3 (5.9)	1 (2.9)
Distal LCx	1 (2.0)	1 (2.9)

Table 3: CT Scan Parameters

*At time of CT image acquisition.

Table 3 - CT scan parameters

Parameter	Rest CTA	Stress CTA	P value
Heart rate (beats/min)*, mean±SD	54.1 ± 5.4	70.1 ± 10.2	<0.0001
Beta-blocker usage, n (%)	25 (93)		
Oral metoprolol	25 (93)		
Intravenous metoprolol	10 (37)		
Beta-blocker dose (mg), mean±SD			
Oral metoprolol	77.6 ± 39.9		
Intravenous metoprolol	6.5 ± 2.5		
Gantry rotations*, n (%)			
1	27 (100)	27 (100)	
2	0 (0)	0 (0)	
Tube Voltage (kV), mean±SD	110 ± 10.2	110 ± 10.2	NS
Tube Current (mA), mean±SD	624.8 ± 188.2	630.8 ± 189.2	NS
Dose Length Product (mGy-cm), mean±SD	229.9 ± 135.6	362.9 ± 163.3	<0.0001
Radiation exposure (mSv), mean±SD	3.2 ± 1.9	5.1 ± 2.3	<0.0001

*At time of CT image acquisition.

Table 4 – Per vessel territory diagnostic accuracy of coronary CTA, TAG and CO difference compared with FFR.

CI = 95% confidence interval, PPV= positive predictive value, NPV= negative predictive value, AUC= area under the curve, ROC = receiver operating characteristics analysis.

	CTA ($\geq 50\%$)	Rest TAG (≤ -15.1)	Stress TAG (≤ -10.0)	Rest CO difference (>55)	Stress Co Difference (>62)	CTA + Rest TAG	CTA + Stress TAG
N	51	51	35	51	35	51	35
True positive	13	13	9	14	9	10	6
True negative	19	29	14	15	15	32	18
False positive	15	5	9	19	8	2	5
False negative	4	4	3	3	3	7	6
Accuracy							
Sensitivity	76.5 (50.1-93.2)	76.5 (50.1-93.2)	75.0 (42.8-94.5)	82.4 (56.6-96.2)	75.0 (42.8-94.5)	58.8 (32.9-81.6)	50.0 (21.1-78.9)
Specificity	55.9 (37.9-72.8)	85.3 (68.9-95.0)	60.9 (38.5-80.3)	44.1 (27.2-62.1)	65.2 (42.7-83.6)	94.1 (80.3-99.3)	78.3 (56.3-92.5)
PPV	46.4 (27.5-66.1)	72.2 (46.5-90.3)	50.0 (26.0-74.0)	42.4 (25.5-60.8)	52.9 (27.8-77.0)	83.3 (51.6-97.9)	54.5 (23.4-83.3)
NPV	82.6 (61.2-95.0)	87.9 (71.8-96.6)	82.4 (56.6-96.2)	83.3 (58.6-96.4)	83.3 (58.6-96.4)	82.1 (66.5-92.5)	75.0 (53.3-90.2)
AUC	0.66 (0.53-0.80)	0.78 (0.63-0.93)	0.75 (0.43-0.95)	0.71 (0.56-0.87)	0.67 (0.47-0.87)	0.76 (0.64-0.89)	0.64 (0.47-0.81)

Table 5 – Incremental value of TAG and CO difference when added to CTA in prediction of significant FFR.

Table 5: Incremental value on CTA alone

	Rest TAG (<-15.1)	Stress TAG (<-10.0)	Rest CO difference (>55)	Stress Co Difference (>62)
IDI	0.33±0.07	0.07±0.05	0.03±0.02	0.08±0.06
P value	<0.0001	0.19	0.24	0.15
NRI	1.24±0.30	0.72±0.36	0.53±0.30	0.80±0.36
P value	<0.0001	0.04	0.07	0.02

Chapter 5

Diagnostic accuracy of the ASLA score: a computed tomography angiographic index to predict functionally significant coronary stenoses in lesions with intermediate stenosis severity

PART B: Suggested Declaration for Thesis Chapter

[This declaration to be completed for each conjointly authored publication and to be placed at the start of the thesis chapter in which the publication appears.]

Monash University

Declaration for Thesis Chapter

Chapter 5: Diagnostic accuracy of the ALSA score: a computed tomography angiographic index to predict functionally significant coronary stenoses in lesions with intermediate stenosis severity.

Declaration by candidate

In the case of Chapter 5, the nature and extent of my contribution to the work was the following:

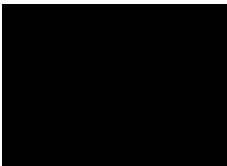
Nature of contribution	Extent of contribution (%)
Conceived the study, interpretation of quantitative CT coronary angiography, statistical analysis, analysis and interpretation of data and co-wrote the manuscript.	70

The following co-authors contributed to the work. If co-authors are students at Monash University, the extent of their contribution in percentage terms must be stated:

Name	Nature of contribution	Extent of contribution (%) for student co-authors only
Dennis Wong	Interpretation of quantitative CT coronary angiography, assisted in the interpretation of data and statistical analysis. Assisted in manuscript revision and presentation of the data	20
James Cameron	Assisted in study design and assisted in manuscript drafting and critical revision	
Darryl Leong	Statistical analysis and manuscript revision	
Siang Soh	Assisted in data collection and revision of manuscript	
Ian Meredith	Assisted in manuscript revision	
Nitesh Nerlekar	Assisted in data collection and revision of manuscript	
Sujith Seneviratne	Assisted in manuscript revision and had a major role in interpretation of the data	

The undersigned hereby certify that the above declaration correctly reflects the nature and extent of the candidate's and co-authors' contributions to this work*.

**Candidate's
Signature**

	Date 16/10/2014
---	----------------------------------

Preface:

Each novel CT technique evaluated thus far, in its current form, may have inherent limitations. Stress perfusion imaging on CT requires additional imaging hence is associated with increased radiation exposure and iodinated contrast usage. FFR CT can only be computed currently by the use of supercomputer, which currently requires at least 4 hours of processing time and hence cannot be conveniently performed at the point of care. While the assessment of TAG is promising and convenient, it requires manual vessel tracking using dedicated research software and the technique remains unvalidated on images acquired using narrow detector CT scanners

Hence there remains an unmet need for a simple and easily accessible approach for the CT angiographer to predict the functional significance of coronary stenoses and to assist in clinical decisions regarding referral for invasive angiography. Recent studies demonstrate that CT angiographic predictors of FFR may include minimal luminal diameter, area stenosis and lesion length – which by themselves remain insufficient predictors of $FFR \leq 0.8$. Moreover the myocardium subtended by the lesion has also been demonstrated to strongly correlate with ischemic burden as assessed by cardiac magnetic resonance imaging and invasive FFR. An advantage is that these parameters are easily accessible and can all be derived conveniently at the point of care using software provided by the vast majority of CT vendor workstations. It is not known whether a score which takes into account such measurements quantified by CT may better predict fractional flow reserve.

Title

Diagnostic accuracy of the ASLA score: a computed tomography angiographic index to predict functionally significant coronary stenoses in lesions with intermediate stenosis severity

Authors

Brian S Ko ¹MBBS (Hons), PhD, Dennis TL Wong ^{1,2} MBBS (Hons), PhD, James D Cameron ¹MBBS, MD, Darryl P Leong ^{2,3} MBBS (Hons), PhD, Siang Soh¹, MBBS, Nitesh Nerlekar¹ MBBS (Hons), Ian T Meredith ¹ MBBS (Hons), PhD, Sujith Seneviratne ¹ MBBS

Affiliation of Authors

¹ Monash Cardiovascular Research Centre, Department of Medicine (Monash Medical Centre) Monash University and Monash Heart, Monash Health, 246 Clayton Road, Clayton, 3168 VIC, Australia

² Discipline of Medicine, University of Adelaide, Adelaide, Australia

³ Discipline of Medicine, Flinders University, Adelaide, Australia

Address correspondence

Dr Brian Ko

MonashHeart, Monash Medical Centre

246 Clayton Road,

Clayton, Victoria, AUSTRALIA



[REDACTED]

[REDACTED]

Word count: 5377 words including body of manuscript, reference, figures, tables and legends

Subject code: [30] CT and MRI

The study has not been submitted to RSNA meeting.

Advances in Knowledge

1. Combined CT assessment of area stenosis, lesion length and myocardium subtended improves prediction of functionally significant coronary stenosis beyond individual indices alone (C-statistic of combined assessment, area stenosis, lesion length and APPROACH score was 0.82, 0.74, 0.75 and 0.71; $P < 0.001$ for trend)

2. This can be conveniently applied using the ASLA score in 103 ± 38 seconds

Implications for Patient Care

Application of this score may decrease the need for further functional testing and invasive angiography.

Abstract

Purpose

To 1) identify CT indices independently associated with $\text{FFR} \leq 0.8$, 2) derive a score which combines CT indices most predictive of $\text{FFR} \leq 0.8$ and 3) evaluate the diagnostic accuracy of the score to predict $\text{FFR} \leq 0.8$.

Materials and Methods

This retrospective study has been approved by institutional review board and informed consent has been waived. We assessed consecutive patients who underwent CT coronary angiography and FFR assessment, with ≥ 1 discrete lesion of intermediate (30% to 70%) severity on CT. Quantitative CT measurements were performed using dedicated software. CT indices evaluated included: plaque burden, minimal-luminal area and diameter, diameter stenosis, area stenosis (AS), lesion length (LL), remodelling index, plaque morphology, calcification severity and APPROACH score, which approximates size of myocardium subtended by a lesion. Using covariates independently associated with $\text{FFR} \leq 0.8$, a score was determined based on modified Akaike's information criteria and the C-statistics of individual and combined indices were compared.

Results

85 patients (mean age 64.2; 66% male, 124 lesions; 38% $\text{FFR} \leq 0.8$) were included. Area stenosis, LL and APPROACH score were the strongest predictors for $\text{FFR} \leq 0.8$, and were used to derive the ASLA score. The optimism-adjusted Harrell's c-statistic for ASLA score was 0.82 which was superior to the corresponding values for AS (0.74), LL (0.75) and APPROACH score (0.71) ($P < 0.001$ for trend). The corresponding incremental discrimination improvement indices (P value) are 0.17 (< 0.001), 0.11 (< 0.001), and 0.19 (< 0.001) suggesting that the score

improves reclassification compared with any one angiographic index. Average time required for score derivation was 102 seconds.

Conclusion

The ASLA score which accounts for CT-derived Area Stenosis, lesion Length and APPROACH score may conveniently improve prediction, beyond individual indices, of functionally significant intermediate coronary lesions.

Key Words: Computed tomography; Myocardial Ischemia; Fractional flow reserve

Computed tomography coronary angiography (CCTA) is recommended as an initial investigation to assess symptomatic patients with low to intermediate risk of coronary artery disease (1). In its current form however CCTA has limited specificity in determining the functional significance of coronary stenoses (2, 3). For this reason patients with moderate stenoses may require referral for non-invasive functional imaging to confirm the presence of ischemia before the decision is made to proceed to invasive angiography.

A number of novel CT techniques have recently been described which may improve the ability of CCTA to predict ischemia. These include the use of adenosine stress CT myocardial perfusion imaging (4, 5), the assessment of the transluminal attenuation gradient (TAG) across coronary stenoses based on resting CCTA images (6), and the non-invasive prediction of a fractional flow reserve (FFR CT) by the application of computational fluid dynamics on resting CCTA images (3, 7). Each technique has been demonstrated to improve the specificity, positive predictive value and overall accuracy of CCTA in prediction of functionally significant coronary stenoses as assessed by invasive fractional flow reserve ($\text{FFR} \leq 0.8$) (3-7).

Each novel technique in its current form however may have limitations. Stress perfusion imaging on CT requires additional imaging hence is associated with increased radiation exposure and iodinated contrast usage. FFR CT can only be computed currently by the use of supercomputer, which currently requires at least 4 hours of processing time (3). Whilst the assessment of TAG is promising and convenient, it requires manual vessel tracking using dedicated research software and the technique remains unvalidated on images acquired using narrow detector CT scanners (6).

Hence there remains an unmet need for a simple and easily accessible approach for the CT angiographer to predict the functional significance of coronary stenoses- in particular intermediate coronary stenoses identified on CT to assist in clinical decisions regarding referral for invasive angiography. Recent studies demonstrate that CT angiographic predictors of FFR may include minimal luminal diameter, area stenosis and lesion length – which by themselves remain insufficient predictors of $\text{FFR} \leq 0.8$ (8, 9). Moreover the myocardium subtended by the lesion has also been demonstrated to strongly correlate with ischemic burden as assessed by cardiac magnetic resonance imaging and invasive FFR (10, 11), though the use of these scores based on CT coronary angiography remain unknown.

We hypothesise that the combined use of angiographic indices may improve prediction of reduced FFR compared to individual indices alone. Our study is therefore performed to 1) identify CT indices independently associated with $\text{FFR} \leq 0.8$, 2) derive a score which combines CT indices most predictive of $\text{FFR} \leq 0.8$ and 3) to evaluate the diagnostic accuracy of the score in prediction of $\text{FFR} \leq 0.8$

Materials and Methods

This retrospective study has been approved by institutional review board and informed consent has been waived. We included consecutive patients who underwent clinically mandated CCTA and non-urgent invasive coronary angiography (ICA) with FFR assessment, performed in at least one discrete lesion of intermediate severity (30-70%) as visually assessed on CCTA, in our institution MonashHEART, between October 2009 and July 2012. Conventional ICA and

FFR was performed at a mean of 11 days after CCTA. Patients were excluded in the case of CT identified total occlusion, if the time interval between CCTA and FFR was longer than 6 months duration, the presence of adverse cardiac events or revascularisation during this time interval, or the presence of acute coronary syndrome in the 3 months prior to the CT, and those with bypass graft lesions or significant left main stenoses. In the patients who met inclusion criteria, uninterpretable vessels on CT and those with >70% stenosis or <30% stenosis, poor CT image quality, small vessel diameter (<2mm), intracoronary stent, excessive calcification and presence of myocardial bridge were excluded.

CT coronary angiography

Patients underwent CCTA using a 320-row detector CT scanner (Aquilion ONE, Toshiba Medical Systems, Japan). Beta-blockers and nitroglycerin were administered to achieve a pre-scan heart rate of <65bpm and to optimise vasodilation in accordance to guidelines(12). A bolus of 55ml of 100% iohexol 56.6g/75mL (Omnipaque 350) was injected into an antecubital vein at a flow rate of 5ml/s, followed by 20ml of a 30:70 mixture of contrast and saline, followed by 30ml of saline. Scan parameters were: Detector collimation 320x0.5mm; tube current 300-500mA (depending on body mass index); tube voltage 120kV; gantry rotation time 350ms; and temporal resolution 175ms. Prospective electrocardiogram gating was used covering phases 70-80% of the R-R interval. For images acquired at heart rates ≤ 65 bpm, scanning was completed with a single R-R interval utilising a 180° segment. In patients with a heart rate >65 bpm data segments from two consecutive beats were used for multi-segment reconstruction with improved temporal resolution of 87ms.

Computed tomography coronary angiography analysis

Analysis was performed in coronary vessels which were >2mm in diameter. All data were transferred to an external workstation (Vitre 6, version 3.0, Vital Images Inc USA) for further analysis. Two angiographers with 5 years experience in CCTA interpretation (BK, DW) blinded to the results of the corresponding ICA and FFR performed the analysis independently. All included vessels were deemed suitable for analysis of the coronary artery and plaque characteristics by the CT interpreters.

Coronary plaques were classified as non-calcified, calcified or mixed. Any plaque that could be assigned to the coronary artery wall with CT attenuation values below the contrast-enhanced coronary lumen was defined as non-calcified; any plaque with high density CT attenuation values that could be visualised separately from the contrast-enhanced coronary lumen was defined as calcified, whereas the presence of calcified and non-calcified components embedded within the same lesion was defined as mixed. The extent of coronary calcium is classified as none, <50% of cross sectional area (CSA) or $\geq 50\%$ of CSA.

Quantification of luminal narrowing and vessel remodelling in the target lesion was performed using a dedicated software tool (Sure Plaque, Vitrea 6, Version 3.0, Vital Images Inc USA and Toshiba Medical Systems, Japan) which has been previously validated against IVUS (13). Automatic vessel tracking was then used to locate the vessel centreline based on the opacification of the lumen. The location and extent of the coronary lesion was manually assigned and the minimal lumen diameter (MLD, mm), minimal lumen area (MLA, mm²) and lesion length (LL, mm) were determined automatically by the software. The reference diameter and area were determined as an average of the vessel dimensions at points proximally and distally to the traced lesion, where minimal or no plaque could be detected. In ostial lesions

only one reference was used. The diameter stenosis (DS, %) was calculated as $100\% \times (\text{reference diameter} - \text{MLD}) / \text{reference diameter}$. The area stenosis (AS, %) was calculated as $100\% \times (\text{reference lumen} - \text{MLA}) / \text{reference lumen}$.

Plaque analysis performed by the software is based on an automatic detection of the outer contour of the vessel (corresponding to the elastic external membrane). Coronary plaque is defined as the area between the outer contour of the vessel and the lumen border, with the lumen border detected by the software based on the contrast in the vessel and the outer vessel border as previously described (8). Measurements were obtained for each plaque and were defined as:

- Plaque burden (mm²) = (vessel area-lumen area)/ vessel area
- Remodelling index = outer vessel area (stenotic segment) / outer vessel area (reference segment)

Modified APPROACH score

The Alberta Provincial Project for Outcome Assessment in Coronary Heart Disease (APPROACH) score is based on the division of the left ventricle into regions in accordance with pathological studies in humans and cardiac catheterisation correlation, which evaluate the proportion of the myocardium perfused by each artery (14-16). The table in the appendix demonstrates the derivation of the APPROACH score as has been previously described (17). Furthermore it has been validated with cardiac magnetic resonance methods to quantify the myocardial area at risk after myocardial infarction (18). The modified score takes into account the location of the lesion (proximal, mid or distal) and dominance and size of the secondary

branches and provides an estimate of the percentage of supplied myocardium beyond the considered coronary lesion (17).

Invasive coronary angiography and fractional flow reserve

Invasive coronary angiography was performed as per standard clinical practice. The pressure wire (Pressure Wire Certus, St Jude Medical, USA) was calibrated and electronically equalised with the aortic pressure before being placed distal to the stenosis in the distal third of the coronary artery being interrogated. Intracoronary glyceryl trinitrate (100 mcg) was injected to minimise vasospasm. Intravenous adenosine was administered (140mcg/kg/min) through an intravenous line in the antecubital fossa. At steady-state hyperemia, FFR was assessed using the RadiAnalyser Xpress (Radi Medical Systems, Sweden), calculated by dividing the mean coronary pressure measured with the pressure sensor placed distal to the stenosis by the mean aortic pressure measured through the guide catheter. A FFR of ≤ 0.8 was taken to define ischaemia in the interrogated artery and its supplied territory (19, 20). This threshold is chosen as it may determine vessel outcome and benefit from revascularisation.(21)

Statistical analysis

Continuous variables are expressed as mean \pm SD or with 95% confidence intervals.. Categorical variables are expressed as percentages. Interobserver variability is performed using the intraclass coefficient. In order to identify the optimal combination of CCTA parameters for the estimation of FFR, linear mixed effects modelling was undertaken. Patient identity was included as a random effect to account for the likelihood of greater correlation between different vessels in a particular patient than between vessels from different patients.

To identify CT angiographic covariates that were independently associated with $\text{FFR} \leq 0.8$, we used generalised estimating equations. The following covariates were considered at univariate level: plaque burden, MLA, MLD, diameter stenosis, area stenosis, lesion length, remodelling index, calcification, plaque morphology, and APPROACH score. Those covariates with a univariate P-value < 0.2 were included in the multivariate analysis, which was performed using the “enter” approach.

To ensure the most parsimonious model, the modified Akaike’s information criterion (AIC) was used(22); models with a lower AIC are preferable to models with a higher AIC.

The ability of the final model to predict $\text{FFR} \leq 0.8$ was assessed by the optimism-adjusted Harrell’s c-statistic on bootstrapped samples with replacement 100 times. The optimal ASLA score threshold is one which maximises sum of sensitivity and specificity with a minimal sensitivity of 75%. Finally the incremental utility of ASLA score was assessed using the integrated discrimination improvement (IDI) index as described by Pencina et al (23):

$$\text{IDI} = (\text{IS}_{\text{new}} - \text{IS}_{\text{old}}) - (\text{IP}_{\text{new}} - \text{IP}_{\text{old}})$$

Where the “new” subscript refers to a model containing a novel diagnostic tool of interest in addition to conventional risk-predictors, and “old” pertains to the model containing only the conventional risk-markers. IS and IP are the integrals of sensitivity and $(1 - \text{specificity})$ respectively. Statistical analysis was performed with SPSS 18.0 (SPSS Inc, Chicago, IL, USA) and STATA 12.1 (StataCorp, College Station, TX, USA). A P value < 0.05 was considered statistically significant.

Results

There were 121 who underwent CT and FFR assessment in our institution during the study period (Figure 1). Ten patients were excluded for the presence of left ventricular dysfunction (n=4), time interval between CCTA and FFR 6 months (n=2), presence of acute coronary syndrome in the 3 months prior to CCTA (n=1), presence of cardiac events or revascularisation between CTA and FFR (n=1), presence of coronary artery bypass graft (n=1) and left main disease (n=1). In the remaining 111 patients including 204 vessels, eighty vessels were excluded from analysis due to the presence of severe ($>70\%$) or minor stenoses (n=34), the presence of poor image quality as a result of excessive noise or motion (n=17), vessel diameter $< 2\text{mm}$ (n=11), intracoronary stent (n=7), excessive calcification (n=6), myocardial bridging (2) and incomplete information (3). The remaining 85 patients (mean age 64.2 ± 11.2 ; 66% male) with 124 vessels were included for analysis. Patient and vessel characteristics are summarised in Table 1.

Fractional flow reserve was performed in all 85 patients, of whom 55 (64.7%) received FFR interrogation in a single vessel, 21 (24.8%) in two vessels, and 9 (10.6%) in three vessels. Overall FFR ranged from 0.39 to 1.0 (mean of 0.84 ± 0.11). Thirty eight vessels (30.6%) were classified as functionally significant with $\text{FFR} \leq 0.8$. There were no adverse events during FFR interrogation.

Accuracy of visual assessment on CT to predict $\text{FFR} \leq 0.8$

On a per vessel basis, 58 (48.6%) vessels had $\geq 50\%$ visual stenosis on CT. The presence of a $\geq 50\%$ visual stenosis on CTA was associated with a 78.9% sensitivity, 67.4% specificity, 51.7% PPV and 87.9% NPV. The area under the curve for visual stenosis to diagnose $\text{FFR} \leq 0.8$ was 0.74 (95% CI: 0.64-0.83).

Accuracy of quantitative CT parameters to predict FFR \leq 0.8

The univariate and multivariate analyses for predictors of FFR are presented in Table 2. According to univariate analysis, MLA, MLD, plaque burden, diameter stenosis, area stenosis, lesion length, remodelling index, presence of calcification, plaque morphology and APPROACH score were all significant predictors of FFR \leq 0.8. By multivariate analysis, plaque burden, area stenosis, lesion length and the APPROACH score remained significant predictors for lesion specific ischemia.

Accuracy of area stenosis quantified on computed tomography to predict FFR \leq 0.8

On a per vessel basis, 56 (45.2%) vessels had \geq 50% area stenosis on QCT. The area stenosis in lesions with FFR \leq 0.8 was $61.5 \pm 22.5\%$ versus $41.8 \pm 22.3\%$ in vessels with FFR >0.8 ($P<0.0001$). Area stenosis measurements were reproducible with an inter-observer intraclass coefficient of 0.98 (95% CI: 0.91-0.99). There was a statistically significant negative correlation between area stenosis and FFR ($r=-0.37$, $P<0.0001$) (Figure 2). The presence of a \geq 50% area stenosis was associated with 65.9% sensitivity, 62.1% specificity, 44.6% PPV and 79.7% NPV. The bootstrapped Harrell's c-statistic for area stenosis to predict FFR \leq 0.8 was 0.74 (95% CI: 0.65-0.83).

Accuracy of lesion length to predict FFR \leq 0.8

The lesion length in vessels with FFR \leq 0.8 was 27.2 ± 12.9 mm versus 16.1 ± 8.9 mm in vessels with FFR >0.8 ($P<0.0001$). There was a statistically significant negative correlation between lesion length and FFR ($r=-0.45$, $P<0.0001$) (Figure 2). The bootstrapped Harrell's c-statistic for lesion length to predict FFR \leq 0.8 was 0.75 (95% CI: 0.66-0.85). The lesion length measurements were highly reproducible with an inter-observer intraclass coefficient of 0.95

(95% CI: 0.83-0.99).

Accuracy of APPROACH score to predict $FFR \leq 0.8$

The APPROACH score in lesions with $FFR \leq 0.8$ was 32.7 ± 11.6 versus 23.7 ± 11.0 in vessels with $FFR > 0.8$. ($P < 0.0001$). There was a statistically significant negative correlation between APPROACH score and FFR ($r = -0.34$, $P = 0.0002$) (Figure 1). The bootstrapped Harrell's c-statistic for the APPROACH score to predict $FFR \leq 0.8$ was 0.71 (95% CI: 0.61-0.81). The APPROACH score demonstrated high reproducibility with a inter-observer intraclass coefficient of 1.0 (1.0-1.0).

Accuracy of plaque burden to predict $FFR \leq 0.8$

The plaque burden in lesions with $FFR \leq 0.8$ was 69.3 ± 14.5 versus 76.5 ± 17.1 in vessels with $FFR > 0.8$ ($P < 0.0001$). There was a statistically significant negative correlation between plaque burden and FFR ($r = -0.27$, $P = 0.003$) (Figure 1). The bootstrapped Harrell's c-statistic for plaque burden to predict $FFR \leq 0.8$ was 0.64 (95% CI: 0.54-0.76).

ASLA SCORE:

The ASLA score was derived by multivariate generalised estimating equation regression, including QCT derived area stenosis and lesion length and the APPROACH Score as ordinal variables categorized using the cut-points described in Table 3. Each was important for the model, as indicated by a likelihood ratio test $P < 0.02$ when each parameter was dropped sequentially from the model. Plaque burden was not taken into account in the score as it did not lower the model's modified AIC substantially, and so was thought not to contribute to the model's clinical performance. An exchangeable correlation structure was selected for the

regression as this minimised the modified AIC compared with other correlation structures. Figure 2 illustrates the application of the ASLA score.

Accuracy of ASLA Score in prediction of $FFR \leq 0.8$

The ASLA score in vessels with $FFR \leq 0.8$ was 10.1 ± 4.77 compared to 4.43 ± 3.62 in vessels with $FFR > 0.8$ ($P < 0.001$). The bootstrapped Harrell's c-statistic of ASLA score in predicting significant FFR was 0.82 (95% confidence interval 0.74-0.91). The ASLA score was a better discriminator of $FFR \leq 0.8$ than area stenosis, lesion length and APPROACH Score (respective ROC AUCs (95% CI) 0.82 (0.74-0.91); 0.74 (0.65-0.83); 0.75 (0.66-0.85); 0.71 (95%CI: 0.61-0.81); $P < 0.001$ for trend). The comparison of ROC curves is presented on Figure 4. A representation of sensitivity and specificity as functional cutoff values over a whole spectrum of ASLA score is presented on Figure 5. A threshold score of 7 provided 76.3% (59.4% -88.0%) sensitivity, 76.7% (66.2%-85.0%) specificity, 59.2% (44.3%-72.7%) positive predictive value, 88.0% (78.0-94.0%) negative predictive value and 76.6% overall accuracy. A score of ≤ 3 was associated with 92% sensitivity and accounted for 50 (40.3%) lesions. Similarly a score of ≥ 11 was associated with 86% specificity and accounted for 21 lesions (16.9%) (Figure 6). In the 50 lesions with score ≤ 3 , four (8%) had $FFR \leq 0.8$ (FFR range 0.68-0.78), including 2 lesions in the left anterior descending artery, one in marginal branch and one in the right coronary artery. In the 21 lesions with score ≥ 11 , four (19%) had $FFR > 0.8$ (FFR range 0.81-0.95), including 3 lesions in the left anterior descending artery, one in the left circumflex artery.

We estimated the integrated discrimination improvement (IDI) indices for the score over and above each of its constituents (area stenosis, lesion length and APPROACH), using the

approach of Pencina(23). The IDI indices (P value) are 0.17 (<0.001), 0.11 (<0.001), and 0.19 (<0.001) suggesting that the score improves reclassification of estimated FFR compared with any one angiographic index.

Time required to perform the ASLA Score

The average time required to perform the ASLA score per lesion was 102.6 ± 37.5 seconds (25% percentile 70.1s; 75% percentile 131.8s).

Discussion

This study derived a score based on information quantified on CT to predict the hemodynamic significance of coronary artery stenoses. It demonstrates that the ASLA score which takes into account area stenosis, lesion length and the APPROACH score is a superior predictor of functionally significant stenoses as assessed using invasive FFR beyond individual CT indices alone or visually assessed $\geq 50\%$ stenosis on CTA. This can be conveniently applied in less than 2 minutes.

Computed tomography derived area stenosis and lesion length

Based on multivariate analysis, area stenosis and lesion length were found to be important predictors of $\text{FFR} \leq 0.8$. Our findings are in agreement with Kristensen et al, who found in a smaller cohort of 56 intermediate stenoses in 42 patients using a similar CT based methodology that area stenosis and lesion length were the strongest determinants of an abnormal FFR(8) and were superior to plaque volume, minimal luminal diameter and minimal luminal area. The incremental value of lesion length when added to standard invasive angiographic measurement

of diameter stenosis to predict FFR significant lesions has been reported (24, 25). However like the previous studies, our results highlight the limited predictive value of individual CT derived parameters for $FFR \leq 0.8$ (8, 9).

Computed tomography derived APPROACH score

It is increasingly recognised that FFR is highly dependent on the area of myocardium supplied beyond the lesion in question (11, 26). The APPROACH score has been used to estimate the myocardium at risk during myocardial infarction and was found to be inversely correlated with FFR (11).

This study describe the correlation of a CT derived APPROACH score with FFR. Our study results demonstrate modest but similar correlation ($r = -0.34$, $P < 0.0001$) with FFR as had been described in invasive angiography (11). We also demonstrate that the score is highly reproducible with minimal interobserver variability (Table 5) which is in agreement with previous reports (11, 18).

ASLA score and fractional flow reserve

The ASLA score taking into account area stenosis, lesion length and APPROACH score was found to be superior and incremental to individual indices alone or visual CT assessment in prediction of $FFR < 0.8$. Visually assessed diameter stenosis on CT currently plays an important role in deciding whether a patient may require further investigation with non-invasive stress testing or invasive angiography (27). Rossi et al demonstrated that area stenosis as derived by quantitative CT may be superior in specificity when compared with visually assessed diameter stenosis in a cohort of 99 symptomatic patients (9). Our results extend upon these results and emphasise the importance to account for the myocardium supplied distal to the lesion and the

length of the lesion in addition to area stenosis. By taking into account all three in the form of a score, it may improve the diagnostic accuracy to predict $\text{FFR} \leq 0.8$.

The Poiseuille equation states that the pressure gradient across a coronary lesion is directly proportional to the coronary blood flow, blood viscosity and lesion length and is inversely proportional to the fourth power of the radius. It would be intuitive for a score to take into account each of these key elements. Accordingly the ASLA score includes the APPROACH score which may act as a surrogate for myocardial blood flow (11), minimal area stenosis which represents the square of the radius of the vessel at the lesion, and the lesion length.

Potential Application of the ASLA score

The ASLA score can be derived using standard rest CTA images, without additional radiation exposure, contrast, medications, reconstruction or cost. The score can also be readily calculated using software available on most currently available reporting workstations during CTA interpretation. The technique is convenient and requires a short processing time.

In our cohort, 57% of intermediate lesions had scores which were ≤ 3 or ≥ 11 . In the former, 92% were not FFR significant and in the latter 81% of lesions were FFR significant. This suggests that the score may have value in differentiating lesions which may or may not require further functional assessment and or invasive angiography. In contrast, in lesions with scores between 4 and 10, the diagnostic performance remains limited. In the 9/25 lesions with scores between 4 to 10, which were FFR significant, the average, median and range of ASLA scores was 7, 6.6, and 4 to 10 respectively. In the 16/25 lesions which were FFR non-significant, the corresponding values for ASLA score were 8, 7.3 and 4 to 10. Our results suggest it will still be important to perform functional assessment or fractional flow reserve.

Notably given the sample size and number of false positive and negative results at the extremes of the ASLA score, our results represent a preliminary report on the described technique. Larger studies with methodological improvements are required to improve the diagnostic performance of the technique and to assess whether the use of the score may save costs and decrease downstream testing.

Limitations:

Our results represent a retrospective single-centre experience involving 85 patients and hence require confirmation with larger studies. The findings are limited to intermediate stenoses alone, and the applicability of the score to vessels with tandem lesions, severe stenoses, in bypass graft lesions and in patients with impaired left ventricular function is not known.

Analysis was restricted to per vessel basis alone. In a proportion of patients who underwent multivessel FFR interrogation, only one vessel was included in the final analysis as the remaining vessels met exclusion criteria. For this reason, the accuracy of the applied technique cannot be extended to the patient per se, but remains true for the vessel. Hence per patient analysis was not performed. The incremental value of the technique upon pre-test information including symptom severity and results of functional testing has also not been evaluated.

We acknowledge that the derivation and validation of the ASLA score was performed in the same cohort, which can optimise the performance of the score through an optimisation bias. We also acknowledge in patients with prior myocardial infarction, fractional flow reserve may be elevated due to the loss of viable myocardial mass (26). The effect of this may have been

minimised in this study as all patients, including the nine patients who had suffered prior myocardial infarction, had documented normal left ventricular ejection fraction on transthoracic echocardiogram or invasive angiography as per the inclusion criteria. However the applicability of the study findings to patients with sizeable loss of viable myocardial mass has not been studied.

Lastly we acknowledge measurements of area stenosis and lesion length in this study were quantified using dedicated software provided by a sole vendor. The applicability of the technique using other vendors remains not known.

Conclusion:

Combined CT angiographic assessment using the ASLA score including area stenosis, lesion length and APPROACH score provides incremental predictive value over individual indices alone for detecting functionally significant coronary artery stenoses.

Conflict of interest / Disclosures: Professor Meredith has received honoraria for serving on strategic advisory boards of Boston Scientific and Medtronic. Dr Seneviratne has been an invited speaker at a Toshiba sponsored meeting. All other authors have reported that they have no relationships relevant to the contents of this paper to disclose. The authors who have no relationships with industry had control of inclusion of all data and information in this manuscript.

Funding: Dr Ko and Dr Wong are funded by the National Heart Foundation of Australia and Robertson Family Scholarship.

References

1. Taylor AJ, Cerqueira M, Hodgson JM, et al. ACCF/SCCT/ACR/AHA/ASE/ASNC/NASCI/SCAI/SCMR 2010 Appropriate Use Criteria for Cardiac Computed Tomography. A Report of the American College of Cardiology Foundation Appropriate Use Criteria Task Force, the Society of Cardiovascular Computed Tomography, the American College of Radiology, the American Heart Association, the American Society of Echocardiography, the American Society of Nuclear Cardiology, the North American Society for Cardiovascular Imaging, the Society for Cardiovascular Angiography and Interventions, and the Society for Cardiovascular Magnetic Resonance. *Circulation* 2010; 122:e525-555.
2. Dorbala S, Hachamovitch R, Di Carli MF. Myocardial perfusion imaging and multidetector computed tomographic coronary angiography: appropriate for all patients with suspected coronary artery disease? *J Am Coll Cardiol* 2006; 48:2515-2517.
3. Koo BK, Erglis A, Doh JH, et al. Diagnosis of ischemia-causing coronary stenoses by noninvasive fractional flow reserve computed from coronary computed tomographic angiograms. Results from the prospective multicenter DISCOVER-FLOW (Diagnosis of Ischemia-Causing Stenoses Obtained Via Noninvasive Fractional Flow Reserve) study. *J Am Coll Cardiol* 2011; 58:1989-1997.
4. Ko BS, Cameron JD, Leung M, et al. Combined CT Coronary Angiography and Stress Myocardial Perfusion Imaging for Hemodynamically Significant Stenoses in Patients With Suspected Coronary Artery Disease: A Comparison With Fractional Flow Reserve. *JACC Cardiovasc Imaging* 2012; 5:1097-1111.
5. Bettencourt N, Chiribiri A, Schuster A, et al. Direct comparison of cardiac magnetic resonance and multidetector computed tomography stress-rest perfusion imaging for detection of coronary artery disease. *J Am Coll Cardiol* 2013; 61:1099-1107.

6. Wong DT, Ko BS, Cameron JD, et al. Translumenal Attenuation Gradient in Coronary Computed Tomography Angiography Is a Novel Noninvasive Approach to the Identification of Functionally Significant Coronary Artery Stenosis: A Comparison With Fractional Flow Reserve. *Journal of the American College of Cardiology* 2013; 61:1271-1279.
7. Min JK, Leipsic J, Pencina MJ, et al. Diagnostic Accuracy of Fractional Flow Reserve From Anatomic CT Angiography. *JAMA* 2012;1-9.
8. Kristensen TS, Engstrom T, Kelbaek H, von der Recke P, Nielsen MB, Kofoed KF. Correlation between coronary computed tomographic angiography and fractional flow reserve. *Int J Cardiol* 2010; 144:200-205.
9. Rossi A, Papadopoulou SL, Pugliese F, et al. Quantitative computed tomographic coronary angiography: does it predict functionally significant coronary stenoses? *Circ Cardiovasc Imaging* 2014; 7:43-51.
10. Jogiya R, Kozerke S, Morton G, et al. Validation of dynamic 3-dimensional whole heart magnetic resonance myocardial perfusion imaging against fractional flow reserve for the detection of significant coronary artery disease. *J Am Coll Cardiol* 2012; 60:756-765.
11. Leone AM, De Caterina AR, Basile E, et al. Influence of the amount of myocardium subtended by a stenosis on fractional flow reserve. *Circ Cardiovasc Interv* 2013; 6:29-36.
12. Abbara S, Arbab-Zadeh A, Callister TQ, et al. SCCT guidelines for performance of coronary computed tomographic angiography: a report of the Society of Cardiovascular Computed Tomography Guidelines Committee. *J Cardiovasc Comput Tomogr* 2009; 3:190-204.

13. Sun J, Zhang Z, Lu B, et al. Identification and quantification of coronary atherosclerotic plaques: a comparison of 64-MDCT and intravascular ultrasound. *AJR Am J Roentgenol* 2008; 190:748-754.
14. Lee JT, Ideker RE, Reimer KA. Myocardial infarct size and location in relation to the coronary vascular bed at risk in man. *Circulation* 1981; 64:526-534.
15. Brandt PW, Partridge JB, Wattie WJ. Coronary arteriography; method of presentation of the arteriogram report and a scoring system. *Clin Radiol* 1977; 28:361-365.
16. Graham MM, Faris PD, Ghali WA, et al. Validation of three myocardial jeopardy scores in a population-based cardiac catheterization cohort. *Am Heart J* 2001; 142:254-261.
17. Ortiz-Perez JT, Meyers SN, Lee DC, et al. Angiographic estimates of myocardium at risk during acute myocardial infarction: validation study using cardiac magnetic resonance imaging. *Eur Heart J* 2007; 28:1750-1758.
18. Moral S, Rodriguez-Palomares JF, Descalzo M, et al. Quantification of myocardial area at risk: validation of coronary angiographic scores with cardiovascular magnetic resonance methods. *Rev Esp Cardiol (Engl Ed)* 2012; 65:1010-1017.
19. Kern MJ, Samady H. Current concepts of integrated coronary physiology in the catheterization laboratory. *J Am Coll Cardiol* 2010; 55:173-185.
20. Tonino PA, De Bruyne B, Pijls NH, et al. Fractional flow reserve versus angiography for guiding percutaneous coronary intervention. *N Engl J Med* 2009; 360:213-224.
21. Johnson NP, Toth GG, Lai D, et al. Prognostic value of fractional flow reserve: linking physiologic severity to clinical outcomes. *J Am Coll Cardiol* 2014; 64:1641-1654.
22. Pan W. Akaike's information criterion in generalized estimating equations. *Biometrics* 2001; 57:120-125.

23. Pencina MJ, D'Agostino RB, Sr., D'Agostino RB, Jr., Vasan RS. Evaluating the added predictive ability of a new marker: from area under the ROC curve to reclassification and beyond. *Stat Med* 2008; 27:157-172; discussion 207-112.
24. Jaffe R, Halon DA, Roguin A, Rubinshtein R, Lewis BS. A Poiseuille-based coronary angiographic index for prediction of fractional flow reserve. *Int J Cardiol* 2013; 167:862-865.
25. Brosh D, Higano ST, Lennon RJ, Holmes DR, Jr., Lerman A. Effect of lesion length on fractional flow reserve in intermediate coronary lesions. *Am Heart J* 2005; 150:338-343.
26. De Bruyne B, Pijls NH, Bartunek J, et al. Fractional flow reserve in patients with prior myocardial infarction. *Circulation* 2001; 104:157-162.
27. Shaw LJ, Hausleiter J, Achenbach S, et al. Coronary Computed Tomographic Angiography as a Gatekeeper to Invasive Diagnostic and Surgical Procedures: Results From the Multicenter CONFIRM (Coronary CT Angiography Evaluation for Clinical Outcomes: An International Multicenter) Registry. *J Am Coll Cardiol* 2012; 60:2103-2114.

Table 1 Patient and vessel characteristics

Patient Characteristics	Value
Age (years, mean \pm SD)	64.2 \pm 11.2
Age in male cohort (years, mean, range)	63.9 (48-82)
Age in female cohort (years, mean, range)	64.7 (51-88)
Difference in age between male and female cohort	P=0.76

Gender	
Male n (%)	56 (65.9)
Female n (%)	29 (34.1)
BMI (kg/m², mean±SD)	28.1 ± 5.1
Symptom (n, %)	
Typical angina	65 (76.5)
Atypical angina or non-cardiac pain	20 (23.5)
Suspected CAD (n, %)	49 (57.6)
Known CAD (n, %)	36 (42.4)
Previous MI	9 (9.5%)
Previous PCI	12 (12.7%)
Cardiovascular risk factors (n, %)	
Diabetes	13 (15.3)
Hypertension	63 (74.1)
Hypercholesterolaemia	63 (74.1)
Current smoker	13 (15.3%)
Family history of IHD	34 (40.0%)
CT Angiographic Findings	
Vessels with a ≥50% stenosis as visually assessed on CCTA (n, %)	
0	36 (42.4)
1	42 (29.4)
2	5 (5.9)
3	2 (2.4)
FFR findings	
Vessels interrogated on FFR (n, %)	
1	55 (64.7)
2	21 (24.8)
3	9 (10.6)
Mean number of vessels interrogated per patient (±SD)	1.6±0.8
Vessels with FFR≤0.8 per patient (n,%)	
0	48 (56.5)
1	35 (41.2)

2	2 (2.4)
Mean number of vessels with FFR \leq 0.8 per patient (\pm SD)	0.46 \pm 0.55
Lesion characteristics, n=124	
CTCA findings	
\geq 50% diameter stenosis on visual assessment (n,%)	58 (46.8)
Quantitative CT findings (mean\pmSD)	
Diameter stenosis (%)	39.4 \pm 20.9
Area stenosis (%)	47.8 \pm 24.0
Minimal luminal diameter (mm)	1.8 \pm 0.8
Minimal luminal area (mm ²)	5.0 \pm 3.5
Lesion length (mm)	19.5 \pm 11.4
Plaque burden	71.5 \pm 15.6
APPROACH score	26.5 \pm 11.9
QCA findings (mean\pmSD)	
Diameter stenosis (%)	37.4 \pm 17.8
Minimal luminal diameter (mm)	1.6 \pm 0.7
Vessel diameter (mm)	2.5 \pm 0.7
FFR findings (mean \pmSD)	
Mean FFR in all lesions	0.84 \pm 0.11
Lesions with FFR \leq 0.8 (n,%)	38 (30.6)
Mean of FFR in lesions with FFR \leq 0.8	0.71 \pm 0.09
Lesion location (n, %)	
Proximal RCA	15 (12.1)
Mid RCA	8 (6.5)
Distal RCA	2 (1.6)
Right PDA or PLV	3 (2.4)
Proximal LAD	31 (25.0)
Mid LAD	23 (18.5)
Distal LAD	4 (3.2)
Diagonal artery	3 (2.4)
Proximal LCx	24 (20.2)

Ramus intermediate	1 (0.8)
Obtuse marginal arteries	7 (5.6)
Distal LCx	2 (1.6)

Table 2: Univariate and multivariate predictors for FFR \leq 0.8

	Univariate coefficient (95% CI)	p-value	Multivariate coefficient (95% CI)	p-value
Plaque burden (%)	0.033 (0.0050 to 0.061)	0.02	-0.071 (-0.13 to - 0.013)	0.02
MLA (mm²)	-0.22 (-0.67 to - 0.070)	0.004	-0.065 (-0.37 to 0.24)	0.7
MLD (mm)	-0.81 (-1.4 to -0.25)	0.004	-1.2 (-2.9 to 0.41)	0.1
Diameter stenosis (%)	0.029 (0.0093 to 0.049)	0.004	-0.044 (-0.10 to 0.014)	0.1
Area stenosis (%)	0.038 (0.019 to 0.056)	<0.001	0.067 (0.015 to 0.12)	0.01
Lesion length (mm)	0.090 (0.051 to 0.13)	<0.001	0.091 (0.036 to 0.15)	0.001
Remodelling index	-0.0068 (-0.018 to 0.0044)	0.2		
Calcification	0.59 (0.023 to 1.2)	0.04	-0.068 (-0.85 to 0.71)	0.9
Plaque morphology	0.31 (-0.16 to 0.77)	0.2		
APPROACH score	0.069 (0.035 to 0.10)	<0.001	0.053 (0 0.0059 to 0.10)	0.03

Table 3: The ASLA Score

Variable	Value	Points
Area stenosis (%)	>63	7
	47-63	2
	31-46	1
	<31	0
Lesion length (mm)	>28	6
	10.8-28	1
	<10.8	0
APPROACH score	>44	5
	25.1-44	2
	18-25	1
	<18	0
Total		Maximum = 18

Table 4: Bootstrapped Harrell's c-statistic

	CTA	Area stenosis	Lesion Length	Plaque burden	APPROACH score	ASLA score
Harrell's c-statistic (95% confidence interval)	0.74 (0.64- 0.83)	0.74 (0.65- 0.83)*	0.75 (0.66- 0.85)*	0.65 (0.54- 0.76)	0.71 (0.61- 0.81)*	0.82 (0.74- 0.91)

Pairwise comparison with the ASLA score P<0.001 for trend

Table 5: Lesion characteristics quantified by CT and interobserver variability

	Mean \pm SD	Inter-observer intraclass coefficient
Area stenosis	47.8 \pm 24.0	0.977 (0.91-0.99)
Lesion Length	19.5 \pm 11.4	0.954 (0.824-0.988)
APPROACH score	26.5 \pm 11.9	1.0 (1.0-1.0)

Figure 1 Patient and vessel flow diagram

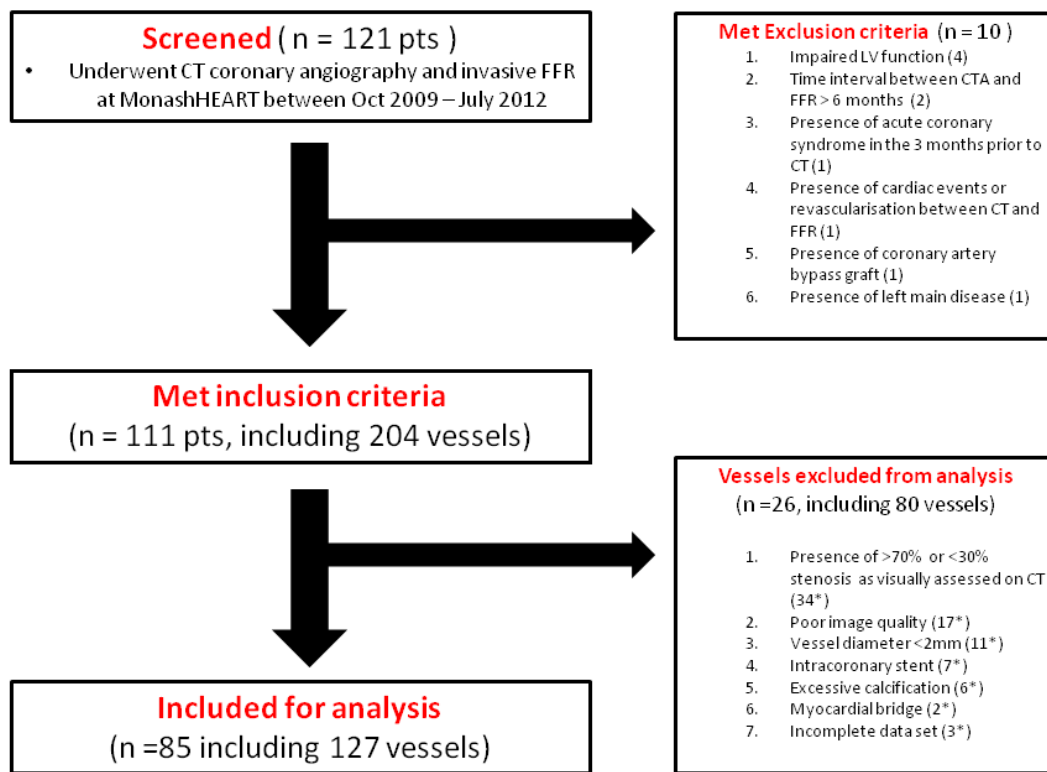


Figure 2 Scatter Plot of FFR and CT angiographic parameters including area stenosis

(A), lesion length (B), APPROACH Score (C) and plaque burden (D) There was a statistically significant inverse relationship between CT area stenosis and FFR ($R = -0.37$; $P < 0.0001$), lesion length ($R = -0.45$, $P < 0.0001$), APPROACH score ($R = -0.34$, $P = 0.0002$) and plaque burden ($R = -0.26$, $P = 0.003$)

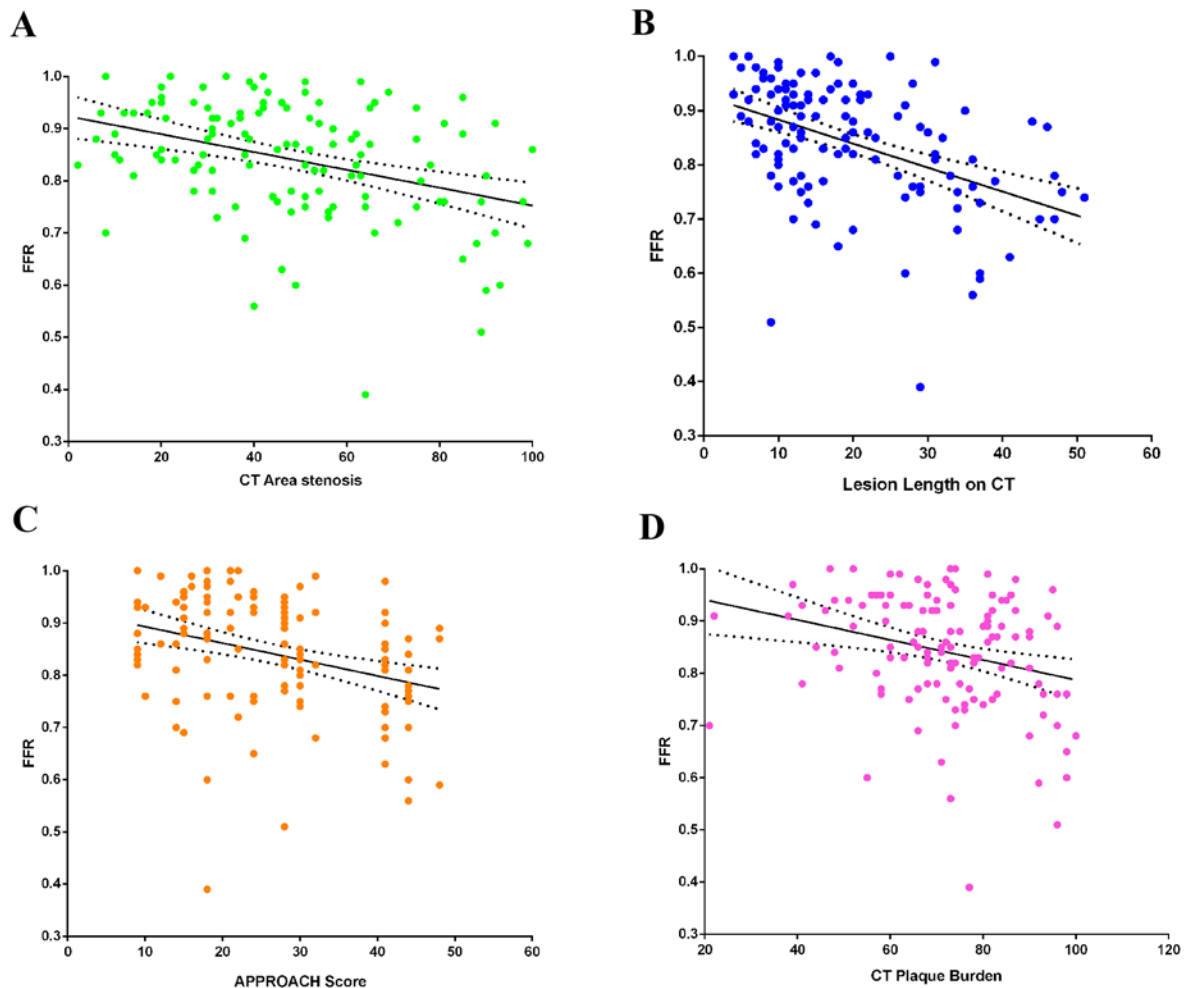


Figure 3: Quantitative computed tomography performed in an intermediate (50-70%) lesion in LCX. The lesion length was 12.4cm (B), area stenosis 77% (C) and APPROACH score was 24.5 (D). The ASLA score was 9 (1 for lesion length + 7 for area stenosis + 1 for lesion length). FFR in the LCX was 0.76.

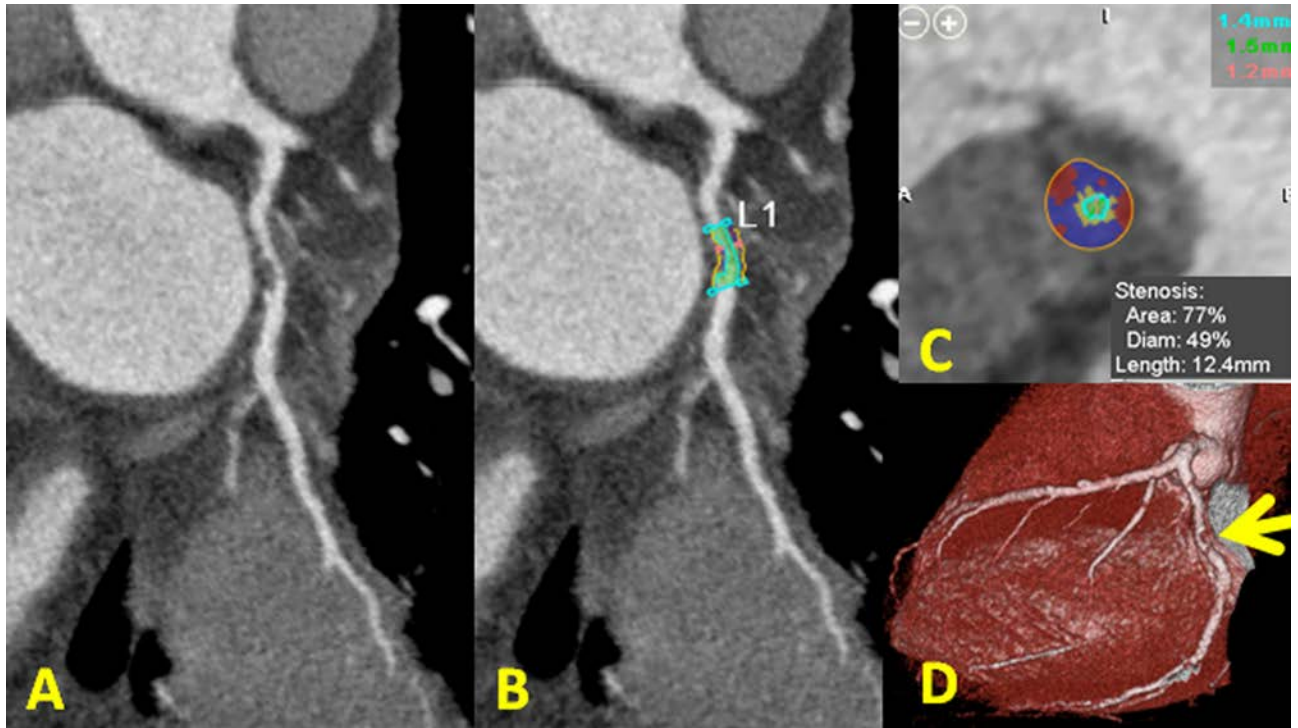


Figure 4– Receiver operating characteristic curve of the ASLA score, APPROACH score, CT quantified area stenosis and lesion length

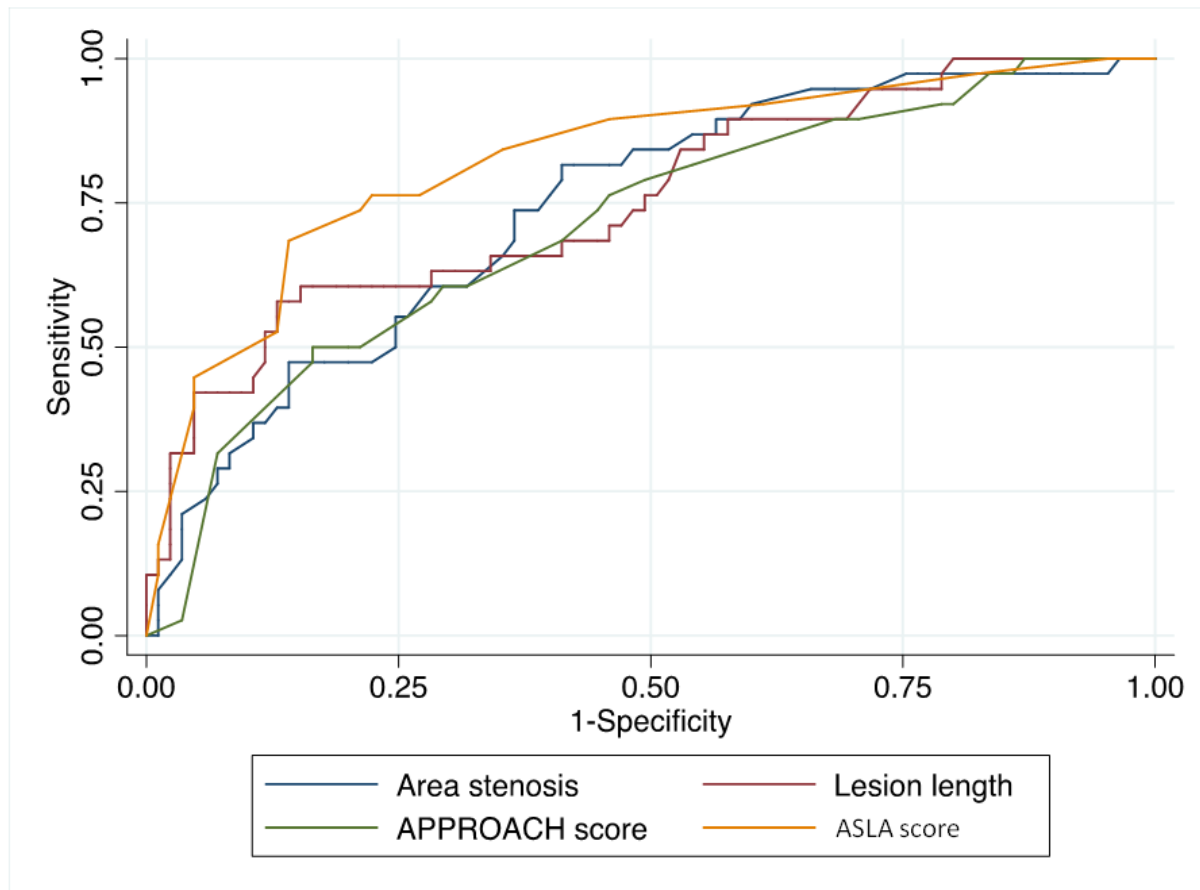


Figure 5– Representation of sensitivity and specificity as functional cutoff values over a whole spectrum of ASLA score.

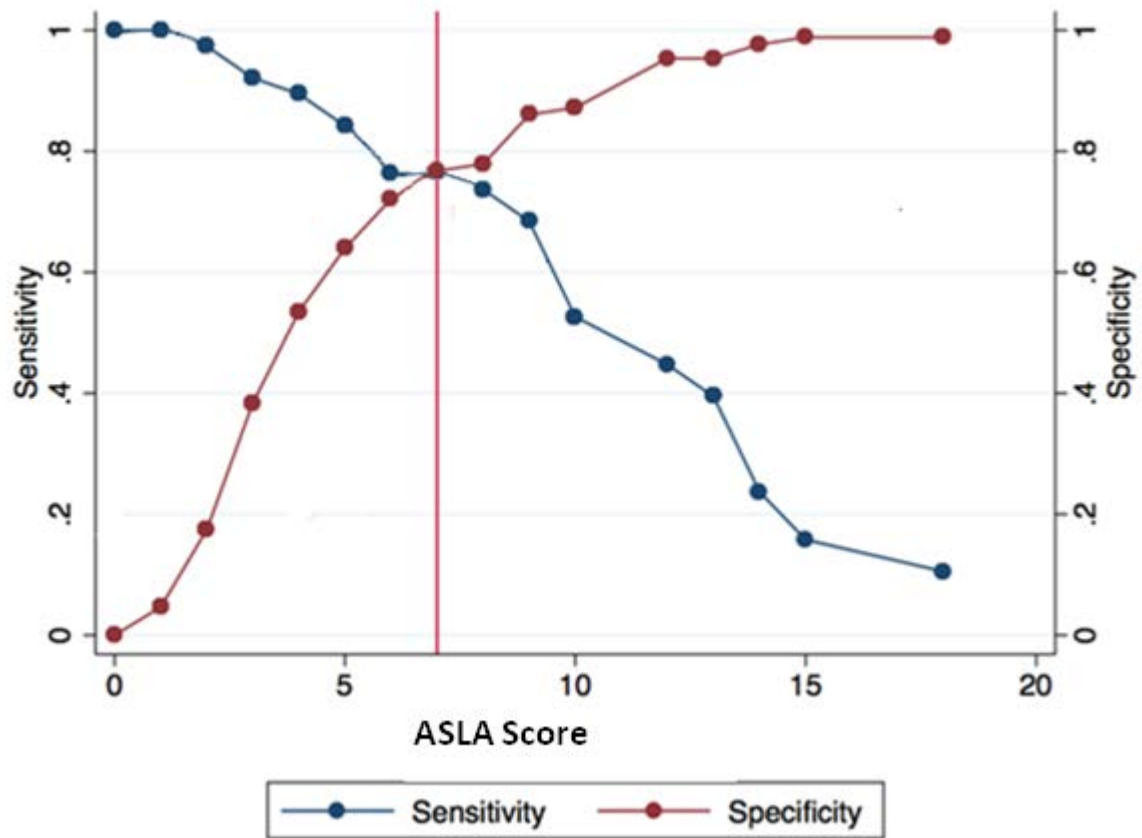
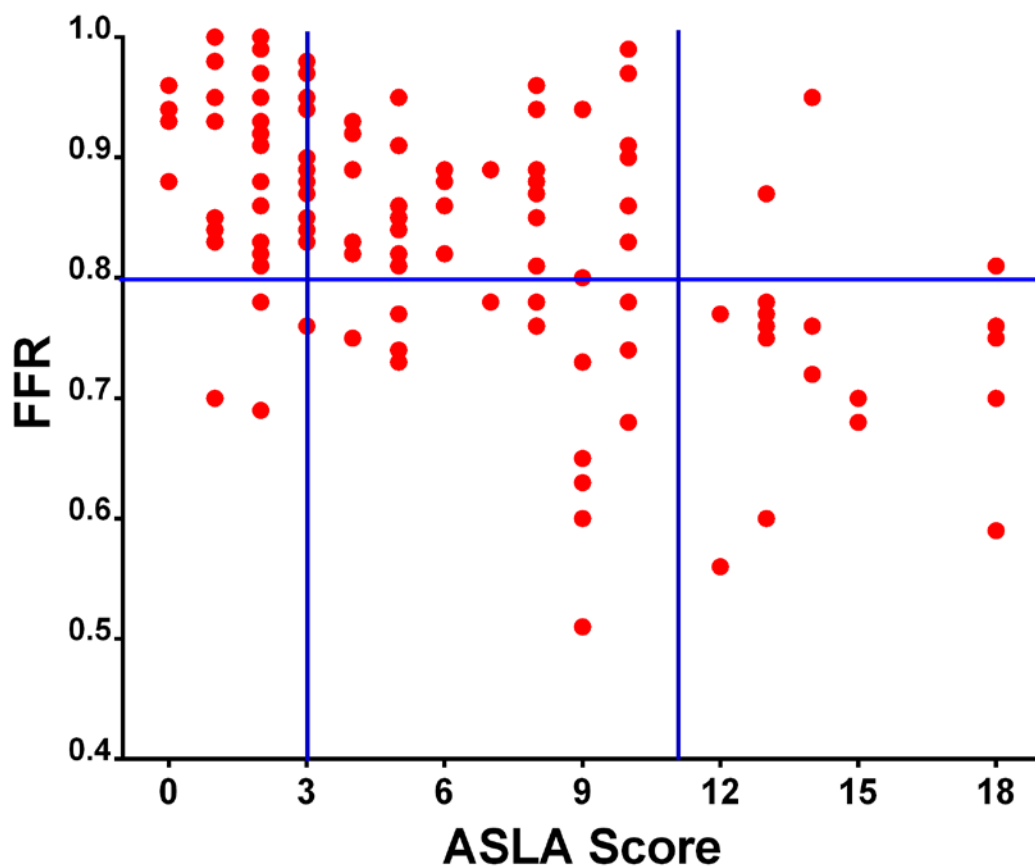


Figure 6: Scatter plot of FFR value and ASLA score. A total of 124 lesions were assessed.

In the 50 lesions with ASLA score ≤ 3 , four (8%) had FFR ≤ 0.8 (FFR range 0.68-0.78), including 2 lesions in the left anterior descending artery, one in marginal branch and one in the right coronary artery. In the 21 lesions with ASLA score ≥ 11 , four (19%) had FFR > 0.8 (FFR range 0.81-0.95), including 3 lesions in the left anterior descending artery, one in the left circumflex artery.



Appendix

Calculation of the Approach score. Table adapted from Ortiz-Perez JT, Meyers SN, Lee DC, Kansal P, Klocke FJ, Holly TA, Davidson CJ, Bonow RO, Wu E. Angiographic estimates of myocardium at risk during acute myocardial infarction: validation study using cardiac magnetic resonance imaging. *Eur Heart J.* 2007;28(14):1750-1758.

Data represents the percentage of left ventricular myocardium volume(17). In this system, the lesion location, dominance and major side branches beyond the lesion are taken into consideration. For example a subject with a left dominant system and a proximal left circumflex lesion who has a medium sized posterior descending artery and small posterolateral branches has a area at risk of 29.5% of the left ventricular myocardium. LAD, left anterior descending artery; LCx, left circumflex artery; LD, left dominance; OM, obtuse marginal; PDA, posterior descending artery; RCA, right coronary artery; RD, right dominance.

Culprit lesion location	Infarct related artery side branches ↓		Diagonal for LAD occlusion only or Posterolateral for all others		
			Small or absent	Medium	Large
LAD (RD or LD)		Distal	13.75	14.8	15.9
		Mid	27.5	29.7	31.8
		Proximal	41.25	44.5	47.75
Proximal LCx (RD)	OM	Small or absent	9.25	12.5	15.75
		Medium	15.25	18.5	21.75
		Large	21.25	24.5	27.75
Proximal LCx (LD)	PDA	Small or absent	23.5	28	32.5
		Medium	29.5	34	38.5
		Large	35.5	40	44.5
Mid LCx (LD) or RCA (RD)	PDA	Small or absent	9.25	12.5	15.75
		Medium	15.25	18.5	21.75
		Large	21.25	24.5	27.75
Mid LCx (RD)			3.25	6.5	9.75

Conclusion and future directions

Conclusion and Future Directions

The results of this thesis have advanced the understanding of the clinical utility of CT in cardiac imaging in four main areas.

Firstly the results presented demonstrate the first attempts at combining and comparing CT functional techniques to better predict functional stenoses as determined by invasive fractional flow reserve (FFR). The findings highlight the feasibility and potentially higher diagnostic accuracy in combining CT techniques to predict FFR such as by combining stress CT myocardial perfusion imaging (CTP), rest derived transluminal attenuation gradient (TAG) and CT coronary angiography. In addition, the findings emphasise the promise in rest-CTA based techniques which require less radiation, contrast, patient discomfort and time when compared with stress-CTA based techniques. Specifically when compared with stress CT myocardial perfusion imaging, rest CT-derived transluminal attenuation gradient (TAG) was demonstrated to have comparable diagnostic performance and incremental value when added to CTA alone. These observations may support the upfront use of rest-CT based functional strategies, and the reservation of stress-CT based functional strategies to be implemented when rest-based strategies cannot be performed or interpreted.

Secondly the results presented compare the difference in diagnostic performance of rest CTA-based functional techniques, namely non invasive FFR derived from CT (FFR_{CT}) and TAG. Compared for the first time in a multicentre cohort of patients as part of an international multicentre sub-study, the results demonstrate that FFR_{CT} performed using wide-detector CT

provided better diagnostic performance for the diagnosis of hemodynamically significant coronary stenoses when compared to CTA and TAG. Importantly the results suggest this may be attributable to an observed superior correlation between FFR_{CT} with invasive FFR than TAG with FFR.

Thirdly the results presented have evaluated methodological improvements aimed to optimise the practical implementation and diagnostic performance of TAG, including the use of a semi-automated method to quantify TAG, and the feasibility of TAG performed on stress CTA. While semi-automated TAG processing may increase the number of lesions in which TAG may be evaluable, the results highlight its potential challenges and pitfalls. The results also demonstrate the lack of improvement in diagnostic performance when TAG is performed on stress CTA when compared with rest CTA. These results emphasise the need for future methodological refinements and for them to be systematically evaluated before they are widely adopted into the technique.

Fourthly, the results presented demonstrate the feasibility in the use of a novel score system based on three parameters namely area stenosis, lesion length and myocardium subtended derived from CT coronary angiography which may improve prediction of functionally significant coronary stenoses compared with the individual indices alone.

Future prospective large multicentre studies are undoubtedly required to further evaluate which CT technique is the best choice to assess the functional significance of coronary artery disease based on its ease of application and diagnostic accuracy, and whether this choice may vary

between patient populations and clinical scenarios. Notably initial single expert centre evaluations are generally performed with more narrow and distinct spectrums of diseased and non diseased patients than are encountered clinically, which may falsely elevate measures of diagnostic performance (1), for example the majority of TAG studies thus far mainly excluded patients with branch vessel disease and distal vessel disease for ease of TAG evaluation. The use of independent core-lab CT analyses will be vital to ensure and promote the integrity of future multicentre studies. In the case of multi-centre data thus far which have evaluated the technique of FFR_{CT} (2-4), all FFR_{CT} values to date have regrettably been derived in a core-lab situated in the company in which FFRCT was first developed and continues to be marketed, which poses as a large conflict of interest.

Large multicentre international registries and prospective studies aimed to evaluate the prognostic significance, cost effectiveness and downstream resource utilisation of the novel CT techniques will be crucial in determining their adoption into guideline and reimbursement recommendations, as had been evident historically in the case of established imaging techniques including CT coronary angiography (5-7) and non-invasive stress imaging such as SPECT MPI and stress echocardiography (8-11). Comparisons made against standard practice will also be important. The ongoing multicentre “Prospective Longitudinal Trial of FFR CT: Outcome and Impact (PLATFORM) Clinical Trials.gov Identifier NCT01943903 will seek to compare the effect of FFR CT guided versus standard diagnostic evaluation on clinical outcomes, resource utilization, costs and quality of life in patients with suspected CAD. In CT perfusion, the final results of the Regadenoson Crossover (A Study of Regadenoson in Subjects Undergoing Stress Myocardial Perfusion Imaging (MPI) Using Multidetector Computed Tomography Compared to Single Photon Emission Computed Tomography (SPECT) trial will be important to assess the diagnostic performance of the technique when applied in a

multivendor trial(12). Outcome studies are also underway including the PRECEPT registry, PeRfusion Evaluation by ComputEd tomography Procedures and Techniques is a multicentre international study which is similar in concept as the CONFIRM registry performed for CT coronary angiography(13). It currently has 14 centres participating worldwide and includes both retrospective and prospective registries of patients evaluated by CTP.

Lastly technical refinements in CT scanner technology and image interpretation software remain much needed to improve the diagnostic performance and clinical application of these techniques. In CT stress myocardial perfusion imaging, the focus of future research will aim to improve CT scanner temporal resolution to facilitate image acquisition at high heart rates during vasodilator induced hyperaemia and to evaluate dose reduction strategies to lower radiation exposure. Furthermore evaluation of dynamic wide detector CTP, refinements in dual energy CTP and improvements in artefact correction algorithms will be important areas of research to improve diagnostic performance and reader confidence to identify perfusion defects. In the case of FFR CT, there remains a need to refine automated image processing methods (2,3) and to shorten the currently required processing time of five hours (3). The current logistics requiring offsite data analysis and the attendant turnaround time (14) may limit the application of the technique especially in more symptomatic patients. Lastly in the case of TAG, apart from the presence of epicardial stenosis, studies are required to evaluate the influence of bifurcations and myocardium subtended on TAG, and whether the limitations of TAG performed using 64-detector CT may be overcome by a correction for the Hounsfield unit differences observed in the descending aorta(15). Furthermore the development and validation of a refined semi-automated program to provide instantaneous TAG analysis is much anticipated (16) and may shorten TAG processing time.

Reference

1. Ransohoff DF, Feinstein AR. Problems of spectrum and bias in evaluating the efficacy of diagnostic tests. *N Engl J Med* 1978;299:926-30.
2. Koo BK, Erglis A, Doh JH, et al. Diagnosis of ischemia-causing coronary stenoses by noninvasive fractional flow reserve computed from coronary computed tomographic angiograms. Results from the prospective multicenter DISCOVER-FLOW (Diagnosis of Ischemia-Causing Stenoses Obtained Via Noninvasive Fractional Flow Reserve) study. *J Am Coll Cardiol* 2011;58:1989-97.
3. Min JK, Leipsic J, Pencina MJ, et al. Diagnostic Accuracy of Fractional Flow Reserve From Anatomic CT Angiography. *JAMA* 2012;1-9.
4. Norgaard BL, Leipsic J, Gaur S, et al. Diagnostic performance of non-invasive fractional flow reserve derived from coronary CT angiography in suspected coronary artery disease: The NXT trial. *J Am Coll Cardiol* 2014;63:1145-55.
5. Min JK, Dunning A, Lin FY, et al. Age- and sex-related differences in all-cause mortality risk based on coronary computed tomography angiography findings results from the International Multicenter CONFIRM (Coronary CT Angiography Evaluation for Clinical Outcomes: An International Multicenter Registry) of 23,854 patients without known coronary artery disease. *J Am Coll Cardiol* 2011;58:849-60.
6. Hadamitzky M, Achenbach S, Al-Mallah M, et al. Optimized Prognostic Score for Coronary Computed Tomographic Angiography: Results From the CONFIRM Registry (CORonary CT Angiography EvaluationN For Clinical Outcomes: An InteRnational Multicenter Registry). *J Am Coll Cardiol* 2013;62:468-76.
7. Chow BJ, Small G, Yam Y, et al. Incremental prognostic value of cardiac computed tomography in coronary artery disease using CONFIRM: COroNary computed

- tomography angiography evaluation for clinical outcomes: an International Multicenter registry. *Circ Cardiovasc Imaging* 2011;4:463-72.
8. Hachamovitch R, Hayes SW, Friedman JD, Cohen I, Berman DS. Comparison of the short-term survival benefit associated with revascularization compared with medical therapy in patients with no prior coronary artery disease undergoing stress myocardial perfusion single photon emission computed tomography. *Circulation* 2003;107:2900-7.
 9. Hachamovitch R, Rozanski A, Shaw LJ, et al. Impact of ischaemia and scar on the therapeutic benefit derived from myocardial revascularization vs. medical therapy among patients undergoing stress-rest myocardial perfusion scintigraphy. *Eur Heart J* 2011;32:1012-24.
 10. Marwick TH, Case C, Vasey C, Allen S, Short L, Thomas JD. Prediction of mortality by exercise echocardiography: a strategy for combination with the duke treadmill score. *Circulation* 2001;103:2566-71.
 11. McCully RB, Roger VL, Mahoney DW, et al. Outcome after abnormal exercise echocardiography for patients with good exercise capacity: prognostic importance of the extent and severity of exercise-related left ventricular dysfunction. *J Am Coll Cardiol* 2002;39:1345-52.
 12. Cury RC, Kitt TM, Feaheny K, Akin J, George RT. Regadenoson-stress myocardial CT perfusion and single-photon emission CT: Rationale, design, and acquisition methods of a prospective, multicenter, multivendor comparison. *J Cardiovasc Comput Tomogr* 2014;8:2-12.
 13. Min JK, Dunning A, Lin FY, et al. Rationale and design of the CONFIRM (COronary CT Angiography EvaluationN For Clinical Outcomes: An InteRnational Multicenter) Registry. *J Cardiovasc Comput Tomogr* 2011;5:84-92.

14. Hecht HS. The Game Changer? J Am Coll Cardiol 2014.
15. Chow BJ, Kass M, Gagne O, et al. Can differences in corrected coronary opacification measured with computed tomography predict resting coronary artery flow? J Am Coll Cardiol 2011;57:1280-8.
16. Wong DT, Ko BS, Cameron JD, et al. Translumenal attenuation gradient in coronary computed tomography angiography is a novel noninvasive approach to the identification of functionally significant coronary artery stenosis: a comparison with fractional flow reserve. J Am Coll Cardiol 2013;61:1271-9.